

**EPITHELIAL SODIUM CHANNELS IN THE BRAIN:
EFFECTS OF HIGH SALT INTAKE ON THEIR EXPRESSION**

Name of student:

Md. Shahrier Amin

Supervisor:

Dr Frans H H Leenen

Committee members:

Dr Balwant S Tuana, Dr Frederique Tesson, Dr Stewart Whitman

This thesis is submitted as a partial fulfillment of the Ph.D. program in Cellular and Molecular Medicine.

Date of Submission:

June 24, 2011

Place of Submission:

Ottawa, Ontario, Canada.

© Md. Shahrier Amin, Ottawa, Canada, 2011

ABSTRACT

Statement of the problem: The epithelial sodium channels (ENaC) play an important role in regulation of blood pressure (BP). Although the genes are identical in Dahl salt sensitive (S) and Dahl salt resistant (R) rats, expression of ENaC subunits is increased in kidneys of S rats on high salt diet. Intracerebroventricular (icv) infusion of ENaC blocker benzamil prevents Na^+ induced hypertension. It was not known whether ENaC subunits are expressed in the brain and whether or not brain ENaC plays a role in regulation of $[\text{Na}^+]$ in CNS.

Hypothesis: 1. Epithelial sodium channels are expressed in the brain. 2. Expression of ENaC is increased in the kidneys and brain of Dahl S rats on high salt diet. 3. ENaC in the brain contributes to regulation of $[\text{Na}^+]$ in the CSF and brain interstitium.

Methods of investigation: We studied expression and distribution of the ENaC subunits and assessed the effects of icv infusion of Na^+ -rich aCSF in Wistar rats or high salt diet in Dahl S rats in different areas of the brain. Function of ENaC in the choroid plexus was evaluated by studying the effects of benzamil and ouabain on Na^+ transport.

Major findings: In Wistar rats, both mRNA and protein of all three ENaC subunits are expressed in brain epithelia and magnocellular neurons in the supraoptic (SON) and paraventricular (PVN) nucleus. ENaC abundance is higher on the apical versus basolateral membrane of choroid cells. Benzamil decreases Na^+ influx into choroid cells by 20-30% and increases CSF $[\text{Na}^+]$ by ~ 8 mmol/L. Na^+ rich aCSF increases apical membrane expression of β ENaC in the choroid cells and of α and β ENaC in basolateral membrane of ependymal cells, but has no effect on neuronal ENaC. Expression of ENaC is higher in choroid cells and SON of Dahl S versus R rats and the higher expression persists on a high salt diet. High salt attenuates the ouabain blockable efflux of Na^+ from choroid cells and has no effect on CSF $[\text{Na}^+]$ in Dahl R rats. In contrast, high salt does not attenuate ouabain blockable efflux of $^{22}\text{Na}^+$ and CSF $[\text{Na}^+]$ increases in Dahl S.

Main Conclusion: ENaC in the brain contributes to Na^+ transport into the choroid cells and appear to be involved in reabsorption of Na^+ from the CSF. Aberrant regulation of Na^+ transport and of $\text{Na}^+\text{K}^+\text{ATPase}$ activity, might contribute to increases in CSF $[\text{Na}^+]$ in Dahl S rats on high-salt diet. ENaC in magnocellular neurons may contribute to enhanced secretion of mediators such as 'ouabain' leading to sympathetic hyperactivity in Dahl S rats.

ACKNOWLEDGMENTS

This thesis is dedicated to the memory of late Dr Stewart C Whitman, whose encouragement and advice was crucial in enabling me get to where I am now. Dr Whitman, you may have left us from this world, but you are always in our memories.

First of all I am and always will be indebted to the painstaking supervision of Dr Frans H H Leenen, without whose support I wouldn't have been able to complete my studies. He was always there whenever we needed him for anything and would always go the extra step to help us. I will especially remember all the weeknights and holidays that I have knocked on his home and disturbed his family life for my papers, presentations and thesis. Thank you Dr Leenen, for your incredible support.

The guidance and contribution of my committee members Dr Balwant Tuana and Dr Frederique Tesson has been crucial. I also am grateful to Dr Hongwei Wang, Mrs Roselyn White, Dr Bing Huang and Dr Monir Ahmed for their advice, help and suggestions for completing these studies.

The collaboration and support of my wife Dr Erona Reza cannot be over-emphasized. As a coworker she did the RNA related studies in most of the experiments. She always offered her benevolent support in each and every step and endured my long work hours, especially after the start of residency. I like to thank my daughters Sumehra Amin, Suhaira Amin and Sumanta Amin and my niece Naza Amin, for keeping me entertained all these years with their playfulness. Indeed the colors in many of my figures are their choice. I like to thank my mother Dr Laila Amin and father Dr Md Nurul Amin, for their support, encouragement and love. Hadn't my mother Dr Laila Amin and mother in law Mrs Rehana Karim taken care of our daughters, life would have been much more difficult for us. Thanks to my wonderful

siblings Dr Shahreen Amin, Md Shahrooz Amin and Md Shahnoor Amin especially for their encouragement and support.

I must also acknowledge the support and consideration I received from my mentors, supervisors and colleagues in the Department of Pathology and Laboratory Medicine, during the last three years. My special gratitude to Dr John Veinot, Dr Jean Michaud, Dr Yasmin Ayroud and Dr Shahidul Islam who always have supported me and given me the extra time to complete my tasks.

Finally but not the least, I would like to acknowledge the Canadian Institutes of Health Research, Pfizer Canada and the Canadian Hypertension Society for the doctoral research award, and the Heart and Stroke Foundation of Ontario for funding our research.

LIST OF ABBREVIATIONS

11 β HSD2 - 11 β -hydroxysteroid dehydrogenase type 2

aCSF – Artificial cerebrospinal fluid

AT1 – Angiotensin II type 1 receptor

AVP – Arginine Vasopressin

BBB – Blood brain barrier

BN – Brown Norway

CNS - central nervous system

CP – Choroid plexus

CRE - cAMP response element

CREB - CRE binding protein

CSF - cerebrospinal fluid

DEG - Degenerin

DMA – Di methyl amiloride

DS – Dahl Salt Sensitive

DR – Dahl Salt Resistant

DOCA – Deoxy Corticosterone Acetate

EIPA – Ethyl iso propyl amiloride

ENaC - epithelial sodium channels

GR – Glucocorticoid receptor

icv - Intracerebroventricular

ISF – Interstitial fluid

MHS – Milan Hypertensive Strain

MNS – Milan Normotensive Strain

MR - mineralocorticoid receptors

Na⁺ - Sodium / sodium ion

Na⁺K⁺ATPase – Sodium potassium ATPase

NHE – Sodium hydrogen exchanger

OVLT - organum vasculosum of lamina terminalis

OLC / 'ouabain' - ouabain-like compound

MnPO - Median preoptic nucleus

PVN - Paraventricular nucleus

QTL - quantitative trait locus

RAAS - renin–angiotensin-aldosterone system

SFO - Subfornical organ

SHR - spontaneously hypertensive rats

SIK - salt-inducible kinase

SON - Supraoptic nucleus

WKY - Wistar–Kyoto rats

TABLE OF CONTENTS

Abstract	ii
ACKNOWLEDGMENTS	iii
LIST OF ABBREVIATIONS	v
Table of contents.....	vii
List of figures.....	xii
List of tables.....	xxix
General Introduction	1
1.1 Overview	1
1.2 The Epithelial Sodium Channel (ENaC)	2
1.2.1 Overview	2
1.2.2 Structure	3
1.2.3 Expression of ENaC in different tissues	4
1.2.4 Transport of Na ⁺ through ENaC	9
1.2.5 Regulation of ENaC.....	11
1.2.6 SGK1 – a crucial regulator of ENaC.....	29
1.3 Sodium, blood pressure (BP) and the role of ENaC	32
1.3.1 Mutations in ENaC genes affect BP	33
1.3.2 Experimental Na ⁺ induced hypertension in Dahl S rats and the role of ENaC.....	34
1.3.3 Central mechanisms of Na ⁺ induced hypertension	42
1.3.4 Rationale of the studies	57
Hypotheses and Objectives	58

2.1 Hypotheses.....	58
2.2 Objectives	59
2.2.1 Studies in Wistar rats	59
2.2.2 Studies in Dahl rats.....	59
Outline of approach to problem	60
3.1 MANUSCRIPT # 1: ENHANCED EXPRESSION OF EPITHELIAL SODIUM CHANNELS IN THE RENAL MEDULLA OF DAHL S RATS.....	62
3.1.1 RELEVANCE TO OVERALL PROJECT	63
3.1.2 CONTRIBUTION	63
3.1.3 Abstract	64
3.1.4 Introduction	65
3.1.5 Materials And Methods	68
3.1.6 Results	73
3.1.7 Discussion.....	79
3.1.8 Acknowledgement	83
3.1.9 Sources of Funding.....	83
3.2 MANUSCRIPT # 2: DISTRIBUTION OF EPITHELIAL SODIUM CHANNELS AND MINERALOCORTICOID RECEPTORS IN CARDIOVASCULAR REGULATORY CENTERS IN RAT BRAIN. 84	
3.2.1 Relevance to overall project.....	85
3.2.2 Contribution	85
3.2.3 Abstract	86
3.2.4 Introduction	87
3.2.5 Materials and Methods.....	89

3.2.6	Results	96
3.2.7	Discussion.....	112
3.2.8	Acknowledgements.....	118
3.3	MANUSCRIPT # 3: EFFECTS OF CENTRAL SODIUM ON EPITHELIAL SODIUM CHANNELS IN RAT BRAIN.	119
3.3.1	RELEVANCE TO OVERALL PROJECT	120
3.3.2	CONTRIBUTION	120
3.3.3	ABSTRACT.....	121
3.3.4	INTRODUCTION	122
3.3.5	MATERIALS AND METHODS	124
3.3.6	Supplemental Methods.....	129
3.3.7	RESULTS.....	136
3.3.8	DISCUSSION.....	156
3.3.9	ACKNOWLEDGEMENTS	166
3.3.10	SOURCES OF FUNDING.....	166
3.4	Manuscript # 4: EXPRESSION OF EPITHELIAL SODIUM CHANNELS AND REGULATORY GENES IN THE BRAIN OF DAHL S AND R RATS.	167
3.4.1	RELEVANCE TO OVERALL PROJECT	168
3.4.2	CONTRIBUTION	168
3.4.3	ABSTRACT.....	169
3.4.4	INTRODUCTION	170
3.4.5	MATERIALS AND METHODS	173
3.4.6	RESULTS.....	180
3.4.7	DISCUSSION.....	193

3.4.8	Limitations of study.....	196
3.4.9	Conclusion	197
3.4.10	Acknowledgement	198
3.4.11	Sources of Funding.....	198
3.5	Manuscript # 5: SODIUM TRANSPORT IN THE CHOROID PLEXUS AND SALT SENSITIVE HYPERTENSION.	199
3.5.1	Relevance	200
3.5.2	CONTRIBUTION	200
3.5.3	ABSTRACT.....	201
3.5.4	INTRODUCTION	202
3.5.5	METHODS.....	205
3.5.6	Supplementary Methods.....	208
3.5.7	RESULTS.....	215
3.5.8	DISCUSSION.....	228
3.5.9	ACKNOWLEDGEMENTS	234
3.5.10	DISCLOSURES	234
3.5.11	SOURCE OF FUNDING	234
3.6	MANUSCRIPT # 6: THE CENTRAL ROLE OF THE BRAIN IN SALT-SENSITIVE HYPERTENSION.	235
3.6.1	Relevance to overall project.....	235
3.6.2	Contribution	235
3.6.3	Abstract	236
3.6.4	Introduction	238
3.6.5	Central nervous system mechanisms contributing to salt-sensitive hypertension.....	239

3.6.6	Role of central nervous system aldosterone, mineralocorticoid receptors, and epithelial sodium channels in salt-sensitive hypertension	245
3.6.7	Genetic determinants of salt sensitivity with focus on the mineralocorticoid receptor – epithelial sodium channels – renin-angiotensin system pathway	250
3.6.8	Conclusion	257
3.6.9	Acknowledgements.....	262
General Discussion		263
4.1	ENaC expression in the choroid plexus.....	264
4.1.1	ENaC Expression in Wistar rats	264
4.1.2	Factors affecting ENaC expression in the choroid plexus.....	264
4.1.3	ENaC expression in Dahl rats.....	265
4.1.4	Effect of high salt diet on ENaC expression in the choroid plexus	266
4.1.5	ENaC function in the choroid plexus	266
4.1.6	Effect of high salt on CSF [Na ⁺], ENaC function and Na ⁺ transport in the choroid plexus 268	
4.2	ENaC expression in the ependyma	269
4.2.1	Effect of Na ⁺ on ENaC expression in ependyma	270
4.3	ENaC expression in magnocellular neurons.....	270
4.3.1	Effect of high salt on expression of ENaC subunits and their regulators in the SON ..	271
4.3.2	Functional implications	272
4.4	CONCLUSION	272
References		276

LIST OF FIGURES

Figure 1.2-1: Cartoons showing the different structural domains of an ENaC subunit (left) and a trimeric $\alpha\beta\gamma$ ENaC in the membrane (right). Both the N- and C- termini are in the cytoplasm. Complete activation of ENaC requires sequential cleavages of the finger domains of α ENaC (purple rectangle) and γ ENaC (red rectangle) by extracellular proteases (Reproduced from Soundararajan et al (Soundararajan et al. 2010)). 5

Figure 1.2-2: Linear model for cleavage of ENaC subunits. Each subunit has two transmembrane domains, short N and C termini and a large extracellular loop with 5-12 N-glycosylation sites. Cleavage sites are shown in yellow and putative sites for trypsin (T), chymotrypsin (CT), elastase (E) or serine proteases (SP) are in green. Depending on cleavage site α ENaC fragments can have molecular weights of 90, 65-70 (active), 50 and 25-37 kDa. β ENaC is not cleaved by furin but maybe cleaved by other proteases and has N-glycosylation sites that can increase its molecular weight from 85 to 100 kDa. γ ENaC has one furin cleavage site as well as cleavage sites for proteases such as CAP, prostasin and elastase generating fragments with molecular weights of 85, 70 (active), 50 and 15 kDa. Reproduced from Rossier and Stutts, 2009 (Rossier & Stutts 2009) 17

Figure 1.2-3: Regulation of trafficking and activation of ENaC by proteases. Uncleaved ENaCs can be cleaved in the trans-Golgi network by furin. These cleaved ENaCs are then transported to the plasma membrane in a highly regulated fashion where they can transport Na^+ . A pool of nascent ENaC can bypass the cleavage step and be directly inserted into the plasma membrane as 'silent' channels. These silent channels can then

be cleaved by cell-attached, extracellular or soluble proteases. Alternatively, silent ENaC may bind to SPLUNC1-, and be targeted for internalization. Reproduced from Gaillard et al (Gaillard et al. 2010). 18

Figure 1.2-4: Concerted regulation of ENaC by hormones. Aldosterone (Ald) and glucocorticoids (Glu) acting through the mineralocorticoid receptor (MR) and glucocorticoid receptor (GR) and vasopressin acting through increases in cAMP and CREB increase transcription of ENaC subunits both directly and through regulators such as SGK1. Nascent ENaC subunits undergo assembly, cleavage and activation, partially in the ER-Golgi complex and partly on the cell surface by extracellular proteases. Aldosterone, vasopressin, insulin and β 2adrenergic activity (β 2AR) also activate the PI3K pathway that activates SGK1 by phosphorylation. Activated SGK1 phosphorylates Nedd4-2, and acting through interacting 14-3-3 proteins decreases ubiquitination and degradation of ENaC. Author's own reproduction. 23

Figure 1.2-5: Synergistic effect of aldosterone and vasopressin on ENaC Po . ENaC is most active when both aldosterone and vasopressin levels are elevated. Reproduced from Bugaj et al, 2009 (Bugaj et al. 2009). 26

Figure 1.2-6: Regulation of SGK1. Glucocorticoids maintain the basal SGK1 levels, while aldosterone and other factors such as cAMP mediate the day-to-day fluctuation by increasing transcription. A number of mediators such as insulin and aldosterone activate SGK1 through PDK1 and PKB dependent phosphorylation, involving other proteins such as WNK1. The SGK1 protein is rapidly degraded in the cell through processes that are facilitated by Nedd4-2 mediated ubiquitination. Author's own reproduction. 31

Figure 1.3-1: Outline of brain and kidney interactions in Na^+ induced hypertension. Reproduced from Leenen, FH, 2010 (Leenen 2010). 45

Figure 1.3-2: Morphology of blood-brain-CSF interfaces: (A) The main CNS compartments and interfaces. The blood-brain and blood-CSF barriers are true barriers with tight junctions between endothelial and epithelial cells, respectively. The brain-CSF interface, because of gap junctions between ependymal (or pia-glia) cells, is more permeable than brain or spinal cord capillaries and choroid plexus. (B) Blood-CSF barrier. The choroid plexus has one cell layer of circumferentially arranged epithelial cells. Plexus capillaries, unlike counterparts in brain, are permeable to macromolecules. (C) Blood-brain barrier: Endothelial cells are linked by tight junctions, conferring low paracellular permeability. Endothelial cell pinocytotic vesicle paucity reflects minimal transcytosis. (D) Brain-CSF interface: Ependymal lining in lateral ventricles maintains the barrier between brain ISF and large-cavity CSF. Motile cilia at ependymal cell apex move CSF downstream to sub-arachnoidal space. Figure reproduced from Johanson et al, 2008 (Johanson et al. 2008), (Praetorius 2007). 46

Figure 1.3-3: Schematic diagram of CSF secretion by the choroid plexus. The apically located $\text{Na}^+\text{K}^+\text{ATPase}$ generates the net driving force of Na^+ secretion into the CSF. Na^+ moves down a concentration gradient via secondary active transport in the basolateral membrane. Transport of other ions and water occurs along their electrochemical gradients through other transporters such as $\text{Na}^+\text{H}^+\text{CO}_3^-$ cotransporter, Na^+ dependent $\text{Cl}^-\text{HCO}_3^-$ exchanger, K^+Cl^- cotransporter and $\text{Cl}^-\text{HCO}_3^-$ countertransporter on the basolateral membrane and $\text{Na}^+2\text{Cl}^-\text{K}^+$ cotransporter, K^+Cl^- cotransporter, other K^+ and Cl^- channels and aquaporins predominantly on the apical CSF side of the membrane.c.a.

= carbonic anhydrase. Reproduced from Johanson et al, 2008 (Johanson et al. 2008, Millar et al. 2007, Praetorius & Nielsen 2006, Johanson 1984, Johanson et al. 1990, Johanson et al. 2011),(Johanson & Murphy 1990, Murphy & Johanson 1990) 48

Figure 1.3-4: Outline of CNS mechanisms activated by an increase in CSF $[Na^+]$. Increased CSF $[Na^+]$ activates the aldosterone-ouabain neuromodulatory pathway that enhances angiotensinergic activity in e.g. the PVN to cause sympathetic hyperactivity and hypertension. Reproduced from Leenen, FH, 2010 (Leenen 2010). 53

Figure 1.3-5: Neuronal connections between the circumventricular organs, SON and PVN. Magnocellular neurons receive synaptic inputs from central Na^+ -sensitive neurons located in the organum vasculosum lamina terminalis (OVLT), subfornical organ (SFO), and median preoptic nucleus (MnPO). In these latter areas, the blood-brain barrier and CSF-brain barrier are partially open, allowing for direct sensing of the ionic composition of the plasma. OVLT and SFO neurons also project to the MnPO. The PVN and SON respond by for example secretion of vasopressin, and their function is additionally affected by the $[Na^+]$ and osmolality of the CSF. IML - Intermediolateral cell column of the thoraco-lumbar spinal cord, RVLM – Rostral ventrolateral medulla, optic chiasma. Adapted from Hussy et al and Orlov and Mongin (Hussy et al. 2000, Orlov & Mongin 2007). 55

Figure 3.1-1: Protein abundance in the inner medulla and immunoreactivity to α , β and γ ENaC in the collecting ducts in Wistar rats after 2 weeks of regular versus low salt diet. Diffuse and mostly cytoplasmic staining was noted in the collecting ducts of Wistar rats on regular salt diet. Low salt increased apical immunoreactivity in the collecting

ducts (arrows) and abundance of 80kDa α ENaC, 85 kDa β ENaC and 70kDa γ ENaC proteins in the inner medulla. 70

Figure 3.1-2: Immunoreactivity to α ENaC in the renal medulla. Immunoreactivity to α ENaC in the inner medulla of Dahl R and S rats after 2 or 4 weeks on regular (RS) or high (HS) salt diet. In R rats, the staining is modest at 2 and 4 weeks, and similar on both salt diets. In contrast, distinct apical immunoreactivity is notable in the IMCD of S rats at 2 weeks and is not affected by a high salt diet. The higher abundance of ENaC subunits in S rats is more apparent after 4 weeks, although at this point the apical immunoreactivity is less contrasting due to the increased cytoplasmic staining. Arrows show apical immunoreactivity in IMCDs in S rats. 74

Figure 3.1-3: β ENaC abundance and immunoreactivity in the renal medulla of Dahl R and S rats after 2 or 4 weeks on regular (RS) or high (HS) salt diet. 3A. Abundance of β ENaC protein in the medulla. Both strains had similar abundance of the protein which was not affected by high salt. 3.3-3B. Distribution of β ENaC in the IMCDs. Apical staining was decreased in the IMCDs of Dahl R on high salt diet, but became more prominent in Dahl S. Arrows show immunoreactivity in IMCDs. 75-76

Figure 3.1-4: γ ENaC protein abundance and immunoreactivity in the inner medulla of Dahl R and S rats after 2 or 4 weeks on regular (RS) or high (HS) salt diet. 3.1-4A. Abundance of γ ENaC protein in the medulla. Dahl S have greater abundance of the protein at both 2 and 4 weeks. 3.1-4B. Distribution of γ ENaC in the IMCDs. Modest apical and cytoplasmic staining can be seen in the IMCDs which is significantly increased by high salt in Dahl S. 77-78

Figure 3.2-1: Real time RT-PCR to detect transcripts of α , β & γ ENaC in different brain areas. Total RNA was isolated from the kidney and different brain areas of Wistar rats. cDNAs were synthesised and subjected to the real-time PCR. 429bp, 220bp and 301bp PCR products were amplified for ENaC α , β & γ subunits respectively by using ENaC specific primers. Kidney served as positive control and the RT reaction with absence of reverse transcriptase served as negative control. 97

Figure 3.2-2: Relative abundance of α , β and γ ENaC mRNA in the kidney, the whole hypothalamus and different brain areas. Total RNA was isolated from the kidney, the whole hypothalamus and different parts of the brain of Wistar rats. cDNAs were synthesized and subjected to real-time quantitative RT-PCR using SYBR Green I. Fig 3.2-2A) Relative abundance of α , β and γ ENaC subunits in kidney. Fig 3.2-2B) Relative abundance of α ENaC in different brain areas. Fig 3.2-2C) Relative abundance of β ENaC in different brain areas. Fig 3.2-2D) Relative abundance of γ ENaC in different brain areas. Data were normalized to endogenous PGK mRNA and represent mean \pm SEM (n=6). 98

Figure 3.2-3: Relative abundance of MR mRNA in the kidney, the whole hypothalamus and different brain areas. Total RNA was isolated from the kidney, the whole hypothalamus and different brain areas of Wistar rats. Relative abundance of MR mRNA was analyzed by real-time quantitative RT-PCR using SYBR Green I. Data were normalized to endogenous PGK mRNA and represent Mean \pm SEM (n=6). 99

Figure 3.2-4: ENaC and MR expression in kidney and colon. Red staining was developed by Nova Red and brown-black with Nickel enhanced DAB. Fig 3.2-4A-C) ENaC α (A, red), β (B, brown-black) and γ (C, red) in renal cortex. Cellular localization is

better shown in the insets. Blue nuclear counterstain with Hematoxylin. There is no staining in the glomeruli. Scale bar – 45 μm Fig 3.2-4 D) MR expression in the renal cortex. Scale bar – 45 μm . Fig 3.2-4E) Omission of the primary antibody abolishes the specific staining. Blue nuclear counterstain with Hematoxylin. Fig 3.2-4 F-H) ENaC α (D, red), β (E, brown-black) and γ (F, red) along the brush border epithelia (arrows) of colon. Blue nuclear counterstain with Hematoxylin. Scale bar – 45 μm . 99

Figure 3.2-5: Colocalization of α and β ENaC with Neu N: double staining with anti- α or - β ENaC and Neu N demonstrates neuronal expression of ENaC. α ENaC (A; red) and Neu N (B; green) in cerebral cortex. C: overlay by exciting both dyes (Texas Red and Alexa Fluor 488) demonstrates double staining (light green to yellow). Scale bar = 37 μm . β ENaC (D; red) and Neu N (E; green) in the amygdala. F: overlay of D and E showing double staining (yellow). Scale bar 37 μm . Arrows in C and F, Neu N- and GFAP-negative cells noted to be α and β ENaC positive. 104

Figure 3.2-6: ENaC and MR staining in different areas in the brain. Red staining was developed by Nova Red and brown-black with Nickel enhanced DAB. Fig 3.2-6A-D) Cerebral cortex showing staining for α (A, red), β (B, brown-black) and γ (C, red) ENaC subunits and MR (D, red). Insets show magnified cells. Note staining along some neuronal processes and the clear nuclear halos. Scale bar – 37 μm . Fig 3.2-6E-H) Pyramidal neurons in the CA subfields of hippocampus showing α (E, brown-black), β (F, brownblack) and γ (G, red) ENaC and MR (H, red). Note some nuclear staining for MR. Scale bar – 37 μm . Fig 3.2-6 I-L) Median preoptic nucleus dorsal part showing α (I, brown-black), β (J, black) and γ (K, red) ENaC and MR (L, red). Scale bar – 37 μm . 105

Figure 3.2-7: ENaC and MR staining in hypothalamic areas. Red staining was developed by Nova Red and brown-black with Nickel enhanced DAB. Fig 3.2 7A-E) Supraoptic nucleus (SON) – omission of the primary antibodies abolished any specific staining (A) whereas inclusion of the specific antibodies shows immunoreactivity to α (B, red), β (C, black) and γ (D, red) ENaC subunits and MR (E, red) in adjacent sections. The staining appears to be on magnocellular cells by morphological criteria. Scale bar – 37 μ m. Fig 3.2 7F-J) The ventral third ventricle (V3V) and adjacent areas. No significant staining is seen in the PeVN and ependyma when the primary antibody is omitted (F). With inclusion of the primary antibody, cells in the periventricular nucleus (PeVN) show staining for α (G, brown-black) and β (H, brown-black) ENaC subunits and MR (J, red) but undetectable staining of γ (I, red) ENaC. The ependyma of the ventral third ventricle is shown in the insets. Scale bar – 37 μ m. Fig 3.2 7K) Double staining for ENaC β and GFAP, most ENaC β positive cells (brown) are GFAP (red) negative. Fig 3.2 7L-O) Paraventricular nucleus (PVN) also shows staining in adjacent sections for α (L, brown-black), β (M, brown-black) and γ (N, brown-black) ENaC and MR (O, red). Note lack of significant staining for γ ENaC and MR in the parvocellular parts. Inset in fig 3.2 7M shows a magnified magnocellular neuron expressing β ENaC. Scale bar - 37 μ m. 106-107

Figure 3.2-8: ENaC and MR in the amygdala, brainstem, CVOs, choroid plexus and blood vessels. Red staining was developed by Nova red and brown-black staining by Nickel enhanced DAB. Fig 3.2 8A-B) ENaC α (A, brown-black) and β (B, brown-black) in medial amygdaloid nucleus. Inset in B shows a magnified neuron. Scale bar – 37 μ m. Fig 3.2 8C-D) Nucleus of tractus solitarius showing β ENaC (C, β ENaC in black, nuclear counterstain in blue) and MR (D, red) staining – note immunopositivity in the large

neurons in the area. Scale bar – 25 μm . Fig 3.2 8E-F) Subfornical organ showing α (E, brown-black) and β (F, red) ENaC staining. Scale bar – 37 μm . Fig 3.2 8G-H) β ENaC (G, brown-black) and MR (H, red) staining in the OVLT. Scale bar – 37 μm . Fig 3.2 8I-L) Immunoreactivity to ENaC α (I, red), β (J, red) and γ (K, brown-black) subunits and MR (L, red) in the choroid plexus and ependyma. Choroidal epithelium is magnified in the insets. Scale bar – 37 μm . Fig 3.2 8M-P) Blood vessels on the ventral surface of the brain showing prominent α (M, red), β (N, brown-black) and γ (O, red) ENaC and MR (P, brown) staining in the endothelia and vascular smooth muscle. Note also staining in the pia-arachnoid membranes. The latter was not due to dye deposition, since it was absent in the negative controls. Scale bar – 37 μm . 108-109

Figure 3.3–1(Next page): Effects of 2 wk of intracerebroventricular (icv) infusion of Na^+ rich artificial cerebrospinal fluid (aCSF) alone or combined with spironolactone (Spir) on α , β , and γ -epithelial Na^+ channel (ENaC) immunostaining (A) and subcellular localization of α ENaC-labeled gold-labeled particles (B) in choroid plexus. Values (means \pm SE, n = 4/group). Insets in A represent percent staining (i.e., fraction of area that was stained).The diamond denotes CSF side. Arrows in B show α -ENaC-gold-labeled particles in apical microvilli of a control rat infused with aCSF and a rat infused with Na^+ -rich aCSF. By 2-way ANOVA, Na^+ -rich aCSF significantly increases β -ENaC immunostaining (F = 16.40, *P < 0.001 vs. aCSF groups). Spironolactone significantly lowers α -ENaC (F = 14.75, aP < 0.005) and β -ENaC (F = 17.41, aP < 0.001) immunostaining, with a significant interaction between spironolactone and Na^+ treatment [F = 5.47, P < 0.05 (for α -ENaC) and F = 6.60, P < 0.05 (for β -ENaC). 137-138

Figure 3.3-2: Effects of 2-week icv infusion of Na⁺-rich aCSF alone or combined with spironolactone (Spir.) on α and β ENaC immunostaining (A) and subcellular localization (B) in the ependyma of the anteroventral third ventricle. Values (means \pm SEM, n= 4/group) in A represent percent staining (fraction of area that was stained). Arrows in B show β ENaC gold-labeled particles in the ependymal basal membrane of an aCSF control rat and a rat infused with Na⁺ rich aCSF. For α ENaC, by two-way ANOVA, Na⁺-rich aCSF significantly increases α ENaC immunostaining (F= 31.73, # p<0.0001 versus aCSF groups) with no effect of spironolactone on α ENaC immunostaining. For β ENaC, Na⁺-rich aCSF significantly increases β ENaC immunostaining (F= 9.84, * p< 0.05 versus aCSF groups). Spironolactone significantly lowered β ENaC immunostaining (F=16.84, ap<0.005. Spir. versus none) with no interaction between spironolactone and Na⁺. 139-140

Figure 3.3-3(previous page): Effects of 2 wk of icv infusion of Na⁺ rich aCSF on α and β ENaC immunostaining and serum/glucocorticoid-inducible kinase 1 (SGK1) protein abundance in the supraoptic nucleus. Values (means \pm SE, n = 4/group) in A represent percent staining (i.e., fraction of area that was stained). Representative Western blots of SGK1 and phosphorylated SGK1 (p-SGK1) are shown in B. Values of SGK1/ β -actin or p-SGK1/ β actin of aCSF group were normalized to 1. 143-144

Figure 3.3-4: Effects of 2 wk of icv infusion of Na⁺ rich aCSF on α and β ENaC immunostaining and SGK1 protein abundance in the paraventricular nucleus. Values (means \pm SE, n = 4/group) in A represent percent staining. Representative Western blots of SGK1 and phosphorylated SGK1 are shown in B. Values of SGK1/ β -actin or p-SGK1/ β -actin of aCSF group were normalized to 1. 145-146

Figure 3.3–5(next page): Effects of icv infusion of aCSF and Na⁺ rich aCSF alone or combined with benzamil (Benz) on CSF and hypothalamic tissue Na⁺ concentration ([Na⁺]). Values are means ± SE (n = 5–7/group). For CSF [Na⁺], by 2-way ANOVA, benzamil significantly increases CSF [Na] [F = 12.13, *P < 0.005 vs. aCSF vehicle (Veh) groups], with no significant difference between 1 and 2 wk of benzamil treatment in control aCSF-treated groups. Na⁺ -rich aCSF significantly increases CSF [Na⁺] (F = 7.65, *P < 0.05 vs. aCSF Veh groups). Benzamil has no significant (F = 3.60, P = 0.07) effect on this increase in CSF [Na⁺]. For hypothalamic tissue [Na⁺], benzamil has a significant effect on tissue [Na⁺] (F = 10.27, *P < 0.005 vs. groups without benzamil), whereas tissue [Na⁺] for different levels of Na⁺ in aCSF did not differ significantly (P = 0.12), and treatment x Na⁺ interaction only showed a tendency (P = 0.08). 147-148

Figure 3.3 S1: ENaC α , β and γ subunit immunostaining in the choroid plexus of rats with out an icv cannula (left panels) and of rats with icv cannula and icv infusion of aCSF (right panel). 149

Figure 3.3 S2: In situ hybridization of ENaC α -subunit in the choroid plexus. Images represent nonradioactive in situ hybridization with specific ENaC α -subunit riboprobes in representative sections of the choroid plexus. Top panel: brain section hybridized using sense riboprobes as negative control. Lower panel: brain section hybridized using antisense riboprobes for localization. Arrows indicate the positive cells with purple staining of the cytoplasm after nuclear counterstaining with methyl-green. 150-151

Figure 3.3 S3: In situ hybridization of ENaC α -subunit in the supraoptic nucleus. Top panel: brain section hybridized using sense riboprobes as negative control. Lower

panel: Antisense riboprobe hybridization for localization. Arrows indicate the positive magnocellular neurons with purple staining of the cytoplasm after nuclear counterstaining with methyl-green. 151

Figure 3.3 S4: Effects of 2-week icv infusion of Na⁺ rich aCSF on α ENaC mRNA staining in the supraoptic nucleus by in situ hybridization. Insets show means \pm SEM for percent staining (%) (fraction of area that was stained). 152

Figure 3.3 S5: Effects of 2-week icv infusion of Na⁺-rich aCSF on α ENaC mRNA staining in the paraventricular nucleus by in situ hybridization. Insets show means \pm SEM for percent staining (%) (fraction of area that was stained). 153

Figure 3.3-6: Schematic outline of location of ENaC in the choroid plexus and ependymal cells and their possible role in Na⁺ transport across the choroid plexus and ependyma in Wistar rats. Under control conditions, ENaC predominates at the apical membrane of the choroid plexus and ependymal cells, presumably leading to net Na⁺ transport into epithelial cells of the choroid plexus or into brain tissue. Consistent with this localization, benzamil increases CSF [Na⁺] but lowers hypothalamic tissue [Na⁺] (top). Infusion of Na⁺ rich aCSF increases ENaC at the apical membrane of the choroid plexus, presumably to increase Na transport from the CSF into epithelial cells of the choroid plexus. ENaC also increases at the basolateral membrane of the ependyma, presumably to allow more Na⁺ out of the brain tissue back into the CSF (bottom).

160-161

Figure 3.4-1: Protein abundance of ENaC subunits in the choroid plexus after 4 weeks on regular or high salt diet. α and β ENaC protein abundance was higher in Dahl S

versus R rats, and this increase persisted on high salt diet. Abundance of 90 and 70 kDa fraction of γ ENaC was also higher in Dahl S on both diets 182

Figure 3.4-2: Immunoreactivity and subcellular distribution of β ENaC in the choroid plexus of Dahl S and R rats. Dahl S shows greater apical immunoreactivity (left panels) and greater abundance of β ENaC in all subcellular compartments (right panels). The higher immunoreactivity and abundance in Dahl S persists on a high salt diet. Insets show mean \pm SEM for cytoplasmic (C) and apical (A) immunoreactivity (n=4-6 rats/group). *p<0.05, Reg vs High salt; #p<0.05, Dahl R vs Dahl S. BM = Basal membrane, V= Ventricle. 183

Figure 3.4-3: Protein abundance of the ENaC subunits in the SON and PVN after 4 weeks on regular versus high salt diet. The arrows show the specific bands that were quantified. Abundance of protein is similar in Dahl R and S rats, and is not affected by a high salt diet. β ENaC protein was not detectable in the SON by Western blot. 186

Figure 3.4-4: Immunoreactivity to β and γ ENaC in the SON of Dahl R and S rats on regular or high salt diet. Immunoreactivity to both β and γ ENaC protein was higher in the SON of Dahl S rats, and remained elevated or further increased with high salt diet. Insets show mean \pm SEM for cytoplasmic (C) and membranous (M) immunoreactivity (n=4-6 rats/group). *p<0.05, Reg vs High salt; #p<0.05, Dahl R vs Dahl S. 187

Figure 3.4-5: Effect of icv infusion of benzamil on CSF [Na⁺] in Dahl R and S rats on regular or high salt diet. On regular salt, icv benzamil increases CSF [Na⁺], somewhat more in Dahl R than Dahl S rats. High salt increases CSF [Na⁺] in Dahl S by \sim 7 mmol/L, but not in R rats. Icv benzamil does not affect CSF [Na⁺] on high salt in either strain.

Values are mean \pm SEM (n=4-10 rats/group). *p<0.05, Reg vs High salt; #p<0.05, Veh vs Benz. 191

Figure 3.5-1: Presence of ENaC subunits in the choroid plexus of Wistar rats on regular salt diet. Fig 1a shows Western blots. The antibodies detected bands at ~80 and 37 kDa for α ENaC, ~85 kDa for β ENaC and ~90 kDa and 70 kDa for γ ENaC. No bands were detected in the presence of the immunizing peptides. Fig 1b shows ENaC immunoreactivity and subcellular localization in the choroid plexus of Wistar rats: Both the microvilli and cytoplasm show strong positive reaction. EM quantification shows 20-40% of subunits on the microvilli and 5-10% on the basolateral membrane. 217

Figure 3.5-2: Effect of drugs on retained ^{22}Na by the choroid plexus of Wistar rats: 1 mM ouabain increased ^{22}Na content by ~40% (n=5-8). 1 nM benzamil did not have a significant effect but higher doses decreased ^{22}Na content in a dose dependent manner (n=8-14). The benzamil induced decrease was not seen in the presence of ouabain (n=7). 1 μM EIPA caused a minimal decrease in ^{22}Na content (n=3). Values are means \pm SEM as percent changes versus control. * p<0.05 vs control. 218

Figure 3.5-3: Immunoreactivity to β and γ ENaC in the choroid plexus of S and R rats on regular or high salt diet for 2 weeks: Immunoreactivity is greater in both the apical membrane and cytoplasm in S than R rats. High salt does not affect immunoreactivity in either strain (n=3-5). Insets show means \pm SEM for % of CP area stained. *p<0.05 S versus R rats. Immuno reactivity to α ENaC was low (see Table 3.5-1) and is not shown. 220

Figure 3.5-4: Effects ouabain and benzamil on ^{22}Na retention in the choroid plexus of Dahl R and S rats on regular or high salt diet. Top panel shows the absolute values, and

the lower panel the absolute and percent changes (in brackets) by ouabain and benzamil. Values are means \pm SEM (n=6-14/group). *p<0.05 Benzamil or ouabain vs aCSF; a : p<0.05 aCSF Dahl S vs Dahl R: b: p<0.05 aCSF Dahl R, regular vs high salt

221

Figure 3.5-5: Effects of ouabain and benzamil on intracellular [Na] ([Na]_i) in the choroid plexus of R and S rats on regular or high salt diet. Top panel shows the absolute values and the lower panel the absolute changes by ouabain and benzamil. Values are means \pm SEM (n=5). *p<0.05 Benzamil vs aCSF or ouabain vs aCSF a p<0.05 Dahl R aCSF, high vs regular salt

222

Figure 3.5-6: Schematic outline of the location of ENaC and Na⁺K⁺ATPase in CP cells and their possible role in Na⁺ transport across the CP in Dahl S and R rats on regular or high-salt diet. Top, CP of Dahl S and R rats on regular salt: (1) enhanced basal Na⁺ influx and apical efflux in S vs R; (2) similar apical Na⁺ efflux by Na⁺K⁺ATPase into CSF in S and R rats; and (3) greater apical ENaC expression and activity (?) in S vs R rats. Bottom, Dahl S and R rats on high salt: (1) enhanced basal Na influx persists in S vs R rats; (2) apical Na⁺K⁺ATPase activity persists in S but decreases in R rats; (3) ENaC expression and activity do not further increase in S rats despite increase in CSF [Na⁺] on high-salt diet; and (4) release of ouabain increases in S vs R rats to inhibit Na-K-ATPase in vivo and to attenuate further increases in CSF [Na⁺].

223-224

Figure 3.5 S1: Evaluation of ²²Na content in the choroid plexus (CP) over time: ²²Na content in CP increases with the duration of incubation and reaches a steady-state by 1 min. 10 nM benzamil decreases ²²Na content in the CP by ~25% suggesting that ENaC

mediate Na influx into the CP. Values are mean \pm SEM (n=7-8/ time point) * p<0.05 at each time point. 225

Figure 3.5 S2: Measurement of intracellular [Na] using Sodium Green fluorescence intensity: Intracellular [Na] increases in choroid cells incubated with Gramicidin according to the [Na] in the aCSF calibrating solutions with varying concentrations of Na. The polynomial equation thus derived was used to calculate [Na]_i. Values are mean \pm SEM (n=4-6/sodium concentration). 226

Figure 3.5 S3: Effect of drugs on Sodium Green fluorescence in the choroid plexus of Wistar rats: 10 nM benzamil decreased fluorescence to background levels. 1 mM ouabain increased fluorescence and offset the benzamil induced decrease. Brightfield images shown in the second and fourth panels demonstrate outline of the cells in the field (n=6). Calculated [Na]_i in mM are shown in the insets. * p<0.05 versus aCSF alone. 227

Figure 3.6-1: Response of CSF [Na⁺] to high salt diet and response of BP to a 5 mmol/L increase in CSF [Na⁺] in Dahl S versus R rats. Left panel: Cerebrospinal fluid (CSF) [Na⁺]_i in Dahl salt-sensitive (S) and salt-resistant (R) rats on high-salt or regular salt intake for 5–7 days. Right panel: Resting mean arterial pressure (MAP) in Dahl S and R rats on regular salt intake after intracerebroventricular infusion of aCSF or Na⁺-rich aCSF for 2 weeks. *P < 0.05, vs. others. a: P < 0.05, vs. Dahl R with intracerebroventricular aCSF (Huang et al. 2001a, Huang et al. 2004). 241

Figure 3.6-2: Outline of putative [Na⁺] transport mechanisms in the central nervous system (CNS) contributing to sympathetic hyperactivity and hypertension in salt-sensitive rats on high-salt intake. In these genetic strains on high-salt intake, Na⁺

transport into cerebrospinal fluid (CSF) is enhanced and $[Na^+]$ in CSF and brain interstitium is increased. For unknown reasons, binding of locally produced mineralocorticoid (MR) (e.g. aldosterone) to MR activates endothelial sodium channels (ENaC) as well as the $Na^+K^+ATPase$ activity in the choroid plexus; ENaC in neurons in (e.g.) the paraventricular (PVN) and supraoptic (SON) nuclei, resulting in an increase in intracellular $[Na^+]$ and $[Ca^{2+}]$; the latter increases neuronal excitability. Both lead to an increase in ouabain-like compound (OLC) release possibly from the SON. OLC inhibits the $Na^+K^+ATPase$ activity in the choroid plexus and prevents a further increase in CSF $[Na^+]$ and activates the renin–angiotensin system. As a result, in spontaneously hypertensive rats and Dahl salt-sensitive rats, high-salt intake increases sympathetic outflow and blood pressure (BP) (Huang et al. 2001a, Huang et al. 2004). 247-248

Figure 4.4–1: Mechanisms in Dahl S rats that may lead to sympathetic hyperactivity and hypertension. High salt decreases ouabain blockable efflux of $[Na^+]$ presumably into CSF in salt resistant strains, but not in Dahl S rats and causes persistent increases in CSF $[Na^+]$. Higher $[Na^+]$ alongwith the greater expression of ENaC in e.g. the magnocellular SON neurons may increase the excitability of these cells and enhance production of mediators such as ‘ouabain’ and vasopressin. The persistence of higher CSF $[Na^+]$ may be responsible for continuous production of ‘ouabain’ in Dahl S and activation of sympathoexcitatory pathways causing hypertension. 275

LIST OF TABLES

- Table 1.2–1: Properties of amiloride-sensitive sodium channels formed by different combinations of ENaC subunits in different tissues (reproduced from Palmer LG, 1992 (Palmer 1992) , Eaton et al (Eaton et al. 2009) and other studies (Garty & Palmer 1997, Palmer 1982, Palmer 1985b, Palmer 1985a, Palmer 1990, Palmer & Andersen 1989, Palmer et al. 1980, Palmer & Frindt 1986, Palmer & Frindt 1988, Palmer & Frindt 1996, Palmer 1992, Eaton et al. 2009, Chen et al. 2002, Jain et al. 1999, Jain et al. 2001) [pS = pico Siemens (1 Siemens = 1 amp/V, 5 pS = 106 ions/sec/channel)] 10
- Table 1.3–1: Common mutations in the genes for ENaC subunits and SGK1 and their association with BP in humans. ICE= ischemic cerebrovascular events, HT = Hypertensive, NT = Normotensive 37
- Table 1.3–2: Components of the $[Na^+]$ transport-regulating gene network – known polymorphisms and expression in response to high salt diet in salt-sensitive rats (Jaitovich & Bertorello , Taub et al. , Sjostrom et al. 2007, Stenstrom et al. 2009, Aoi et al. 2007, Aoi et al. 2006, Aoi et al. 2004, Kakizoe et al. 2009, Umemura et al. 2006, Farjah et al. 2003, Cover et al. 1995, Matsukawa et al. 1993, Huang et al. 2006a, Murrell et al. 2005). MHS = Milan Hypertensive rat; HSD = Hydroxysteroid dehydrogenase, ? = Not confirmed subsequently. 40
- Table 3.2–1: Primer sequences used to detect α , β and γ ENaC and MR mRNA transcript. 91
- Table 3.2–2: Relative abundance of α , β and γ ENaC and MR immunopositive cells in selected brain areas 101

Table 3.3 S1: Primer sequences used for analysis of expression of ENaC subunits, SGK1, Nedd4-L, CYP11B1 and CYP11B2. 126

Table 3.3–1: Relative abundance of ENaC subunits, MR, SGK1, Nedd4L, CYP11B1, and CYP11B2 mRNA in different brain areas after 2-wk of icv infusion of aCSF or Na⁺rich aCSF. 141

Table 3.3–2: Abundance of α , β and γ ENaC in different cellular compartments in the choroid plexus and ependyma after 2-wk of icv infusion of Na⁺ rich aCSF. Values are means \pm SE, expressed as number of gold particles per 100 μ m². Na⁺ = Na⁺-rich aCSF. * 3-fold change in response to Na⁺-rich aCSF infusion. 142

Table 3.3 S2: (Next page) Relative mRNA abundance of ENaC subunits, MR, SGK1, Nedd4L, CYP11B1 and B2 in different brain areas after 2-week icv infusion of aCSF or Na⁺-rich aCSF alone or combined with spironolactone (Spir.) Data for the 2 groups without spironolactone are also shown in table 3.2-1. Values are Mean \pm SEM (n=6/group). By two-way ANOVA, there is a significant effect of Na⁺-rich aCSF on β ENaC mRNA levels (F=5.15, * p<0.05 versus aCSF groups) with no effect of spironolactone on this increase. Whole nuclei were punched from the brain and homogenized for total RNA extraction. BD: below detection. 153-155

Table 3.4-S1: Primer sequences used in qRT-PCR analysis of expression of the ENaC subunits, MR, SGK1 and 11 β HSD2. 176

Table 3.4–1: Effect of high salt diet on expression of ENaC subunits in the choroid plexus of Dahl R and S rats. 181

Table 3.4–2: Subcellular localization of ENaC subunits in the choroid cells of Dahl R and S rats on regular or high salt diet for 12-14 days. 184

Table 3.4–3: Effect of high salt diet on expression of ENaC subunits in the supraoptic nucleus of Dahl R and S rats.	185
Table 3.4–4: Effect of high salt diet on expression of ENaC subunits in the paraventricular nucleus of Dahl R and S rats.	188
Table 3.4–5: Effect of high salt diet on mRNA expression of MR, SGK1 and 11βHSD2 in the choroid plexus, SON and PVN of Dahl R and S rats.	189
Table 3.5–1: Abundance of mRNA and protein and cellular distribution of ENaC subunits in the CP of S and R rats on regular or high salt diet for 2 weeks.	216
Table 3.6–1: Components of the Na ⁺ transport regulating gene network: known polymorphisms and expression in response to high salt diet in salt sensitive rats. NS, not studied or not studied in salt-sensitive rats on high-salt diet; Dahl R, Dahl salt-resistant rats; SIK, salt-inducible kinase; MHS, Milan Hypertensive rat; OLC, ouabain-like compound; BN, Brown Norway rat; ENaC, epithelial sodium channels; Dahl S, Dahl salt-sensitive rats; AVP, arginine vasopressin.	259-261

GENERAL INTRODUCTION

1.1 OVERVIEW

Blood pressure (BP) sensitivity to salt is seen in 40-60% of patients with essential hypertension and in ~20-30% of the general population (Franco & Oparil 2006, Hanneman 1996). The kidneys may act as a sensor and effector organ regulating BP, but studies from our and other groups suggest that the central nervous system acts both as a sensor and as the ultimate determinant of the BP response to salt (Huang et al. 2006a, Leenen et al. 2002, Gomez-Sanchez et al. 1996, Geerling & Loewy 2008, Orlov & Mongin 2007). Analyses of human forms of monogenic hypertension and of common genetic variants in patients with essential hypertension identified the epithelial sodium channel (ENaC) to be associated with salt sensitivity (Grunder et al. 1997, Kreutz et al. 1997, Knight et al. 2006, Tamura et al. 1996, Poch et al. 2000, Iwai et al. 2002, Karet & Lifton 1997, Luft 2004, Iwai et al. 2001, Jones et al. 2010, Rayner et al. 2003, Matsubara et al. 2002, Nkeh et al. 2003, Su et al. 1996). Expression of ENaC is affected by dietary salt, and plays a major role in determining the way the body handles sodium (Na^+) (Stokes & Sigmund 1998, Masilamani et al. 1999, Loffing et al. 2000b, Hager et al. 2001, Greig et al. 2002, Masilamani et al. 2002, Rossier et al. 2002, Karet & Lifton 1997, O'Shaughnessy & Karet 2004). Under physiological conditions, in normotensive rats (Dahl Salt Resistant (R) / Wistar / Sprague-Dawley) there is either no change in expression or decreased expression of ENaC in the kidneys in response to a high salt diet (Aoi et al. 2007, Kakizoe et al. 2009, Farjah et al. 2003, Wolf et al. 2001, Frindt et al. 2008, Loffing et al. 2000a, Loffing et al. 2000b). In contrast, high salt was found to

increase expression of α ENaC in the whole kidneys of Dahl Salt Sensitive (S) rats (Aoi et al. 2004). Intracerebroventricular (icv) infusion of benzamil – a potent blocker of ENaC – prevents the sympathetic hyperactivity and hypertension in Dahl S rats on high salt diet (Gomez-Sanchez & Gomez-Sanchez 1995, Nishimura et al. 1998, Wang & Leenen 2002, Huang & Leenen 2002). At the start of this thesis project, expression of the three ENaC subunits in different parts of the kidneys in Dahl S versus Dahl R rats and the mechanisms responsible for abnormal regulation had not yet been studied. Presence and functions of ENaC in the brain had never been demonstrated. A paradoxical increase in renal abundance of Serum and Glucocorticoid Regulated Kinase 1 (SGK1), one of the regulators of ENaC, was noted in the kidneys of Dahl S versus R rats on high salt diet (Farjah et al. 2003). Whether or not differences in the SGK1 gene contributed to the differential expression of ENaC had not yet been studied.

In the next sections, I will provide a brief overview of ENaC, regulators of ENaC and their role in the regulation of Na^+ homeostasis. Subsequently I will discuss transport of Na^+ into the central nervous system and how Na^+ appears to activate central pathways involved in the regulation of BP.

1.2 THE EPITHELIAL SODIUM CHANNEL (ENaC)

1.2.1 Overview

ENaC is a member of the DEG/ENaC family of cation selective ion channels (Canessa et al. 1994b, Canessa et al. 1995, Canessa et al. 1993a). DEG/ENaC are a large group of Na^+ channels, which includes acid sensing ion channels (ASICs), brain Na^+ channels (BNaC), degenerins (DEG), FMRF amide gated Na^+ channels (FaNaC) and other smaller subfamilies (Kellenberger & Schild 2002). Despite functional heterogeneity between

members of the family, they share some common functional domains for channel activity and pore formation.

1.2.2 Structure

Functional ENaC was thought to be a heteromultimer of the three subunits α , β and γ with a 2:1:1 (Kosari et al. 1998, Firsov et al. 1998) or 3:3:3 stoichiometry (Snyder et al. 1998). Recent studies show a heteromultimeric complex with equal numbers of each type of subunit being involved in channel formation on the membrane (Staruschenko et al. 2005). ENaC subunits are 70-90 kDa glycoproteins composed of 530 to 750 amino acids (Rat: α – 699 aa, β – 638 aa, γ – 650 aa) with 30-35% sequence identity between subunits (Kellenberger & Schild 2002, Alvarez de la Rosa et al. 2000, Barbry & Lazdunski 1996). Topographically (Fig 1) there are two hydrophobic trans-membrane segments (M1 and M2), one large extracellular domain with multiple N-glycosylation sites and cytoplasmic amino (NH₂) and carboxy (COOH) termini in each subunit (Canessa et al. 1994b, Snyder et al. 1994). The large extracellular loop is hydrophilic and contains two highly conserved cysteine rich domains (CRD1 and CRD2) spanning almost 50% of the loop. It is presumed that this domain is involved in maintaining the tertiary structure of the protein, protein-protein interactions and in efficient transport of the assembled subunits to the cell membrane (Firsov et al. 1999, Benos & Stanton 1999). The cytoplasmic NH₂ terminus contains two key regions – one with an endocytotic motif important for channel retrieval from the plasma membrane and a second region just before the M1 domain involved in channel gating (Chalfant et al. 1999, Booth et al. 2003). The cytoplasmic COOH terminus contains a conserved proline rich PPXY (proline-proline-aa-tyrosine) motif which interacts with the WW domain of the ubiquitin protein ligases, Neurally

Expressed Developmentally Downregulated (NEDD4L) and is important for channel endocytosis and degradation (Staub et al. 1996, Staub et al. 1997, Kamynina & Staub 2002). A fourth subunit of ENaC – δ ENaC has subsequently been described in *Homo sapiens*, *Xenopus laevis*, *Mus musculus* and several other species but not *Rattus norvegicus* (rat). δ ENaC shares considerable sequence similarity to α ENaC and may form functional channels in several tissues including brain, pancreas, testes and ovaries (Bangel-Ruland et al. 2010, Brockway et al. 2002, Ji & Benos 2004, Ji et al. 2006). We limited our studies to the better-characterized α , β and γ ENaC that were known to be expressed in rats.

1.2.3 Expression of ENaC in different tissues

ENaC subunits are expressed in several tissues. The epithelia of the kidneys, colon, salivary and sweat gland ducts and lungs had been considered as the predominant site of ENaC expression (Matsushita et al. 1996, McDonald et al. 1995, Canessa et al. 1993a, Canessa et al. 1994a, Canessa et al. 1994b, Duc et al. 1994). Recent studies show a more extensive distribution including blood vessels, peripheral neurons and sensory receptors. The function of the subunits depends on the cell type and ranges from Na^+ transport to mechanotransduction and sensory perception.

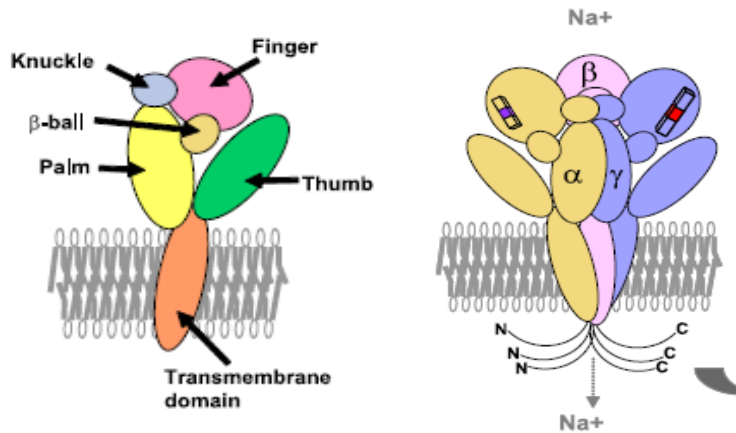


Figure 1.2–1: Cartoons showing the different structural domains of an ENaC subunit (left) and a trimeric $\alpha\beta\gamma$ ENaC in the membrane (right). Both the N- and C- termini are in the cytoplasm. Complete activation of ENaC requires sequential cleavages of the finger domains of α ENaC (purple rectangle) and γ ENaC (red rectangle) by extracellular proteases (Reproduced from Soundararajan et al (Soundararajan et al. 2010)).

1.2.3.1 Renal ENaC

The aldosterone sensitive distal nephron (ASDN), which comprises the late distal convoluted tubule (DCT), connecting tubule (CNT), principal cells of cortical collecting duct (CCD), outer medullary collecting duct (OMCD) and inner medullary collecting duct (IMCD) is the major site of ENaC expression in the kidneys (Duc et al. 1994, Hager et al. 2001, Loffing et al. 2000a, Loffing et al. 2000b, Loffing et al. 2001b, Ergonul et al. 2006, Frindt et al. 2007, Frindt et al. 2008, Palmer & Frindt 1986). ENaC in the renal tubules contributes to the reabsorption of filtered Na^+ from the lumen. Under physiological conditions and on regular salt diet, ENaC expression is relatively low in the IMCD (Duc et al. 1994, Hager et al. 2001). As will be discussed later (1.2.5 and 1.3.3),

the pattern of expression of the different subunits and their cellular localization changes with a variety of factors, most importantly salt intake.

1.2.3.2 ENaC in other Na⁺ absorbing epithelia

ENaC is also abundant in other Na⁺-transporting epithelia, such as those in the colon, lungs, salivary glands and sweat glands (Duc et al. 1994, Stokes & Sigmund 1998, McDonald et al. 1995, Amasheh et al. 2000, Reddy & Quinton 2003). In surface enterocytes of the distal colon α ENaC is constitutively present, but all three subunits are present only in the salt depleted state when aldosterone levels are elevated (Stokes & Sigmund 1998). All three subunits are highly expressed in small and medium sized distal airways of the lungs (Burch et al. 1995, Farman et al. 1997, Matalon et al. 2002, Swezey et al. 1998). In lung alveoli, ENaC subunits form two types of channels, highly selective channels composed of all three subunits and nonselective channels composed of α ENaC alone (Chen et al. 2002, Eaton et al. 2004, Eaton et al. 2009, Jain et al. 1999, Jain et al. 2001, Jain & Eaton 2006, Johnson et al. 2006). Both types are found with equal abundance and contribute to alveolar fluid clearance and maintenance of alveolar surface liquid (Jain & Eaton 2006, Eaton et al. 2009). ENaC subunits in the cochlear epithelium contribute to the maintenance of low [Na⁺] in the endolymph (Couloigner et al. 2001, Grunder et al. 2001). Functional studies also suggest the presence of ENaC in the ciliary epithelium in the eye where it contributes to formation of aqueous humor (Civan et al. 1997, Mirshahi et al. 2000, Mirshahi et al. 2001, Mirshahi et al. 1999, Mongin & Orlov 2001, Dyka et al. 2005).

1.2.3.3 ENaC in vasculature

Electrophysiological and uptake studies had suggested the existence of an amiloride sensitive Na⁺ transport mechanism in brain capillaries and cultured endothelial cells from brain microvessels (Vigne et al. 1989, Betz 1983, Betz & Goldstein 1986). But expression in the brain vasculature had not been studied. Recently all three subunits were found to be expressed in rat cerebral arteries, freshly dissociated vascular smooth muscle cells from cerebral (Drummond 2009, Drummond et al. 2004, Jernigan & Drummond 2005, Jernigan & Drummond 2006, Jernigan et al. 2008, Jernigan et al. 2009, Guan et al. 2009, Kusche-Vihrog et al. 2008) and mesenteric arteries (Jernigan et al. 2008) and in vascular endothelium (Kusche-Vihrog et al. 2010, Kusche-Vihrog et al. 2008). Interestingly, only β and γ ENaC were found to be expressed in renal interlobar arteries (Grifoni et al. , Drummond 2009, VanLandingham et al. 2009, Jernigan et al. 2009, Jernigan & Drummond 2006, Jernigan & Drummond 2005). While some studies suggest that ENaC in the vasculature may be involved in mechanosensation, myogenic constriction and regulation of blood flow (Drummond 2009, Drummond et al. 2004, Drummond et al. 2008a, Drummond et al. 2008b, Jernigan & Drummond 2005, Jernigan & Drummond 2006, Jernigan et al. 2008, Jernigan et al. 2009), concern remains regarding specificity of the blockade due to the high doses of the blockers used (Loutzenhiser & Aaronson 2010, Guan et al. 2009).

1.2.3.4 ENaC in the peripheral nervous system

ENaC subunits are expressed in a number of sensory end organs. The role of ENaC subunits in sensory functions has been shown in a number of *in vitro* models and cell types (Awayda et al. 1995, Awayda & Subramanyam 1998, Benos 2004, Berdiev & Benos 2006, Brockway et al. 2005, Ismailov et al. 1997, Ji et al. 2006, Kapoor et al.

2009, Ross et al. 2007, Althaus et al. 2007, Morimoto et al. 2006, Satlin et al. 2001, Satlin et al. 2006, Kizer et al. 1997, Fronius et al. 2010, Fronius & Clauss 2008). *In vivo*, there is a tissue and cell type specific differential expression of individual subunits that suggests specific roles in each cell type. Only β and γ ENaC are found in Merkel cell neurite complexes, Meissner-like corpuscles and small lamellated corpuscles of skin (Drummond et al. 2000). All three subunits are present in anterior taste buds and lingual epithelium but predominantly α ENaC is found in the posterior vallate papillae of the tongue (Kretz et al. 1999, Lindemann et al. 1998, Lin et al. 1999). The spiral ligament of cochlea expresses all three subunits, while only α and γ ENaC are found in the spiral ganglion (Couloigner et al. 2001). In the retina α ENaC is expressed in photoreceptors and bipolar cells (Golestaneh et al. 2001, Golestaneh et al. 2000, Golestaneh et al. 2002, Mirshahi et al. 1999), both α and β ENaC are found in Muller, amacrine and ganglion cells (Brockway et al. 2002), but γ ENaC expression is detectable only under conditions of increased intraocular pressure (Dyka et al. 2005). β and γ but not α ENaC are expressed in the neurons of the dorsal root, trigeminal and nodose ganglion as well as the carotid baroreceptors (Drummond et al. 1998, Drummond et al. 2001, Fricke et al. 2000, Drummond et al. 2004, Drummond et al. 2008a, Drummond et al. 2008b).

1.2.3.5 ENaC in the central nervous system

Functional studies showed the existence of an amiloride blockable transport mechanism in the choroid plexus which was thought to be mediated by the sodium hydrogen exchanger (Murphy & Johanson 1989b). In early studies evaluating expression of ENaC subunits in different tissues, mRNA of ENaC subunits was not detectable in whole brain extracts by northern blot analyses (Canessa et al. 1993a, Canessa et al. 1994b).

Expression of ENaC subunits in brain had not been further studied. However, functional studies, as described later (1.3.4), suggested the presence of ENaC in the brain.

1.2.4 Transport of Na⁺ through ENaC

ENaC is a voltage-insensitive Na⁺ channel that is highly selective for ions such as Li⁺ and Na⁺. Transport of Na⁺ through ENaC is passive in that it is dependent on the gradient of [Na⁺] across the membrane. In polarized transporting epithelia, such as the CCD, transport of Na⁺ by ENaC depends on the electrochemical gradient created by basolateral Na⁺K⁺ATPase (DeLong & Civan 1984, Palmer et al. 1980, Rubera et al. 2003, Bens et al. 1999). Studies in homologous and heterologous expression systems such as *Xenopus* oocytes, A6 cells or CHO cells, show that all three subunits are necessary for maximal channel function, and when all three subunits are expressed a heteromultimeric conformation is favored over homomeric channels (Palmer et al. 1990, Baxendale-Cox & Duncan 1999, Eaton et al. 2001, Blazer-Yost et al. 2001, Spindler et al. 1997, Staruschenko et al. 2005). However, expression of individual subunits alone or in differing combinations can still create different levels of activity, as summarized in Table 1.2-1 (Firsov et al. 1996, Canessa et al. 1994a, Bonny et al. 1999, Firsov et al. 1998, Palmer et al. 1990). In the CCD for example, over-expression of γ ENaC is sufficient to increase Na⁺ transport (Volk et al. 2005). In most epithelia where all three subunits are expressed, the predominant channels are of highly- or moderately- selective type, while in the sensory organs variable combinations of two or three subunits are seen. Recent studies suggest that newly formed, inserted or activated channels appear to have lower selectivity and are later converted to the more highly selective channels by post-translational modifications. This selectivity filter in ENaC is formed by a stretch of three

conserved amino acid sequence motifs (G/S-aa-S) at the initial segment of the second hydrophobic domain of each subunit (Figure 1) (Kellenberger et al. 1999, Kellenberger et al. 2001). This region interacts with and removes the water of hydration of small monovalent cations, shrinking the size of the ions and enabling passage through the pore. Post-translational modifications alter the structure of the pore and are thus able to convert moderately selective channels to highly selective ones (Palmer 1990, Palmer 1992, Palmer & Frindt 1996, Sariban-Sohraby et al. 1984).

Table 1.2–1: Properties of amiloride-sensitive sodium channels formed by different combinations of ENaC subunits in different tissues (reproduced from Palmer LG, 1992 (Palmer 1992) , Eaton et al (Eaton et al. 2009) and other studies (Garty & Palmer 1997, Palmer 1982, Palmer 1985b, Palmer 1985a, Palmer 1990, Palmer & Andersen 1989, Palmer et al. 1980, Palmer & Frindt 1986, Palmer & Frindt 1988, Palmer & Frindt 1996, Palmer 1992, Eaton et al. 2009, Chen et al. 2002, Jain et al. 1999, Jain et al. 2001) [pS = pico Siemens (1 Siemens = 1 amp/V, 5 pS = 106 ions/sec/channel)]

<i>Channel property</i>	Channel type		
	Highly-Selective Channels	Moderately-Selective Channel	Non-Selective Channel
<i>Na⁺/K⁺ selectivity (P_{Na}/P_K)</i>	>10	3-4	1
<i>Single channel conductance (pS)</i>	4-6	7-15	20-28
<i>Mean open time / Mean closed time (T_{open}/T_{closed}) (sec)</i>	Slow channels 2-3/3-4	Faster channels 0.03-0.04/0.03-0.1	Faster channels 0.04/0.05
<i>K_i for Amiloride (μM)</i>	0.1-0.5	0.1-0.5	1800
<i>Known regulatory mechanisms</i>	Aldosterone, ADH	G proteins, proteases	ANP

<i>Channel property</i>	Channel type		
	Highly-Selective Channels	Moderately-Selective Channel	Non-Selective Channel
<i>Time line of activation</i>	Hours to days	Minutes	---
<i>Composition</i>	Active $\alpha\beta\gamma$ ENaC	Nascent $\alpha\beta\gamma$ ENaC	α , β or γ ENaC alone, $\beta\gamma$ ENaC
<i>Sites of expression and models studied</i>	CCD, colon, skin, alveolus, <i>Xenopus</i> , A6	Bladder, kidney A6	Smooth muscle, vascular endothelial cell <i>Xenopus</i>

1.2.5 Regulation of ENaC

A number of different hormones, chemical mediators and neural activity affect ENaC expression and function, which depends on the tissue type, the subunits expressed and the mediators involved. The effect on function e.g. net transport of Na^+ depends on the abundance at the surface membrane and open probability (P_o) of individual channels. These mechanisms are linked by events such as regulation of trafficking, endocytosis and recycling of the channels. When studied *in vitro* individual regulators have distinct effects on expression and net transport of Na^+ , but *in vivo* the result depends on a delicate interplay of all the different regulators and mechanisms involved, and is often difficult to ascribe to a particular variable (Farman et al. 1997, Escoubet et al. 1997, Asher et al. 1996, Reif et al. 1986, Renard et al. 1995).

I will first discuss the major cellular mechanisms that regulate transcription and translation of ENaC subunits, their trafficking, membrane expression and ultimately P_o . Next I will discuss the effects of major hormonal regulators on ENaC expression in

different tissues. Considering their importance in ENaC regulation, special emphasis will be placed on aldosterone and SGK1.

1.2.5.1 Cellular mechanisms of ENaC regulation

1.2.5.1.1 **Regulation of transcription**

Transcriptional regulation controls tissue specific expression of the ENaC subunits and long-term effects of hormones on Na⁺ transport. Factors that regulate gene expression such as chromatin remodelling, histone modification, DNA methylation, RNA-associated gene silencing or chromosomal inactivation and imprinting are only recently being elucidated for the ENaC genes (Rat: α ENaC - Scnn1a on 4q42; β ENaC - Scnn1b on 1q36-q41; γ ENaC - Scnn1g on 1q36-q41; Human: α ENaC - Scnn1a on 12p13; β ENaC - Scnn1b on 16p12.2-p12.1; γ ENaC - Scnn1g on 16p12) and their regulators such as SGK1 (Rat – 1p12; Human – 6q23). Hormones regulate ENaC transcription both directly by binding of transcriptional activators, repressors and epigenetic mechanisms and indirectly by regulation of other factors. As an example, in the kidneys under basal conditions, α ENaC expression is inhibited by a Disruptor Of Telomeric silencing alternative splice variant a (Dot1a) and ALL1-fused gene from chromosome 9 (Af9) repressor complex that regulates targeted histone H3 Lys-79 methylation of the chromatin associated with the α ENaC promoter (Reisenauer et al. 2009, Zhang et al. 2007, Zhang et al. 2006, Zhang et al. 2009, Vogel & Gruss 2009, Nakamura et al. 2007, Kone et al. 2007), while, excess β and γ ENaC are ubiquitinated and targeted for degradation in the proteasome (Staub et al. 1997, Valentijn et al. 1998). Direct transcriptional regulation by aldosterone and vasopressin is mediated by specific consensus motifs in the promoter regions of all three ENaC subunits which bind homo- or heterodimers of the mineralocorticoid receptor

(MR) and/or glucocorticoids receptor (GR) for aldosterone and cAMP response element binding protein (CREB) for vasopressin (Canessa et al. 1993a, Canessa et al. 1994a, Canessa et al. 1994b, Djelidi et al. 1997, Eaton et al. 2001, Ecelbarger et al. 2000, Ecelbarger et al. 2001, Escoubet et al. 1996, Farman et al. 1997, Loffing et al. 2006, Shigaev et al. 2000, Snyder et al. 2004a, Wang et al. 2001, Fuller et al. 2000). Aldosterone inhibits Dot1a and Af9 expression and phosphorylates Af9 through SGK1, thus increasing α ENaC gene expression (Zhang et al. 2007, Zhang et al. 2006, Zhang et al. 2009, Reisenauer et al. 2009) in the kidney.

1.2.5.1.2 Regulation of translation

Efficient translation of ENaC mRNAs depends on their stability in the tissue and is regulated by specific RNA-binding proteins (RBP) that interact with *cis*-elements in the 5' and 3' untranslated regions (UTR) of the transcripts (Otulakowski et al. 1999, Wilkie et al. 2003, McCarthy 1998, Pesole et al. 2000, Pesole et al. 2001, Shi et al. 2009). The mRNA may also reside in a translational inactive state in post-polysomal messenger ribonucleoprotein (mRNP) complexes. In the lungs, α ENaC mRNA is much more abundant than β and γ ENaC although protein abundance is similar, suggesting that translational efficiency is much higher for β and γ ENaC (Otulakowski et al. 2006, Otulakowski et al. 2004, Banasikowska et al. 2004). The α ENaC mRNA contains a long GC rich 5' UTR of 550/750 (rat/human) nucleotides while that of γ ENaC contains a long AU-rich element (Otulakowski et al. 2001, Perlewitz et al. 2010). Alternative splicing of α ENaC mRNA leads to various lengths of α ENaC transcripts. Translation of mRNAs with such long GC-rich 5'UTRs is sensitive to the amount of translation initiation factor eIF4F and the mRNA 5'-cap binding complex (McCarthy 1998, Pesole et al. 2000, Pesole

et al. 2001, Shi et al. 2009). O₂ and dexamethasone increase α ENaC translation in the lungs at birth, by affecting the 5'-cap binding complex through increased phosphorylation of eIF4F by mTOR kinases (Otulakowski et al. 2007). In mouse CCDs under basal conditions, 40% of γ ENaC mRNA is stored in translational inactive mRNP pools, while most of α and β ENaC are translated by polyribosomal complexes (Perlewitz et al. 2010). Aldosterone and vasopressin promote γ ENaC translation by affecting the interaction of the AU-rich element with AU-rich element binding proteins such as HuR, AUF1 and TTP (Perlewitz et al. 2010).

1.2.5.1.3 Regulation of subunit maturation and trafficking

Nascent ENaC is transported from the endoplasmic reticulum in an inactive form to the Golgi complex where it undergoes post-translational modifications before being trafficked to the cell surface (Butterworth et al. 2009). ENaC processing is tissue dependent and generally inefficient. Studies in Chinese hamster ovary and Madin-Darby canine kidney type 1 epithelial cells showed that when expressed alone the molecular weight of ENaC subunits are: α ENaC – 95 kDa, β ENaC – 96 kDa and γ ENaC – 93 kDa. When $\alpha\beta\gamma$ ENaC are expressed together Na⁺ transport is highest and at this point a second band is seen for each subunit (65 kDa for α ENaC, 110 kDa for β ENaC and 75 kDa for γ ENaC) (Hughey et al. 2003)(Fig 1.2-2 and 1.2-3). In the rat kidney, activation by aldosterone and salt depletion also involves cleavage of full-length 85kDa α ENaC to 50 (active) and 35 kDa fractions, glycosylation of β ENaC and cleavage of full-length 90 kDa γ ENaC to 70 (active) and 20 kDa fractions (Ergonul et al. 2006, Frindt et al. 2007, Frindt et al. 2008, Hughey et al. 2004a, Hughey et al. 2007, Masilamani et al. 1999). Much of the intracellular processing by proteolysis is carried out by convertase type proteases such

as furin (Gaillard et al. 2010, Harris et al. 2008, Hughey et al. 2004a, Sheng et al. 2006, Carattino et al. 2006, Bruns et al. 2007, Hughey et al. 2007, Carattino et al. 2008). Only a small fraction (~1% in *Xenopus* oocytes, ~20% in A6 cells) of synthesized subunits make it to the cell surface (Valentijn et al. 1998, Weisz et al. 2000). The cellular pool of synthesized ENaC has a half life of ~40-120 minutes in cultured cells (May et al. 1997, Staub et al. 1997, Weisz & Johnson 2003) and somewhat longer (~3.5-4 hrs) in *Xenopus* oocytes (Valentijn et al. 1998). The transfer process is blockable by inhibitors of trafficking (Myerburg et al. , Butterworth et al. 2009) and is most efficient when an $\alpha\beta\gamma$ ENaC complex is formed (Asher et al. 1996, Escoubet et al. 1997, Ono et al. 1997, Stokes & Sigmund 1998, Butterworth et al. 2009). Much of the unassembled and some of the assembled $\alpha\beta\gamma$ ENaC is ubiquitinated and degraded by the proteasome (Rotin et al. 2001). Increases in cAMP in response to e.g. vasopressin promotes exocytosis of newly synthesized (Snyder 2000, Snyder 2002, Snyder 2005) and recycling (Butterworth et al. 2005) channels to the cell surface. SNARE (soluble N-ethylmaleimide sensitive factor attachment receptor) proteins such as syntaxin 1A are involved in targeting of ENaC towards the apical membrane (Peters et al. 2001, Qi et al. 1999).

1.2.5.1.4 **Regulation of channel open probability (P_o)**

Two pools of ENaC can be found on the cell surface – active channels that have already undergone proteolytic cleavage and silent channels that have – by yet unknown mechanisms – bypassed the cleavage steps and were directly inserted into the membrane (Palmer 1992) (Fig 1.2-3). Thus the P_o of ENaC at the cell surface is variable. It is affected by a number of mechanisms including activity of second messengers such as cAMP (Knowles et al. 1983, Boucher et al. 1986, Hallows et al. 2009, Stutts et al. 1997,

Butterworth et al. 2005, Yang et al. 2006, Turnheim 1991) , Ca^{2+} (Morimoto et al. 2006, Jernigan & Drummond 2005, Loffing et al. 2001a, Ismailov et al. 1997, Yu et al. 2007, Yu et al. 2008, Turnheim 1991) ; intra- and extracellular concentrations of ions e.g. Na^+ , Cl^- , H^+ and K^+ (Turnheim 1991, Turnheim et al. 1977, Collier & Snyder 2010, Collier & Snyder 2009a, Collier & Snyder 2009b, Bize & Horisberger 2007, Yu et al. 2007, Yu et al. 2008); interaction with other channels such as CFTR (cystic fibrosis transmembrane regulator) (Reddy et al. 1999, Reddy & Quinton 2003, Reddy & Quinton 2005) and membrane tension (Morimoto et al. 2006, Jernigan & Drummond 2005, Kizer et al. 1997, Ismailov et al. 1997, Satlin et al. 2001, Awayda et al. 1995, Awayda & Subramanyam 1998, Carattino et al. 2007).

Proteolytic activity has by far the greatest effect (Gaillard et al. 2010, Hughey et al. 2007) with three classes of proteases that can affect P_o of ENaC – a) intracellular convertase type proteases e.g. furin (**1.2.5.1.3**); b) extracellular cell-attached proteases e.g. CAP1 (Vallet et al. 1997, Vuagniaux et al. 2002) and c) soluble extracellular proteases e.g. trypsin and neutrophil elastase (Caldwell et al. 2005, Guipponi et al. 2002). The activity of the proteases in turn is affected by factors that change the cellular microenvironment such as composition and flow of surface liquids. As an example, cleavage of specific sites in the extracellular domains of α and γ ENaC by furin, converts inactive ($P_o = 0.02$ s) channels to active ($P_o = 0.6$ to 0.7 s) ones (Caldwell et al. 2004). Another class of proteases such as the short palate lung and nasal epithelial clone 1 (SPLUNC1) was

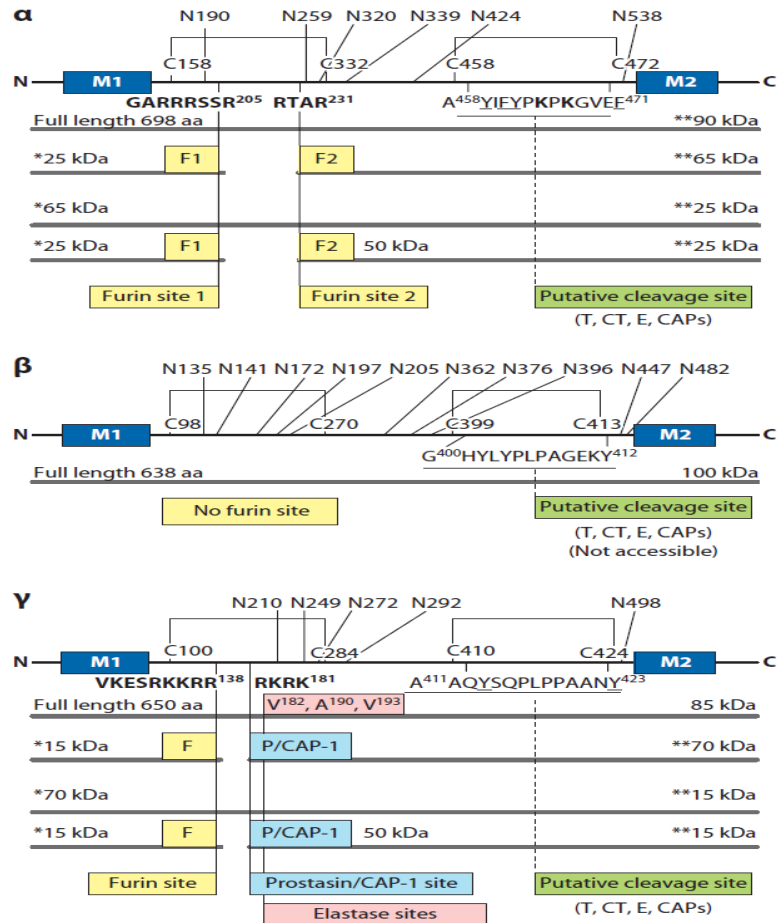


Figure 1.2–2: Linear model for cleavage of ENaC subunits. Each subunit has two transmembrane domains, short N and C termini and a large extracellular loop with 5-12 N-glycosylation sites. Cleavage sites are shown in yellow and putative sites for trypsin (T), chymotrypsin (CT), elastase (E) or serine proteases (SP) are in green. Depending on cleavage site α ENaC fragments can have molecular weights of 90, 65-70 (active), 50 and 25-37 kDa. β ENaC is not cleaved by furin but maybe cleaved by other proteases and has N-glycosylation sites that can increase its molecular weight from 85 to 100 kDa. γ ENaC has one furin cleavage site as well as cleavage sites for proteases such as CAP, prostatic and elastase generating fragments with molecular weights of 85, 70 (active), 50 and 15 kDa. Reproduced from Rossier and Stutts, 2009 (Rossier & Stutts 2009)

recently found that prevent proteolysis of ENaC but decrease ENaC mediated current in *Xenopus* oocytes and cultured alveolar epithelial cells (Garcia-Caballero et al. 2009). SPLUNC1 which is secreted from some epithelial cells in an autocrine / paracrine fashion appears to bind to ENaC, prevents it from being cleaved (Garcia-Caballero et al. 2009) and may also reduce the number of ENaC that are inserted into the membrane (Rollins et al. 2010).

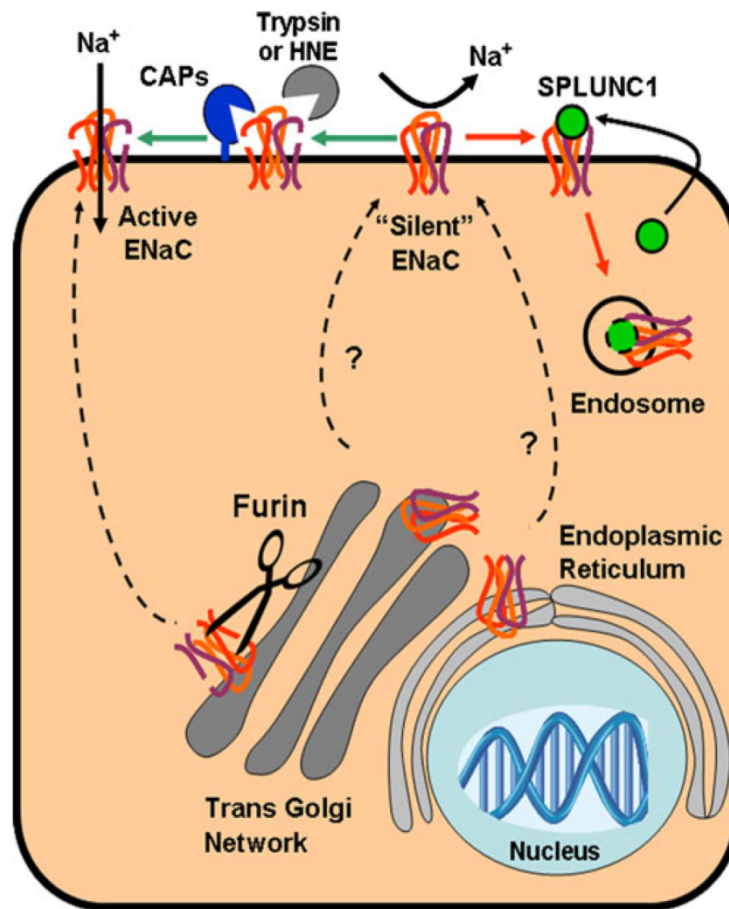


Figure 1.2–3: Regulation of trafficking and activation of ENaC by proteases. Uncleaved ENaCs can be cleaved in the trans-Golgi network by furin. These cleaved ENaCs are then transported to the plasma membrane in a highly regulated fashion where they can

transport Na⁺. A pool of nascent ENaC can bypass the cleavage step and be directly inserted into the plasma membrane as 'silent' channels. These silent channels can then be cleaved by cell-attached, extracellular or soluble proteases. Alternatively, silent ENaC may bind to SPLUNC1-, and be targeted for internalization. Reproduced from Gaillard et al (Gaillard et al. 2010).

1.2.5.1.5 **Regulation of membrane abundance and degradation**

Mature ENaC at the cell surface is an unstable protein with a half-life of about 1-3 hours (Butterworth et al. 2009, Hanwell et al. 2002, Rotin et al. 2001, Yu et al. 2008). Cell surface expression of ENaC subunits requires a conserved PPPXYXXL sequence (P= Proline, X = unknown amino acid, Y = Tyrosine, L = lysine) in the C-terminal sequence of the proteins (Snyder et al. 1995, Schild et al. 1996). The endocytosis motifs – NPXY and YXXΦ in this sequence mediate ENaC endocytosis (Snyder et al. 1995, Shimkets et al. 1997). The PY motif interacts and binds with the WW-domain in NEDD4 family of E3 ubiquitin-ligases (Staub et al. 1996, Harvey et al. 2001, Harvey et al. 1999, McDonald et al. 2002, Snyder et al. 2001, Asher et al. 2001, Asher et al. 2003), most importantly NEDD4-2 (Snyder et al. 2004b). NEDD4-2 mediated ubiquitylation of ENaC subunits changes their conformation affecting accessibility to other proteases (Ruffieux-Daidie & Staub 2011) and destines them for endocytosis (Hicke 1997, Hicke 2001) and lysosomal degradation (Goulet et al. 1998). Nedd4-2 induced binding of hepatocyte growth factor-regulated tyrosine kinase substrate (Hrs), a component of the endosomal sorting complexes has recently been shown to be involved in sorting of ENaC vesicles to the lysosome versus a recycling pool (Zhou et al. 2010). Many hormones regulate ENaC mediated Na⁺ transport by converging on NEDD4-2, through SGK1 and protein kinase A

(PKA). Both SGK1 and PKA phosphorylate NEDD4-2 at three Ser/Thr residues (Ser-221, Thr-246 and Ser-327) and through 14-3-3 interacting proteins (Lee et al. 2008, Liang et al. 2008, Liang et al. 2006, Wiemuth et al. 2010) prevent its binding to ENaC (Snyder et al. 2004a, Snyder et al. 2002, Debonneville et al. 2001). Among other regulators arachidonic acid analogs (Carattino et al. 2003), AMP activated kinase (Carattino et al. 2005) and protein kinase C (Booth & Stockand 2003) also decrease surface expression of ENaC, while phosphatidyl inositol 4,5 bis-phosphate (Staruschenko et al. 2004) and I κ B kinase- β (Lebowitz et al. 2004) increase surface expression. Functional blockade of the channel with for example amiloride also has recently been shown to cause rapid disappearance of the channels from the cell surface and from intracellular pools, indicating either rapid degradation and/or membrane pinch-off (Kusche-Vihrog et al. 2008).

1.2.5.2 Hormonal regulators of ENaC

Hormones regulating the body's Na⁺ homeostasis and fluid balance are the most important extrinsic regulators of ENaC expression and function. Among these I will briefly discuss the more important ones and their effects on ENaC mediated regulation of Na⁺ transport. The effect of sympathetic activity will also be discussed as it affects Na⁺ reabsorption directly and by modulation of arterial blood flow. Fig 1.2-4 shows a brief overview of how the different mechanisms are integrated together.

1.2.5.2.1 **Aldosterone**

The steroid hormone aldosterone, synthesized principally in the zona glomerulosa of the adrenal cortex, is the final endocrine signal in the renin-angiotensin-aldosterone (RAS) system. Aldosterone secretion and physiological actions are under feedback control by

serum K^+ , ACTH and angiotensin II (Aguilera et al. 1996, Condon et al. 2002, Ye et al. 2003). Aldosterone regulates ENaC by both non-genomic and genomic mechanisms. The effects are tissue specific. For example, aldosterone increases expression of α but not β and γ ENaC in rat kidney (Masilamani et al. 1999, Masilamani et al. 2002, Escoubet et al. 1997), while in the colon aldosterone increases β and γ ENaC but not α ENaC (Escoubet et al. 1997, Fuller et al. 2000). In most epithelia, aldosterone increases net Na^+ transport in two phases – a) an early phase taking place within 0.5 – 3 hours when Na^+ transport increases by 2-3 fold; and b) a late phase starting after ~3 hours and characterized by a progressive, larger (~20 fold after 24 hours) increase in Na^+ transport that wanes in the next few days (Alvarez de la Rosa et al. 2000). In the early phase, aldosterone increases P_o and decreases internalization of channels already at the surface. In the late phase there is further increase in Na^+ transport due to both increased abundance of ENaC subunits and increased abundance of regulators.

Genomic effects: The genomic actions of aldosterone are mediated by its binding to the high-affinity mineralocorticoid receptor (MR) and to a lesser extent the lower affinity glucocorticoid receptor (GR). Aldosterone binding to MR or GR induces dimerization of the receptors and translocation to the nucleus where they modulate the expression of two major classes of genes – aldosterone induced transcripts (AIT) and aldosterone repressed transcripts (ART), by binding to steroid response elements in the promoter regions of the target genes (Fig 2). One of the important AITs that increase in both the early and late phase of aldosterone action is SGK1 (Fig 1.2-6). Some AITs such as activators of MAPK, act to limit the extent of aldosterone action (Verrey 1995, Stockand et al. 1999, Stockand 2002, Pearce & Kleyman 2007, Pearce 2001, Naray-Fejes-Toth et al. 1999,

Bhargava et al. 2001). ARTs such as Dot1a, Af9 are involved in tissue specific regulation of ENaC expression and may also have a role in limiting the duration of Na⁺ transport by providing feedback regulation (Robert-Nicoud et al. 2001, Reisenauer et al. 2009, Zhang et al. 2009, Zhang et al. 2006, Zhang et al. 2007).

Non-genomic effects: Exposure of rabbit CCDs to 100 nM aldosterone increases ENaC mediated Na⁺ transport within 1-2 minutes. The effect is not prevented by spironolactone (Zhou & Buben 2001). These rapid actions of aldosterone on ENaC are independent of translation and transcription and are thought to be mediated by a membrane associated, non-classical aldosterone receptor (Figure 1.2-4) acting through the PKC pathway (Kusche-Vihrog et al. 2010, Zhou & Buben 2001). Activation of other signaling mechanisms such as angiotensin II and epidermal growth factor receptor signaling pathways may also be responsible for these non-genomic effects (Grossmann & Gekle 2009, Mihailidou 2006).

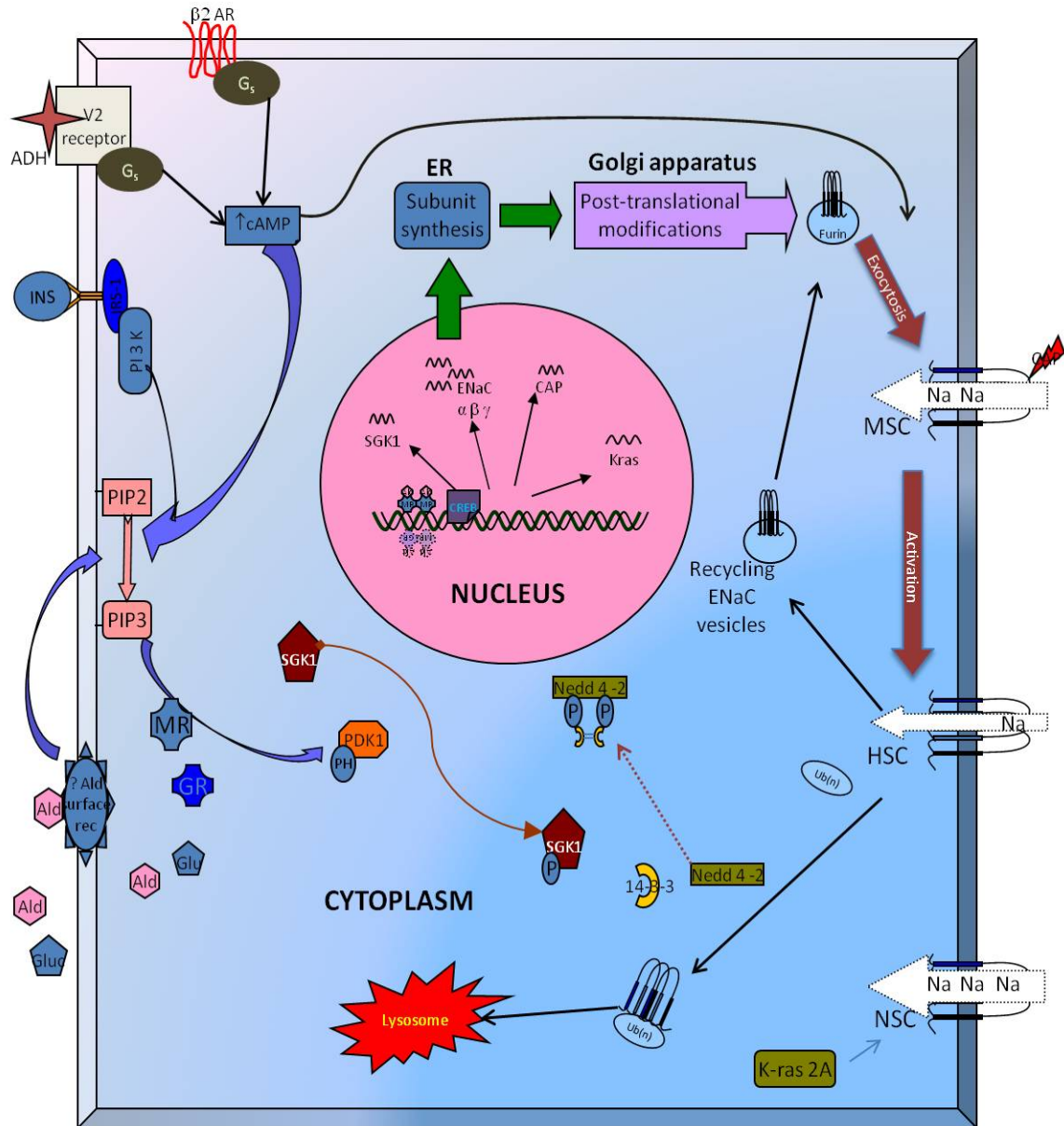


Figure 1.2–4: Concerted regulation of ENaC by hormones. Aldosterone (Ald) and glucocorticoids (Glu) acting through the mineralocorticoid receptor (MR) and glucocorticoid receptor (GR) and vasopressin acting through increases in cAMP and CREB increase transcription of ENaC subunits both directly and through regulators such as SGK1. Nascent ENaC subunits undergo assembly, cleavage and activation, partially in the ER-Golgi complex and partly on the cell surface by extracellular proteases.

Aldosterone, vasopressin, insulin and β 2adrenergic activity (β 2AR) also activate the PI3K pathway that activates SGK1 by phosphorylation. Activated SGK1 phosphorylates Nedd4-2, and acting through interacting 14-3-3 proteins decreases ubiquitination and degradation of ENaC. Author's own reproduction.

1.2.5.2.2 **Corticosteroids**

Corticosteroids act through similar genomic and non-genomic mechanisms by short- and long- term processes as aldosterone, but produce distinct, tissue-dependent effects on ENaC expression and activity. Since the circulating levels of aldosterone are 100-1000 times lower than those of corticosteroids, the effects are most prominent in tissues where the enzyme 11- β hydroxysteroid dehydrogenase that converts active glucocorticoids to their inactive keto metabolites (Albiston et al. 1994, Stewart et al. 1994, Zhou et al. 1995, Bertram et al. 2001, Gardner et al. 1997, Moisan et al. 1992, Robson et al. 1998, Wan et al. 2002), and thereby confers selective binding of aldosterone to steroid receptors is not expressed. In classic aldosterone sensitive epithelia of kidney and distal colon, glucocorticoids synergize the effects of aldosterone and assume a significant role in conditions such as stress (Schulz-Baldes et al. 2001, Fuller et al. 2000). Corticosteroid regulation is especially important in the lungs for preferentially increasing the number of highly selective channels at the expense of non selective channels to clear alveolar surface fluid (Thome et al. 2003, Bonvalet 1998, Eaton et al. 2004, Eaton et al. 2001) and in the semicircular canal ducts to control cationic composition of the inner ear (Pondugula et al. 2004, Pondugula et al. 2006, Kim et al. 2009).

1.2.5.2.3 Vasopressin

Vasopressin as the major antidiuretic hormone regulates serum and interstitial fluid osmolarity and as an anti-natriuretic hormone increases Na^+ reabsorption (Frindt & Burg 1972, Reif et al. 1984, Tomita et al. 1985, Bankir et al. 2005, Bankir et al. 2010). The effects of vasopressin are tissue and species specific. In most mammalian collecting ducts vasopressin increases transepithelial voltage, decreases transepithelial resistance and increases amiloride-sensitive, unidirectional luminal-to-basolateral Na^+ flux (Chen et al. 1990, Sauter et al. 2006, Nicco et al. 2001, Schafer et al. 2000, Husted et al. 1994, Chen et al. 1991, Frindt & Burg 1972, Reif et al. 1986). The effects are additive to the effects of aldosterone suggesting synergy between the two hormones (Figure 1.2-5) (Chen et al. 1990, Reif et al. 1986, Bugaj et al. 2009).

In the short term, vasopressin acting through adenylyl cyclase-PKA increases channel P_o in a rapid (within 2-3 min) but sustained manner (Bugaj et al. 2009). In the long term vasopressin increases the abundance of a deubiquitylating enzyme ubiquitin-specific protease 10 (Usp10) that stabilizes sorting nexin 3 (SNX3) and promotes cell surface expression of ENaC (Boulikroun et al. 2008). Acting via V2 receptors and adenylyl cyclase-cAMP signaling vasopressin also promotes trafficking and insertion of subunits into the apical membrane (Bugaj et al. 2009, Bankir et al. 2010, Bankir et al. 2005).

In the long term, vasopressin induced increased cAMP also increases transcription and translation of ENaC subunits such as α and γ ENaC in mouse CCDs (Perlewitz et al. 2010) and β and γ ENaC in rat CCDs (Djelidi et al. 1997) by binding of cAMP response element (CRE) through CRE binding proteins (CREB) in the promoter regions of the genes. Long-term exposure to vasopressin and water restriction result in a similar

increase in P_o with a significant increase in the number of active channels in the apical membrane appearing over time (Bugaj et al. 2009, Nicco et al. 2001).

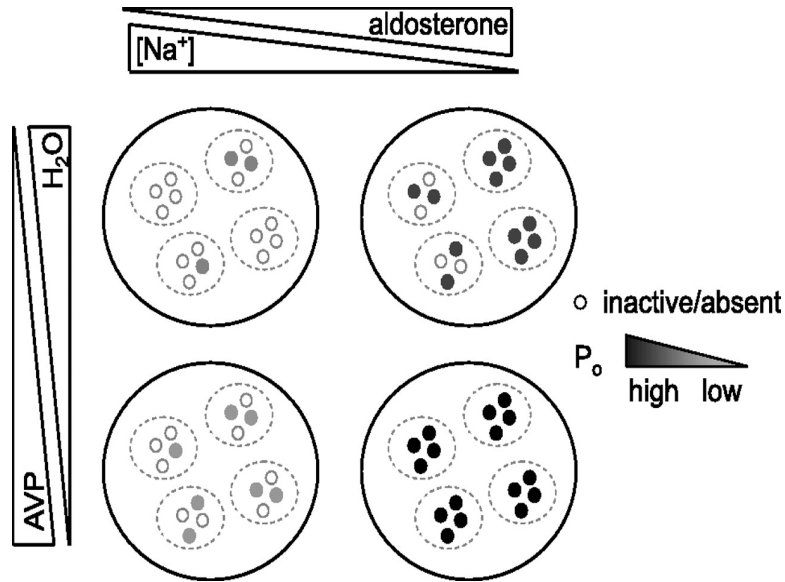


Figure 1.2–5: Synergistic effect of aldosterone and vasopressin on ENaC P_o . ENaC is most active when both aldosterone and vasopressin levels are elevated. Reproduced from Bugaj et al, 2009 (Bugaj et al. 2009).

1.2.5.2.4 Insulin

Insulin has acute anti-natriuretic effects that are independent of blood glucose levels (DeFronzo et al. 1975) but additive to the effects of aldosterone (Record et al. 1998, Blazer-Yost et al. 1998). Chronic infusion of insulin in Sprague-Dawley rats does not increase total abundance of ENaC subunits in the renal cortex, outer medulla or inner medulla but increases apical localization in the principal cells of CCD and increases the

natriuretic response to benzamil (Song et al. 2006). In A6 and CCD cell lines insulin increases Na^+ transport through ENaC by phosphorylating ENaC subunits (Zhang et al. 2005, Shimkets et al. 1998) and by phosphorylation of SGK1 via the Phosphatidylinositol-3-Kinase (PI3K) pathway (Record et al. 1998) (Figure 4). Insulin binding causes allosteric changes in the tyrosine kinase receptor on the cell membrane and via a transduction pathway involving several adapter proteins that ultimately couple PI3K activity activates SGK1 through phosphodiesterase kinases – PDK1 or PDK2. The net effect is increased P_o (Marunaka et al. 1992) and increase in density of functional channels (Blazer-Yost et al. 1998) in the cell surface.

1.2.5.2.5 **Angiotensin II (AngII)**

In isolated perfused CCDs, AngII significantly increases ENaC mediated Na^+ transport (Peti-Peterdi et al. 2002). Infusion of AngII in rats increases α ENaC but not β and γ ENaC protein abundance in the renal cortex (Beutler et al. 2003), and decreases immunolabeling for β and γ ENaC by ~18% in vascular smooth muscle cells in renal interlobar arteries (Jernigan et al. 2009). AT_1 receptor blockade with candesartan decreases abundance of α ENaC mRNA and protein and increases β and γ ENaC protein but not mRNA abundance in the renal cortex (Beutler et al. 2003). Spironolactone does not prevent the effects of AT_1 receptor blockade on α ENaC (Beutler et al. 2003). The abundance of α ENaC is markedly decreased, while β and γ ENaC are markedly increased in AT_1 receptor knockout mice versus wild type mice on low (0.02%) NaCl diet (Brooks et al. 2002). On regular (0.4%) or high (6%) NaCl diet the decreased abundance of α ENaC persists in the AT_1 receptor knockout mice, while the increase in β and γ ENaC abundance is abolished (Brooks et al. 2002). In the rectum of mice on regular but not low or high NaCl diet,

amiloride sensitive potential difference, presumably through ENaC, is higher in the afternoon than morning. AT₁ receptor blockade increases the amiloride-sensitive rectal potential difference in the afternoon suggesting that AngII modulates the diurnal pattern of ENaC mediated Na⁺ transport (Wang et al. 2000).

1.2.5.2.6 **Neural activity**

Acting through the adenylyl cyclase-PKA pathway, both adrenergic and dopaminergic activity regulates ENaC activity, depending on the subcellular compartment involved. Activation of basolateral β -adrenergic receptors in type II alveolar epithelial cells produces a PKA-dependent increase in the number of ENaC in the apical membrane with little or no change in the activity of individual channels (Chen et al. 2002). In contrast, activation of D1 receptors in the apical compartment of these cells produces a PKA-independent increase in P_o with little or no change in the number of channels (Helms et al. 2006a, Helms et al. 2006b).

1.2.6 *SGK1 – a crucial regulator of ENaC*

1.2.6.1 Overview

Serum and glucocorticoid regulated kinases are serine-threonine kinases that phosphorylate the R-X-R-X-X-S/T-Φ (R = arginine, X = any amino acid, Φ = a hydrophobic amino acid) consensus sequence in target proteins (Bhargava et al. 2001, Pearce 2001, Pearce & Kleyman 2007, Vallon & Lang 2005, Lang et al. 2006, Waldegger et al. 1998, Waldegger et al. 1997). Three isoforms SGK1, SGK2 and SGK3 have been described, that share 80% amino acid identity (Lang et al. 2006, Kobayashi et al. 1999, Friedrich et al. 2003). SGK1 is the best characterized isoform and an immediate early gene that is transcriptionally stimulated by a number of factors, most notably aldosterone, glucocorticoids and cell shrinkage (Waldegger et al. 1998, Waldegger et al. 1997). SGK1 plays a central role in mediating the effects of a number of hormones on ENaC (Alvarez de la Rosa et al. 2004, Loffing et al. 2006).

1.2.6.2 Expression of SGK1

SGK1 is ubiquitously expressed in virtually all tissues (Waldegger et al. 1998, Waldegger et al. 1997, Lang et al. 2006, Loffing et al. 2006). Transcript and protein abundance of SGK1 are profoundly different between different cell types in any given tissue such as kidney (Chen et al. 1999, Alvarez de la Rosa et al. 2003, Loffing et al. 2001b, Lang et al. 2000, Hou et al. 2002, Friedrich et al. 2002), brain (Gonzalez-Nicolini & McGinty 2002, Nishida et al. 2004, Tsai et al. 2002, Warntges et al. 2002), eye (Rauz et al. 2003b, Schniepp et al. 2004), lung (Waerntges et al. 2002), liver (Waldegger et al. 2000) or intestine (Waldegger et al. 1999). Cellular localization of SGK1 also depends on the functional state of the cell. For example, activation of SGK1 with serum causes a nuclear

localization (Maiyar et al. 2003) while activation with increased osmolarity or glucocorticoids causes a cytoplasmic localization (Firestone et al. 2003).

1.2.6.3 Regulation of SGK1

Figure 1.2-6 shows a simplified cartoon on regulation of SGK1. Transcription of SGK1 is rapidly regulated by a wide variety of stimulators and inhibitors. Glucocorticoids are one of the most powerful regulators of SGK1 expression. Approximately half of the basal level of SGK1 in e.g. kidneys is maintained by glucocorticoids while fluctuations of aldosterone produce minor changes in SGK1 abundance under physiological conditions. The SGK1 promoter in the rat contains motifs for binding factors such as the GR, MR, CREB, peroxisome proliferator-activated receptor gamma, p53, Sp1, nuclear factor kB etc. that are activated by binding of receptors and signaling molecules such as GR, MR, protein kinase C, cAMP, p53, cytosolic Ca²⁺ (Shelly & Herrera 2002, Hong et al. 2003, Maiyar et al. 1997, Lang & Cohen 2001, Firestone et al. 2003, Lang et al. 2006). In order to be fully functional SGK1 requires activation by PDK1-dependent phosphorylation of ²⁵⁶Thr in the activation loop and PDK2/H motif kinase dependent phosphorylation of ⁴²²Ser in the hydrophobic motif of the protein (Lang et al. 2006). Phosphorylation of ²⁵⁶Thr by PDK1 requires scaffolding by WNK1 (with no lysine kinase 1) and is facilitated by prior phosphorylation of ⁴²²Ser. A number of factors such as insulin, neuronal depolarization, cAMP etc. trigger SGK1 activation through the PI3K pathway. The half-life of SGK1 in the cells is about 30 minutes. Phosphorylation of Nedd4-2 increases ubiquitination and degradation of SGK1 (Zhou & Snyder 2005).

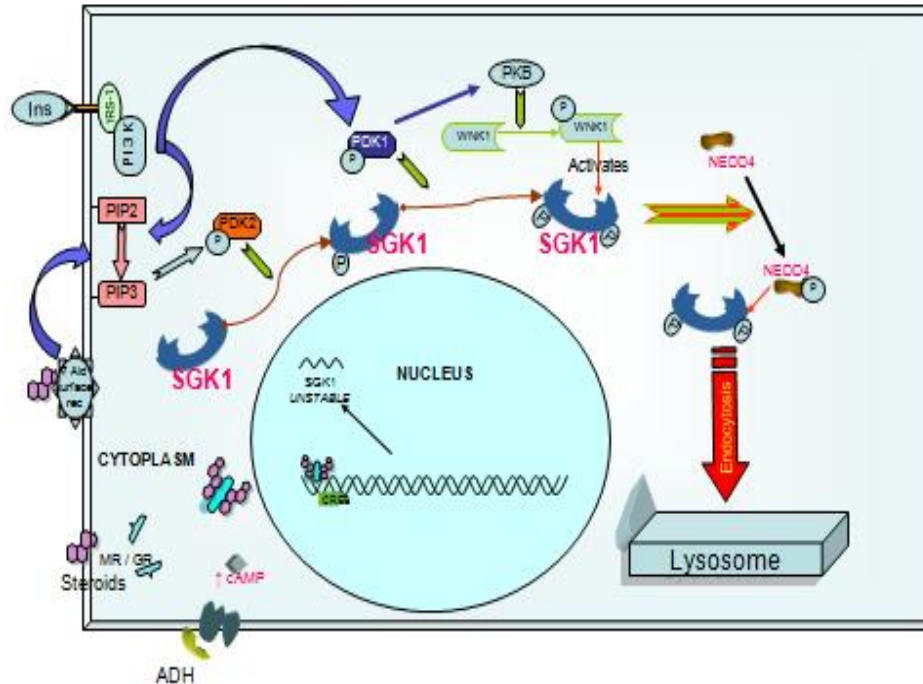


Figure 1.2–6: Regulation of SGK1. Glucocorticoids maintain the basal SGK1 levels, while aldosterone and other factors such as cAMP mediate the day-to-day fluctuation by increasing transcription. A number of mediators such as insulin and aldosterone activate SGK1 through PDK1 and PKB dependent phosphorylation, involving other proteins such as WNK1. The SGK1 protein is rapidly degraded in the cell through processes that are facilitated by Nedd4-2 mediated ubiquitination. Author’s own reproduction.

1.2.6.4 Role of SGK1 in regulation of ENaC

Activated SGK1 acts on ENaC by at least three different mechanisms:

- a. Post-translational effects on Nedd4-2 (as described above in 1.2.5.1.5): SGK1 phosphorylates Nedd4-2, thereby preventing ubiquitinylation and endocytosis of ENaC
- b. Post-translational Nedd4-2 independent effects: SGK1 directly phosphorylates the intracellular C-terminal tail of α ENaC and activates the channel (Diakov & Korbmacher 2004). Indirectly SGK1 affects channel abundance and P_o through effects on

CAP (Vuagniaux et al. 2002) or Na⁺ transport by stimulating the activity of Na⁺K⁺ATPase (Alvarez de la Rosa et al. 2004, Zecevic et al. 2004).

c. Effects on transcription: active SGK1 regulates expression of late aldosterone responsive genes. SGK1 increases abundance of α ENaC by phosphorylating Af9, which reduces the interaction between Af9 and Dot1a (Zhang et al. 2007) (1.2.5.1.1).

1.3 SODIUM, BLOOD PRESSURE (BP) AND THE ROLE OF ENAC

High BP or hypertension affects approximately 25% of the population and is a major risk factor for cardiovascular mortality and morbidity (Burt et al. 1995a, Burt et al. 1995b). Dietary salt is a major risk factor for hypertension (Cirillo et al. 1994, Wen 1973, Beevers 2002, Gibbs et al. 2000, Sasaki 1962, Oliver et al. 1975, Liebman et al. 1985, INTERSALT 1986, INTERSALT 1988, Elliott et al. 1989, Luft 1989, Weinberger 1993b, Luft 1995, Rossier 1997, Weinberger 2000, O'Shaughnessy & Karet 2004, Weinberger 2004, O'Shaughnessy & Karet 2006). Although epidemiological studies in the general population found only a weak association between dietary salt intake and changes in BP (Hanneman 1996, Elliott et al. 1996, Sullivan 1991, Kaplan 1990, Elliott et al. 1989, Rose & Stamler 1989, INTERSALT 1988, INTERSALT 1986, Obarzanek et al. 2003, Sacks et al. 2001, Svetkey et al. 2004), stronger associations are found in specific groups (Weinberger et al. 2001, Sasaki 1962, Sasaki 1964, Weinberger 1996a, Weinberger 1996b, Weinberger 1993a, Weinberger & Fineberg 1991, Luft et al. 1991, Luft et al. 1988a, Luft et al. 1988b, Luft et al. 1987, Bjerregaard et al. 2003, Bjerregaard et al. 2004). The term 'Salt Sensitive' was coined to designate individuals who respond to

a high salt diet by an increase in BP, while those in whom BP does not change are considered ‘Salt Resistant’ (Franco & Oparil 2006, Brier & Luft 1994, Luft 1989, Luft 1995, Wedler et al. 1992, Weinberger 2006, Weinberger 2004, Weinberger 1991, Kimura et al. 1990). Both genetic and environmental factors are thought to contribute to salt sensitivity, but the exact mechanisms linking dietary sodium to the rise in arterial pressure are not completely understood.

1.3.1 Mutations in ENaC genes affect BP

Both gain of function and loss of function of ENaC, resulting from frameshift, premature termination, deletion or missense mutations of the genes affect Na⁺ homeostasis and response to dietary salt. Loss of function can result from mutations in α , β or γ ENaC to cause pseudohypoaldosteronism 1 (PHA1) – a rare, autosomal recessive disease characterized by severe Na⁺ wasting and hypotension associated with hyperkalaemia, metabolic acidosis and unresponsiveness to mineralocorticoid hormones (Chang et al. 1996, Strautnieks et al. 1996a, Strautnieks et al. 1996b, Schild 1996). Knockout of β or γ ENaC (Barker et al. 1998, McDonald et al. 1999) or decreased expression of α ENaC (Hummler et al. 1996, Hummler et al. 1997) in mice produces a similar phenotype. In contrast, gain of function due to mutations in the β and γ ENaC genes involving the PPPXYXXL motif in the C termini, cause increased surface expression and constitutive increase in P_o (Hansson et al. 1995a, Shimkets et al. 1994, Findling et al. 1997, Hansson et al. 1995b, Inoue et al. 1998, Schild 1996, Schild et al. 1995, Schild et al. 1996). These activating mutations result in a rare, autosomal dominant disease, known as Liddle’s syndrome (pseudoaldosteronism), which is characterized by early onset of hypertension associated with hypokalemic alkalosis, reduced plasma renin activity and low plasma

aldosterone levels (Liddle 1973, Liddle et al. 1974, Liddle et al. 1973, Liddle et al. 1976, Liddle et al. 1963, Warnock 2001, Jackson et al. 1998).

Recent observations suggest that Liddle's syndrome may be under-diagnosed and its incidence is greater than originally appreciated (Takeuchi 2002, Takeuchi et al. 1989, Ono et al. 1975, Tamura et al. 1996, Gadallah et al. 1995, Warnock 2001). In fact, several variants in the ENaC genes are relatively common in different populations and also show strong associations with the level of BP, response to dietary Na⁺ and diuretics (Table 1.3-1). For example, lymphocytes of T594M variant carriers show increased Na⁺ conductance in response to cAMP and loss of inhibition by PKC in vitro (Cui et al. 1997). This variant is found in 6-8% of African Americans, who also show better anti-hypertensive response to the diuretic amiloride (Baker et al. 1998, Pratt 2005, Swift & MacGregor 2004, Baker et al. 2002). It is presumed that hypertension in Liddle's syndrome is secondary to Na⁺ retention and volume expansion, but actual expansion of the extracellular volume has not been demonstrated in Liddle's patients and some of the patients even appear to be volume contracted (Rezkalla & Borra 2000, Mutoh et al. 1986, Bubien 2010).

1.3.2 Experimental Na⁺ induced hypertension in Dahl S rats and the role of ENaC

In order to study the cellular pathways and mechanisms that cause salt sensitivity, Dahl and colleagues developed inbred rat strains – the Dahl Salt Sensitive (S) and Dahl Salt Resistant (R) rats (Dahl et al. 1962a, Dahl et al. 1962b, Iwai et al. 1973, Dahl et al. 1974, Rapp 1982). BP increases steadily in Dahl S rats placed on a 4-8% salt diet, whereas there are no changes in the BP of Dahl R rats (Rapp 1982). Selective loading of Dahl S

rats with either Na^+ or Cl^- fails to induce changes in BP (Whitescarver et al. 1984, Liebman et al. 1985, Whitescarver et al. 1986, Kurtz & Morris 1983, Luft et al. 1988c) suggesting that both Na^+ and Cl^- in salt are necessary for the hypertensinogenic effects of high salt in Dahl S rats. Despite efforts by many groups worldwide the exact pathways and mechanisms that lead to salt sensitivity in the Dahl S model have not yet been identified.

1.3.2.1 Renal mechanisms of hypertension and possible role of ENaC

The kidneys have the capacity to return altered arterial pressure to baseline levels by increasing or decreasing water and electrolyte excretion in response to elevated or reduced systemic arterial pressure (Guyton 1990c, Guyton 1990a, Guyton 1990b, Hall et al. 1990, Campese & Park 2006). Renal transplantation studies in both humans and animal models (Curtis et al. 1983, Guidi et al. 1996, Dahl & Heine 1975, Dahl et al. 1972, Dahl et al. 1974, Bianchi et al. 1977, Bianchi et al. 1973, Bianchi et al. 1975, Morgan et al. 1990, Rettig & Grisk 2005) show that both renal and extra-renal factors play an important role in the regulation of BP. The renal contribution to regulation of BP is largely executed by fine-tuning Na^+ excretion to match Na^+ intake (Johns 2002, Abe et al. 1987, Ackermann 1975, Chou et al. 1984, Cowley 1997, Crowley & Coffman 2007, Crowley et al. 2007, Crowley et al. 2005, DiBona 1986, Grim et al. 1979, Hall 1986, Hall et al. 1996, Hall et al. 1986, Kopp et al. 2003, Lee et al. 1993, Manitius et al. 1985, Marunaka 1997, Mattson 2003, Mills 1970). While most of the filtered Na^+ is reabsorbed in the early segments of the nephron, fine-tuning Na^+ intake to urinary output occurs predominantly in the distal nephron where reabsorption of the remaining tubular Na^+ is modulated by a variety of hormonal and neural inputs including the renin-angiotensin-

aldosterone system and sympatho-renal interactions. ENaC is a key transporter of Na^+ in this segment of the nephron (Duc et al. 1994, Stokes & Sigmund 1998, Wolf et al. 2001, Frindt et al. 2007, Volk et al. 1995).

In normotensive strains such as the Sprague–Dawley or Wistar rats, low-salt diet increases mRNA abundance of α ENaC in the inner medulla but not cortex or outer medulla, and has no effect on β or γ ENaC mRNA abundance (Stokes & Sigmund 1998).

In the medulla, low salt diet also increases abundance of both the full-length 90 kDa α ENaC and its 30kDa cleavage product, increases abundance of β ENaC forms that have endoglycosidase-H resistant glycosylation, increases abundance of 70 kDa form of γ ENaC and causes increased apical membrane localization of the proteins. These are associated with a robust increase in amiloride sensitive Na^+ current (Ergonul et al. 2006, Frindt et al. 2007, Frindt et al. 2008, Masilamani et al. 1999, Masilamani et al. 2002). Studies on the effect of high Na^+ diet on renal ENaC expression have shown variable changes when compared to regular or low Na^+ diet. Lim et al (Lim et al. 2004) reported decreased α ENaC mRNA in the kidney, while Wolf et al (Wolf et al. 2001) reported no change in ENaC mRNA abundance with high Na^+ diet. Three weeks of 4% NaCl also did not cause any change in α and γ ENaC proteins in whole kidneys of Sprague Dawley rats but caused a redistribution of β ENaC from the low density plasma membrane enriched fractions to higher density intracellular membrane enriched fractions (Yang et al. 2008, Ergonul et al. 2006, Lim et al. 2004, Wolf et al. 2001). Altogether the different studies suggest that the $[\text{Na}^+]$ in what is considered a regular Na^+ diet already suppresses much of ENaC expression in the kidneys and explains why ENaC abundance is already lowish on

Table 1.3–1: Common mutations in the genes for ENaC subunits and SGK1 and their association with BP in humans. ICE= ischemic cerebrovascular events, HT = Hypertensive, NT = Normotensive

Gene	Locus / Mutation	Study population	Effects and association with BP	Ref
α ENaC	<p>1. Evaluated 4 polymorphisms in the promoter, 3 in the exonic and 1 in the first intron resp.</p> <p>2. Trp493Arg and Ala663Thr</p>	<p>1. Japanese (n=3898)</p> <p>2. Caucasian (n=3516, 1399 with ICE and 1076 controls)</p>	<p>1. Promoter activity of the G (2139) allele was higher than that of the A (2139) allele. A (2139) G polymorphism significantly increased BP in the Japanese. Odds ratio for HT with the GA⁺GG genotype 1.31 (p = 0.0154) in the total population and 1.77 (p = 0.0035) among subjects <60 yrs. of age.</p> <p>2. Effect of the 493Arg allele not known, but carriers have a 1.78 fold higher increased risk for ICE compared with Trp/Trp carriers. Relative risk higher (3.26) in younger women.</p>	(Iwai et al. 2002, Hsieh et al. 2005)
β ENaC	<p>1 & 3. T594M in exon 12</p> <p>2 & 3. G442V variant in exon 8</p> <p>4. R563Q</p> <p>5. T594M</p> <p>6. T594M and G442V</p>	<p>1. South African (n: 519 HT, 514 NT)</p> <p>2. African American</p> <p>3. Japanese HT and general population</p> <p>4. 136 South Africans kindred with R563Q</p> <p>5. Black UK (206 HT, 142 NT)</p> <p>6. African Black UK (n=279)</p>	<p>T594M alters a binding site for PKC and increases ENaC activity; G442V not known to have any effect on Na⁺ transport</p> <p>1. 4-4.5% of South Africans carry the T594M mutation. Genotype frequency is similar between HT and NT.</p> <p>2. G442V and T594M are present in 6-8% African Americans and show increased cAMP responsiveness.</p> <p>3. G442V and T594M mutations in β ENaC are absent in the Japanese.</p> <p>4. R563Q mutation is 3 amino acids from R566X truncation in Liddle's syndrome. R563Q causes a mild form of Liddle's syndrome. BP higher in R563Q heterozygous group (p = 0.005), 80% are/become hypertensive.</p> <p>5. Incidence of hypertension higher in T594M carriers (OR 4.17).</p> <p>6. T594M in ~5% African Blacks and more common in HT.</p>	(Nkeh et al. 2003, Matsubara et al. 2002, Su & Menon 2001, Su et al. 1996, Warnock 1996, Jones et al. 2010, Rayner et al. 2003, Baker et al. 1998, Dong et al. 2001)

Gene	Locus / Mutation	Study population	Effects and association with BP	Ref
γENaC	16p12 and several promoter polymorphisms	General population in Japan (n=4075)	Promoter activity of A(-173) is lower than that of G(-173) allele. The A(-173) allele is recessive and occurs in 0.7% Japanese. Carrying the AA genotype is associated with an 11 mm Hg lower SBP, 8 mm Hg lower PP and with a higher prevalence of hypotension (p=0.005)	(Iwai et al. 2001)
SGK1	1. 3 SNPs 2. SGK1 risk (inheritance of Intron 6 CC + exon 8 CC/CT) 3. SNPs in exons 4,5,8 and 10-12 4. SNPs C to T in exon 8 and T to C in exon 7	1. Swedish - >4600 HT & NT 2. Mixed population, most Caucasian (Swiss German) 3. Mixed, N=591; among which are 311 ESRD pts presumed to be salt-sensitive 4. German twins	1. C homozygosity at intron 6 caused higher diastolic BP (~2 mmHg); at least one C allele at exon 8 caused higher SBP(~5 mmHg); Carriers of both intron 6 CC and exon 8 CC/CT had higher SBP (~5 mmHg) and DBP (~2 mmHg) 2. SBP and DBP increased by 2.1 and 0.8 mmHg/yr in risk carriers (n=65) compared to other genotypes (n=2005) with more uncontrolled (61.1% vs 43.9%) or poorly controlled (27.8% vs 8.9%) HT 3. No significant association shown 4. Linkage of SGK1 gene locus to DBP and evidence of linkage for SBP	(Trochen et al. 2004, Busjahn et al. 2002, Busjahn & Luft 2003, von Wörmern et al. 2005)

regular salt diet (Hager et al. 2001, Masilamani et al. 1999, Duc et al. 1994, Loffing et al. 2000b, Volk et al. 1995).

Early studies by Husted et al (Husted et al. 1996) showed that IMCD cell monolayers obtained from pre-hypertensive Dahl S rats transported Na⁺ at twice the rate as monolayers from age-matched Dahl R rats. The exact molecular mechanisms were not clear but the apical ENaC in the distal nephron and the basolateral Na⁺K⁺ATPase – both appeared to be attractive candidates. A number of studies attempted to identify possible polymorphisms in the ENaC genes or their regulators. Sequence analyses did not reveal any relevant mutations in the coding regions of the three ENaC genes in genetically

hypertensive strains including Dahl S rats (Grunder et al. 1997, Kreutz et al. 1997, Huang et al. 1995). Observed SNPs were not found to be functionally significant using *in vitro* assays in *Xenopus* oocytes. In our lab, screening of coding regions as well as 5' UTR of α , β and γ ENaC identified a number of SNPs in Dahl S and R rats, some of which are also present in Wistar rats (Shehata et al. 2007), but there were no differences between Dahl S and R rats.

The A1079T transversion of the *Atp1a1* gene resulting in a single amino acid substitution Q276L was presumed to be associated with increased activity of the Na^+K^+ ATPase in Dahl S versus R rats (Canessa et al. 1993b, Glorioso et al. 2001, Glorioso et al. 2007, Herrera et al. 1988, Herrera et al. 1994, Herrera et al. 1987, Herrera et al. 2001, Herrera & Ruiz-Opazo 1990, Herrera et al. 1998, Kaneko et al. 2005, Ruiz-Opazo et al. 1994, Ruiz-Opazo et al. 1997a, Ruiz-Opazo & Herrera 1992, Ruiz-Opazo et al. 1997b, Song et al. 2001, Sweadner et al. 1994, Harris & Barnard 2006a), however, other groups have not been able to reproduce the findings (Mokry & Cuppen 2008, Simonet et al. 1991, Barnard et al. 2001, Harris & Barnard 2006b, Harris & Barnard 2006a).

Table 1.3-2 summarizes some of the known genetic differences between Dahl S and R rats, as they relate to ENaC expression or function.

1.3.2.2 Enhanced expression of ENaC in Dahl S rats

Despite no evidence for significant variations in ENaC genes, ENaC expression has consistently been found to be different between Dahl S and R rats. Abundance of the ENaC subunits was comparable in whole kidneys or cortical extracts of Dahl S and R rats

Table 1.3–2 Components of the $[Na^+]$ transport-regulating gene network – known polymorphisms and expression in response to high salt diet in salt-sensitive rats (Jaitovich & Bertorello, Taub et al., Sjöstrom et al. 2007, Stenstrom et al. 2009, Aoi et al. 2007, Aoi et al. 2006, Aoi et al. 2004, Kakizoe et al. 2009, Umemura et al. 2006, Farjah et al. 2003, Cover et al. 1995, Matsukawa et al. 1993, Huang et al. 2006a, Murrell et al. 2005). MHS = Milan Hypertensive rat; HSD = Hydroxysteroid dehydrogenase, ? = Not confirmed subsequently.

	Mutations in coding regions	Kidney expression	Brain expression	Activity
11-β-hydroxylase	R127C, V351A, V381L, I384L and V443M substitutions in Dahl R	No change	Not studied	Decreased in Dahl R versus Dahl S
Aldosterone synthase	E136D & Q251R substitutions in Dahl R due to 7 mutations in the gene	Decreased	Dahl rats not studied	AS in Dahl R catalyzes the conversion of 11-deoxycorticosterone to aldosterone at a greater rate in Dahl S or Sprague-Dawley rats
SGKI	Not studied	Increased in Dahl S	Not studied	Not studied
Side Chain Cleavage	Not studied	Not studied	4 fold increase in MHS hypothalamus, Dahl S not studied	Increased OLC in Dahl S and MHS hypothalamus
HSD isomerase	Not studied	Not studied	5 fold increase in MHS hypothalamus, Dahl S not studied	Increased OLC in Dahl S and MHS hypothalamus
ENaC	No differences found in Dahl S and R	Increased α , β & γ ENaC in Dahl S	Not studied	Increased in Dahl S

	Mutations in coding regions	Kidney expression	Brain expression	Activity
Nedd4L	Not studied	Increased in Dahl R; no change in Dahl S	Not studied	Not studied
AngII/AVP receptor	N119S & C163R substitutions in Dahl S	Not studied	Not studied	Increased affinity for AVP and AngII in Dahl S
Na⁺K⁺ ATPase	Q276L substitution in α 1 subunit in Dahl S (?)	Not studied	Not studied	Increased Na:K coupling in Dahl S (?)

on regular salt diet. Aldosterone increases α ENaC mRNA in kidneys of both Dahl S and R rats by threefold but decreases β ENaC and γ ENaC mRNA levels in Dahl S rats only with no effect in Dahl R rats (Aoi et al. 2006). Aoi et al (Aoi et al. 2004) reported that in the kidneys of Dahl S rats, high-salt diet for 4 weeks increases α ENaC mRNA by 2.5-fold. In a further study by the same group, high salt diet for 4 weeks was found to cause the expected decrease in α ENaC mRNA in whole kidneys of Dahl R but caused modest increases in α , β and γ ENaC mRNA in whole kidneys of Dahl S rats compared to levels on regular salt diet (Aoi et al. 2007). These studies were not known at the beginning of this project. We also sought to study expression of the genes, to identify the tubular segments that showed abnormal ENaC expression, and evaluated ENaC mRNA and protein abundance and distribution in the different regions of kidneys, particularly the medulla after 2 and 4 weeks of high salt diet.

1.3.2.3 SGK1 and Na⁺ induced hypertension

SGK1 plays an important role in the regulation of renal Na^+ excretion and salt appetite which is evident from studies in SGK1 knockout (SGK1^{-/-}) mice. On a regular salt diet, SGK1^{-/-} mice show normal renal water and electrolyte excretion like their wild type counterparts. However, when challenged with a low salt diet, SGK1^{-/-} mice are not able to adequately decrease Na^+ excretion despite increased serum aldosterone levels and proximal tubular Na^+ and fluid reabsorption, leading to decreased BP (Wulff et al. 2002). SGK1^{-/-} mice have decreased ability to retain Na^+ in response to insulin (Huang et al. 2006c) and do not increase their salt intake in response to DOCA (Vallon et al. 2005). The salt wasting phenotype observed in SGK1^{-/-} mice is milder than the severe Na^+ wasting observed in mice lacking either MR (Berger et al. 1998), αENaC (Hummler et al. 1996), or βENaC (McDonald et al. 1999) suggesting that renal ENaC function is not completely dependent on SGK1. Studies in humans also show that variants in the SGK1 gene or its promoter are associated with changes in BP in different populations (Table 1.3-1).

In Dahl S kidneys expression and protein abundance of SGK1 is similar to that of Dahl R or SD rats (Aoi et al. 2007, Farjah et al. 2003). High salt diet decreases expression of SGK1 in the salt resistant strains. In contrast, expression and protein abundance of SGK1 increases in Dahl S rats on high salt diet. The SGK1 mRNA sequence was found to be similar between Dahl S and SD rats (Farjah et al. 2003). Whether or not the SGK1 coding and non-coding regions are different between Dahl R and Dahl S rats was not studied.

1.3.3 Central mechanisms of Na^+ induced hypertension

Cross transplantation studies show that a kidney from a normotensive strain does not necessarily lower BP in an otherwise genetically salt sensitive rat (Morgan et al. 1990,

Rettig & Grisk 2005, Dahl & Heine 1975, Dahl et al. 1972, Dahl et al. 1974), suggesting that extrarenal mechanisms also may play an important role in Na^+ induced hypertension. In Dahl S rats as well as several other experimental models, high salt diet increases sympathetic activity and total peripheral resistance (Brooks et al. 2005, Brooks et al. 2001, Carlson et al. 2001, Huang et al. 2006a, Leenen 2010, Leenen et al. 2002). Activation of sympathetic nerves to the kidneys *per se* also increases tubular Na^+ reabsorption, renin release and renal vascular resistance (DiBona & Kopp 1997). Blockade of the increased sympathetic activity by e.g. peripheral sympathectomy or denervation of the renal nerves prevents Na^+ induced hypertension (Takeshita et al. 1979, Friedman et al. 1979, Iwai et al. 1980). Acute specific or non-specific blockade of certain brain areas, such as the rostral ventrolateral medulla (RVLM), produce profound and rapid decrease in BP in animals indicating that these areas are important in setting the basal sympathetic tone. Lesions in more proximal brain areas such as the anteroventral third ventricle (AV3V) and paraventricular nucleus (PVN) cause a similar effect in experimental models including those of Na^+ induced hypertension (Carithers et al. 1980, Gordon et al. 1982, Erinoff et al. 1975, Fink & Bryan 1982, Gauthier et al. 1981, Marson et al. 1985, Marson et al. 1983, Sanders et al. 1989). The neural pathways leading to hypertension, do not appear to be driven by the osmotic effect of the ions, nor due to the effects of Cl^- , but rather by $[\text{Na}^+]$ *per se* (Wei & Wu 1979, Bunag & Miyajima 1984, Leksell et al. 1982, Gabor & Leenen 2009b, Huang et al. 2006b, Jin et al. 2001). How the increases in $[\text{Na}^+]$ are being sensed and translated into increased neuronal activity leading to sympathoexcitation has not yet been resolved (Orlov & Mongin 2007). Na^+ sensitive cells that respond to changes in plasma and CNS extracellular $[\text{Na}^+]$ are present in several

brain areas such as the OVLT, SFO and MnPO (Bourque & Oliet 1997). While the terminal responses such as thirst and vasopressin release can be mimicked by different mechanisms, NaCl elicits the greatest response for the pressor effects and sympathoexcitatory activity (Chen & Toney 2001, Kadekaro et al. 1995, Voisin & Bourque 2002). Special tanycytes are interspersed along the ependymal lining of the anteroventral 3rd ventricle. Tanycytes sense the concentration of substances in the CSF and relate it to deeper located nuclei in the hypothalamus (Jarvis & Andrew 1988, Bruni et al. 1985). Tanycyte signaling is especially important in neuroendocrine regulation (Rodriguez et al. 2005, Sanchez et al. 2009, Bruni 1998, Flament-Durand & Brion 1985, Gotoh et al. 2008, Lechan & Fekete 2007, Wittkowski 1998). Interestingly, both tanycytes and SON neurons also show increased Fos immunoreactivity in response to changes in water and salt overload (Zambotti-Villela et al. 2008). $[\text{Na}^+]$ can affect neuronal function in several ways. For example, Na^+ may activate the central pathways directly through voltage sensitive channels that sense $[\text{Na}^+]$ and relate it to an action potential. Enhanced transport of Na^+ into the cell via a voltage insensitive channel can also cause a general decrease in the depolarization threshold of that cell. How Na^+ preferentially affects sympathetic pathways in salt sensitive strains to increase BP is not completely understood. Fig 1.3-1 shows how the renal and neural mechanisms may interplay in regulation of BP.

I will first discuss the mechanisms that are involved in the transport of Na^+ from plasma into the brain and discuss the studies that show abnormal transport of Na^+ into the brain may underlie the primary pathology in Dahl S rats. Next I will discuss how increased

[Na⁺] activates neural pathways and mechanisms that lead to enhanced sympathetic activity and hypertension, especially in Dahl S rats on high salt diet.

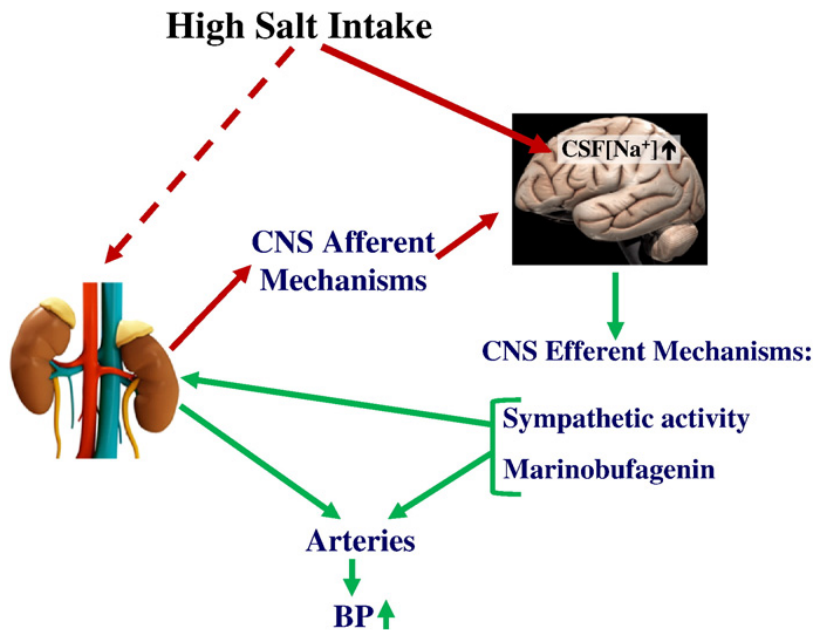


Figure 1.3–1: Outline of brain and kidney interactions in Na⁺ induced hypertension. Reproduced from Leenen, FH, 2010 (Leenen 2010).

1.3.3.1 Na⁺ transport in the brain

Na⁺ can enter the CNS interstitial fluid (ISF) and affect neuronal function either a) directly through the blood brain barrier (BBB), or b) secondarily from the CSF via the blood-CSF and CSF-brain barriers. Figure 1.3-2 shows the morphology of the blood-brain-CSF interfaces.

1.3.3.1.1 Na⁺ transport across the CSF-brain barrier

CSF bathes the exterior of the CNS and fills the ventricles of the brain, spinal canal and subarachnoid spaces (Brown et al. 2004, Brown et al. 1985, Johanson et al. 2008, Praetorius 2007, Praetorius & Nielsen 2006). About two-thirds of the CSF is produced by

the choroid plexus (Brown et al. 2004, Brown et al. 1985, Johanson et al. 2008, Praetorius 2007, Praetorius & Nielsen 2006, Wright 1972b, Wright & Saito 1986).

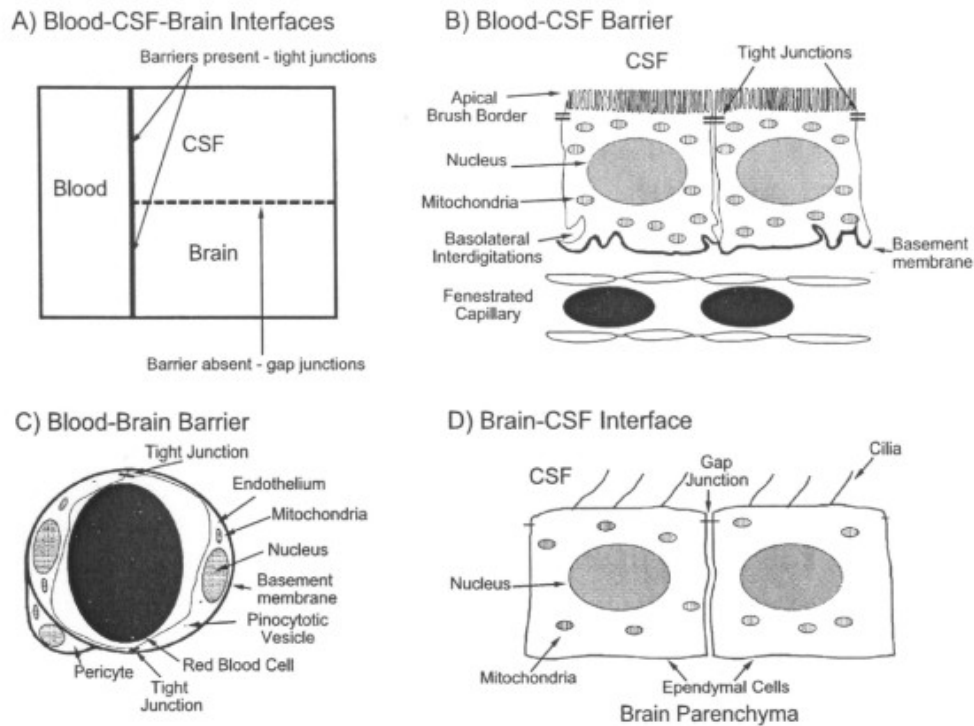


Figure 1.3–2: Morphology of blood-brain-CSF interfaces: (A) The main CNS compartments and interfaces. The blood-brain and blood-CSF barriers are true barriers with tight junctions between endothelial and epithelial cells, respectively. The brain-CSF interface, because of gap junctions between ependymal (or pia-glial) cells, is more permeable than brain or spinal cord capillaries and choroid plexus. (B) Blood-CSF barrier. The choroid plexus has one cell layer of circumferentially arranged epithelial cells. Plexus capillaries, unlike counterparts in brain, are permeable to macromolecules. (C) Blood-brain barrier: Endothelial cells are linked by tight junctions, conferring low paracellular permeability. Endothelial cell pinocytotic vesicle paucity reflects minimal transcytosis. (D) Brain-CSF interface: Ependymal lining in lateral ventricles maintains the barrier between brain ISF and large-cavity CSF. Motile cilia at ependymal cell apex

move CSF downstream to sub-arachnoidal space. Figure reproduced from Johanson et al, 2008(Johanson et al. 2008),(Praetorius 2007).

The transchoroidal secretion of water, ions and other macromolecules drives the bulk flow of CSF along the ventriculo-cisternal axis and accounts for the 11 times daily renewal in the rat (Parandoosh & Johanson 1982, Johanson et al. 2008). The choroid plexus is responsible for the precise maintenance of the composition of CSF through a combination of absorption and secretion of solutes and solvents (Brown et al. 2004, Brown et al. 1985, Johanson et al. 2008, Praetorius 2007, Praetorius & Nielsen 2006). Studies with tracers injected into the CSF showed that the CSF and brain tissue can exchange both across the bulk of the ependyma lining the cerebral ventricles, and across the pial/glial layer at the surface of the brain facing the subarachnoid space suggesting that there is dynamic exchange at the ependymal and pia-glial surfaces of the brain (Bruni et al. 1985, Del Bigio 1995b, Del Bigio 1995a, Del Bigio & Bruni 1986, Jarvis & Andrew 1988, Sarnat 1992b, Sarnat 1992a, Sarnat 1998, Johanson et al. 2008, Abbott 2004). However, the bulk flow rate of interstitial fluid in rat brain is 0.15–0.3 μ l/min/g of brain, which is much lower than that of CSF formation at approximately 3-4 ml/min/g at the blood-CSF-brain barrier (Abbott 2004).

[Na⁺] in the CSF taken from the subarachnoid spaces is significantly higher than plasma [Na⁺] in several species including the rat, suggesting that Na⁺ is actively transported into the CSF rather than being passively filtered (Brown et al. 2004, Johanson et al. 2008, Praetorius 2007, Quinton et al. 1973, Saito & Wright 1982, Wright 1970, Wright 1972b, Wright 1972a, Wright 1974, Wright 1977, Wright 1978, Wright & Saito 1986, Wright et al. 1977, Zeuthen & Wright 1978, Saito & Wright 1983, Saito & Wright 1984, Saito &

Wright 1987). Figure 1.3-3 shows the current model of CSF formation in the rat. The apically located $\text{Na}^+\text{K}^+\text{ATPase}$ of the choroid plexus cells actively secretes Na^+ into the ventricles, and drives the process of CSF secretion (Wright 1970, Wright 1972b, Wright 1972a, Wright 1977, Wright 1978, Wright & Saito 1986, Wright et al. 1977). The basolateral uptake of Na^+ and Cl^- - another essential step in CSF formation, is facilitated by carriers functionally dependent upon the transmembrane gradient for Na^+ , Cl^- , H^+ and HCO_3^- . Decreases in CSF formation rate by i.v. amiloride, supports this theory and the presence of a Na^+ transporter/exchanger at the basolateral membrane.

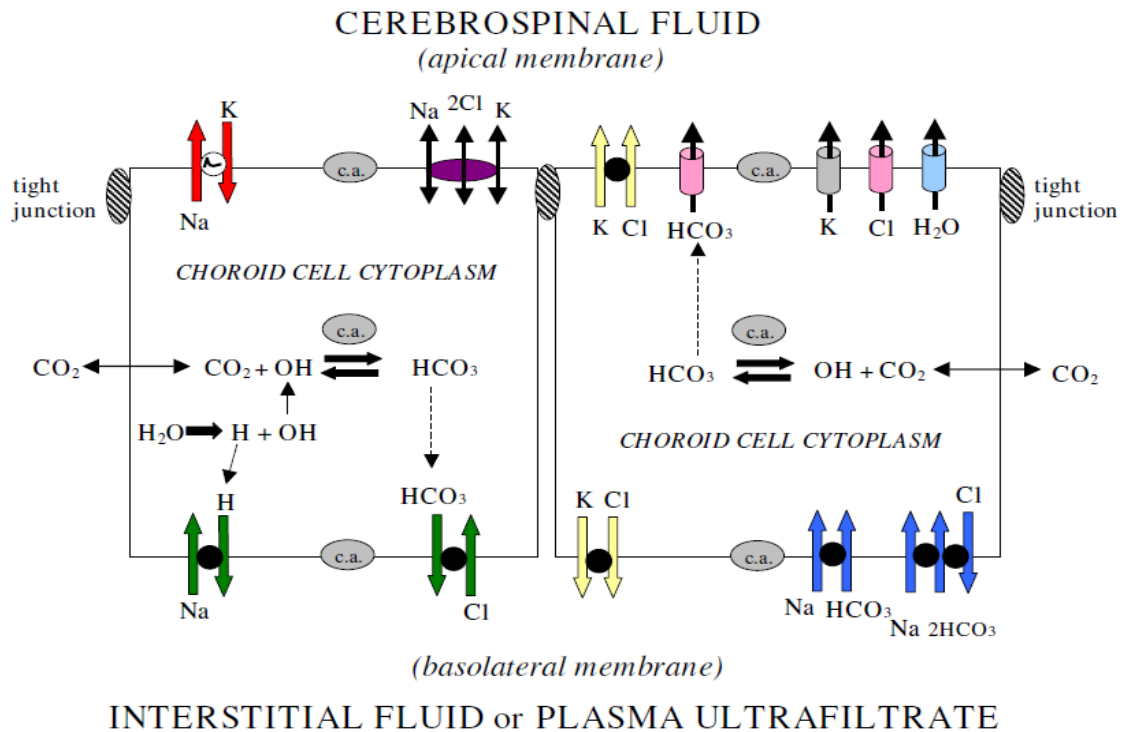


Figure 1.3–3: Schematic diagram of CSF secretion by the choroid plexus. The apically located $\text{Na}^+\text{K}^+\text{ATPase}$ generates the net driving force of Na^+ secretion into the CSF. Na^+ moves down a concentration gradient via secondary active transport in the basolateral membrane. Transport of other ions and water occurs along their electrochemical

gradients through other transporters such as $\text{Na}^+\text{H}^+\text{CO}_3^-$ cotransporter, Na^+ dependent $\text{Cl}^-\text{HCO}_3^-$ exchanger, K^+Cl^- cotransporter and $\text{Cl}^-\text{HCO}_3^-$ countertransporter on the basolateral membrane and $\text{Na}^+2\text{Cl}^-\text{K}^+$ cotransporter, K^+Cl^- cotransporter, other K^+ and Cl^- channels and aquaporins predominantly on the apical CSF side of the membrane.c.a. = carbonic anhydrase. Reproduced from Johanson et al, 2008 (Johanson et al. 2008, Millar et al. 2007, Praetorius & Nielsen 2006, Johanson 1984, Johanson et al. 1990, Johanson et al. 2011),(Johanson & Murphy 1990, Murphy & Johanson 1990)

Although NHE1 mRNA appears to be expressed in the lateral ventricle choroid plexus (Kalaria et al. 1998), NHE1 protein has not been detected in the choroid plexus (Alper et al. 1994, Brown et al. 2004, Praetorius & Nielsen 2006). Whether or not ENaC channels are expressed in the choroid plexus was not studied before. The possible role of an amiloride (or more specifically benzamil) blockable Na^+ transporter in the setting of Na^+ induced hypertension was also not yet investigated.

1.3.3.1.2 Na^+ transport across the Blood Brain Barrier (BBB)

The BBB forms the primary barrier between Na^+ in the plasma and the brain interstitial fluid (ISF). In contrast to other vascular beds, the endothelial cells in brain capillaries lack fenestrations or transendothelial channels, have a limited transcellular vesicular transport and very high transcellular resistance to polar solutes that can support high transcellular concentration gradients for ions and potential differences of 35 mV (Crone & Olesen 1982, Betz & Goldstein 1978, Betz & Goldstein 1980, Betz & Goldstein 1986, Bowman et al. 1983, Goldstein & Betz 1986, Shivers et al. 1984). Two separate saturable mechanisms are thought to contribute to Na^+ transport across the BBB. Under physiological conditions, the transfer constant of Na^+ from blood to brain in Long-Evans

rats was found to be about $1.1 \pm 0.2 \mu\text{l/g/min}$ (Ennis et al. 1996), and increased to $3.2 \pm 0.4 \mu\text{l/g/min}$ when the perfusate $[\text{Na}^+]$ was decreased to 0.2 mM, suggesting carrier-mediated transport of Na^+ at the BBB. The unidirectional transport of Na^+ from blood to brain is decreased by 28% with 25 μM dimethyl-amiloride (DMA, IC_{50} : NHE – 7.0 μM , ENaC – 8.75 μM) and by 22% with 25 μM phenamil (IC_{50} : NHE - 8400 μM , ENaC – 0.02 μM) (Kleyman & Cragoe 1988a). A more specific blocker of NHE ethyl isopropyl amiloride (IC_{50} : NHE – 0.38 μM , ENaC – 8.75 μM) was not used. The true identity of this DMA and phenamil sensitive Na^+ transporter in the luminal membrane of BBB capillaries remains to be known but combined with the abluminal $\text{Na}^+\text{K}^+\text{ATPase}$ it contributes to Na^+ transport into the brain (Ennis et al. 1996).

1.3.3.1.3 Na^+ transport in the brain of Dahl S versus R rats

The relationship of CSF to plasma $[\text{Na}^+]$ appears to be altered in Dahl S rats. Intravenous injection of $^{22}\text{NaCl}$ is associated with 5-8 times higher CSF $^{22}\text{Na}^+$ counts in Dahl S rats than Dahl R rats. However, on regular salt diet, CSF $[\text{Na}^+]$ is similar in Dahl R, Dahl S and Wistar rats, indicating that compensatory mechanisms may help to normalize the increased transport of Na^+ into the CSF on regular salt diet. The extent of this difference is further enhanced by high salt diet (Simchon et al. 1999). CSF $[\text{Na}^+]$ also does not change significantly in salt resistant animals such as Wistar and Dahl R rats on high salt diet, but CSF $[\text{Na}^+]$ increases in Dahl S on high salt diet and precedes the onset of hypertension by a few days (Haywood et al. 1984, Huang et al. 2004, Yamashita et al. 1992, Nakamura & Cowley 1989). The nature of the Na^+ transporting protein/s that may be involved in enhanced transport of Na^+ into the brain remained to be explored.

1.3.3.2 Central mechanisms mediating the sympathoexcitatory responses to increases in $[\text{Na}^+]$

The functional integrity of the sympathetic nervous system is required for the effects of a high salt diet on BP (Hano et al. 1989, Saavedra et al. 1983, Takeshita et al. 1979). In Dahl S rats high salt diet causes enhanced sympathetic activity, which is characterized by impairment of baroreflex function, enhanced renal sympathetic nerves activity (RSNA) and enhanced pressor responses to environmental stressors such as air jet (Huang & Leenen 1995b, Huang & Leenen 1998). These effects can be blocked by inhibitors of components of the renin-angiotensin-aldosterone system (RAAS) such as AT_1 receptor blockers, both by infusion into the cerebral ventricles and by injection into specific nuclei such as the para-ventricular nucleus (PVN) or subfornical organ (SFO) suggesting that central angiotensinergic pathways play a crucial role in high salt induced sympathetic hyperactivity (Ackermann & Azizi 2000, Gabor & Leenen 2009b, Tagawa & Dampney 1999, Wei et al. 2008, Gyurko et al. 1993, Ito et al. 2003, Ito et al. 2002, Muders et al. 2001). The phenotype in Dahl S rats on high salt diet, can be mimicked by increasing $[\text{Na}^+]$ in the brain through infusion of Na^+ rich aCSF into the cerebral ventricles and also by local increase of $[\text{Na}^+]$ in specific areas such as the paraventricular nucleus (PVN). These effects are enhanced in Dahl S rats compared to salt resistant Dahl R or Wistar rats (Huang et al. 1992, Huang et al. 1998). Altogether these studies suggest that an increase in CSF $[\text{Na}^+]$ activates angiotensinergic pathways causing increased sympathetic hyperactivity.

1.3.3.2.1 **Increases in aldosterone and ouabain like compounds ('ouabain') in the central nervous system (CNS) mediate the effects of increased [Na⁺]**

Recent studies show that the increased sympathetic activity in response to increases in [Na⁺] is mediated by brain mechanisms involving aldosterone and 'ouabain'. Although high versus regular salt diet inhibits circulating aldosterone, it increases hypothalamic aldosterone by ~35% in Dahl S rats versus decreases in Dahl R rats (Huang et al. 2009b). High salt also increases hypothalamic but not peripheral 'ouabain' in Dahl S rats by ~2 fold (Wang & Leenen 2002). In normotensive Wistar rats, icv infusion of Na⁺ rich aCSF also increases hypothalamic aldosterone by ~33% and of 'ouabain' by ~50% (Huang et al. 2006b). Chronic icv infusion of low doses of aldosterone (that have no systemic effect), increases hypothalamic 'ouabain' in normotensive, salt resistant animals such as Wistar rats by ~30% and causes sympathoexcitation and hypertension (Wang & Leenen 2003). The extent of the increase in BP by icv aldosterone depends on the [Na⁺] in the vehicle (Wang & Leenen 2003). Both icv or specific injection of ouabain into areas such as the median preoptic nucleus (Budzikowski & Leenen 1997), PVN (Gabor & Leenen 2009b) or rostral ventrolateral medulla (Teruya et al. 1997) cause dose-dependent increase in sympathetic activity and BP. 'Ouabain' binding Fab fragments block the effects of icv aldosterone and increased CSF [Na⁺] on BP and sympathetic hyperactivity in Wistar rats and prevent hypertension in Dahl S rats on high salt diet (Wang et al. 2003a). The sympathoexcitatory effects of high salt in Dahl S rats and of central aldosterone or Na⁺ rich aCSF infusion in Wistar rats, are blockable by MR antagonists such as RU28318 or spironolactone (Gomez-Sanchez et al. 1994, Huang et al. 2005, Huang & Leenen 1998, Huang & Leenen 1999, Huang & Leenen 2002, Huang et al.

2009a, Rahmouni et al. 2001, Rahmouni et al. 1999, Gomez-Sanchez et al. 1992). Altogether, as discussed in detail in recent reviews the results indicate that high Na^+ either from a high salt diet or through icv infusion, activates central pathways involving aldosterone which via MR increase ‘ouabain’ production and release (Huang et al. 2006a, Leenen 2010, Leenen et al. 1993b, Leenen et al. 2002). It appears that the responses to increases in aldosterone and ‘ouabain’ are a general characteristic in all strains to varying degrees and not specific to Dahl S, and that this pathway may be activated to prevent the further increase in CSF $[\text{Na}^+]$, but as a side effect increase activity in the angiotensinergic pathways via enhanced AT_1 receptor stimulation to produce sympathetic hyperactivity and hypertension (Huang et al. 2006a, Leenen 2010, Leenen et al. 1993b, Leenen et al. 2002). Figure 1.3-4 shows a schematic outline of the involved neuromodulatory mechanisms that are activated by an increase in CSF $[\text{Na}^+]$.

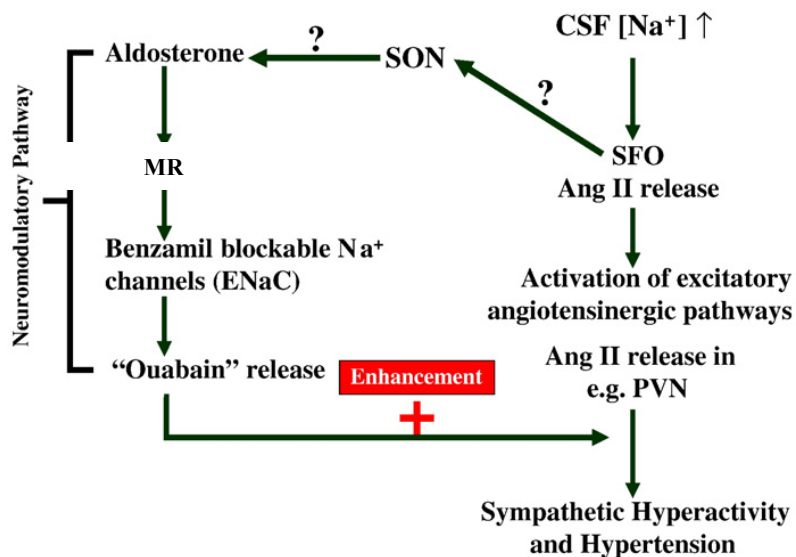


Figure 1.3–4: Outline of CNS mechanisms activated by an increase in CSF $[\text{Na}^+]$. Increased CSF $[\text{Na}^+]$ activates the aldosterone-ouabain neuromodulatory pathway that

enhances angiotensinergic activity in e.g. the PVN to cause sympathetic hyperactivity and hypertension. Reproduced from Leenen, FH, 2010 (Leenen 2010).

1.3.3.2.2 **Benzamil blockable Na⁺ channels mediate the effects of increased [Na⁺]**

Gomez-Sanchez et al, first showed that icv infusion of benzamil at doses that did not have any effect on BP when infused subcutaneously, prevent the increase in BP in several rat models of mineralocorticoid induced hypertension (Gomez-Sanchez & Gomez-Sanchez 1994, Gomez-Sanchez & Gomez-Sanchez 1995). Nishimura et al showed that, icv benzamil abolished the increase in BP caused by central mechanisms such as icv infusion of Na⁺ rich aCSF in Wistar rats and not by peripheral mechanisms such as aortic ligation between origin of the renal arteries in Sprague Dawley rats (Nishimura et al. 1998). Subsequent studies showed that, at low icv doses benzamil also prevents the increase in brain ‘ouabain’ content, the hyperactivity of angiotensinergic neurons and the increase in sympathetic tone, that are caused by a high salt diet in Dahl S rats or icv infusion of Na⁺ rich aCSF in Wistar rats (Wang et al. 2003a, Wang & Leenen 2002, Wang & Leenen 2003, Huang & Leenen 2005, Wang et al. 2003b). As stated previously (section 1.3.4.1.2) this amiloride analogue can dose-dependently block a number of channels, including NHE, sodium calcium exchanger and ASICs, but it is most potent in blocking ENaC (Kleyman & Cragoe 1988a, Kleyman & Cragoe 1988b).

Figure 1.3-5 shows the neuronal circuitry involved in sensing changes in [Na⁺] by the brain. Through Na_x – a recently discovered, voltage sensitive, amiloride or tetrodotoxin resistant, Na⁺ channel that is expressed in the glial processes, the glia in the SFO respond to changes in extracellular [Na⁺] from 145 to 170 mM (EC₅₀ 157 mM) and through yet unknown mechanisms transmit it to the neurons (Noda 2006, Shimizu et al. 2007,

Watanabe et al. 2002, Watanabe et al. 2003, Hiyama et al. 2010, Hiyama et al. 2004, Hiyama et al. 2002). Direct neuronal projections from the SFO and OVLT or indirect neuronal projections through the MnPO to the SON and PVN regulate electrical activity of the magnocellular

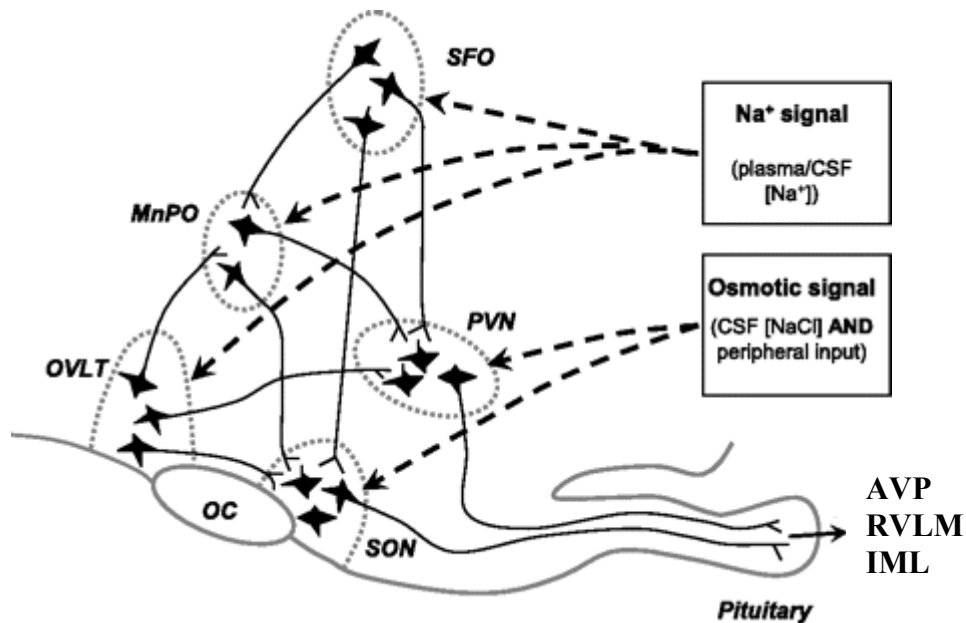


Figure 1.3–5: Neuronal connections between the circumventricular organs, SON and PVN. Magnocellular neurons receive synaptic inputs from central Na⁺-sensitive neurons located in the organum vasculosum lamina terminalis (OVLT), subfornical organ (SFO), and median preoptic nucleus (MnPO). In these latter areas, the blood-brain barrier and CSF-brain barrier are partially open, allowing for direct sensing of the ionic composition of the plasma. OVLT and SFO neurons also project to the MnPO. The PVN and SON respond by for example secretion of vasopressin, and their function is additionally affected by the [Na⁺] and osmolality of the CSF. IML - Intermediolateral cell column of the thoraco-lumbar spinal cord, RVLM – Rostral ventrolateral medulla, oc- optic chiasma. Adapted from Hussy et al and Orlov and Mongin (Hussy et al. 2000, Orlov & Mongin 2007).

neurons and thereby their secretory e.g. vasopressin release or sympathoexcitatory functions (Orlov & Mongin 2007, Hussy et al. 2001, Hussy et al. 2000, Hussy et al. 1997, Kolaj & Renaud 2007). Knockout experiments of the Na_x channel show that it is predominantly involved in regulation of salt appetite (Watanabe et al. 2003). The exact mechanisms by which an increase in $[\text{Na}^+]$ lead to sympathetic hyperactivity remain yet unresolved. In peripheral tissues, such as the macula densa in the kidney increases in luminal $[\text{NaCl}]$ for example lead to increases in intracellular concentration of the ions $[\text{Na}^+]$ and $[\text{Cl}^-]$ after transport into the cell via the apically located Na-K-2Cl transporter. The increase in the intracellular concentration of the ions triggers increases in cytosolic calcium and leads to cell depolarization. Cl^- exits the cell through a basolateral channel while Na exits via an apically located $\text{H}^+(\text{Na}^+)\text{K}^+$ ATPase (Lapointe et al. 2003, Bell et al. 2003b, Bell et al. 2003a). Mechanisms of ion sensing in the brain are still poorly understood. Members of the transient receptor potential vanilloid (TRPV) family of cation channels have been proposed to mediate at least some of the effects of changes in $[\text{Na}^+]$ (Bourque 2008). However, unlike the native nonselective sodium channels recombinant homomultimeric TRPV2 and TRPV4 channels were not found to be affected by hyperosmolality. Rather a group of stretch responsive and nonselective cation channels are possibly responsible as the key mediators in the transduction of CNS extracellular $[\text{Na}^+]$ to neuronal activity in the SON and PVN (Chakfe & Bourque 2001) followed by downstream neuronal projections from the PVN to other areas such as the RVLM and IML that regulate sympathetic outflow.

1.3.4 Rationale of the studies

Genetic factors contribute to an individual's sensitivity to Na⁺. ENaC and SGK1 have been shown to be associated with hypertension both in population based studies and from rarer disorders that lead to Na⁺ induced hypertension. However, the underlying mechanisms have not yet been elucidated.

Dahl S rats represent an excellent model for studying Na⁺ induced hypertension, while Dahl R are their resistant control. Increases in the CSF [Na⁺] and subsequent activation of neural pathways through aldosterone – MR – benzamil blockable channels – ouabain plays an important role in the pathogenesis of Na⁺ induced hypertension in this model. Expression of ENaC and SGK1 were found to be paradoxically increased in the kidneys of Dahl S rats on high salt diet. Since the ENaC genes were found to be identical between Dahl S and R rats, we sequenced the SGK1 gene in these rats for possible genetic mutations. Expression of ENaC in the CNS and the effects of high salt diet on ENaC expression and distribution had never been studied. Our first study showed strong expression of ENaC in the choroid plexus, ependyma, SON and PVN. We therefore focused on these areas and studied the effects of increasing CSF [Na⁺] and of high salt diet on expression of ENaC and some of its regulators. Considering the importance of the choroid plexus in regulation of CSF [Na⁺] we further evaluated the functional role of ENaC in the choroid plexus.

HYPOTHESES AND OBJECTIVES

2.1 HYPOTHESES

1. ENaC subunits are expressed in brain epithelia and cardiovascular regulatory centers.
2. ENaC in the choroid plexus contributes to changes in CSF $[\text{Na}^+]$.
3. Increased CSF $[\text{Na}^+]$ acting through aldosterone increases expression of ENaC subunits in different brain cardiovascular regulatory centers.
4. Expression of ENaC subunits is enhanced and not downregulated by high salt in the kidneys and brain of Dahl S rats due to genetic mutations in the SGK1 gene, and contributes to increased transport of Na^+ into the CSF and increased neuronal response to Na^+ .

2.2 OBJECTIVES

2.2.1 Studies in Wistar rats

1. Study the expression of ENaC subunits in the brain.
2. Study ENaC mediated Na⁺ transport in the choroid plexus.
3. Study the effect of increases in CSF [Na⁺] on expression of ENaC subunits and its regulation by aldosterone in the brain.

2.2.2 Studies in Dahl rats

1. Study the expression of ENaC subunits in the kidneys and brain of Dahl S and R rats on regular versus high salt diet.
2. Study the effect of high salt diet on Na⁺ transport by the choroid plexus in Dahl S versus R rats.
3. Investigate the possible presence and significance of polymorphisms in the SGK1 gene between Dahl S and Dahl R rats.

OUTLINE OF APPROACH TO PROBLEM

The following manuscripts detail our categorical approach to test and prove/disprove our hypotheses.

1. Manuscript # 1: **Amin MS**, Reza E, El-Shahat E, Wang H, Tesson FC, Leenen FH. Enhanced expression of epithelial sodium channels in the renal medulla of Dahl S rats. *Canadian Journal of Physiology and Pharmacology*, 2011, 89: 159-168 (*Amin et al. 2011*).
2. Manuscript # 2: **Amin MS**, Wang HW, Reza E, Whitman SC, Tuana BS, Leenen FH. Distribution of epithelial sodium channels and mineralocorticoid receptors in cardiovascular regulatory centers in rat brain. *American journal of physiology, Regulatory, Integrative and Comparative Physiology* 2005; 289: R1787-1797 (*Amin et al. 2005*).
3. Manuscript # 3: Wang HW, **Amin MS**, El-Shahat E, Huang BS, Tuana BS, Leenen FH. Effects of central sodium on epithelial sodium channels in rat brain. *American Journal of Physiology: Regulatory, Integrative and Comparative Physiology*, 2010; 299, R222-233 (*Wang et al. 2010a*).
4. Manuscript # 4: **Amin MS**, Reza E, Wang H, El-Shahat E, White R, Huang BS, Tesson FC, Leenen FH. Expression of epithelial sodium channels and regulatory genes in the brain of Dahl S and R rats. (Submitted to 'Neurochemistry international')
5. Manuscript # 5: **Amin MS**, Reza E, Wang H, Leenen FH. Sodium transport in the choroid plexus and salt sensitive hypertension. *Hypertension* 2009; 54(4):860-867(*Amin et al. 2009*).

6. Manuscript # 6 (review): Huang BS, **Amin MS**, Leenen FH. The central role of the brain in salt-sensitive hypertension. *Current opinion in cardiology* 2006; 21:295-304 (Huang et al. 2006a).

3.1 MANUSCRIPT # 1: ENHANCED EXPRESSION OF EPITHELIAL SODIUM CHANNELS IN THE RENAL MEDULLA OF DAHL S RATS.

Md Shahrier Amin^{a,c}, Erona Reza^{a,c}, Esraa El-Shahat^{a,b}, Hong-Wei Wang^a, Frédérique Tesson^{b,d} and Frans HH Leenen^{a,c}.

^aHypertension Unit, and

^bLaboratory of Genetics of Cardiac Disease, University of Ottawa Heart Institute, Ottawa, Ontario, Canada.

^cDepartment of Cellular and Molecular Medicine, and

^dFaculty of Health Sciences, University of Ottawa, Ottawa, Ontario, Canada

Status

This article has been published in the 'Canadian Journal of Physiology and Pharmacology, 2011, 89: 159-168 (*Amin et al. 2011*).

3.1.1 RELEVANCE TO OVERALL PROJECT

In this study we first evaluated the distribution of ENaC in the kidneys and tested our hypothesis #4, regarding evaluating the expression of ENaC subunits in the kidneys of Dahl rats. We also generated and characterized our own antibodies for ENaC subunits. Previous studies had shown that ENaC expression was dysregulated in Dahl S rats. Concurrent to our studies, two others were also published showing similar results. However, none of them evaluated distribution of ENaC and expression in different areas of the kidneys.

3.1.2 CONTRIBUTION

Responsible for the overall project and performed the following:

1. Responsible for overall co-ordination of the project.
2. Generated anti ENaC antibodies in rabbits, as these were not commercially available at the time.
3. Performed all of the protein assays such as immunoblots and immunohistochemistry and analyses.
4. Assisted in tissue collection, processing and data gathering for most measurements.
5. Prepared the manuscript.

3.1.3 Abstract

Inner medullary collecting duct (IMCD) cells from salt-sensitive (S) Dahl rats transport twice more Na⁺ than cells from salt-resistant (R) rats, possibly related to dysregulation of the renal epithelial sodium channel (ENaC). The effect of high salt diet on ENaC expression in the inner medulla of S versus R rats has not yet been studied. Young, male S and R rats were placed on regular (0.3%) or high (8%) salt for 2 or 4 weeks. mRNA and protein expression of ENaC subunits were studied by RT-PCR and immunoblotting. Intracellular distribution of the subunits in the IMCD was evaluated by immunohistochemistry. On regular salt, abundance of the mRNA of β and γ ENaC was higher in the medulla of S rats versus R rats. This was associated with greater protein abundance of 90 kDa γ ENaC and higher immunoreactivity for both α and γ ENaC. High salt did not affect mRNA abundance in either strain and decreased apical staining of γ ENaC in IMCD of R rats. In contrast, high salt did not affect the higher apical staining for α ENaC and further increased the apical membrane staining for β and γ ENaC in the IMCD of S rats. Expression of ENaC subunits is enhanced in the medulla of S versus R rats on regular salt, and further increased on high salt. Increased apical localization of β and γ ENaC may contribute to greater retention of sodium in S rats on high salt diet.

Keywords

Kidney, Salt, ENaC, RT-PCR, immunohistochemistry.

3.1.4 Introduction

Blood pressure sensitivity to salt is seen in 40-60% of patients with essential hypertension and in ~20-30% of the general population (Franco et al. 2006). Genetic analyses of human monogenic hypertension and some common variants of essential hypertension identified the epithelial sodium channel (ENaC) to be associated with salt sensitivity (Kreutz et al, 1997; Luft 2004; Iwai et al. 2002). Expression of ENaC in the kidneys is affected by dietary salt, and may play a major role in determining the way the body handles sodium (Rossier et al. 2002; Masilamani et al. 2002). Better understanding of the mechanisms contributing to salt sensitivity is crucial to developing new strategies for treatment.

ENaC are members of the DEG/ENaC family of cation selective ion channels (Canessa et al. 1995; Canessa et al. 1994). The functional channel is thought to be a heteromultimer of three subunits α , β and γ with a 2:1:1 (Firsov et al. 1998; Kosari et al. 1998) or 3:3:3 stoichiometry (Snyder et al. 1998). Individual ENaC subunits show a tissue specific expression and regulation. Channels with all three subunits show maximal function but different combinations of subunits also form active channels and post-translational modifications affecting one or more subunits can also affect Na^+ transport. In the collecting ducts of the kidneys, all three subunits are expressed and ENaC mediates transport of Na^+ along an electrochemical gradient created by basolateral $\text{Na}^+\text{K}^+\text{ATPase}$ (Kudo et al. 1990; Palmer et al. 1980). The final rate limiting steps of sodium reabsorption in the distal nephron segments are mediated by ENaC. The aldosterone-mineralocorticoid receptor (MR) complex increases ENaC surface expression and activity by increasing transcription of the subunits and by increasing transcription of

regulators which in turn activate the channel (Snyder, 2005; Snyder et al. 2002). Among these are the serum and glucocorticoid regulated kinase-1 (SGK1), an early aldosterone inducible protein kinase, which upregulates ENaC activity by phosphorylating neural precursor cells expressed developmentally down-regulated-4 like gene (Nedd4L), thereby reducing the interaction between ENaC and Nedd4L (Snyder et al. 2004; Snyder et al. 2002).

In Dahl S rats the expression and function of ENaC appear to be dysregulated. The conductive permeability of the apical membrane to Na^+ and the rate of Na^+ transport is higher in monolayers of cultured cells from inner medullary collecting ducts of S versus R rats, suggesting that ENaC are intrinsically different or differently regulated in S and R rats (Husted et al. 1996, 1997). Comprehensive screening did not show any variations in the ENaC genes between S and R rats (Shehata et al. 2007). However, high salt for 4 weeks caused the expected decrease in mRNA levels of α ENaC in whole kidneys of R rats, but caused modest increases of α , β and γ ENaC in S rats (Aoi et al. 2007). In a more recent study, high salt for 4 weeks did not affect α ENaC and increased both mRNA and protein of β and γ ENaC in the cortex of Dahl S rats (Kakizoe et al. 2009).

All previous studies on renal ENaC in Dahl rats only studied homogenates of whole kidneys or the renal cortex, and did not evaluate the medulla and distribution of the proteins. Whether or not mRNA, protein abundance and distribution of ENaC and regulators such as SGK1 and Nedd4L are differently regulated in the renal medulla of S and R rats has not yet been studied. We hypothesized that enhanced ENaC expression is present in the renal medulla of S rats on regular salt intake and persists on high salt. To test this hypothesis, we evaluated the mRNA abundance, protein abundance and

intracellular distribution of ENaC subunits in the renal medulla of S and R rats on regular versus high salt for 2 or 4 weeks.

3.1.5 Materials And Methods

Male 3-4 weeks old Dahl salt sensitive (SS/Jr-Hsd: S) and Dahl salt resistant (SR/Jr-Hsd: R) rats were purchased from Harlan Sprague-Dawley (Indianapolis, Indiana). The rats were housed two per cage under standard conditions on a 12 hour light-dark cycle at 24°C and were allowed a 3-5 days acclimatization period on normal rat chow and tap water before entering the study. All procedures were performed according to the guidelines of the Canadian Council on Animal Care and were approved by the University of Ottawa Animal Care Committee.

3.1.5.1 Experimental protocol

Dahl S and R rats were assigned randomly to either regular (120 $\mu\text{mol Na}^+/\text{gm}$) or high (1,370 $\mu\text{mol Na}^+/\text{gm}$) salt diet for 2 or 4 weeks (n=6-8 per group). At the end of 2 or 4 weeks of salt diet, BP was recorded and blood samples obtained for plasma aldosterone and plasma angiotensin II. Under pentobarbital anesthesia the rats were perfused transcardially first with cold PBS (pH 7.4) to drain all the blood. This was followed by perfusion over 20-30 minutes with ~300-400 ml per rat of RNase free cold PBS (pH 7.4) for RNA and protein extraction or 4% paraformaldehyde plus 0.05% glutaraldehyde in phosphate buffer (pH 7.4) for immunohistochemistry.

3.1.5.2 mRNA studies

Real time PCR: Total RNA was isolated from the kidney medulla as described previously (Amin et al. 2005). Specific primers for α , β and γ ENaC and phosphoglycerate kinase1 (PGK1) were the same as described previously (Amin et al. 2005, Umemura et al. 2006). The amplicon length of the PCR products were: PGK1 (263 bp), α ENaC (429

bp), β ENaC (220 bp), γ ENaC (301 bp). Real-time PCR was performed with Roche Light Cycler using Fast start DNA master SYBR Green I dye (Roche Diagnostics, QC, Canada). The PCR conditions were set as follows: initial at 95°C for 10 min to activate Taq polymerase and followed by 45 cycles of denaturation at 95° C for 5 sec; annealing for 10 sec at 62°C for PGK and α ENaC, and 65°C for β and γ ENaC. Extension time was determined by target amplicon length/25. The specificity of the real-time PCR products were determined by both melting curve analysis and agarose gel electrophoresis. External standard curves were created using serial dilutions of plasmids containing cDNA fragment for different gene with the same PCR conditions as described above. mRNA expression was normalized to PGK1 mRNA levels.

3.1.5.3 Protein studies

ENaC antibodies were generated as described previously (Ergonul et al. 2006, Masilamani et al. 1999).

Characterization of the antibodies: The α ENaC antibodies detected bands at ~80 (uncleaved) kDa. In addition, bands at 120, 50 and 37 kDa (aggregates or cleaved inactive fragments) were variably detected, but not quantifiable in most samples. α ENaC protein was also not consistently detectable in all inner medulla samples. The β ENaC antibody detected a major band at 85 kDa and the γ ENaC antibody detected bands at ~90 (uncleaved) and 70 (cleaved active fragment) kDa. These bands were abolished by pre-adsorbition with the immunizing peptides. Omission of the primary antibody or co-incubation with the immunizing peptide also abolished immunostaining. As a positive control, the effects of low (10 μ mol Na⁺/gm) versus regular salt diet for 2 weeks were studied in Wistar rats. Consistent with previous studies (Masilamani et al. 1999, Frindt et

al. 2007), low salt diet for 2 weeks increased the abundance of 80kDa α ENaC by ~40%, β ENaC by ~70% and 70kDa band of γ ENaC by ~20% in the inner medulla and also increased the apical immunoreactivity in the collecting ducts (Fig 3.1-1).

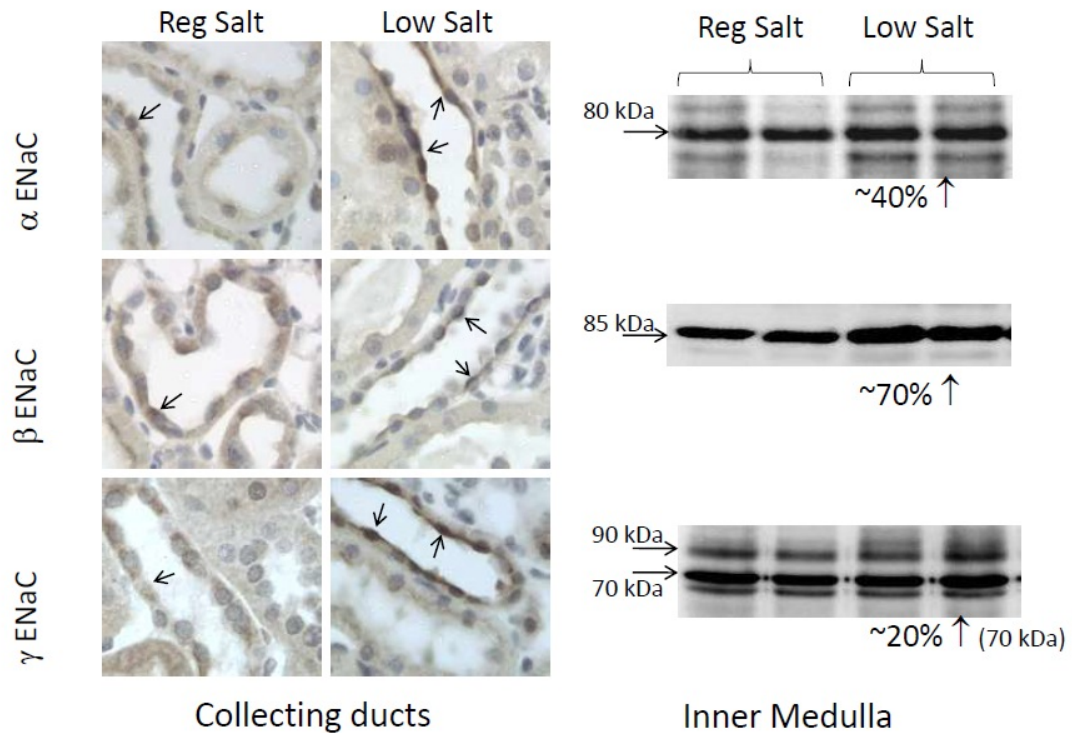


Figure 3.1-1: Protein abundance in the inner medulla and immunoreactivity to α , β and γ ENaC in the collecting ducts in Wistar rats after 2 weeks of regular versus low salt diet. Diffuse and mostly cytoplasmic staining was noted in the collecting ducts of Wistar rats on regular salt diet. Low salt increased apical immunoreactivity in the collecting ducts (arrows) and abundance of 80kDa α ENaC, 85 kDa β ENaC and 70kDa γ ENaC proteins in the inner medulla.

Immunoblotting: Whole protein was extracted from macroscopically dissected inner medullas and homogenized in ice-cold solution (pH 7.5) containing 300 mM sucrose and 10 mM Triethanolamine (ENaC) containing 1% protease inhibitor cocktail (Sigma). The

membranes were probed with the respective primary antibodies overnight at 4°C [α ENaC and Nedd4L - 1:1000, β and γ ENaC - 1:5000], followed by incubation in goat anti-rabbit secondary antibody conjugated with horseradish peroxidase (1:5000, Santa Cruz biotechnology, California). The membranes were stripped and re-probed with anti- β actin antibody (Sigma). Signal was developed with ECL⁺ system (Perkin Elmer) and visualized using Alpha-Ease system. The results are expressed in arbitrary units (percent change of normalized densitometry of target gene versus β actin from control).

Immunohistochemistry: Sagittal sections were cut on a rotary microtome at a thickness of 7 μ m. Antigen retrieval was done by heating the sections with 1.0 mM Tris (pH 8.0) at 90°C for 25 min and incubation in 1% sodium borohydride for 30 min. Non-specific IgG binding and endogenous peroxidase activity were blocked by incubation in 50mM NH₄Cl for 30 min and 0.5% H₂O₂ in 20% methanol in PBS for 30 min. Sections were blocked with a cocktail of 1% normal goat serum, 0.02% gelatin, 0.05% Triton X-100 and 1% BSA in PBS (pH 7.4) for 2 hours. Endogenous biotin was blocked with avidin-biotin blocking solution (Vector Laboratories, Burlington, ON). The sections were then incubated for 12 hours with the respective primary antibodies diluted appropriately in the blocking solution (α ENaC 1:250, β ENaC and γ ENaC 1:100). Further processing was done with Vectastain Elite ABC kit for rabbit IgG and visualized using DAB kit with Nickel enhancement (Vector Laboratories, Burlington, ON). Slides were counterstained with Vector hematoxylin, dehydrated, cleared and coated with Permount (Fisher Scientific, Ottawa, ON).

Images were captured using a Spot digital camera attached to a high resolution bright-field transmitted light microscope (Olympus BX60). The inner medullary collecting ducts

(IMCD) were identified based on predominance of cuboidal cells, centrally located nucleus with clear outline and a large sized lumen (Mills 2008). Tubules that had uniformity of staining and were sectioned in the same plane were used for analysis. Immunostaining was assessed blindly by two individuals (MSA and ER). A score of 1 (<30% cells and/or mild staining intensity), 2 (30-70% cells stained and moderate staining intensity) or 3 (>70% cells stained with strong staining intensity) was given for immunostaining in the apical membranes and in the cytoplasm.

3.1.5.4 Statistical Analysis

Values are presented as mean \pm SEM. All comparisons between groups were determined by two way analysis of variance (ANOVA) followed by the Student-Newman-Keuls test where applicable. A value of $p < 0.05$ was considered statistically significant.

3.1.6 Results

3.1.6.1 Blood pressure, plasma aldosterone and angiotensin II (Table 3.1-1)

On regular salt, mean arterial pressure (MAP) tended to be higher in S compared to R rats. High salt intake did not affect MAP in R rats but increased MAP moderately after 2 weeks and markedly after 4 weeks in S rats. On regular salt, R rats had higher plasma Ang II but lower plasma aldosterone than S rats. On high salt intake, plasma Ang II was decreased particularly in R rats and plasma aldosterone in S rats.

3.1.6.2 ENaC expression in the renal medulla

α ENaC: Abundance of α ENaC mRNA was not significantly different in the renal medulla of S and R rats on regular salt diet (Table 3.1-2). However, apical immunoreactivity in IMCDs was greater in S rats on regular salt diet at both 2 and 4 weeks and cytoplasmic reactivity higher at 4 weeks (Table 3.1-3, Fig 3.1-2). High salt diet did not affect α ENaC mRNA expression in either strain and immunoreactivity remained increased in S rats (Tables 3.1-2 and 3.1-3, Figure 3.1-2).

β ENaC: The abundance of β ENaC mRNA was similar in the medulla of both strains after 2 weeks, but significantly higher in S rats after 4 weeks; β ENaC protein abundance and cytoplasmic staining were similar (Tables 3.1-2 and 3.1-3, Figure 3.1-3). On high salt, the higher mRNA abundance persisted in S rats. High salt did not affect β ENaC protein in either strain, but decreased apical immunoreactivity in IMCDs of R rats and transiently increased apical staining in S rats (Tables 3.1-2 and 3.1-3, Figure 3.1-3).

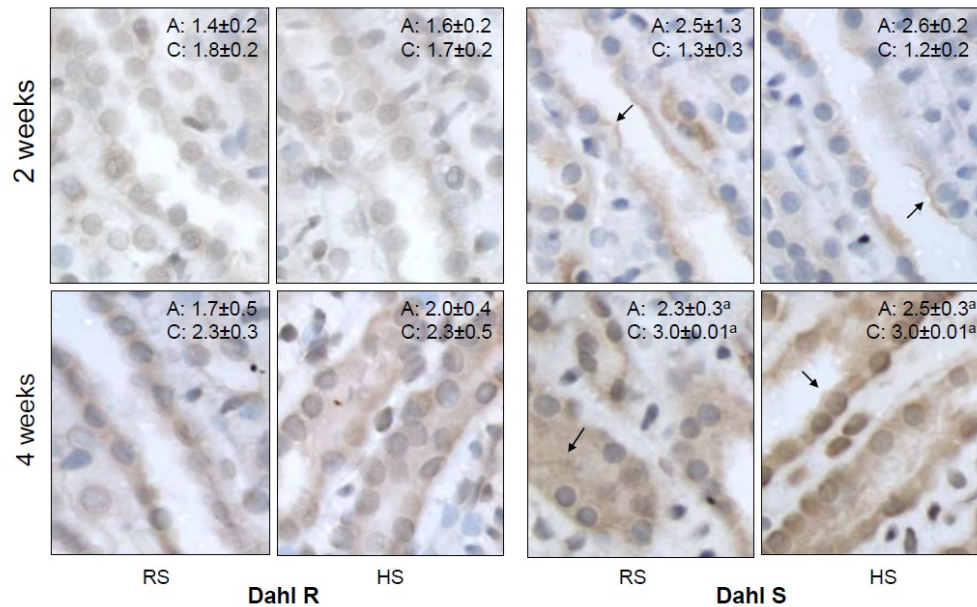


Figure 3.1–2: Immunoreactivity to α ENaC in the renal medulla. Immunoreactivity to α ENaC in the inner medulla of Dahl R and S rats after 2 or 4 weeks on regular (RS) or high (HS) salt diet. In R rats, the staining is modest at 2 and 4 weeks, and similar on both salt diets. In contrast, distinct apical immunoreactivity is notable in the IMCD of S rats at 2 weeks and is not affected by a high salt diet. The higher abundance of ENaC subunits in S rats is more apparent after 4 weeks, although at this point the apical immunoreactivity is less contrasting due to the increased cytoplasmic staining. Arrows show apical immunoreactivity in IMCDs in S rats.

γ ENaC: On regular salt γ ENaC mRNA abundance was similar in the two strains at 2 weeks, but S rats had greater abundance of the mRNA at 4 weeks and of both protein fractions at both 2 and 4 weeks (Tables 3.1-2 and 3.1-3, Figure 3.1-4). Apical membrane staining was similar in the IMCDs of the 2 strains on regular salt. In R rats, high salt intake caused a modest, transient increase in the 90 kDa fraction but not in the active 70 kDa band or in staining of γ ENaC. In contrast, high salt intake did not affect the elevated

mRNA and protein of S rats and clearly increased both cytoplasmic and apical immunoreactivity in IMCDs of S rats (Tables 3.1-2 and 3.1-3, Figure 3.1-4).

Fig 3.1-3A: β ENaC protein abundance in inner medulla

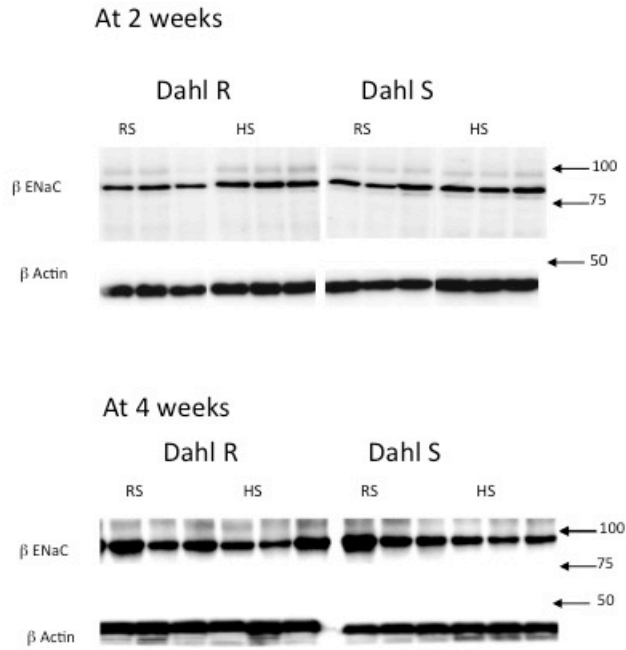


Fig 3.1-3B: β ENaC immunoreactivity in inner medulla

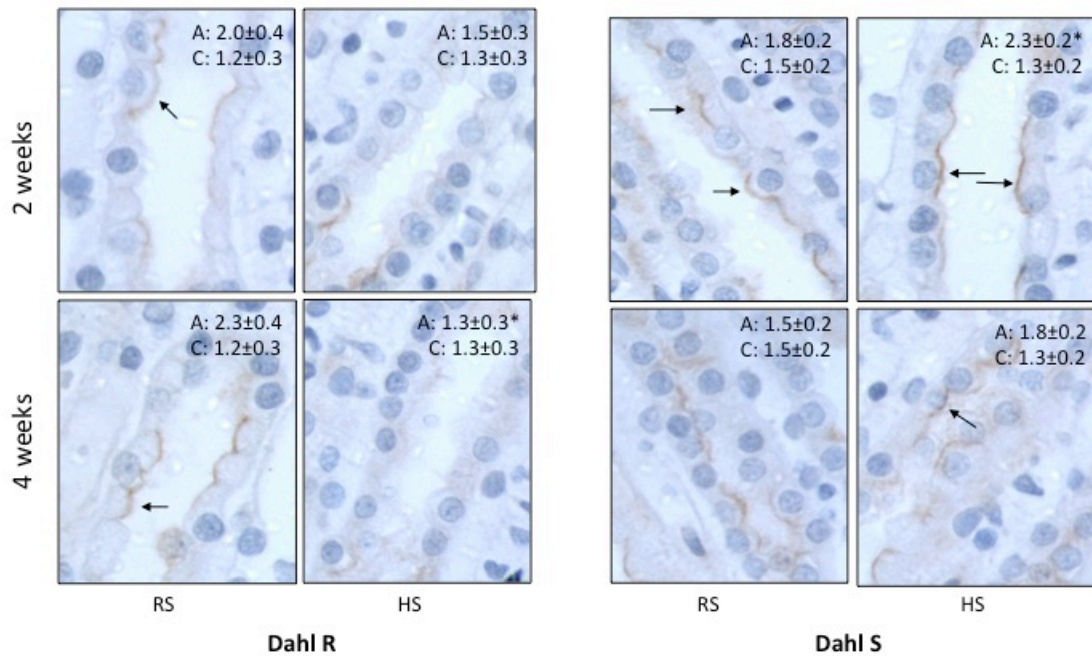


Figure 3.1–3: β ENaC abundance and immunoreactivity in the renal medulla of Dahl R and S rats after 2 or 4 weeks on regular (RS) or high (HS) salt diet. 3.3-3A. Abundance of β ENaC protein in the medulla. Both strains had similar abundance of the protein which was not affected by high salt. 3.3-3B. Distribution of β ENaC in the IMCDs. Apical staining was decreased in the IMCDs of Dahl R on high salt diet, but became more prominent in Dahl S. Arrows show immunoreactivity in IMCDs.

Fig 3.1-4A: γ ENaC protein abundance in inner medulla

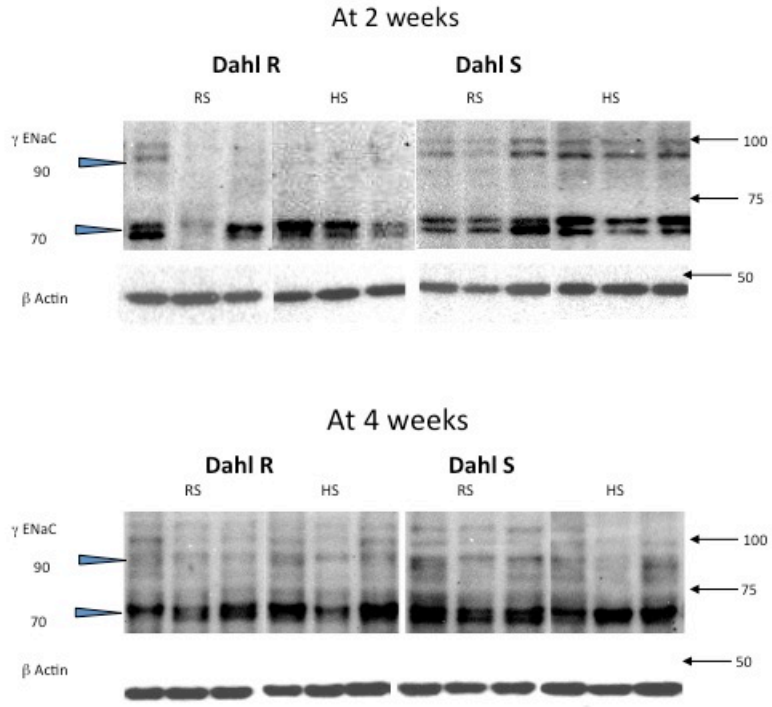


Fig 3.1-4B: γ ENaC immunoreactivity in inner medulla

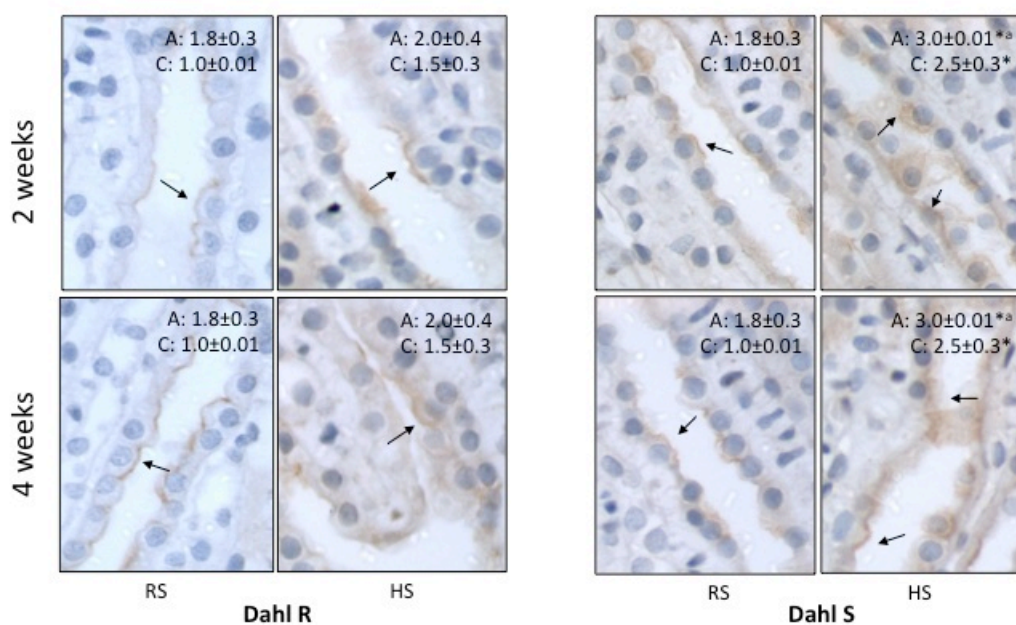


Figure 3.1–4: γ ENaC protein abundance and immunoreactivity in the inner medulla of Dahl R and S rats after 2 or 4 weeks on regular (RS) or high (HS) salt diet. 3.1-4A. Abundance of γ ENaC protein in the medulla. Dahl S have greater abundance of the protein at both 2 and 4 weeks. 3.1-4B. Distribution of γ ENaC in the IMCDs. Modest apical and cytoplasmic staining can be seen in the IMCDs which is significantly increased by high salt in Dahl S.

3.1.7 Discussion

The current study shows as major new findings that on regular salt, abundance of mRNA (β and γ ENaC), protein (γ ENaC) and apical staining (α ENaC) of ENaC is higher in the medulla of S rats. On high salt, in S rats the higher abundance persists, and apical membrane staining further increases for β ENaC at 2 weeks and for γ ENaC at both 2 and 4 weeks.

3.1.7.1 Renal ENaC on regular salt

ENaC subunits are expressed predominantly along the aldosterone sensitive distal nephron (Duc et al. 1994) and are the major Na^+ transporter in the IMCD (Frindt et al. 2007, Volk et al. 1995). ENaC expression and distribution in the IMCD of R and S rats has not been studied before. In the medulla of S rats β and γ ENaC mRNA abundance was higher and associated with more γ ENaC protein and higher apical membrane immunoreactivity to α ENaC in the IMCD. Increased abundance at the cell surface of active α ENaC alone has been shown to be sufficient for increased ENaC activity (Rotin et al. 1994). These expression data and previous in vitro studies showing increased rate of Na^+ -transport in monolayers of cultured IMCD in S versus R rats (Husted et al. 1996, Husted et al. 1997), suggest that in Dahl S higher ENaC expression may contribute to increased Na^+ reabsorption, even on regular salt diet.

3.1.7.2 Renal ENaC on high salt

In Wistar or Sprague-Dawley rats, high salt diet causes time-dependent, modest decreases in abundance of one or more subunits in the medulla (Farjah et al. 2003, Loffing et al. 2000b, Masilamani et al. 1999, Masilamani et al. 2002). In R rats, Aoi et al (Aoi et al. 2006, Aoi et al. 2007) showed that high salt for 4 weeks decreased mRNA levels of

α ENaC in the whole kidney. Our results in R rats show only modest changes by high salt that may reflect at the most a minor decrease in ENaC activity in different nephron segments. The magnitude of the changes appears similar to those in Wistar rats, and is substantially less than low versus regular salt (Figure 3.1-1) suggesting that regular salt intake already causes most of the decrease.

In S rats, Aoi et al (Aoi et al. 2006, Aoi et al. 2007) reported increased mRNA expression of all three subunits in whole kidneys after 4 weeks high salt. In contrast, Kakizoe et al reported no change in α ENaC mRNA but an increase in β and γ ENaC mRNA and protein in the cortex (Kakizoe et al. 2009). These studies (Kakizoe et al. 2009, Aoi et al. 2007, Aoi et al. 2006) did not evaluate expression in the medulla nor intracellular distribution. In the present study, on high salt diet the higher mRNA and protein expression of β and γ subunits in the medulla of S rats and abundance of α ENaC in the apical membrane of IMCDs persisted, whereas apical staining of β and γ ENaC increased. Increased apical staining in the medulla of S versus R rats – for only α ENaC on regular salt and for all three subunits on high salt – may reflect enhanced transport to the membrane and/or decreased removal from the membrane. These changes are distinctly different from those of salt-resistant strains and indicate that high salt in S rats affects mechanisms that regulate sub-cellular distribution and therefore presumably activity of the subunits and Na^+ -transport.

3.1.7.3 Regulators of renal ENaC

The absence of differences in the regulatory and coding sequences of ENaC genes between S and R rats (Shehata et al. 2007) suggests that the greater abundance on regular salt and the opposite response i.e. persistence or increase with high salt in kidneys of

Dahl S is due to differential regulation of the ENaC subunits. Aldosterone acting through the mineralocorticoid receptor is a major regulator of ENaC. While studies in the early '90s showed lower levels for plasma aldosterone in S versus R (Cover et al. 1995), recent studies show similar or higher levels in S rats (Manger et al. 2009, Takeda et al. 2007). Plasma aldosterone concentration decreased with high salt in both strains, consistent with previous studies (Aoi et al. 2007, Farjah et al. 2003) but remained somewhat higher in S. This suggests similar regulation of plasma aldosterone by high salt. In contrast, the activity of the intra-renal renin-angiotensin-aldosterone system is increased by high salt intake in S rats (Zhu et al. 2009), and may contribute to increased ENaC expression in Dahl S on high salt. Classically aldosterone increases expression of α ENaC in the kidney and of β and γ ENaC in the colon (Duc et al. 1994). This pattern may be disrupted in S rats and aldosterone contributes to the higher expression of β and γ ENaC in the medulla of S rats. Alternatively, other regulators such as vasopressin may contribute to the dysregulated expression of ENaC subunits in S versus R rats on high salt diet. High salt does not affect plasma vasopressin levels in R rats, but increases vasopressin levels by ~2.6 fold in S rats (Wainford & Kapusta 2010). Vasopressin affects post-transcriptional expression of the α and γ ENaC subunits (Perlewitz et al. 2010) and increases amiloride blockable luminal Na^+ transport across the IMCD (Kudo et al. 1990).

3.1.7.4 Perspectives

Expression of ENaC subunits is enhanced in the IMCD of S versus R rats on regular salt diet and is further enhanced by high salt diet. This supports the concept that in genetically predisposed individuals increased retention of Na^+ by the renal tubules contributes to salt sensitivity. Since Dahl S rats were not found to have any mutations in ENaC genes, tt

remains to be established whether increases in aldosterone-MR activation or other regulators are responsible for these changes. Functional studies are needed to assess whether this higher expression is associated with increased ENaC activity and leads to greater Na⁺ reabsorption in S rats. Unraveling the mechanisms that contribute to more apical localization of ENaC in salt sensitive individuals may provide new strategies to prevent and treat hypertension.

3.1.8 Acknowledgement

The authors would like to acknowledge Ms. Danielle Oja for her excellent skills in assisting in the preparation and formatting of this article. Dr. Leenen holds the Pfizer Chair in Hypertension Research, an endowed chair supported by Pfizer Canada, University of Ottawa Heart Institute Foundation and Canadian Institutes of Health Research.

3.1.9 Sources of Funding

This research was supported by operating grant FRN: MOP-74432 from the Canadian Institutes of Health Research. Md Shahrier Amin was supported by a Pfizer/CIHR/Canadian Hypertension Society doctoral research award and program grant PRG5275 from the Heart and Stroke Foundation of Ontario.

**3.2 MANUSCRIPT # 2: DISTRIBUTION OF
EPITHELIAL SODIUM CHANNELS AND
MINERALOCORTICOID RECEPTORS IN
CARDIOVASCULAR REGULATORY CENTERS
IN RAT BRAIN.**

Md Shahrer Amin¹, Hong-Wei Wang¹, Erona Reza, Stewart C Whitman, Balwant S
Tuana, Frans H H Leenen²

Hypertension Unit, University of Ottawa Heart Institute, Ottawa, Ontario, Canada.

1. Joint primary authors.

2. Pfizer Chair in Hypertension Research, an endowed chair supported by Pfizer Canada,
University of Ottawa Heart Institute Foundation and Canadian Institutes of Health
Research.

Running head

Brain ENaC and MR

Status

This article was published in the American Journal of Physiology, Regulatory, Integrative
and Comparative Physiology, 2005; Vol. 289: Pages R1787-1797.

3.2.1 Relevance to overall project

This is our first study to test hypothesis #1. We evaluated the expression of ENaC subunits in the brain at both the messenger and protein levels and mapped the areas with prominent expression.

3.2.2 Contribution

Responsible for the overall project and performed the following:

1. Design and planning of the experiments
2. Tissue collection and processing for the entire experiment.
3. Set up of the methods and punching of specific brain areas for RT-PCR.
4. Performed and analyzed all the immunohistochemistry and immunofluorescence experiments.
5. Compilation of all data and preparation of the manuscript.

3.2.3 Abstract

Epithelial sodium channels (ENaC) are important for regulating sodium transport across epithelia. Functional studies indicate that neural mechanisms acting through mineralocorticoid receptors (MR) and sodium channels – presumably ENaC – are crucial to the development of sympathoexcitation and hypertension in experimental models of salt sensitive hypertension. However, expression and localization of the ENaC in cardiovascular regulatory centers of the brain have not yet been studied. RT-PCR and immunohistochemistry were performed to study ENaC and MR expression at the mRNA and protein levels respectively. Both mRNA and protein for α , β and γ ENaC subunits and MR were found to be expressed in the rat brain. All three ENaC subunits and MR were present in the supraoptic nucleus and magnocellular paraventricular nucleus, hippocampus, choroid plexus, ependyma and brain blood vessels suggesting the presence of multimeric channels and possible regulation by mineralocorticoids. In most cortical areas, thalamus, amygdala and suprachiasmatic nucleus notable expression of ENaC γ was undetectable, whereas ENaC α and β were abundantly expressed pointing to the possibility of a heterogeneous population of channels. The findings suggest that stoichiometrically different populations of ENaC may be present in both epithelial and neural components in the brain, which may contribute to regulation of CSF and interstitial $[\text{Na}^+]$ as well as neuronal excitation.

Key words

ENaC, MR, RT-PCR, Immunohistochemistry

3.2.4 Introduction

Epithelial sodium channels (ENaC) are members of the DEG/ENaC family of voltage-insensitive, amiloride blockable cation channels. They are generally composed of three subunits (α , β , γ), approximately 650-700 amino acids in length. ENaC are present in e.g. the kidney, colon, lungs, sweat and salivary gland ducts – where expression at the apical membrane mediates unidirectional absorption of Na^+ (Duc et al. 1994, Garty & Palmer 1997, Renard et al. 1995). In tongue fungiform papillae (Lin et al. 1999) and baroreceptor mechanotransducer of the aortic arch (Drummond et al. 1998) ENaC contribute to the electrogenic movement of Na^+ . Expression of the subunits was also reported in the retina (Brockway et al. 2002, Dyka et al. 2005), cochlea (Couloigner et al. 2001, Zhong & Liu 2004) sensory nerve endings in the rat foot pad (Drummond et al. 2000), as well as trigeminal mechanosensory neurons (Fricke et al. 2000). Their function in these tissues has not yet been clarified. Other members of the DEG/ENaC superfamily such as Brain Na^+ Channels (BNaC) and Acid Sensing Ion Channels (ASIC) are highly expressed in the central nervous system (Alvarez de la Rosa et al. 2003). So far, ENaC expression has not been demonstrated in the rat brain. A variety of functional studies suggest the presence of specific Na^+ channels, presumably ENaC, in the brain that are activated by aldosterone or high salt diet and blocked by amiloride or benzamil. In Wistar rats, intracerebroventricular (icv) infusion of aldosterone or Na^+ rich aCSF increases blood pressure (BP) and renal sympathetic nerve activity (RSNA) (Wang et al. 2003a). In Dahl S (salt sensitive) but not R (salt resistant) rats, high salt diet or icv infusion of aldosterone causes sympathoexcitation and hypertension. The blood brain barrier (BBB) in Dahl S rats is 5-8 times more permeable to Na^+ than that in Dahl R rats (Simchon et al. 1999).

Increases in CSF Na^+ are observed in Dahl S rats but not Dahl R rats on high salt diet and precede changes in BP by 1-2 days (Huang et al. 2004). Importantly, the responses to aldosterone or Na^+ rich aCSF in Wistar rats and to aldosterone or high salt diet in Dahl S rats can all be prevented by icv infusion of benzamil or spironolactone (Wang et al. 2003a). These findings suggest that mineralocorticoid receptor (MR) mediated activation of sodium channels in the brain is responsible for mechanisms leading to increased sympathetic outflow and hypertension.

MR expression is well characterized in the brain (Ahima & Harlan 1991). In contrast, ENaC expression in the brain has not yet been demonstrated. The objectives of the current studies were therefore, 1) to evaluate expression of ENaC subunits and their relative abundance in different brain areas and nuclei, and 2) to assess whether MR are present in the same areas as ENaC.

3.2.5 Materials and Methods

Adult male Wistar rats (Charles River, Montreal, PQ, Canada) were housed under standard conditions (12 hour light cycle, ambient temperature $23 \pm 2^{\circ}\text{C}$) and received standard laboratory chow and tap water *ad libitum* for 5 days before entering the study. All procedures were carried out in accordance with the guidelines of the Canadian Council on Animal Care, which conform to NIH guidelines and were approved by the University of Ottawa Animal Care Committee.

3.2.5.1 RT-PCR

RNA isolation and RT-PCR: Brains and kidneys from 6 rats were rapidly removed and quickly frozen in liquid nitrogen and stored at -80°C until use. Whole kidney and hypothalamus were homogenized in TRIzol Reagent (Invitrogen, Burlington, ON) using a polytron. Total RNA was isolated from tissues according to the manufacturer's instructions. In an additional experiment, 6 rats were perfused with chilled DEPC-treated PBS (pH 7.4) under pentobarbital anesthesia. The brains were removed, immediately frozen in isopentane and placed on dry ice and then stored at -80°C until use. Serial 80 μm thick coronal slices were cryosectioned and the brain punches of specific areas were taken with pre-chilled 25 μL Drummond Microdispensers (Drummond Scientific Company, USA). The tissue pellet was homogenized in 0.2 ml TRIzol Reagent by using a pestle (Bel-Art-Products, Pequannock, NJ) driven by a pellet pestle motor and 0.3ml TRIzol Reagent was then added. To eliminate potential genomic DNA contamination, 20 μg total RNA from the kidney, hypothalamus or total RNA from the different punched brain areas was treated with DNase I (Ambion, Inc., Austin, TX) before the reverse transcription reaction (RT).

cDNAs were synthesized by incubation with 200U Superscript II RNase H⁻ Reverse Transcriptase (Invitrogen, Burlington, ON) at 42° C for 50 min. 2 µL of the above RT reaction were subjected to PCR as follows: an initial denaturation step at 94° C for 2 min, then 40 cycles of 94° C for 50 sec, 57° C for 45 sec, and 72° C for 1 min. Specific primers for α , β and γ ENaC subunits, MR and the house keeping gene phosphoglycerate kinase (PGK) (Table 3.2-1) were designed based on published sequence information (Gene Bank accession Nos. X70947, X77932, X77933, M36074 and NM053291 respectively). All PCR products of the ENaC subunits (α , β and γ) were sequenced and analyzed for homology with the published rat kidney ENaC sequences.

Real time RT-PCR: Real-time PCR amplifications were performed with a Roche Light Cycler using Fast Start DNA Master SYBR Green I (Roche Diagnostics, Germany). 2µL of 1:10 diluted RT product from kidney or hypothalamus or undiluted RT product of different brain areas were used for the PCR reaction. The primers for ENaC α , β , γ subunits, MR and PGK were the same as the primers used in conventional RT-PCR. The real-time PCR conditions were as follows: 95° C for 10 min, followed by 45 cycles of denaturation at 95° C for 5 sec, annealing the primers to the target for 5 sec at 65° C for the α and β ENaC and at 62° C for γ ENaC, MR and PGK. An extension step was performed at 72° C and the extension time was determined by the formula of amplicon length/25 sec. The specificity of real-time PCR products was documented with a melting curve analysis. In addition, a high resolution gel electrophoresis was performed which resulted in the amplification of a single product of the appropriate size (Table 3.2-1). Real-time RT-PCR analysis was performed in duplicate.

Table 3.2–1: Primer sequences used to detect α , β and γ ENaC and MR mRNA transcript.

<i>Gene</i>		<i>Sequence</i>	<i>Amplicon Length</i>
α -ENaC	Forward	5'-GTTCTGTGACTACCGAAAGCAGAG-3'	429bp
	Reverse	5'-CGTAGCAGCATGAGAAGTGTGATG-3'	
β -ENaC	Forward	5'-ACCCTGAGCAGGAAGGGTAT-3'	220bp
	Reverse	5'-ACAGGAGGCCACTAGCTTGA-3'	
γ -ENaC	Forward	5'-CGTCAGTGGCACAAAGCCAA-3'	301bp
	Reverse	5'-GAGAGCCTCCTCAAACCATG-3'	
MR	Forward	5'-GCTCAACATTGTCCAGTACA-3'	260bp
	Reverse	5'-GCACAGGTGGTCCTAAGATT-3'	
PGK	Forward	5'-GCTGCAGAACTCAAATCTCT-3'	263bp
	Reverse	5'-TGTGTGCAGTCCCAAAGCA-3'	

Plasmids containing the cDNA of α , β and γ ENaC, MR and PGK were used to generate standard curves. All of the construct concentrations were quantified by absorbance at 260nm. Serial 10-fold dilution (e.g. 100pg, 10pg, 1pg, 0.1pg, 0.01pg, 0.001pg etc.) of each subunit of ENaC, MR and PGK plasmid clones were used to generate an external standard individually. Expression was normalized to PGK levels as an endogenous reference. Normalization was achieved by dividing the amount of cDNA of each ENaC subunit or MR by the PGK quantity. Real-time PCR efficiencies were calculated according to the equation $E=10^{[-1/\text{slope}]}$: for α - 1.98; β - 1.91; γ - 1.93; MR - 1.86 & PGK - 1.94.

3.2.5.2 Immunohistochemistry

Under pentobarbital anesthesia, rats were perfused transcardially with chilled normal saline followed by 4% paraformaldehyde and 0.1% glutaraldehyde in PBS (pH – 7.4). The brains were removed and kept in the perfusion solution for 5 - 6 hours followed by cryoprotection with several changes of 20% sucrose in PBS over the next 48 hours. Then the brains were rapidly frozen to -30° C in precooled isopentane and stored at -80° C until use.

5 μ m coronal sections of brain were cut in a rostral to caudal direction in a cryostat (-30° C) and thaw mounted on superfrost plus slides (VWR Scientific, West Chester, PA). Precautions were taken to maintain similar coronal planes while cutting the brain sections. 5-7 consecutive sections were collected on different slides in the hypothalamic areas (main area of interest) before proceeding to the next, which would be about 50-70 μ m caudal. This ensured a distance of about 100 μ m between two successive sections so that the same cells were not included in both. In more rostral or caudal areas of the brain the distance between two sets of collections was about 300-500 μ m. Slides were then dried and stored in freezer at -20° C until further processing.

Just before staining the slides were placed in the same fixative solution for 5-10 minutes followed by several washes in PBS. To quench endogenous peroxidase the slides were treated with 1% sodium borohydride (Sigma-Aldrich, Oakville, ON) in PBS for 30 minutes and then with 1% H_2O_2 in methanol for another 30 minutes. Following several washes in PBS the slides were incubated with blocking solution (1.5% normal sera from the secondary antibody species and 1% bovine serum albumin in PBS) for 2 hours at room temperature. The sections were then incubated with the respective primary

antibodies diluted appropriately in blocking solution (MR 2 $\mu\text{g/ml}$; α ENaC 0.4 $\mu\text{g/ml}$; β ENaC 0.5 $\mu\text{g/ml}$ and γ ENaC 0.7 $\mu\text{g/ml}$). The antibodies against α , β and γ ENaC (LL766AP, LL558AP, LL550AP respectively) were a kind gift from Dr. Mark A. Knepper (National Institutes of Health, Bethesda, Maryland, USA) and had been raised against synthetic peptides corresponding to predicted amino acid sequences in the rat (Canessa et al. 1994b), (Canessa et al. 1993a): α ENaC (amino acids 46-68) NH_2 -LGKGDKREEQGLGPEPSAPRQPTC-COOH, β ENaC (amino acids 617-638) NH_2 -CNYDSLRLQPLDTMESDSEVEAI-COOH and γ ENaC (amino acids 629-650) NH_2 -CNTLRLDRAFSSQLTDTQLTNEL-COOH. These antibodies detect specific bands at 85-90 kDa in membrane fractions of rat renal cortex (Masilamani et al. 1999). Use of different antibodies for α ENaC (Chemicon, Temecula, CA) and β ENaC (Alpha Diagnostic International, San Antonio, TX) showed a similar distribution in the brain. Antibodies for MR were obtained from Santa Cruz Biotechnology (Santa Cruz, CA) and were directed against a 17 amino acid sequence at the N-terminus of rat MR (MCR N-17) or a 19 amino acid sequence at the C terminus (MCR C-19). In preliminary studies no significant differences in immunopositive signal distribution in the areas of interest were observed between the two antibodies and experiments were continued with the MCR N-17.

Following overnight incubation with the primary antibody, the slides were processed using the Vectastain Elite ABC kit (Vector Laboratories, Burlington, ON) for rabbit (ENaC) or goat (MR) IgG or the ABC staining system for goat primary antibody (Santa Cruz Biotechnology, Santa Cruz, CA) for MR. Briefly, these consisted of incubating with the biotinylated secondary antibody for 45 minutes, several washes in PBS and

incubation with biotinylated horseradish peroxidase for another 45 minutes. The antigens were visualized using either the Vector Nova red (red color) or Vector DAB kit (black color). Some slides were counterstained with Vector Hematoxylin, and all dehydrated in graded alcohol, cleared in xylene and coverslipped with Permount (Fisher Scientific, Ottawa, ON).

Several control experiments were performed to rule out non-specific staining. For MR the positive controls were paraffin embedded kidney or heart sections of rats perfused with 4% paraformaldehyde and 0.2% picric acid in 0.1M phosphate buffer (pH 7.3), while for ENaC these were the frozen sections of kidney and colon from rats perfused with 4% paraformaldehyde and 0.1% glutaraldehyde in cacodylate buffer. Prolonged freezing adversely affected immunoreactivity to the MR antibodies. Omission of the primary antibodies or incubation with the nonimmune IgG from goat (MR) or rabbit (ENaC), with all other steps left identical were used as negative control in all cases. In addition some sections were incubated with the primary antibody preadsorbed with excess of the immunizing peptide (MCR N-17). The peptide control experiments for the ENaC antibodies could not be performed due to lack of the specific immunizing peptides.

Double staining: Adjacent sections were studied to determine whether the ENaC or MR immunostaining was in neurons or glia and whether MR and ENaC were expressed in the same cells. Rabbit polyclonal antibodies to Neuron Specific Enolase (NSE, Chemicon) or Neuron specific nuclear protein (Neu N, Alexa488 conjugated, Chemicon) were used as neuronal markers and to glial fibrillary acidic protein (GFAP, Sigma) were used as glial cell marker. For double staining slides were first incubated with anti α or β ENaC primary antibody followed by Alexa red conjugated goat anti rabbit secondary antibody

(Vector Laboratories, Burlington, ON) and then with Alexa 488 conjugated Neu N antibody.

Microscopy and morphological analysis: The slides were studied with a high resolution brightfield transmitted light microscope (Olympus BX60 with 2x, 20x & 40x objectives) and images were captured using Spot digital camera and Spot software. For fluorescent microscopy, the same microscope was used with appropriate emission spectra and filters. Complete labeling in immunoperoxidase staining was confirmed by the presence of uniform Nova red or DAB label intensity. All major nuclei and structures could readily be identified by morphological criteria based on labeling pattern and facilitated by the thinness of the sections. Neuroanatomical localization was confirmed by hematoxylin or Nissl counterstained sections and a rat brain atlas (Paxinos & Watson 1998b). Staining intensity was not assessed in the current study. Relative density of cellular staining was rated as: none (-) if no staining was observed, low (+) if <30% of cells in an area were stained; moderate (++) if 30-70% of cells in an area were stained; and high (+++) if more than 70% of cells in an area were stained.

3.2.6 Results

3.2.6.1 Transcripts encoding ENaC and MR in brain

Figure 3.2-1 shows various lengths of real-time PCR products (α - 429 bp; β - 220 bp and γ - 301 bp) that were amplified in different brain areas – organum vasculosum of lamina terminalis (OVLT), subfornical organ (SFO), supraoptic nucleus (SON), paraventricular nucleus (PVN), median preoptic nucleus (MnPO), choroid plexus (CP) and hippocampus, were of comparable size to the PCR amplified transcripts of each subunit predicted from the kidney. There was no amplification when reverse transcriptase was absent. The putative ENaC subunit transcripts were sequenced by PCR and the DNA sequences of α , β and γ ENaC from Wistar rat brain were identical to the published ENaC subunits nucleotide sequences (data not shown).

Figure 3.2-2 shows the relative abundance of α , β and γ ENaC mRNA in the whole kidney, hypothalamus and specific brain areas. In the kidney, mRNA levels of the α ENaC subunit were ~6-fold higher than β and ~10-fold higher than γ , and in the hypothalamus ~30 fold higher than β and ~60-fold higher than γ . However, mRNA levels of the ENaC subunits in specific brain areas exhibited different patterns from those in the whole hypothalamus. For α , mRNA levels were similar to or higher than in the whole hypothalamus, particularly in the OVLT, SFO and PVN. For β , levels in the OVLT, SON and hippocampus were lower than in the whole hypothalamus, but mRNA levels in MnPO and CP were much higher. For γ , mRNA levels in most brain areas were higher, and in the SFO and MnPO were up to ~40-fold higher than in the whole hypothalamus (Fig 3.2-2).

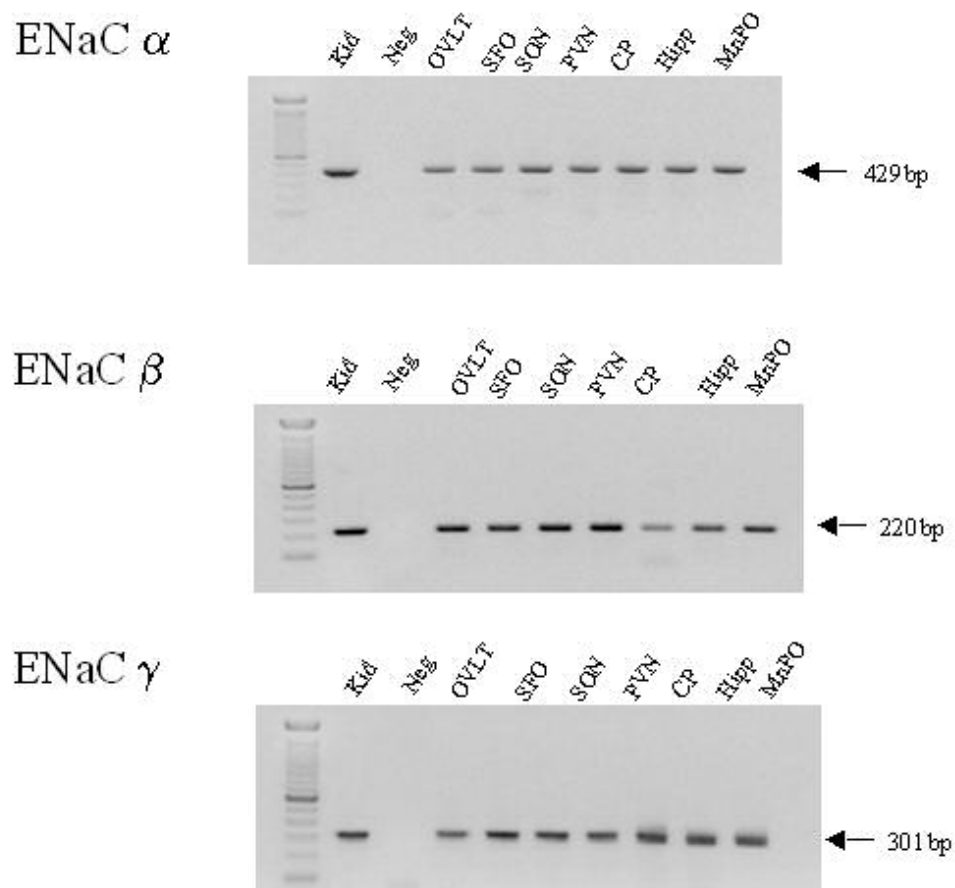


Figure 3.2–1: Real time RT-PCR to detect transcripts of α , β & γ ENaC in different brain areas. Total RNA was isolated from the kidney and different brain areas of Wistar rats. cDNAs were synthesised and subjected to the real-time PCR. 429bp, 220bp and 301bp PCR products were amplified for ENaC α , β & γ subunits respectively by using ENaC specific primers. Kidney served as positive control and the RT reaction with absence of reverse transcriptase served as negative control.

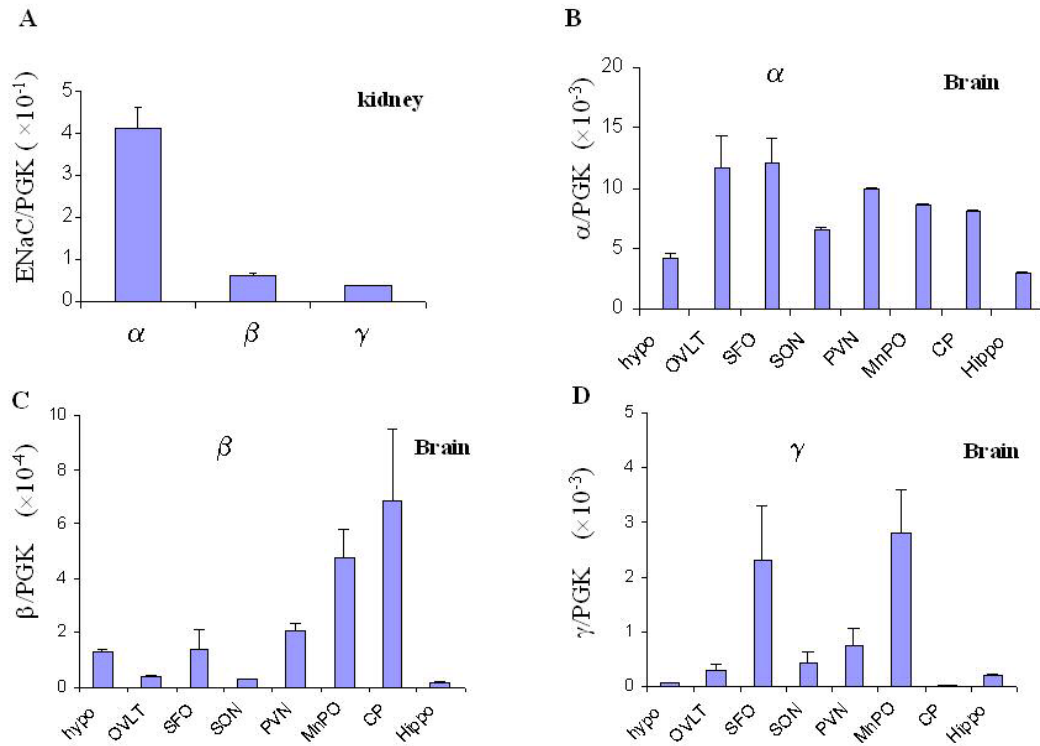


Figure 3.2-2: Relative abundance of α , β and γ ENaC mRNA in the kidney, the whole hypothalamus and different brain areas. Total RNA was isolated from the kidney, the whole hypothalamus and different parts of the brain of Wistar rats. cDNAs were synthesized and subjected to real-time quantitative RT-PCR using SYBR Green I. Fig3.2- 2A) Relative abundance of α , β and γ ENaC subunits in kidney. Fig 3.2-2B) Relative abundance of α ENaC in different brain areas. Fig 3.2-2C) Relative abundance of β ENaC in different brain areas. Fig 3.2-2D) Relative abundance of γ ENaC in different brain areas. Data were normalized to endogenous PGK mRNA and represent mean \pm SEM ($n=6$).

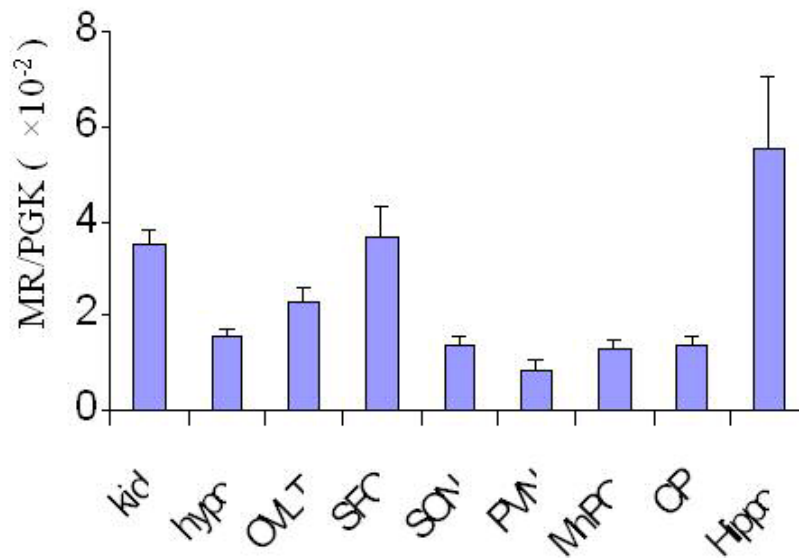


Figure 3.2-3: Relative abundance of MR mRNA in the kidney, the whole hypothalamus and different brain areas. Total RNA was isolated from the kidney, the whole hypothalamus and different brain areas of Wistar rats. Relative abundance of MR mRNA was analyzed by real-time quantitative RT-PCR using SYBR Green I. Data were normalized to endogenous PGK mRNA and represent Mean \pm SEM (n=6).

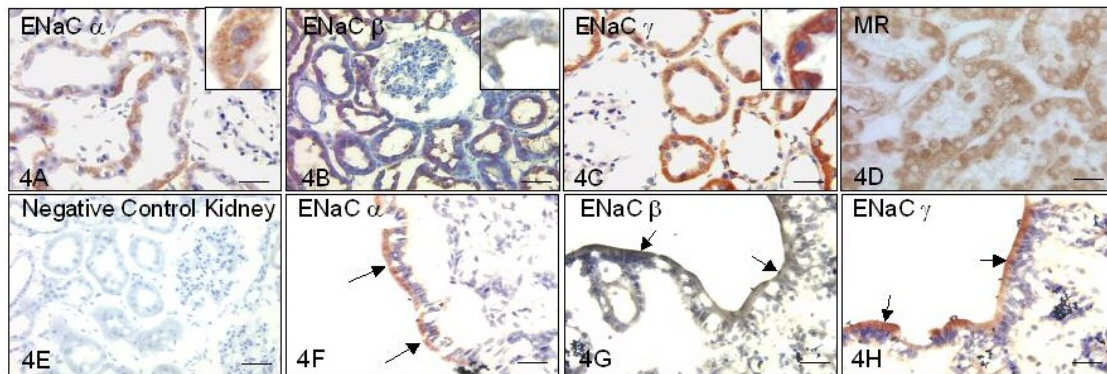


Figure 3.2-4: ENaC and MR expression in kidney and colon. Red staining was developed by Nova Red and brown-black with Nickel enhanced DAB. Fig 3.2-4A-C) ENaC α (A, red), β (B, brown-black) and γ (C, red) in renal cortex. Cellular localization is better shown in

the insets. Blue nuclear counterstain with Hematoxylin. There is no staining in the glomeruli. Scale bar – 45 μ m Fig 3.2-4 D) MR expression in the renal cortex. Scale bar – 45 μ m. Fig 3.2-4E) Omission of the primary antibody abolishes the specific staining. Blue nuclear counterstain with Hematoxylin. Fig 3.2-4 F-H) ENaC α (D, red), β (E,brown-black) and γ (F, red) along the brush border epithelia (arrows) of colon. Blue nuclear counterstain with Hematoxylin. Scale bar – 45 μ m.

Figure 3.2-3 shows the relative MR mRNA levels in the whole kidney, hypothalamus and different brain areas. The mRNA levels were ~2-fold less in the whole hypothalamus than in the kidney. Most of the examined brain areas showed similar mRNA levels of MR to the whole hypothalamus except the SFO and hippocampus. In the hippocampus, mRNA levels of MR were ~3.5-fold higher than in the whole hypothalamus and ~1.5-fold than in the kidney. mRNA levels in the SFO were ~2-fold higher than in the hypothalamus and similar to levels in the kidney.

3.2.6.2 Distribution of α , β and γ ENaC

In rat kidney, staining for all ENaC subunits (Fig 3.2-4A-C) was prominent in the distal tubules and collecting ducts in cortex and outer medulla, with no labeling in the glomeruli. The expression was diffusely cytoplasmic. No labeling was seen with omission of the primary antibodies (Fig 3.2-4E). In the colon, all three subunits showed prominent immunoreactivity along the brush border of the enterocytes (arrows in Fig 3.2-4F-H). Distribution in kidney and colon was consistent with previous studies (Duc et al. 1994, Hager et al. 2001, Renard et al. 1995). Immunohistochemistry of frozen coronal sections of rat brain demonstrated specific immunoreactivity with negligible background

to all three ENaC subunits. Omission of the primary antibodies abolished the entire specific staining (Fig 3.2-7A & 3.2-7F). Incubation with normal IgG did show high background, non-specific nuclear staining in some areas, but these were clearly different from the staining obtained with the specific antibodies. Distinct morphological appearance and double staining with Neu N or, GFAP demonstrated that ENaC immunostaining in most parts of the brain was neuronal (Fig 3.2-5) except for the epithelia of the choroid plexus, ventricular ependyma and blood vessels. Some Neu N and GFAP negative cells were noted that were ENaC α and β positive. These included the magnocellular cells of the SON and PVN and other dispersed groups of cells.

In the brain both α and β ENaC showed similar widespread distribution. However, γ ENaC signal was weak in most parts. The weak γ signal was not due to antibody concentrations since similar concentrations in other tissues resulted in prominent immunostaining and changing the antibody concentrations in the brain did not affect regional distribution. The clear nuclear halos in magnified views of most cells suggest a cytoplasmic and/or membranous distribution of ENaC subunits (insets in figures). Nuclear immunoreactivity was noted in some cells consistent with previous studies (Brockway et al. 2002). Table 3.2-2 shows relative distribution of the ENaC subunits and MR in the areas of the brain that were examined.

Table 3.2–2: Relative abundance of α , β and γ ENaC and MR immunopositive cells in selected brain areas

Region of brain studied	ENaC α	ENaC β	ENaC γ	MR
Cortex	++	++	+/-	++
Hippocampus				
Cornu Ammonis pyramidal subfields	+++	+++	++	+++
Dentate gyrus	+++	+++	++	+++
Amygdala				
Medial amygdaloid nucleus	++	++	-/+	++
Lateral amygdaloid nucleus	++	++	-/+	++
Hypothalamus				
Suprachiasmatic nucleus	+++	+++	-/+	++
Median preoptic nucleus	++	++	-/+	+
Periventricular nucleus	++	++	-/+	++
Supraoptic nucleus	+++	+++	+++	+++
Paraventricular nucleus				
<i>Magnocellular division</i>	+++	+++	+++	++
<i>Parvocellular division</i>	++	++	-/+	+
Arcuate nucleus	++	++	-	+++
Medial preoptic nucleus	++	++	-/+	++

Region of brain studied	ENaC α	ENaC β	ENaC γ	MR
Brain stem				
Nucleus of tractus solitarius	++	++	+	++
Circumventricular organs				
Organum vasculosum of lamina terminalis	++	++	-/+	++
Subfornical organ	++	++	-/+	+ / ++
Area postrema	+ / ++	+ / ++	- / +	++
Ventricles				
Choroid plexus cuboidal epithelium	+++	+++	++	+++
Vasculature in the choroid plexus	+	+	+	++
Ventricular ependyma	+++	+++	++	+++
Pia-arachnoid	++	++	++	+++
Blood vessels				
(Small and medium sized vessels and capillaries)				
Endothelia	++	++	++	++
Vascular Smooth Muscle Cells	++	++	++	++

Relative density of cellular staining was rated as “none” (-) if no staining was observed, “low” (+) if <30% of cells in an area were stained, “moderate” (++) if 30–70% of cells in an area were stained, and “high” (+++) if >70% of cells in an area were stained.

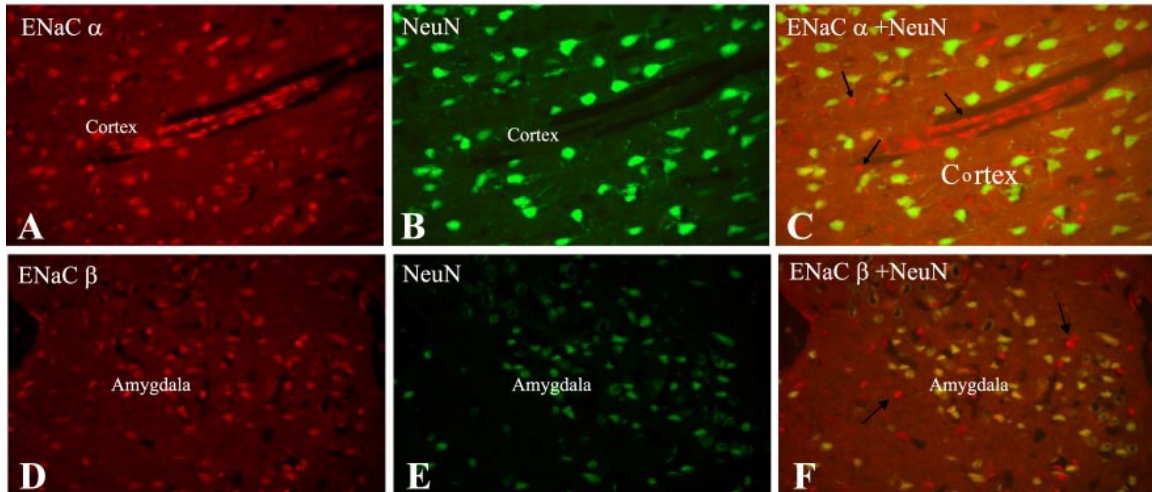


Figure 3.2–5: Colocalization of α and β ENaC with Neu N: double staining with anti- α or - β ENaC and Neu N demonstrates neuronal expression of ENaC. α ENaC (A; red) and Neu N (B; green) in cerebral cortex. C: overlay by exciting both dyes (Texas Red and Alexa Fluor 488) demonstrates double staining (light green to yellow). Scale bar = 37 μ m. β ENaC (D; red) and Neu N (E; green) in the amygdala. F: overlay of D and E showing double staining (yellow). Scale bar 37 μ m. Arrows in C and F, Neu N- and GFAP-negative cells noted to be α and β ENaC positive.

Cortex – α (Fig 3.2-6A) and β (Fig 3.2-6B) ENaC immunopositive neurons were noted in all parts of the cerebral cortex. γ ENaC immunopositivity (Fig 3.2-6C) was restricted to parts of the cingular and piriform cortex. Immunoreactivity was usually restricted to the layers II-VI in the soma of the pyramidal neurons and some of their processes.

Hippocampus - In the hippocampus immunoreactivity to α (Fig 3.2-6E) and β ENaC (Fig 3.2- 6F) and weaker immunoreactivity to γ ENaC (Fig 3.2-6G) was noted in the pyramidal layers of all the cornu ammonis (CA) subfields and the dentate gyrus (DG). Immunoreactivity was usually limited to the soma and some proximal processes of the neurons.

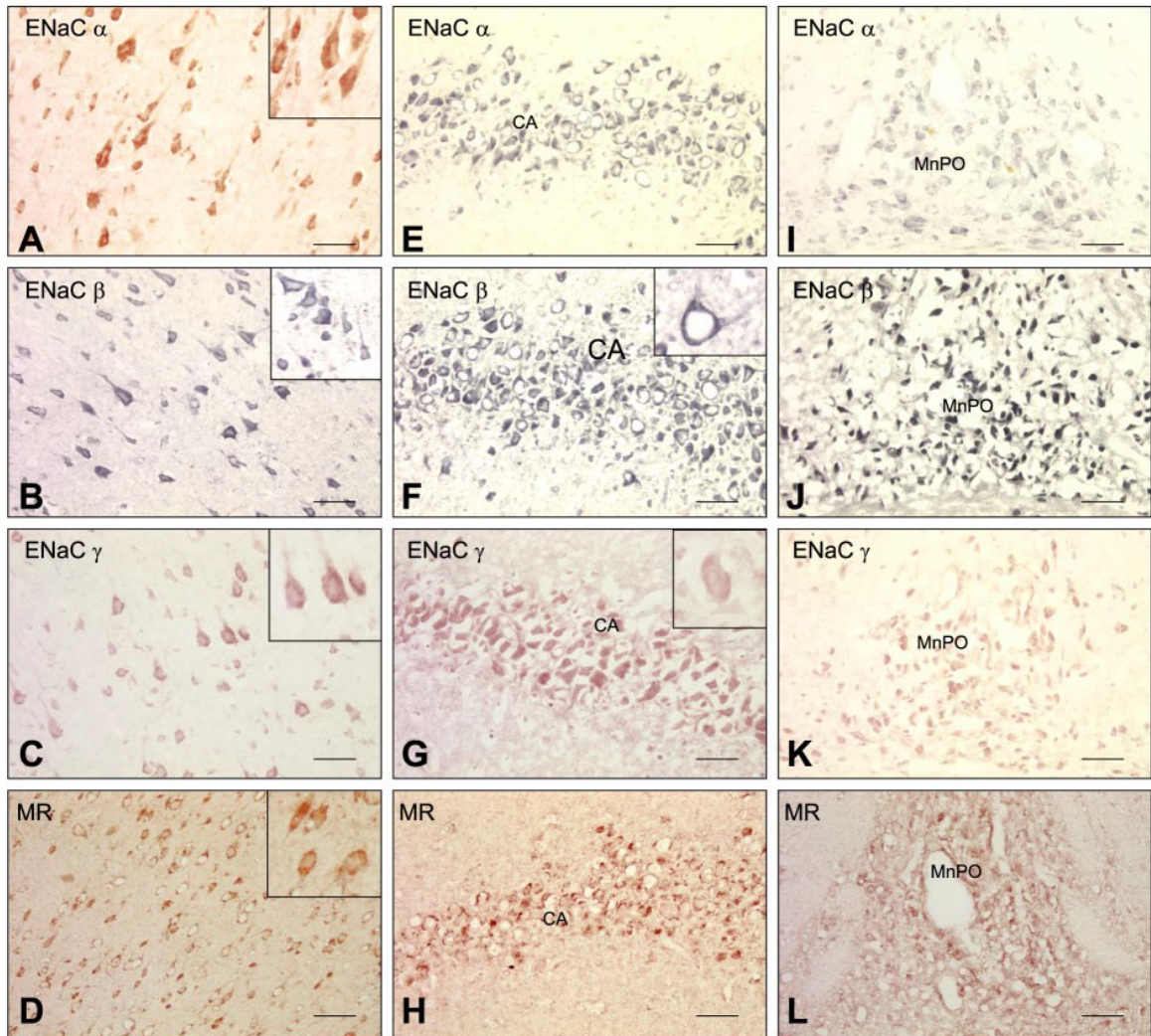


Figure 3.2–6: ENaC and MR staining in different areas in the brain. Red staining was developed by Nova Red and brown-black with Nickel enhanced DAB. Fig 3.2-6A-D) Cerebral cortex showing staining for α (A, red), β (B, brown-black) and γ (C, red) ENaC subunits and MR (D, red). Insets show magnified cells. Note staining along some neuronal processes and the clear nuclear halos. Scale bar – 37 μ m. Fig 3.2-6E-H) Pyramidal neurons in the CA subfields of hippocampus showing α (E, brown-black), β (F, brownblack) and γ (G, red) ENaC and MR (H, red). Note some nuclear staining for MR. Scale bar – 37 μ m. Fig 3.2-6 I-L) Median preoptic nucleus dorsal part showing α (I, brown-black), β (J, black) and γ (K, red) ENaC and MR (L, red). Scale bar – 37 μ m.

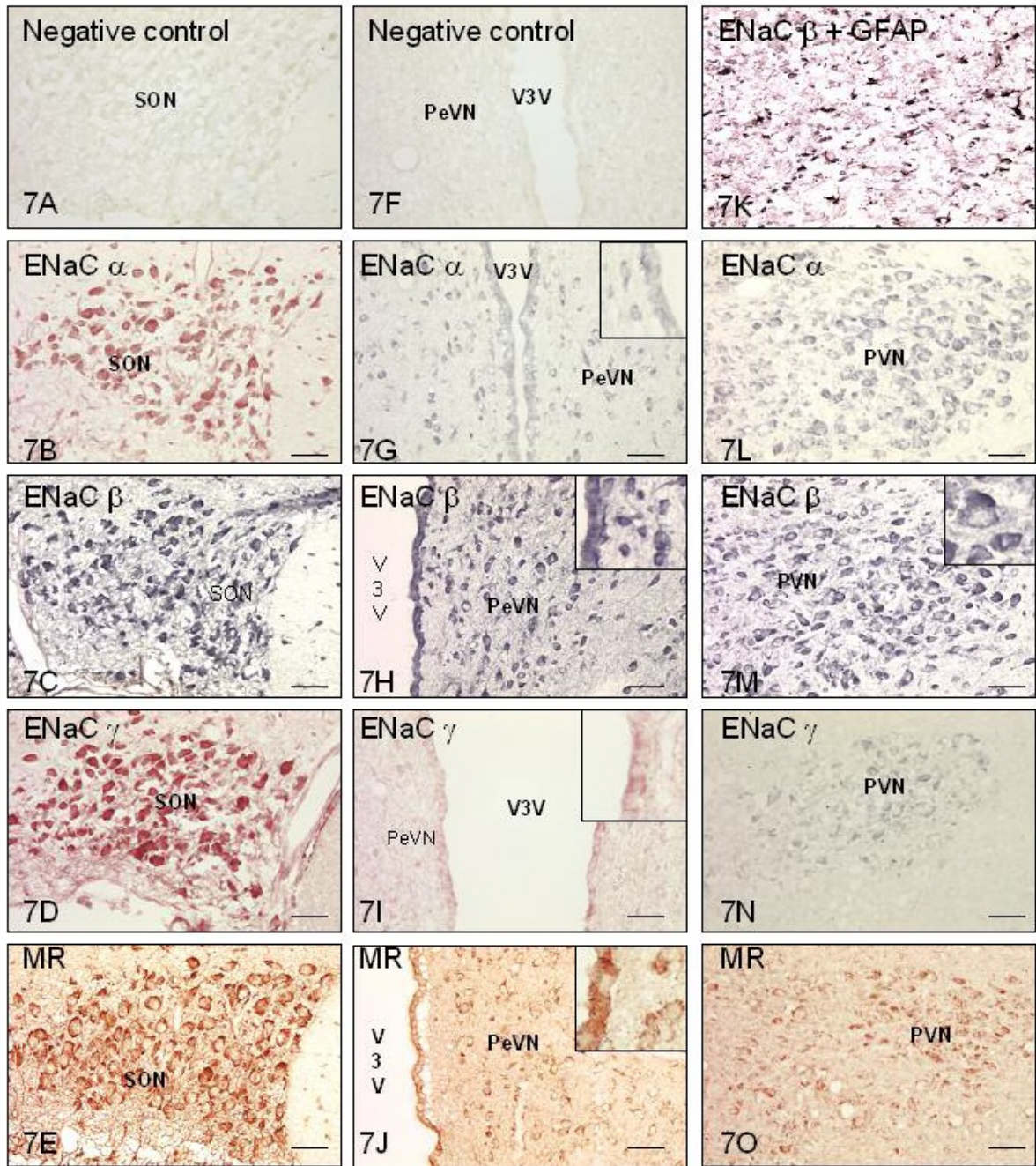


Figure 3.2–7: ENaC and MR staining in hypothalamic areas. Red staining was developed by Nova Red and brown-black with Nickel enhanced DAB. Fig 3.2-7A-E) Supraoptic nucleus (SON) – omission of the primary antibodies abolished any specific staining (A) whereas inclusion of the specific antibodies shows immunoreactivity to α (B, red), β (C, black) and γ (D, red) ENaC subunits and MR (E, red) in adjacent sections. The staining

appears to be on magnocellular cells by morphological criteria. Scale bar – 37 μm . Fig 3.2-7F-J) The ventral third ventricle (V3V) and adjacent areas. No significant staining is seen in the PeVN and ependyma when the primary antibody is omitted (F). With inclusion of the primary antibody, cells in the periventricular nucleus (PeVN) show staining for α (G, brown-black) and β (H, brown-black) ENaC subunits and MR (J, red) but undetectable staining of γ (I, red) ENaC. The ependyma of the ventral third ventricle is shown in the insets. Scale bar – 37 μm . Fig 3.2-7K) Double staining for ENaC β and GFAP, most ENaC β positive cells (brown) are GFAP (red) negative. Fig 3.2-7L-O) Paraventricular nucleus (PVN) also shows staining in adjacent sections for α (L, brown-black), β (M, brown-black) and γ (N, brown-black) ENaC and MR (O, red). Note lack of significant staining for γ ENaC and MR in the parvocellular parts. Inset in fig 3.2-7M shows a magnified magnocellular neuron expressing β ENaC. Scale bar - 37 μm .

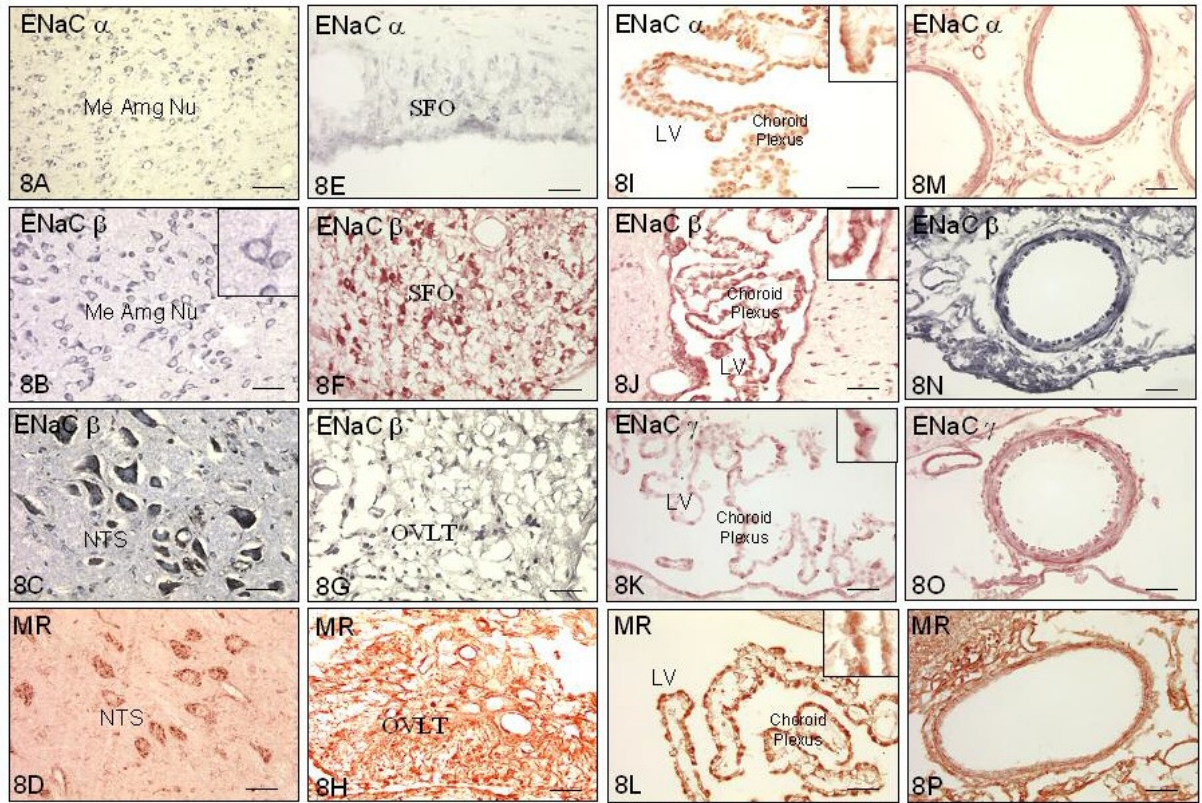


Figure 3.2–8: ENaC and MR in the amygdala, brainstem, CVOs, choroid plexus and blood vessels. Red staining was developed by Nova red and brown-black staining by Nickel enhanced DAB. Fig 3.2-8A-B) ENaC α (A, brown-black) and β (B, brown-black) in medial amygdaloid nucleus. Inset in B shows a magnified neuron. Scale bar – 37 μ m. Fig 3.2-8C-D) Nucleus of tractus solitarius showing β ENaC (C, β ENaC in black, nuclear counterstain in blue) and MR (D, red) staining – note immunopositivity in the large neurons in the area. Scale bar – 25 μ m. Fig 3.2-8E-F) Subfornical organ showing α (E, brown-black) and β (F, red) ENaC staining. Scale bar – 37 μ m. Fig 3.2-8G-H) β ENaC (G, brown-black) and MR (H, red) staining in the OVLT. Scale bar – 37 μ m. Fig 3.2-8I-L) Immunoreactivity to ENaC α (I, red), β (J, red) and γ (K, brown-black) subunits and MR (L, red) in the choroid plexus and ependyma. Choroidal epithelium is magnified

in the insets. Scale bar – 37 μ m. Fig 3.2-8M-P) Blood vessels on the ventral surface of the brain showing prominent α (M, red), β (N, brown-black) and γ (O, red) ENaC and MR (P, brown) staining in the endothelia and vascular smooth muscle. Note also staining in the pia-arachnoid membranes. The latter was not due to dye deposition, since it was absent in the negative controls. Scale bar – 37 μ m.

Hypothalamus – Immunoreactivity to all three ENaC subunits was present in the MnPO (Fig 3.2- 6I-K), SON (Fig 3.2-7B-D) and magnocellular PVN (Fig 3.2-7L-N). Studies of adjacent sections suggested expression in the same cells. Weaker expression of α and β ENaC and undetectable expression of γ ENaC was noted in the parvocellular PVN. Other parts of the hypothalamus such as the suprachiasmatic nucleus, periventricular nucleus (Fig 3.2-7G-I), preoptic areas and anterior and posterior hypothalamic areas showed specific staining only for α and β ENaC.

Other areas - Prominent immunoreactivity to α and β ENaC was noted in the amygdala (Fig 3.2-5 D-F, 3.2-8A-B), the nucleus of tractus solitarius (NTS, β - Fig 3.2-8C) and in the circumventricular organs such as the SFO (Fig 3.2-8E-F) and OVLT (β - Fig 3.2-8G). γ immunoreactivity in these areas was low or undetectable.

Brain epithelial components and blood vessels – The cuboidal epithelium of the choroid plexus and the ventricular ependyma expressed all three ENaC subunits (Fig3.2-8I-K). Notable was expression of all three subunits along the ependyma on a single layer of cells lining the cavity (Fig 3.2-7G-I, 3.2-8I-K) and only β ENaC in the subependymal zone. The pia-arachnoid membrane surrounding the brain also showed

very dense ENaC staining. ENaC immunopositivity was also present in the endothelia and smooth muscle cells of blood vessels (Fig 3.2-8M-O).

3.2.6.3 Distribution of MR

MR immunoreactivity was specific with no staining when the primary antibody was omitted. Incubation with normal IgG or pre-adsorption with the immunizing peptide abolished all specific staining. MR was localized in the distal convoluted tubules, collecting ducts, loops of Henle and uroepithelia in the kidney with no staining in the glomeruli or proximal tubules (Fig 3.2-4D), consistent with previous studies (Rundle et al. 1989). In freshly stained brain sections, the cell nucleus showed low or undetectable levels of MR in many areas (insets of figures); much of the immunolabel was clustered in the peri-nuclear region of the cells. Similar to previous findings (Ahima et al. 1991, Han et al. 2005, Sanchez del Pino et al. 1995) high levels of MR were found in pyramidal subfields of the hippocampus (Fig 3.2-6H). Similar or greater immunodensity was also observed in the supraoptic nucleus (Fig 3.2-7E), magnocellular paraventricular nucleus (Fig 3.2-7O), suprachiasmatic nucleus, periventricular nucleus (Fig 3.2-7J), choroid plexus (Fig 3.2-8L), ventricular ependyma (Fig 3.2-7J, 3.2-8L), endothelia and smooth muscle cells of blood vessels (Fig 3.2-8P) and the pia-arachnoid. Immunoreactivity was also present in the cortex (Fig 3.2-6D), MnPO (Fig 3.2-6L) and the circumventricular organs – OVLT (Fig 3.2-8H) and SFO.

3.2.6.4 Co-expression of α , β and γ ENaC with MR

In the kidney, expression of both MR and ENaC subunits was found on the known aldosterone responsive epithelia. In non-neural components of the brain such as the choroid plexus, ependyma, the pia-arachnoid, endothelia and VSMC all three ENaC

subunits were expressed in parallel with MR. In brain tissue itself, ENaC expression was mainly observed on neurons i.e. GFAP negative but Neu N positive cells, as assessed by double-stained sections (Fig 3.2-5 & Fig 3.2-7K) and morphological appearance. Expression of all three ENaC subunits and MR were abundant in the SON, MnPO and magnocellular PVN, cingular and piriform cortex and the hippocampus. Double labeling did not yield fine resolution images with peroxidase staining. Study of adjacent sections however, suggested that all three ENaC subunits and MR were expressed in the same groups of cells in the different regions. In areas such as the suprachiasmatic nucleus, arcuate nucleus, most cortical areas, amygdala and the SFO immunoreactivity was prominent only for the α and β ENaC and MR but undetectable for γ ENaC. Immunoreactivity to α and β ENaC subunits usually paralleled MR positivity.

3.2.7 Discussion

This study demonstrates for the first time that α , β and γ subunits of ENaC are all expressed in the rat brain. By RT-PCR we showed the presence of mRNA transcripts of all three ENaC subunits and MR in regional extracts from the adult rat brain. By immunohistochemistry we mapped the relative distribution of α , β and γ ENaC and showed their parallel localization with MR.

Canessa et al (Canessa et al. 1994b, Canessa et al. 1993a, Canessa et al. 1994a) cloned ENaC subunit cDNAs from rat kidney, distal colon and lung. No transcripts were detected in rat brain. By Northern blot analysis, we also did not detect transcripts in the brain. By RT-PCR, the ENaC subunit transcripts are indeed expressed in rat brain. Recently α ENaC gene expression was reported in the cortex and cerebellum of mice (Dyka et al. 2005). mRNA transcript levels in the whole hypothalamus are approximately 100 fold lower than the kidney, which explains why ENaC transcripts cannot be detected in the brain by Northern blot. Sequence analysis shows that the DNA sequences are the same in the brain and kidney.

The topology of each of the subunits includes two membrane-spanning segments, cytoplasmic N and C termini, and a large glycosylated extracellular domain (Canessa et al. 1994b, Kellenberger & Schild 2002). A low level of amiloride-sensitive current can be observed after expression of α ENaC alone in oocytes but expression of β or γ subunits individually does not induce an amiloride-sensitive current (Canessa et al. 1994b) (Canessa et al. 1993a). Expression of combinations of $\alpha\beta$ or $\alpha\gamma$ ENaC generates a higher level of current than after expression of α ENaC alone, but still only 5% of the maximal current observed after coexpression of the three subunits in oocytes (Canessa et al.

1994b). In different tissues the three subunits may be synthesized in a differential fashion, with one or two subunits expressed constitutively while the other(s) are induced by different physiological stimuli in parallel with increased channel activity (Weisz & Johnson 2003). Different assemblies of the subunits, alone or with other DEG/ENaC family members, may also be responsible for different functions (Kellenberger & Schild 2002). β and γ ENaC appear to form mechanosensitive complexes in baroreceptor nerve endings (Drummond et al. 1998) and smooth muscle cells of cerebral (Drummond et al. 2004) and renal (Jernigan & Drummond 2005) blood vessels.

In the whole hypothalamus of Wistar rats, α ENaC mRNA was found to be ~30 fold more abundant than β and γ . In individual brain nuclei, higher levels of β and γ ENaC mRNA were detected. Interestingly, γ ENaC mRNA levels in some areas were of comparable values to α ENaC, while β ENaC levels were still ~10 fold lower (Fig 3.2-2). Whereas levels of ENaC mRNA in the brain are low compared to the kidney, immunohistochemistry demonstrated that all three ENaC subunits are abundantly expressed in areas such as the MnPO, SON, PVN, hippocampus, choroid plexus and ependyma. The different relation between mRNA and protein levels in different brain areas compared to the kidneys may reflect higher turnover of mRNA and/or lower protein turnover. Immunoreactivity for γ ENaC was undetectable in the SFO and OVLT, where appreciable amount of γ ENaC mRNA was present. This absence may relate to lack of translation of the γ ENaC mRNA, high protein turnover or post-translational modifications affecting detection of the protein.

The combined approach of RT-PCR and immunohistochemistry establishes that not only ENaC mRNA transcripts are present in the brain, but are also functional, i.e. lead to

abundant presence of channel protein recognized by appropriate antibodies. However, this approach does not establish whether or not active channels are present. Some argue against the presence of truly silent or nonconductive channels at the cell membrane (Firsov et al. 1996); others indicate that distinct pools of mature and immature channels can be present (Hughey et al. 2004b). In the context of the present study it is difficult to comment on this issue. In the peripheral nervous system, ENaC expression has been noted in a variety of tissues e.g. retina (Brockway et al. 2002, Dyka et al. 2005), cochlea (Couloigner et al. 2001, Zhong & Liu 2004), tongue (Lin et al. 1999), skin (Drummond et al. 2000) and baroreceptors (Drummond et al. 1998). Functionally active ENaC have so far been demonstrated only in the tongue (Lin et al. 1999) and baroreceptors (Drummond et al. 1998). Benzamil – a specific blocker of ENaC – had no effect on hypertonicity induced depolarization in MnPO neurons of normal Wistar rats (Grob et al. 2004). Intracerebroventricular infusion of benzamil also has no demonstrable effects in rats on regular salt diet but prevents sympathetic hyperactivity and hypertension in Dahl S rats on high salt diet, suggesting that ENaC in the brain can become functionally active (Gomez-Sanchez & Gomez-Sanchez 1995), (Wang & Leenen 2002).

3.2.7.1 Cardiovascular regulatory centers of hypothalamus and brainstem

Hypothalamic nuclei such as the MnPO, SON and magnocellular PVN showed prominent MR and ENaC immunoreactivity. MR expression was previously documented in the SON and PVN (Ahima & Harlan 1991),(Han et al. 2005), (MacKenzie et al. 2000). Pietranera et al (Pietranera et al. 2001) however, did not find immunoreactivity in the SON and PVN of Sprague-Dawley rats with the MCR N-17 antibody. An explanation of the different findings is not readily apparent but variations in experimental conditions and

fixatives could be contributing. The immunosignal in the SON and PVN for MR and all ENaC subunits was as strong as the signal in the hippocampus. Lack of GFAP costaining and morphological criteria suggests expression in the magnocellular neurons, which are vital in osmoregulation and salt sensitive hypertension via synthesis of a range of hormones and neurotransmitters including vasopressin and possibly ouabain-like compounds (Wang et al. 2003a). ENaC and MR were further detected in regions of the anteroventral third ventricle including the SFO and OVLT. AV3V lesions inhibit salt sensitivity and mineralocorticoid hypertension (Gomez-Sanchez et al. 1997). The actual pathways activated by ENaC in these brain areas remain to be determined.

3.2.7.2 Hippocampus, Amygdala and other brain areas

MR and ENaC α and β subunits were abundantly expressed in the amygdala, hippocampus and different cortical areas. The γ ENaC signal was weak or undetectable in several of these areas. In the amygdala, aldosterone via MR modulates salt appetite (Sakai et al. 2000). In the hippocampus and cortical areas MR modulate the hypothalamo-hypophysial-adrenal axis and higher brain functions (Gesing et al. 2001, Yau et al. 1999, De Kloet 2004). One may speculate that ENaC may be the actual mediator of these actions.

3.2.7.3 ENaC and MR in regulation of CSF $[Na^+]$

Prominent expression of all ENaC subunits and MR in the choroidal epithelia and ependyma is consistent with a role of ENaC in regulation of CSF $[Na^+]$. In most tissues, Na^+ transport by ENaC is dependent on the electrochemical gradient generated by $Na^+K^+ATPase$. In renal tubules, $Na^+K^+ATPase$ is localized on the basolateral membrane and ENaC on the apical membrane favoring unilateral transport of Na^+ from the tubular

lumen towards the interstitium. In the choroid plexus and BBB, $\text{Na}^+\text{K}^+\text{ATPase}$ activity is primarily located on the abluminal membrane, but 25% of the activity is of luminal origin. $\text{Na}^+\text{K}^+\text{ATPase}$ activities associated with each membrane show different ouabain sensitivities, consistent with the presence of different isoenzymes at the luminal (mainly α_2/α_3) and abluminal (mainly α_1) membranes (Sanchez del Pino et al. 1995). Blockade of Na^+ channels by amiloride decreases the rate of Na^+ entry into the CSF and choroid plexus both in vivo and in vitro (Murphy & Johanson 1989b). Our finding that ENaC is indeed expressed in the choroidal epithelia supports a functional role for ENaC in regulation of CSF $[\text{Na}^+]$.

3.2.7.4 Brain blood vessels

All three ENaC subunits and MR were expressed in the brain vasculature in the endothelia as well as smooth muscle cells (Fig 3.2-8 M-P). In contrast, Drummond et al (Drummond et al. 2004) detected mRNA of all three ENaC subunits by PCR from isolated cerebral vessels but could not detect α ENaC expression by immunoassay or RT-PCR of freshly isolated smooth muscle cells or vessels. It was postulated that, ENaC as stretch receptors in blood vessels may be involved in autoregulation of cerebral blood flow. Increased incidence of ischemic cerebrovascular events appears to occur in individuals with ENaC polymorphisms (Hsieh et al. 2005), possibly a consequence of dysregulation of this autoregulation. ENaC in endothelia and BBB, on the other hand, may affect transport of Na^+ from the plasma into the interstitium.

3.2.7.5 Perspectives

In salt sensitive rats – Dahl S and SHR – increases in CSF $[\text{Na}^+]$ on high salt intake and enhanced neuronal response to CSF Na^+ contribute to the development of sympathetic

hyperactivity and hypertension (Huang et al. 2004, Wang et al. 2003a, Wang & Leenen 2002, Wang & Leenen 2003). In rats, following myocardial infarction sympathetic activity increases contributing to progressive cardiac dysfunction and heart failure (Huang & Leenen 2005). In both scenarios, sympathetic hyperactivity and disease progression can be prevented by central infusions of spironolactone or benzamil (Huang & Leenen 2005, Wang et al. 2003a, Wang & Leenen 2002, Wang & Leenen 2003, Huang et al. 2004). These functional studies suggest a pivotal role for MR and ENaC in the activation of central pathways leading to sympathetic hyperactivity. The present study demonstrates for the first time that subunits of the amiloride/benzamil blockable sodium channel – ENaC, are present in the brain on different populations of cells and in neurons localized in e.g. the PVN, SON, amygdala and hippocampus as well as choroid plexus and ependyma. Parallel localization of MR with ENaC provides a mechanism for control of ENaC channel activity. Different combinations of ENaC subunits in different cells may be involved in regulation of cardiovascular function and CSF $[Na^+]$ as well as development, memory and higher brain functions. The actual cellular mechanisms remain to be determined. Further molecular, biochemical and physiological characterization of these channels will give insight into their different roles in the central nervous system.

3.2.8 Acknowledgements

This research was supported by operating grant MOP-74432 from the Canadian Institutes of Health Research and program grant PRG5275 (for support of core Pathology laboratory) from the Heart and Stroke Foundation of Ontario. Full length cDNA α , β and γ ENaC plasmid were kindly provided by Dr. Bernard C. Rossier (Univ. of Lausanne, Switzerland). α , β and γ ENaC antibodies were kindly provided by Dr. Mark A. Knepper (National Institutes of Health, Bethesda, Maryland, USA).

3.3 MANUSCRIPT # 3: EFFECTS OF CENTRAL SODIUM ON EPITHELIAL SODIUM CHANNELS IN RAT BRAIN.

Hong-Wei Wang¹, Md Shahrier Amin¹, Esraa El-Shahat, Bing S Huang, Balwant S
Tuana, Frans H H Leenen²

Hypertension Unit, University of Ottawa Heart Institute, Ottawa, Ontario, Canada.

1. Joint primary authors.

2. Pfizer Chair in Hypertension Research, an endowed chair supported by Pfizer Canada,
University of Ottawa Heart Institute Foundation and Canadian Institutes of Health
Research.

Running Head

Brain ENaC and MR

Status

This article was published in:

American Journal of Physiology: Regulatory Integrative and Comparative Physiology,
2010, Volume 299: Pages 222-233.

3.3.1 RELEVANCE TO OVERALL PROJECT

In this study we tested our hypothesis #2, by evaluating the effect of icv infusion of Na rich aCSF on expression of ENaC subunits in the brain of Wistar rats. The MR blocker – spironolactone prevents the effects of icv aldosterone on sympathetic activity and hypertension. We therefore also evaluated the effect of icv spironolactone with Na⁺ rich aCSF on ENaC expression.

3.3.2 CONTRIBUTION

Responsible for the overall project and performed the following:

1. Design and planning of most of the initial experiments.
2. Tissue collection, processing and punching of specific brain areas for initial RT-PCR experiments.
3. Performed the experiments and studied protein distribution by immunohistochemistry and studied sub-cellular distribution by EM.
4. Set up the methods for measuring CSF [Na⁺] and performed initial measurements of CSF [Na⁺] following icv infusion of benzamil.
5. Assisted in gathering the data and preparation of the manuscript.

3.3.3 ABSTRACT

We evaluated the effects of intracerebroventricular (icv) infusion of Na⁺-rich artificial cerebro-spinal fluid (aCSF) with or without the mineralocorticoid receptor (MR) blocker spironolactone, on epithelial sodium channel (ENaC) subunits and regulators such as MR, serum and glucocorticoid-inducible kinase 1, neural precursor cells expressed developmentally downregulated 4 like gene, 11 β hydroxylase and aldosterone synthase in brain regions of Wistar rats. The effects of icv infusion of the amiloride analogue, benzamil, on brain tissue and CSF [Na⁺] were also assessed. In the choroid plexus and ependyma of the anteroventral third ventricle, ENaC are present in both apical and basal membranes. Na⁺-rich aCSF increased β ENaC mRNA and immunoreactivity in the choroid plexus and increased α and β ENaC immunoreactivities in the ependyma. Na⁺-rich aCSF increased α and β ENaC-gold-labeled particles in the microvilli of the choroid plexus and α and β ENaC-gold-labeled particles in basolateral membranes of the ependyma. Spironolactone only prevented the increase in β ENaC immunoreactivity in the choroid plexus and ependyma. In the supraoptic nucleus, paraventricular nucleus and subfornical organ, Na⁺-rich aCSF did not affect mRNA expression levels of the studied genes. Benzamil significantly increased CSF [Na⁺] in the control, but not in the Na⁺-rich aCSF group. In contrast, benzamil prevented the increase in hypothalamic tissue [Na⁺] by Na⁺-rich aCSF. These results suggest that CSF sodium upregulates ENaC expression in the brain epithelia but not in the neurons of hypothalamic nuclei. ENaC in the choroid plexus and ependyma appear to contribute to regulation of Na⁺ homeostasis in the brain.

KEYWORDS

Na⁺-rich aCSF, ENaC, brain, benzamil, CSF [Na⁺]

3.3.4 INTRODUCTION

In salt-sensitive rats, i.e. Dahl salt sensitive (S) and spontaneously hypertensive rats (SHR), high salt intake increases cerebro-spinal fluid (CSF) $[\text{Na}^+]$ by 4-6 mmol/L which appears to contribute to the development of sympathetic hyperactivity and hypertension on high salt intake (Huang et al. 2001b, Huang et al. 2004). Intracerebroventricular (icv) infusion of Na^+ -rich artificial CSF (aCSF), increasing CSF $[\text{Na}^+]$ by 5-7 mmol/L, increases blood pressure (BP) by ~15 mmHg in Wistar rats and by ~35 mmHg in Dahl S rats (Huang et al. 2001b, Wang & Leenen 2003). These increases in BP can be prevented by icv infusion of spironolactone to block mineralocorticoid receptors (MR) (Huang et al. 2006b) or of benzamil to block presumably epithelial sodium channels (ENaC) (Wang & Leenen 2003), suggesting that MR and ENaC play an important role in the pressor responses to an increase in CSF $[\text{Na}^+]$. ENaC is composed of three homologous subunits (α , β , and γ) which share ~30-35% sequence identity (Canessa et al. 1994b). All three ENaC subunits and MR are co-localized in the supraoptic nucleus, paraventricular nucleus and subfornical organ as well as in the choroid plexus and the ependyma of the anteroventral third ventricle (Amin et al. 2005). Regulators of ENaC expression and activity such as aldosterone, SGK1 (serum/glucocorticoid-inducible kinase 1) and Nedd4L (neural precursor cells expressed developmentally downregulated 4 like gene, previously named Nedd4-2 in rats) are also present in the rat brain (Imaizumi et al. 1994, Anan et al. 1998, Gomez-Sanchez et al. 2005a). SGK1 acts at multiple levels to regulate ENaC expression and activity. In the kidney, SGK1 is activated by phosphorylation, and phosphorylated SGK1 increases α ENaC transcription (Zhang et al. 2007) as well as enhances ENaC surface expression by phosphorylation of Nedd4L, an ubiquitin-protein

ligase (Debonneville et al. 2001). Phosphorylation of Nedd4L disrupts the interaction between channel and ligase and therefore decreases channel internalization and degradation. In addition, phosphorylated SGK1 may physically interact with ENaC by phosphorylating the C-terminus of α ENaC, resulting in increased channel open probability (Diakov & Korbmacher 2004).

In Wistar rats, icv infusion of Na^+ -rich aCSF increases hypothalamic aldosterone and BP both of which can be prevented by icv infusion of an aldosterone synthase inhibitor suggesting that locally produced aldosterone mediates the central actions of Na^+ (Huang et al. 2008). In the rat, 11β -hydroxylase (*CYP11B1*) and aldosterone synthase (*CYP11B2*) convert 11-deoxycorticosterone to corticosterone and aldosterone respectively. The transcripts of *CYP11B1* and *CYP11B2* can be detected in the brain, although the levels are much less (~100 to 1000 fold) in the central nervous system relative to adrenal *CYP11B1* and *CYP11B2* (MacKenzie et al. 2000).

To test the hypothesis that Na^+ upregulates ENaC in the brain and ENaC contributes to regulation of Na^+ homeostasis, we assessed in Wistar rats: (1) effects of central infusion of Na^+ -rich aCSF on ENaC expression, by measuring both mRNA and protein abundance and subcellular distribution of ENaC subunits in the epithelial cells of the ependyma and choroid plexus as well as in neurons of hypothalamic nuclei; (2) effects of central infusion of Na^+ -rich aCSF on mRNA levels of ENaC regulatory genes such as MR, SGK1 (and protein levels), Nedd4L as well as *CYP11B1* and *CYP11B2*; (3) whether blockade of MR by spironolactone prevents any increases in ENaC expression, and (4) whether icv infusion of benzamil influences increases in hypothalamic tissue and CSF [Na^+] by Na^+ -rich aCSF.

3.3.5 MATERIALS AND METHODS

Male Wistar rats (150 ~ 200g) were purchased from Charles River (Montreal, PQ, Canada) and housed under standard conditions (12 hour light cycle, ambient temperature $23 \pm 2^{\circ}\text{C}$). After arrival, rats received standard laboratory chow and tap water *ad libitum* for 5 days for acclimatization before entering the study. All procedures were carried out in accordance with the guidelines of the Canadian Council on Animal Care, which conform to NIH guidelines and were approved by the University of Ottawa Animal Care Committee. All surgery was performed under isoflurane anesthesia. For details of biochemical and molecular biological techniques, see the online supplement at <http://www.the-aps.org>

3.3.5.1 Experimental Protocols

3.3.5.1.1 Protocol 1) Biochemistry and Molecular biology measurements

Two experiments were performed. In the first experiment, 2 sets of 5 groups of Wistar rats were studied for real-time quantitative RT-PCR (n=6/group) and immunohistochemistry (n=4/group), respectively. An icv cannula was implanted into the left lateral cerebral ventricle, and connected to an osmotic mini-pump (Alzet, model 2ML2, ALZET Corp., CA) for chronic infusion at $5\mu\text{l/hr}$ for 14 days. Considering that the secretion rate of CSF in rats is $120\text{-}320\mu\text{l/hr}$ (Davson & Segal 1996), this low rate of icv infusion unlikely affects CSF pressure. Rats were randomized to the following groups: (i) aCSF ($[\text{Na}^+]$ 145 mmol/L), (ii) aCSF combined with spironolactone (100 ng/h), (iii) Na^+ -rich aCSF ($[\text{Na}^+]$ 800 mmol/L), or (iv) Na^+ -rich aCSF with spironolactone. One control group did not receive an icv cannula. In Wistar rats, icv infusion of Na^+ -rich aCSF at this concentration and rate of infusion for 1~2 weeks

increases CSF $[Na^+]$ by 5-7 mmol/L, sympathetic activity, and BP by 15 mmHg. Concomitant infusion of spironolactone (or benzamil as in protocol 2) at the rates used in the present study prevents the increases in sympathetic activity and BP (Huang et al. 2006b, Wang & Leenen 2003). In the second experiment, 3 sets of 2 groups of rats receiving icv infusion of aCSF or of Na^+ -rich aCSF were studied for western blot (n=4-5/group), cellular localization by *in situ* hybridization (n=4-5/group), and subcellular localization by immuno-electron microscopy (n=3/group). All rats remained on regular salt diet and normal tap water. Abundance of mRNA for *CYP11B1*, *CYP11B2*, MR and Nedd4L, and both mRNA and protein levels of ENaC and SGK1 were evaluated in the choroid plexus, ependyma, supraoptic nucleus, paraventricular nucleus and subfornical organ. Subcellular distribution of ENaC subunits was assessed in the choroid plexus and ependyma. To eliminate a possible effect of the icv cannula *per se*, the choroid plexus was obtained from the lateral ventricle opposite to the infusion site. Ependyma was obtained in the area of the anteroventral third ventricle. Assessment of ENaC subunits transcripts was attempted by laser capture microscopy and real-time PCR, but the mRNA abundance was too low to be detected and only immunohistochemistry and immuno-electron microscopy were used for evaluation of ENaC in the ependyma. The extracts from the whole supraoptic nucleus, paraventricular nucleus and subfornical organ were studied for mRNA and protein.

3.3.5.1.2 Protocol 2) Tissue and CSF $[Na^+]$ measurements

In the first experiment, 2 groups of rats had icv cannulae implanted and connected to osmotic mini-pumps for 1 week icv infusion of aCSF plus vehicle, or aCSF plus benzamil (4 μ g/kg/h in vehicle, n=5/group). In a second experiment, in 4 groups of rats

the icv cannulae were connected to osmotic mini-pumps for 2 weeks icv infusion of (i) aCSF plus vehicle, (ii) aCSF plus benzamil, (iii) Na⁺-rich aCSF plus vehicle, or (iv) Na⁺-rich aCSF plus benzamil (n=6-7/group). Benzamil was dissolved in 15% propylene glycol. At the end of each of these two experiments, under halothane anesthesia, each rat was placed in a stereotaxic frame, and 100-200 µL of CSF sample was withdrawn from the cisterna magna, as described previously (Huang et al. 2004). Rats were then decapitated and brains were collected and stored at -80°C.

3.3.5.2 Real-Time Quantitative RT-PCR

RNA was isolated from brain punches of specific nuclei using TriZol Reagent (Invitrogen, Burlington, ON, Canada) and cDNA was synthesized using QuantiTect Reverse Transcription kit with elimination of genomic DNA (Qiagen, Mississauga, ON, Canada). Real-time PCR was performed in duplicate using a Roche LightCycler and Fast-start DNA Master SYBR Green I dye (Roche Diagnostics, Laval, QC, Canada). Phosphoglycerate kinase 1 (PGK1) was used as the housekeeping gene. The sequences of the specific primers are described in Table 3.3-S1.

3.3.5.3 In situ hybridization

The 429bp PCR product of α ENaC was subcloned into pCRII-TA cloning vector (Invitrogen). A non-radioactive DIG RNA labeling kit (Roche Diagnostics) was used to synthesize antisense and sense digoxigenin-labeled RNA probes for α ENaC using SP6 and T7 RNA polymerase (Roche Diagnostics) respectively. The hybridization was performed on 7µm thickness coronal brain sections with sense and antisense DIG-labeled RNA probes at 42 °C for 16 hours. Semi-quantification was performed using Image Pro software version 4.02.03.

Table 3.3-S1 Primer sequences used for analysis of expression of ENaC subunits, SGK1, Nedd4-L, CYP11B1 and CYP11B2.

Gene	Sequence	Amplicon length
α ENaC	Forward: 5' - GTTCTGTGACTACCGAAAGCAGAG -3'	429 bp
	Reverse: 5' - CGTAGCAGCATGAGAAGTGTGATG -3'	
β ENaC	Forward: 5' -TGGATCACTGTCATCAAGCTAGTG-3'	440 bp
	Reverse: 5' -TGGTACCAGCATCTTGACCCTATG-3'	
γ ENaC	Forward: 5' - CGTCAGTGGCACAAAGCCAA -3'	301 bp
	Reverse: 5' - GAGAGCCTCCTCAAACCATG -3'	
Sgk1	Forward: 5' - GCGCAATGTTCTGTTGAAGA -3'	314bp
	Reverse: 5' - TGTGCTCGATGTTCTCCTTG -3'	
Nedd4L	Forward: 5' - ACAGAAGATCCAACCATGG -3'	330bp
	Reverse: 5' - ATCAAGCTAGGTCGGTGCCA-3'	
CYP11B1	Forward: 5' - GTCTATAAACATTGAGTCCAA-3'	324 bp
	Reverse: 5' - ATCTCGGATATGACACTCC-3'	
CYP11B2	Forward: 5' - CCCTGGTAGCCTGAAGTTCATC -3'	203bp
	Reverse: 5' - TCTGAGAGCTGCCGAGTCTG -3'	

3.3.5.4 Immunohistochemistry and Immuno-Electron Microscopy

Protein expression in different brain areas was studied by immunohistochemical staining of 5 μ m coronal sections. The slides were incubated with primary antibodies against α , β and γ ENaC (Masilamani et al. 1999) and developed with Vectastain Elite ABC and DAB kits (Vector Laboratories, Burlington, ON, Canada).

Immuno-electron microscopy was done to assess the subcellular distribution of ENaC subunits in select sections from the choroid plexus and ependyma. Following incubation

with the primary antibodies against ENaC subunits, 15-nm gold particle conjugated secondary antibodies (EY laboratories, San Mateo, CA) were used to demarcate subcellular localization of the proteins. The gold-labeled particles in each subcellular compartment were counted manually in a blinded fashion and are expressed as number / 100 μm^2 .

3.3.5.5 Western Blotting

Immunoblotting was performed on 40 μg protein from brain punches of the supraoptic and paraventricular nuclei, using antibodies against SGK1 (GeneX Inc, Hayward, CA) and phosphorylated SGK1 (p-SGK1:Thr²⁵⁶; Santa Cruz Biotechnology, Santa Cruz, CA).

3.3.5.6 CSF and Tissue $[\text{Na}^+]$ Assessment

CSF $[\text{Na}^+]$ and $[\text{Na}^+]$ in the hypothalamus were measured using an ion selective electrode (model MI-425, Microelectrodes Inc, Bedford, NH). Briefly, aCSF was prepared without NaCl, and NaCl was then added to have standards ranging from 120-180 mmol/L at 5 mmol/L increments, for the CSF $[\text{Na}^+]$ assay. For hypothalamic $[\text{Na}^+]$, each hypothalamus was dissected, weighed, and placed in a disposable polypropylene cryovial with 500 μl HNO_3 (EMD OmniTrace Ultra High Purity Grade) on ice, and then 100 μl H_2O_2 (EMD, Suprapur Grade) was added. After gentle mixing, the tubes were capped and left for 72 hours at room temperature for digestion of the tissue (Edelfors 1975). After neutralization with NH_4OH (EMD OmniTrace Ultra), sample volume was adjusted with ddH₂O to 5 ml in acid-washed glass volumetric flasks. Standards ranging from 0.1 to 5 mmol/L were prepared in a similar mixture of HNO_3 , H_2O_2 , and NH_4OH in ddH₂O, for the tissue assay. The electrode was connected to a standard pH meter (VWR, West Chester, PA) and relative millivolts (RmV) readings were recorded for the standards and

samples. Log standard $[\text{Na}^+]$ was against the RmV readings, and unknowns calculated from the appropriate standard curve.

3.3.5.7 Statistical Analysis

Data are expressed as means \pm SEM. Two-way ANOVA was used to analyze data with 4 groups for real-time PCR, immunohistochemistry, CSF and tissue $[\text{Na}^+]$. When the F-value was significant for a main effect, a Student-Newman-Keuls test was performed as posthoc test for multiple comparisons. A Student's t-test was performed to analyze data with 2 groups for *in situ* hybridization, western blot and immuno-electron microscopy. Statistical significance was defined as $p < 0.05$.

3.3.6 **Supplemental Methods**

3.3.6.1 Real-Time Quantitative RT-PCR

After perfusion with chilled diethyl pyrocarbonate (DEPC, Sigma-Aldrich Canada Ltd, Oakville, ON, Canada) treated phosphate-buffered saline (PBS, pH 7.4) the brains were removed and snap-frozen in liquid nitrogen and then stored at -80°C . Serial 80 μm thick coronal slices were cryosectioned and the specific areas were micro-punched out for total RNA isolation as described previously (Amin et al. 2005).

One μg of total RNA was used for cDNA synthesis by QuantiTect Reverse Transcription kit with elimination of genomic DNA (Qiagen Inc., Mississauga, Ontario, Canada). The primers, PCR conditions and external standards for MR, α , β and γ ENaC subunits and the house keeping gene phosphoglycerate kinase 1 (PGK1) were the same as previously described (Amin et al. 2005) except that different primer sequences were used for β ENaC. Sequences of the specific primers for α , β and γ ENaC (NM_012648.1), SGK1

(NM_019232), Nedd4L (Umemura et al. 2006) (XM57416), *CYP11B1* (NM_012537.2) and *CYP11B2* (NM_012538.1) are listed in table 3.3-S1. Specific primers for *CYP11B1* and *CYP11B2* were selected in the region of the lowest homology in DNA sequences by alignment analysis of those two genes as described previously (Ye et al. 2003). For *CYP11B1*, a 324-bp PCR fragment corresponding to positions 552–875 was amplified. For *CYP11B2*, we designed a pair of primers to amplify a 203-bp fragment corresponding to positions 651-853.

Real-time PCR was performed with a Roche Light Cycler using FastStart DNA Master SYBR Green I dye (Roche Diagnostics, Lava, QC, Canada). The PCR conditions were set as follows: initial at 95 °C for 10 min (5min for *CYP11B2*) followed by 45-50 cycles of denaturation at 95 °C for 5 sec (10 sec for *CYP11B2*); annealing for 10 sec at 65 °C for SGK1 or 60 °C for Nedd4L, 5 sec at 55 °C for *CYP11B1* or 65 °C for *B2*; extension at 72 °C. The PCR products of SGK1, Nedd4L, *CYP11B1* and *CYP11B2* were subcloned into pCRII-TA vector (Invitrogen, Burlington, ON, Canada), followed by restriction endonuclease and sequencing analysis. The concentration of each construct was quantified by absorbance at 260nm. Serial 10-fold dilutions of each plasmid clone were used to generate individual external standards with the same PCR conditions as described above. Expression was normalized to PGK1 levels as an endogenous reference. Normalization was achieved by dividing the amount of cDNA of each gene by the PGK1 quantity.

3.3.6.2 In Situ Hybridization

The 429bp PCR product of α ENaC was amplified under the following conditions: an initial denaturation step at 94 °C for 2 min, then 30 cycles of 94 °C for 50 sec, annealing

for 10 sec at 57 °C and extension for 1 min at 72 °C. The forward and reverse primer sequences are described in Table S1. The PCR products were purified by High Pure PCR product purification kit (Roche Diagnostics) and then were subcloned into pCRII-TA cloning vector (Invitrogen). The correct insert was analyzed by restriction enzyme and sequencing. A nonradioactive DIG RNA labeling kit (Roche Diagnostics) was used to synthesize antisense and sense digoxigenin-labeled RNA probes using SP6 and T7 RNA polymerase (Roche Diagnostics) respectively. Dot blotting was performed to confirm the efficiency of the labeling reaction and product yield.

Coronal brain sections, 7µm thick, were cut in a cryostat and thaw mounted onto Superfrost plus slides. Sections were post-fixed in 4% paraformaldehyde in PBS (pH 7.4) for 20 min, then rinsed three times in PBS, and washed in DEPC water for 10 min. The slides were immersed in 0.1 M HCl for 10 min for mild deproteinization. After rinsing with PBS, the slides were acetylated for 20 min in 0.1 M triethanolamine and 0.25% acetic anhydride. Subsequently, slides were rinsed twice in PBS, stepwise dehydrated (5 min each in 70, 80, and 95% ethanol) and air-dried. Sections were incubated with prehybridization solution [final concentrations: 50% deionized formamide (Sigma), 50 mM Tris-Cl pH 7.6, 25 mM EDTA, pH 8.0 20 mM NaCl, 0.25 mg/ml tRNA from yeast (Roche), and 2.5x Denhardt's solution (Sigma)] for 2 h at 42°C, followed by incubation for 16 h at 42°C in a moist chamber with 100 µl hybridization buffer [final concentrations: 50% deionized formamide, 20 mM Tris·HCl pH 7.6, 1 mM EDTA pH 8.0, 0.33 M NaCl, 0.2 M dithiothreitol, 0.5 mg/ml tRNA, 0.1 mg/ml sonicated denatured DNA from herring sperm (Roche), 1x Denhardt's solution, 10% dextran sulfate, and 1 ng/µl denatured riboprobe]. After two 15 min washes in 2xSSC at room temperature, the

slides were treated with 10 µg/ml RNase A for 30 min at 37°C, followed by two 1 hour washes at 49°C, first in 1x SSC and then in 0.5x SSC with 50% formamide. The slides were then rinsed at room temperature in 0.5x SSC for 15 min, in 0.2x SSC for 10 min, and equilibrated for 10 min in Tris buffer (100 mM Tris·HCl, 150 mM NaCl, pH 7.4). The sections were pre-blocked with 1% sheep serum (Chemicon, Temecula, CA) in TBS for 30 min, then incubated with alkaline phosphatase-coupled anti-digoxigenin antibody (dilution 1:500, Roche) for 2 hours at room temperature. The color reactions were performed with NBT/BCIP (Roche) according to the manufacturer's protocol. Specific signal of ISH was verified by parallel comparison between antisense and sense probes (Fig. 3.3-S2 and 3.3S3).

The slides were studied with a high resolution bright field light microscope (Olympus Bx60 with 2x, 20x and 40x objectives) and images were captured in .tiff format using a Spot digital camera and Spot software. Nuclear localization was confirmed by methyl green (Sigma) counterstaining. For semi-quantification, measurements were made using Image Pro software version 4.02.03. Images were first converted to Grayscale 16 type to facilitate quantification by eliminating differences due to color variation. The threshold of optical density for measurement in each area of specific brain nuclei was adjusted manually to include positive staining but exclude the background. Each area was evaluated for percent staining (calculated as a fraction of area that is positively stained, which indicates the changes in number of cells expressing the transcripts).

3.3.6.3 Immunohistochemistry and electron microscopy

Immunohistochemistry: Brains were perfusion-fixed with 4% paraformaldehyde and 0.05% glutaraldehyde either in PBS (pH 7.4) for immunostaining, or in 0.1 M Na-

cacodylate buffer for electron microscopy. 5 µm coronal sections of the brain areas of interest were cut in a rostral to caudal direction using a cryostat (-30° C) and thaw mounted onto superfrost plus slides. Immunoperoxidase histochemistry was carried out using an avidin-biotin method as described previously (Amin et al. 2005). The primary antibodies (1:250 for α, γ or 1:500 for βENaC)(Masilamani et al. 1999) were diluted in blocking solution and used at the same dilutions throughout the experiment. Following overnight incubation at 4°C with the primary antibodies, slides were processed using Vectastain Elite ABC and DAB kits (Vector Laboratories, Burlington, ON, Canada).

Complete labeling of a section was confirmed by the presence of uniform Nova red or DAB intensity in most parts. For semi-quantification, images were captured in *.tiff* format using the Spot digital camera and Spot software and high resolution bright field Olympus light microscope described above. Following visual assessment of cellular distribution, percent staining was assessed by Image Pro software version 4.02.03 as described above. For each area of interest, the averages of at least 8 individual measurements from at least two slides from each rat were used to evaluate percent staining.

3.3.6.4 Immuno-electron microscopy

Brains were post-fixed in perfusion fixative for 30 min, dissected under a stereomicroscope and the sections stored in 0.1 mol/L Na-Cacodylate buffer at 4°C. Tissues were dehydrated in a series of graded alcohols, infiltrated with LR White resin and polymerized at 50° C. 50-90nm sections were mounted on Formvar coated nickel grids and placed onto drops of 1% BSA for 30 min. Without rinsing, the grids were then placed onto drops of primary antibodies diluted in 0.1% BSA in PBS (1:100) and incubated overnight at 4°C. After rinsing in PBS the grids were incubated at room

temperature for 1 hour on drops of secondary goat anti-rabbit IgG conjugated to 15 nm gold particles (EY Laboratories, 1:100). Grids were counterstained with 3% uranyl acetate and lead citrate.

Sections were imaged in a Jeol 1230 TEM using AMT software. Low magnification (1000×) images were used for area calculation by Image Pro. The number of gold particles (per 100 μm^2) in subcellular compartments (cytoplasm, apical or basal membrane) were counted from highly magnified images (8000-20000×) using ACDSee software. A total of 9500 square microns (~4000 electron microscopy fields) were quantified.

3.3.6.5 Western Blotting

Brain punches were performed as described above, then homogenized in ice-cold *RIPA* buffer containing 1% protease inhibitor cocktail (Sigma). The homogenate was spun at 4,000 g for 20 minutes at 4°C, and the supernatant was collected. Total protein was measured using a Micro BCA assay (Pierce, Rockford, IL), and 40 μg protein was separated on 10% SDS-PAGE gels, and then transferred onto PVDF membranes (Bio-Rad, Reinach, Switzerland). After blocking 1 hour at room temperature with 5% non-fat milk in 1×TBS-T for total SGK1, or 6-8 hours at 4°C with TBS Blotto B blocking reagent (Santa Cruz Biotechnology Inc. Santa Cruz, CA) for phosphorylated SGK1 (p-SGK1), the membranes were incubated overnight at 4°C with the primary antibodies against total SGK1(1:3000, GeneX Inc, Hayward, CA) or p-SGK1 (1:200, Santa Cruz). Goat anti-rabbit IgG conjugated with horseradish peroxidase (HRP) (1:10,000, Santa Cruz) and donkey anti-goat IgG-HRP (1:20,000, Santa Cruz) were used as secondary antibodies for total SGK1 or p-SGK1 respectively. The membranes were stripped and

reprobed with anti β -actin antibody (1:10,000, Sigma). After detection with Western Lightning Plus ECL⁺ reagents (Perkin Elmer, Shelton, CT), protein bands were visualized using an Alpha Innotech Imager (Alpha Innotech, San Leandro, CA), and band densities quantified by Alpha Ease software. The results are expressed in arbitrary units, as a percentage change in normalized densitometry of the target protein versus that at β -actin.

3.3.7 RESULTS

Real-time quantitative RT-PCR (qPCR) analysis showed that icv infusion of control aCSF did not affect mRNA abundance of the three ENaC subunits, MR, SGK1, or Nedd4L in different brain areas compared with values in rats without an icv infusion (data not shown). Immunohistochemistry analysis revealed appreciable levels of α , β and γ ENaC immunostaining in the choroid plexus without icv infusion (Fig. 3.3-S1). However, icv infusion *per se* decreased immunoreactivity of γ ENaC to low levels in all areas (Fig 3.3-S1) and could not be reliably quantified.

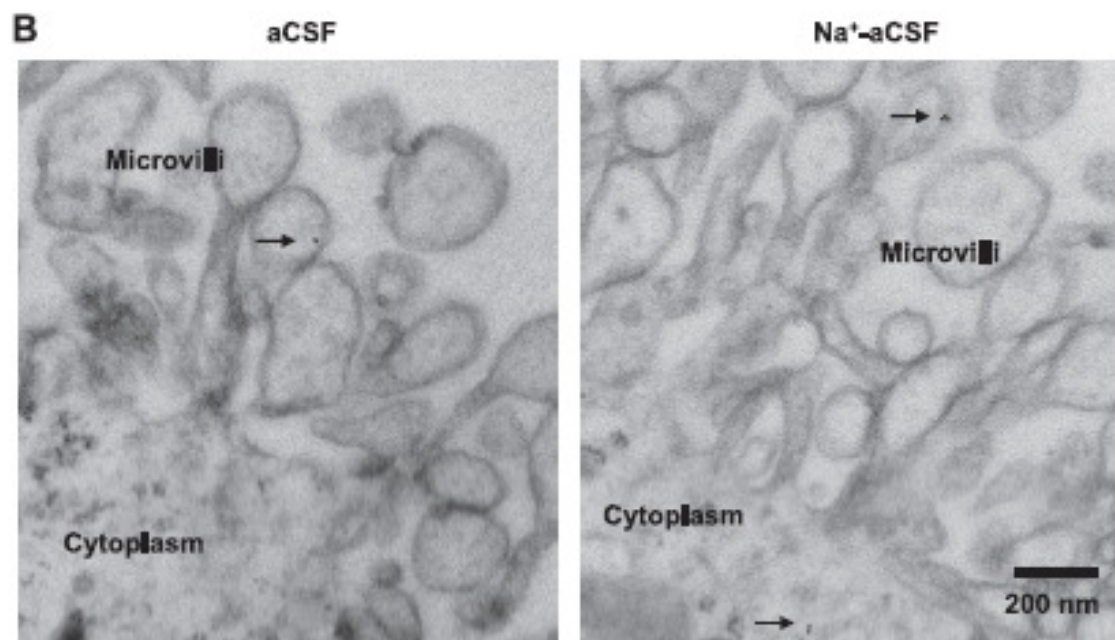
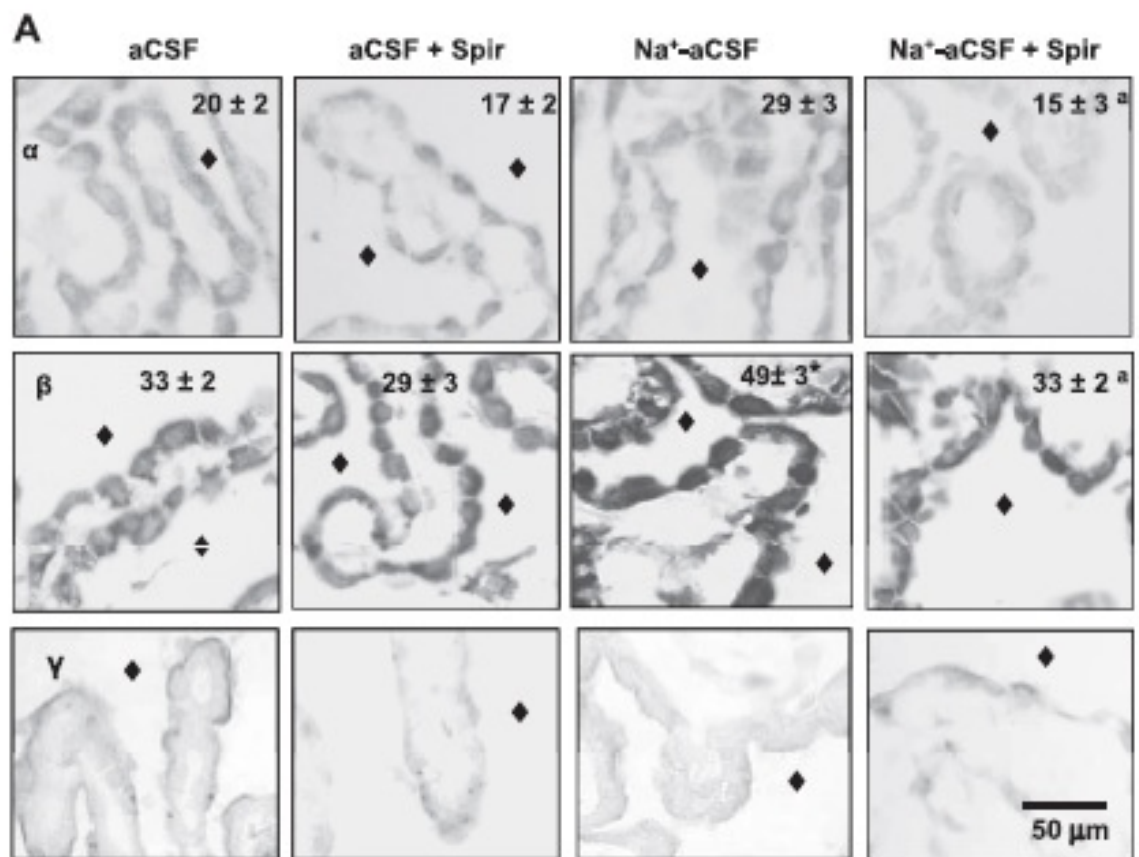
3.3.7.1 Choroid Plexus

Icv infusion of Na⁺-rich aCSF did not affect mRNA levels of α and γ ENaC, measured by qPCR (Table 3.3-1). Immunohistochemistry analysis showed that icv infusion of Na⁺-rich aCSF also had no effect on percent staining of α ENaC (Fig. 3.3-1A). Na⁺-rich aCSF infusion increased β ENaC mRNA abundance by approximately 2 fold ($p < 0.05$, Table 3.3-1) and percent staining by 50% ($p < 0.005$, Fig. 3.3-1A). Spironolactone did not significantly change α ENaC mRNA levels (Table 3.3-S2) but decrease percent staining for immunoreactivity in the Na⁺-rich aCSF group ($F = 5.47$, $p < 0.05$, Fig. 3.3-1A). Spironolactone prevented the increase in percent staining of β ENaC ($F = 6.60$, $p < 0.05$, Fig. 3.3-1A) but had no effect on the increase in β ENaC mRNA abundance (Table 3.3-S2). Spironolactone did not affect γ ENaC mRNA levels (Table 3.3-S2).

To study the localization of ENaC transcripts, α ENaC was assessed by *in situ* hybridization because the α -subunit showed the highest mRNA levels (Table 3.3-1). Positive signals specific for α -subunit antisense riboprobes were more prominent in the

choroid cells than endothelia of blood vessels. Sense riboprobes failed to generate obviously detectable signals (Fig. 3.3-S2).

*Figure 3.3–1(Next page): Effects of 2 wk of intracerebroventricular (icv) infusion of Na⁺ rich artificial cerebrospinal fluid (aCSF) alone or combined with spironolactone (Spir) on α , β , and γ -epithelial Na⁺ channel (ENaC) immunostaining (A) and subcellular localization of α ENaC-labeled gold-labeled particles (B) in choroid plexus. Values (means \pm SE, n = 4/group). Insets in A represent percent staining (i.e., fraction of area that was stained). The diamond denotes CSF side. Arrows in B show α -ENaC-gold-labeled particles in apical microvilli of a control rat infused with aCSF and a rat infused with Na⁺-rich aCSF. By 2-way ANOVA, Na⁺-rich aCSF significantly increases β -ENaC immunostaining ($F = 16.40$, $*P < 0.001$ vs. aCSF groups). Spironolactone significantly lowers α -ENaC ($F = 14.75$, $^aP < 0.005$) and β -ENaC ($F = 17.41$, $^aP < 0.001$) immunostaining, with a significant interaction between spironolactone and Na⁺ treatment [$F = 5.47$, $P < 0.05$ (for α -ENaC) and $F = 6.60$, $P < 0.05$ (for β -ENaC)].*



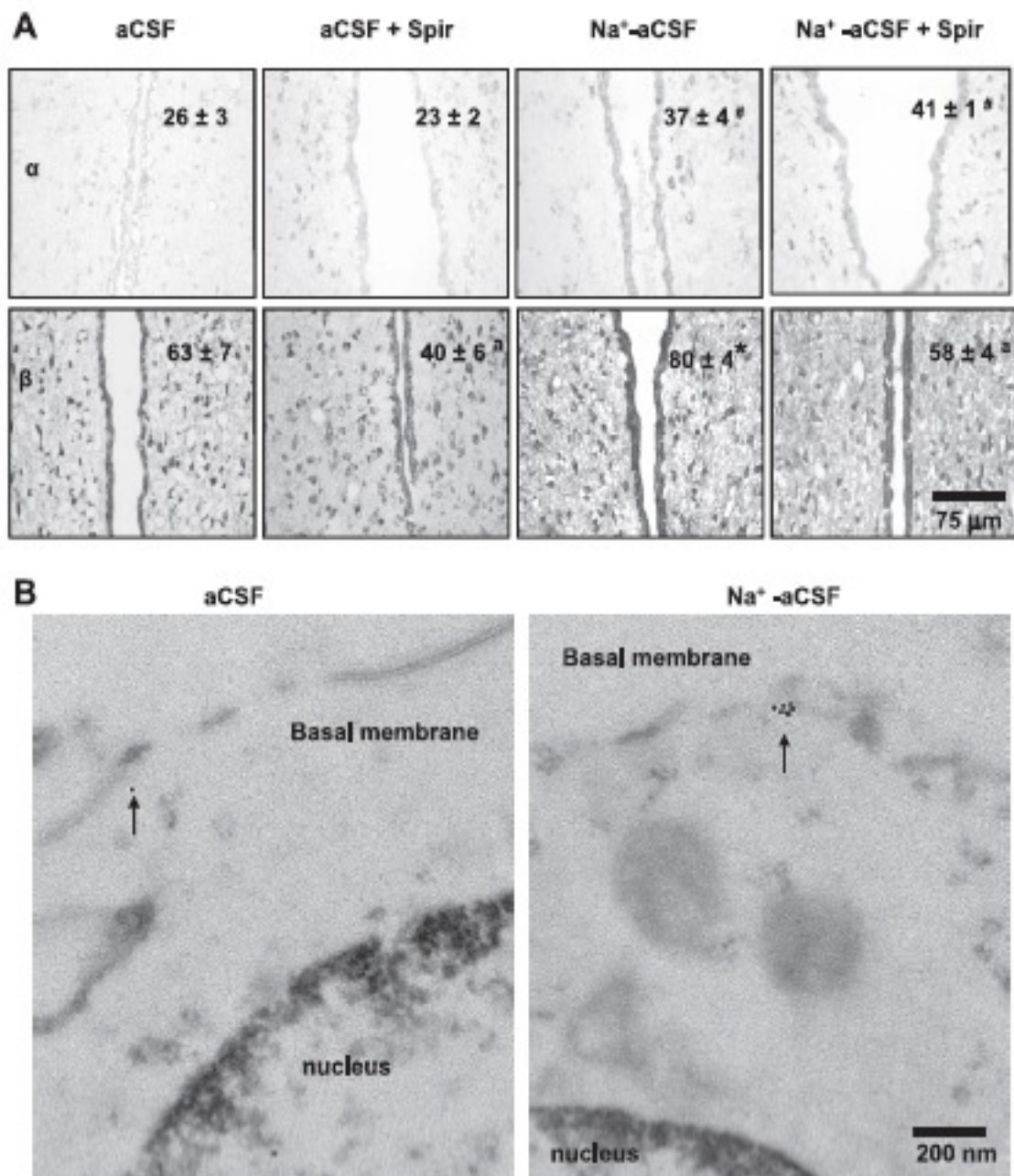


Figure 3.3–2: Effects of 2-week icv infusion of Na⁺-rich aCSF alone or combined with spironolactone (Spir.) on α and β ENaC immunostaining (A) and subcellular localization (B) in the ependyma of the anteroventral third ventricle. Values (means \pm SEM, n=4/group) in A represent percent staining (fraction of area that was stained). Arrows in B

show β ENaC gold-labeled particles in the ependymal basal membrane of an aCSF control rat and a rat infused with Na^+ rich aCSF. For α ENaC, by two-way ANOVA, Na^+ -rich aCSF significantly increases α ENaC immunostaining ($F= 31.73$, # $p<0.0001$ versus aCSF groups) with no effect of spironolactone on α ENaC immunostaining. For β ENaC, Na^+ -rich aCSF significantly increases β ENaC immunostaining ($F= 9.84$, * $p< 0.05$ versus aCSF groups). Spironolactone significantly lowered β ENaC immunostaining ($F=16.84$, $ap<0.005$. Spir. versus none) with no interaction between spironolactone and Na^+ .

Immunohistochemistry (Fig. 3.3-1A) and immuno-electron microscopy (Fig. 3.3-1B and table 3.3-2), showed that ENaC was most prominent in the cytoplasm as well as in the apical membranes and present to a lesser extent in the basolateral membranes. Immuno-electron microscopy indicated that Na^+ -rich aCSF induced a greater number of α ENaC-gold-labeled particles especially in the microvilli by approximately 4 fold (Fig 3.3-2B and table 3.3-2), and did not significantly ($p=0.07$) affect α ENaC-gold-labeled particles in the basal membrane. Na^+ -rich aCSF also increased β ENaC-gold-labeled particles ($p<0.05$) in the apical membrane (Table 3.3-2). No significant effects of Na^+ -rich aCSF on the γ subunits were noted (Table 3.3-2).

Na^+ -rich aCSF did not affect the mRNA abundance of *CYP11B1*, MR, SGK1 or Nedd4L (Table 3.3-1). *CYP11B2* transcripts were below the detection limit in the choroid plexus.

Table 3.3–1: Relative abundance of ENaC subunits, MR, SGK1, Nedd4L, CYP11B1, and CYP11B2 mRNA in different brain areas after 2-wk of icv infusion of aCSF or Na⁺rich aCSF.

Brain Areas	aCSF	Na ⁺ -Rich aCSF	aCSF	Na ⁺ -Rich aCSF
	α -ENaC/PGK1 ($\times 10^{-3}$)		β -ENaC/PGK1 ($\times 10^{-3}$)	
Choroid plexus	2.1 \pm 0.2	2.6 \pm 0.7	0.9 \pm 0.2	1.9 \pm 0.3*
Supraoptic nucleus	1.8 \pm 0.2	1.5 \pm 0.1	0.9 \pm 0.2	1.3 \pm 0.1
Paraventricular nucleus	1.4 \pm 0.2	1.3 \pm 0.2	1.0 \pm 0.1	0.9 \pm 0.1
Subformal organ	4.1 \pm 0.6	3.7 \pm 0.3	2.0 \pm 0.4	2.3 \pm 0.3
	γ -ENaC/PGK1 ($\times 10^{-4}$)		MR/PGK1 ($\times 10^{-2}$)	
Choroid plexus	0.9 \pm 0.2	0.8 \pm 0.1	2.0 \pm 0.1	3.3 \pm 0.3
Supraoptic nucleus	1.1 \pm 0.1	1.1 \pm 0.2	1.8 \pm 0.1	1.8 \pm 0.1
Paraventricular nucleus	0.8 \pm 0.1	0.8 \pm 0.1	1.3 \pm 0.1	1.3 \pm 0.1
Subformal organ	3.7 \pm 0.4	3.1 \pm 0.8	2.2 \pm 0.5	2.0 \pm 0.2
	Sgk1/PGK1 ($\times 10^{-4}$)		Nedd4L/PGK1 ($\times 10^{-2}$)	
Choroid plexus	3.4 \pm 0.4	3.4 \pm 0.4	7.4 \pm 0.6	9.7 \pm 1.5
Supraoptic nucleus	1.1 \pm 0.1	1.0 \pm 0.1	6.7 \pm 0.6	9.5 \pm 3.4
Paraventricular nucleus	0.9 \pm 0.2	1.0 \pm 0.2	7.0 \pm 0.5	5.8 \pm 0.6
Subformal organ	3.4 \pm 0.2	3.8 \pm 0.3	9.7 \pm 0.8	8.7 \pm 0.6
	CYP11B1/PGK1 ($\times 10^{-4}$)		CYP11B2/PGK1 ($\times 10^{-4}$)	
Choroid plexus	17.1 \pm 4.1	19.9 \pm 2.9	BD	BD
Supraoptic nucleus	10.5 \pm 1.2	13.1 \pm 2.1	1.1 \pm 0.1	1.3 \pm 0.2
Paraventricular nucleus	6.7 \pm 0.7	4.7 \pm 0.4	1.0 \pm 0.1	0.7 \pm 0.1
Subformal organ	3.4 \pm 0.6	4.1 \pm 0.8	0.2 \pm 0.04	0.2 \pm 0.03

Values are means \pm SE (n = 6/group). Whole nuclei were punched from the brain and homogenized for total RNA extraction. ENaC, epithelial Na⁺ channel; aCSF, artificial cerebrospinal fluid; MR, mineralocorticoid receptor; PGK1, phosphoglycerate kinase 1; BD, below detection. By 2-way ANOVA, spironolactone had no significant effect and there were no interaction effects on any of the expression levels. Only data from the 2 groups without spironolactone are shown. (See supplemental table for data from all groups, i.e., aCSF or Na⁺rich aCSF with or without spironolactone.) By 2-way ANOVA for the 4 groups, there is a significant effect of Na⁺ rich aCSF on β ENaC mRNA levels (F = 5.15, *P 0.05 vs. aCSF groups) with no effect of spironolactone on this increase (see supplemental Table 3.3-S2).

Table 3.3–2: Abundance of α , β and γ ENaC in different cellular compartments in the choroid plexus and ependyma after 2-wk of icv infusion of Na^+ rich aCSF. Values are means \pm SE, expressed as number of gold particles per $100 \mu\text{m}^2$. Na^+ = Na^+ -rich aCSF. * 3-fold change in response to Na^+ -rich aCSF infusion.

	α -ENaC		β -ENaC		γ -ENaC	
	aCSF	Na^+	aCSF	Na^+	aCSF	Na^+
Cytoplasm						
Choroid plexus	30 \pm 14	73 \pm 4	25 \pm 2	26 \pm 3	29 \pm 10	23 \pm 3
Ependyma	23 \pm 12	33 \pm 20	14 \pm 0.7	26 \pm 7	19 \pm 4	34 \pm 0.2
Basal membrane						
Choroid plexus	15 \pm 10	41 \pm 9	9 \pm 5	6 \pm 0.3	8 \pm 3	4 \pm 0.3
Ependyma	4 \pm 1	14 \pm 4*	3 \pm 0.6	15 \pm 5*	5 \pm 0.7	3 \pm 0.3
Microvilli						
Choroid plexus	45 \pm 21	161 \pm 23*	13 \pm 5	26 \pm 5	22 \pm 11	20 \pm 2
Apical membrane						
Ependyma	28 \pm 6	25 \pm 14	13 \pm 3	33 \pm 20	7 \pm 1	14 \pm 2

3.3.7.2 Ependyma

In the ependyma of the anteroventral third ventricle, ENaC immunoreactivity was present in the cytoplasm as well as in the apical and basal membranes of the epithelial lining (Fig 3.3-2A). By electron microscopy, ENaC particles were prominent in the cytoplasm with similar or lesser numbers in the apical and basal membranes (Table 3.3-2, Fig 3.3-2B). By immunohistochemistry, Na^+ -rich aCSF increased percent staining for α ($p < 0.0001$) and β ENaC ($p < 0.05$) immunoreactivities by $\sim 30\%$ (Fig. 3.3-2A). Spironolactone had no effect on the increase in α ENaC, but lowered percent staining of β ENaC in both the CSF and Na^+ -rich aCSF groups ($p < 0.005$, Fig. 3.3-2A). By electron microscopy, Na^+ -rich aCSF significantly increased the number of α and β ENaC-gold-labeled particles in the basolateral membranes and of γ ENaC in the cytoplasm (Table 3.3-2, Fig. 3.3-2B).

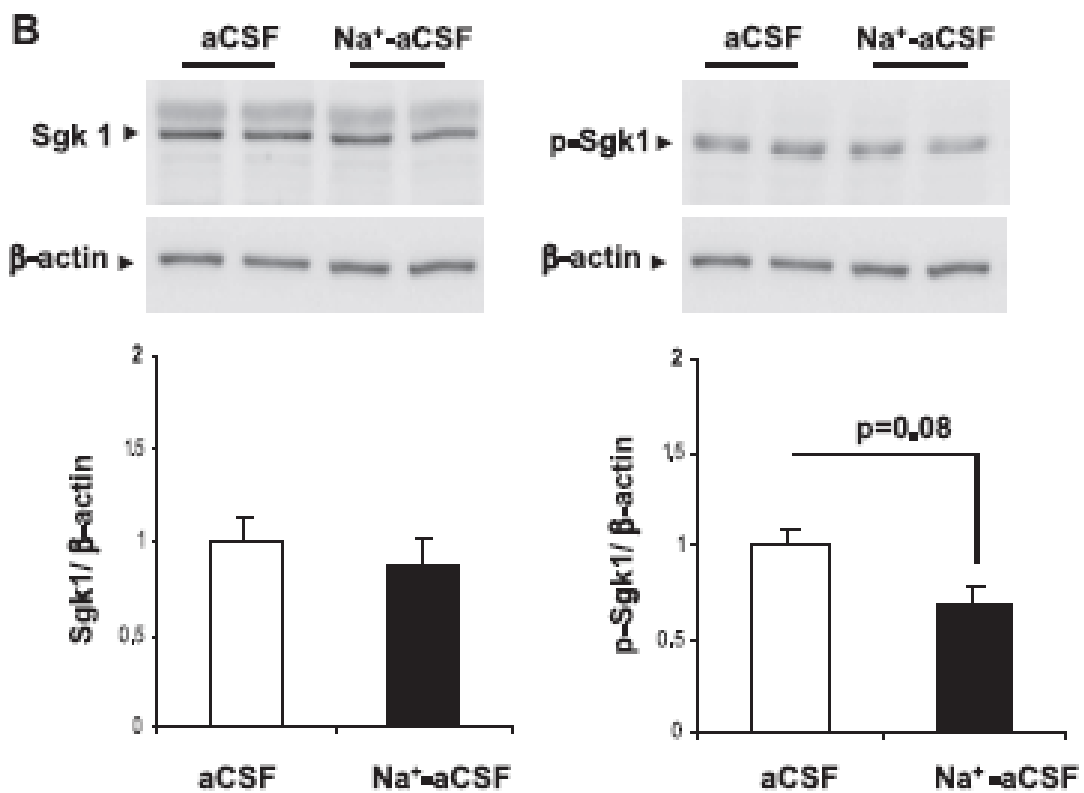
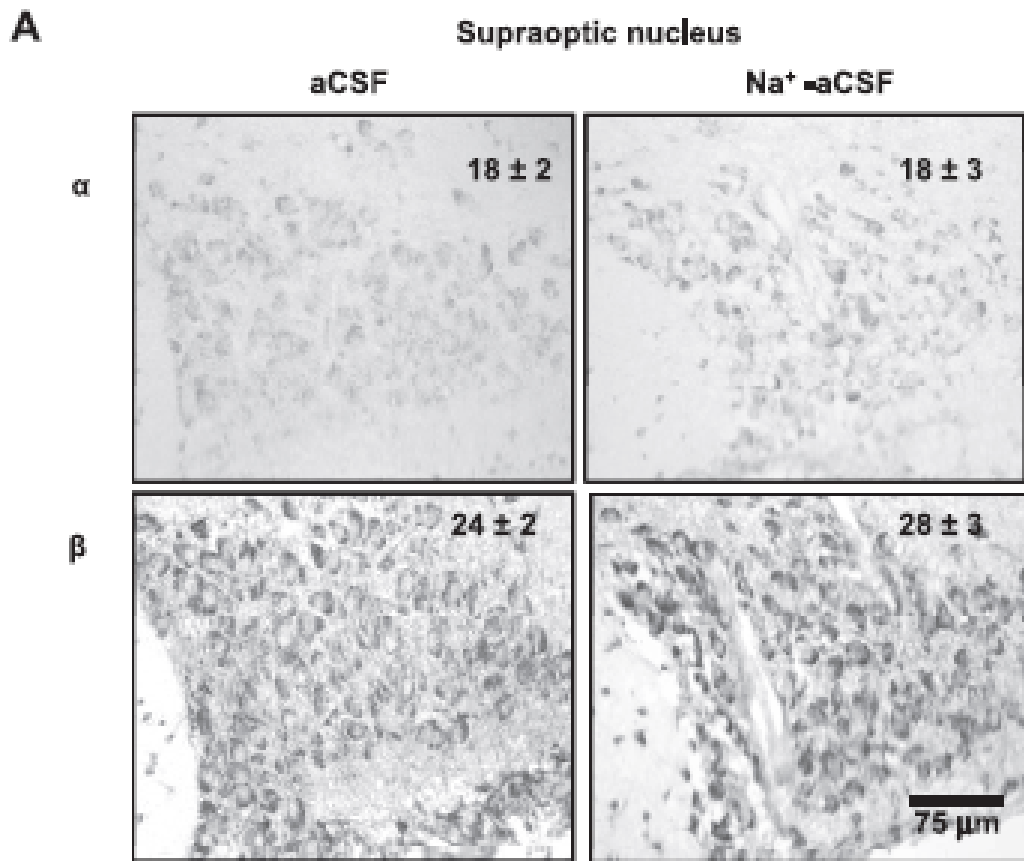


Figure 3.3–3(previous page): Effects of 2 wk of icv infusion of Na⁺ rich aCSF on α and β ENaC immunostaining and serum/glucocorticoid-inducible kinase 1 (SGK1) protein abundance in the supraoptic nucleus. Values (means \pm SE, n = 4/group) in A represent percent staining (i.e., fraction of area that was stained). Representative Western blots of SGK1 and phosphorylated SGK1 (p-SGK1) are shown in B. Values of SGK1/ β -actin or p-SGK1/ β -actin of aCSF group were normalized to 1.

3.3.7.3 Supraoptic Nucleus

In situ hybridization showed more abundant expression of α ENaC transcripts in magnocellular neurons than adjacent glial cells (Fig. 3.3-S3). Immunoreactivity of ENaC subunits was most prominent in the cytoplasm of the magnocellular neurons. qPCR showed that icv infusion of Na⁺-rich aCSF did not alter mRNA abundance of α , β or γ ENaC (Table 3.3-1). Consistent with the PCR data, Na⁺-rich aCSF did not affect staining for α ENaC transcription, as measured by *in situ* hybridization, in the magnocellular neurons of the supraoptic nucleus (Fig 3.3-S5). There was also no effect of Na⁺-rich aCSF on staining for α or β ENaC immunoreactivity, as measured by immunostaining (Fig. 3.3-3A).

Na⁺-rich aCSF did not affect SGK1 mRNA levels (Table 3.3-1). Western blotting analyses indicated that Na⁺-rich aCSF did not significantly affect phosphorylated SGK1 (p=0.08) or total SGK1 protein levels in the supraoptic nucleus (Fig. 3.3-3B). Na⁺-rich aCSF did not alter *CYP11B1*, *CYP11B2*, MR, or Nedd4L mRNA levels (Table 3.3-1).

3.3.7.4 Paraventricular nucleus

By *in situ* hybridization, the staining of α ENaC transcripts was more abundant in magnocellular than in parvocellular neurons (Fig 3.3-S5). Immunoreactivity of ENaC

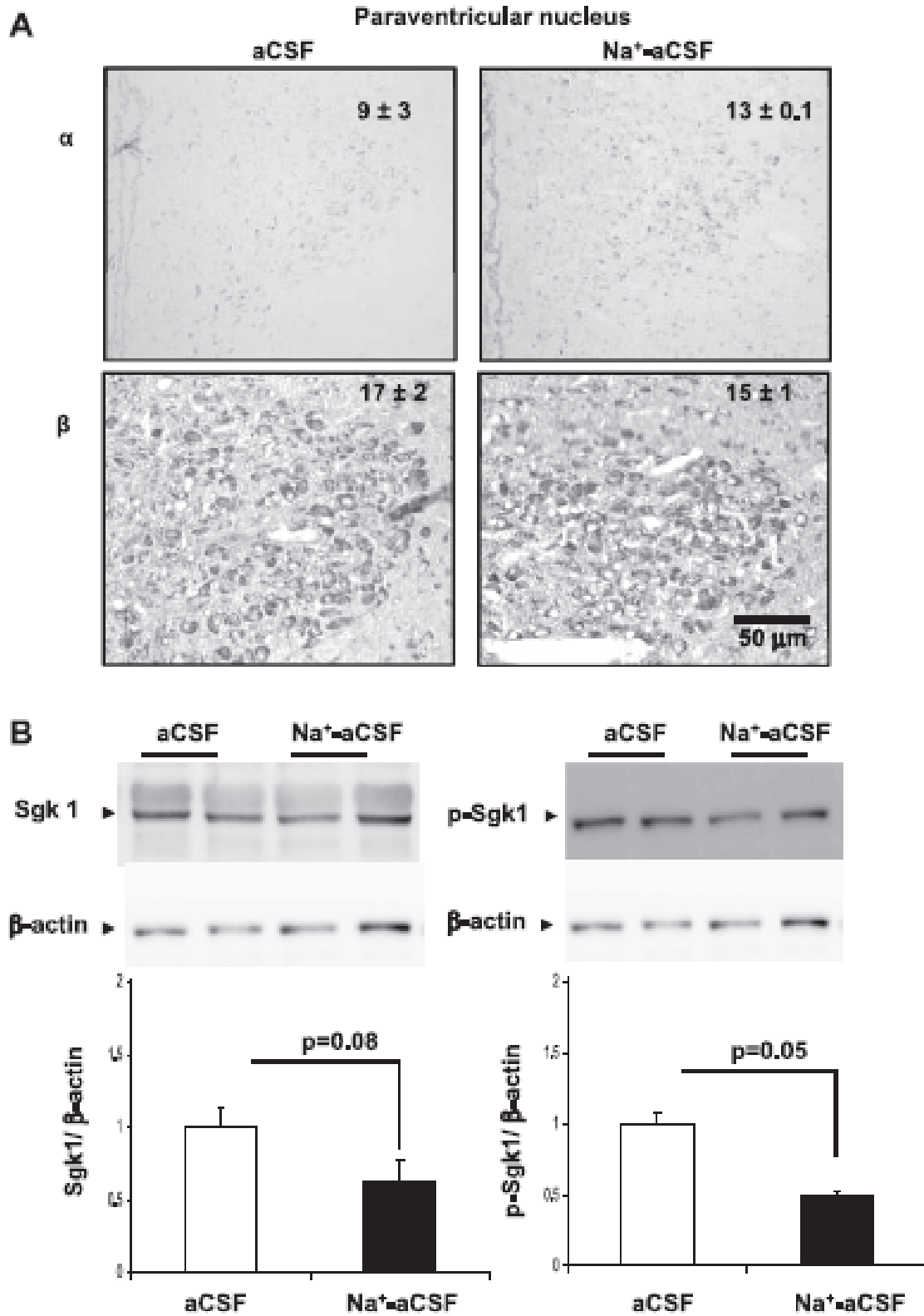


Figure 3.3-4 Effects of 2 wk of icv infusion of Na⁺ rich aCSF on α and β ENaC immunostaining and SGK1 protein abundance in the paraventricular nucleus. Values

(means \pm SE, $n = 4$ /group) in A represent percent staining. Representative Western blots of SGK1 and phosphorylated SGK1 are shown in B. Values of SGK1/ β -actin or p-SGK1/ β -actin of aCSF group were normalized to 1.

subunits was more abundant in the cytoplasm of magnocellular neurons than in adjacent glial cells. Almost no immunoreactivity for ENaC subunits was noted in the parvocellular neurons. Na⁺-rich aCSF did not alter the mRNA abundance of ENaC subunits in the whole paraventricular nucleus, as measured by either qPCR (Table 3.3-1) or *in situ* hybridization (Fig 3.3-S5). Immunohistochemistry showed that Na⁺-rich aCSF also did not affect immunoreactive staining for α or β subunits in the magnocellular neurons of the paraventricular nucleus (Figure 3.3-4A).

Na⁺-rich aCSF did not affect SGK1 mRNA levels (Table 3.3-1), but appeared to decrease phosphorylated SGK1 ($p=0.05$) without significantly ($p=0.08$) altering total SGK1 protein abundance, as measured by western blot (Fig. 3.3-4B). Na⁺-rich aCSF had no effect on the mRNA abundance of *CYP11B1*, *CYP11B2*, MR or Nedd4L (Table 3.3-1).

3.3.7.5 Subfornical organ

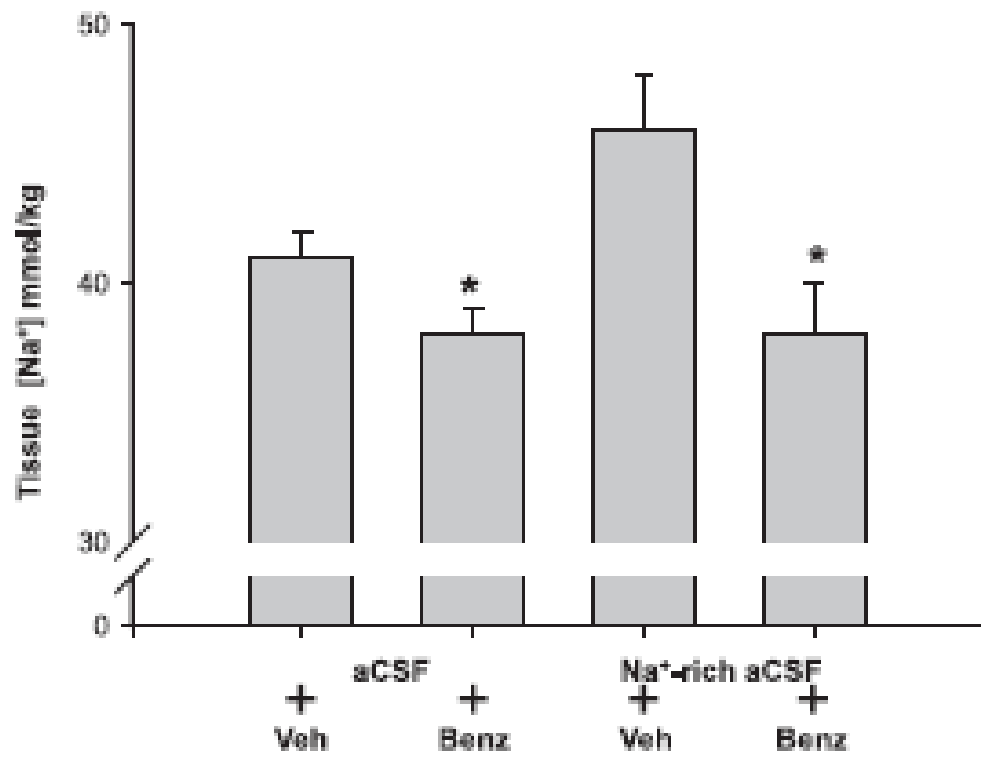
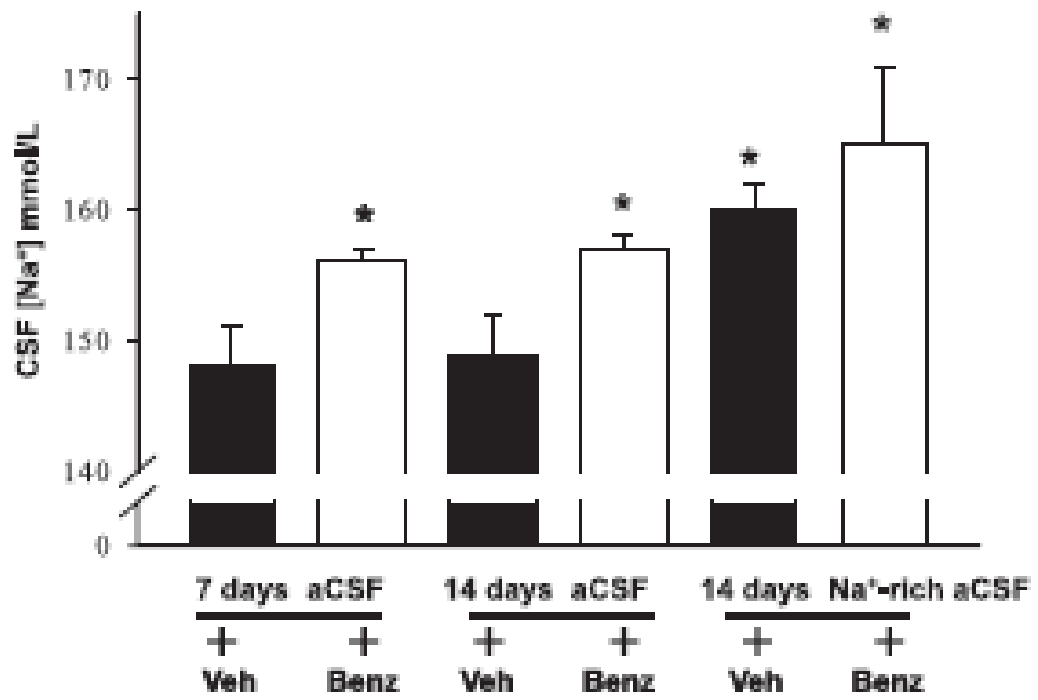
mRNA of all three ENaC subunits was found in the subfornical organ. Immunoreactivity for ENaC subunits was diffuse in the cytoplasm of neurons in this nucleus and very low for α ENaC (data not shown). Na⁺-rich aCSF infusion did not affect mRNA levels of the three ENaC subunits (Table 3.3-1) or percent staining for α or β ENaC immunoreactivity (data not shown).

Na⁺-rich aCSF did not affect mRNA abundance of *CYP11B1* and *CYP11B2*, MR, SGK1 or Nedd4L (Table 3.3-1).

3.3.7.6 CSF and hypothalamic tissue [Na⁺]

In rats with icv infusion of control aCSF, concomitant infusion of benzamil increased CSF [Na⁺] (F=12.13, p<0.005, Fig. 3.3-5 top) similarly after 1 week and 2 weeks. In rats with icv infusion of Na⁺-rich aCSF, CSF [Na⁺] significantly (F=7.65, p<0.05) increased to 160 ± 2 mmol/L and together with benzamil to 166 ± 6 mmol/L (non-significant versus Na⁺-rich aCSF alone, Fig. 3.3-5, top,). Icv infusion of Na⁺-rich aCSF increased hypothalamic tissue [Na⁺] by 5.8 mmol/kg compared to the aCSF treated group. Concomitant benzamil infusion fully prevented the increase in hypothalamic tissue [Na⁺] by Na⁺-rich aCSF but did not affect hypothalamic tissue [Na⁺] in the aCSF treated group (Fig. 3.2-5, bottom).

*Figure 3.3–5(next page): Effects of icv infusion of aCSF and Na⁺ rich aCSF alone or combined with benzamil (Benz) on CSF and hypothalamic tissue Na⁺ concentration ([Na⁺]). Values are means ± SE (n = 5–7/group). For CSF [Na⁺], by 2-way ANOVA, benzamil significantly increases CSF [Na] [F = 12.13, *P < 0.005 vs. aCSF vehicle (Veh) groups], with no significant difference between 1 and 2 wk of benzamil treatment in control aCSF-treated groups. Na⁺ -rich aCSF significantly increases CSF [Na⁺] (F = 7.65, *P < 0.05 vs. aCSF Veh groups). Benzamil has no significant (F = 3.60, P = 0.07) effect on this increase in CSF [Na⁺]. For hypothalamic tissue [Na⁺], benzamil has a significant effect on tissue [Na⁺] (F = 10.27, *P < 0.005 vs. groups without benzamil), whereas tissue [Na⁺] for different levels of Na⁺ in aCSF did not differ significantly (P = 0.12), and treatment x Na⁺ interaction only showed a tendency (P = 0.08).*



Choroid Plexus

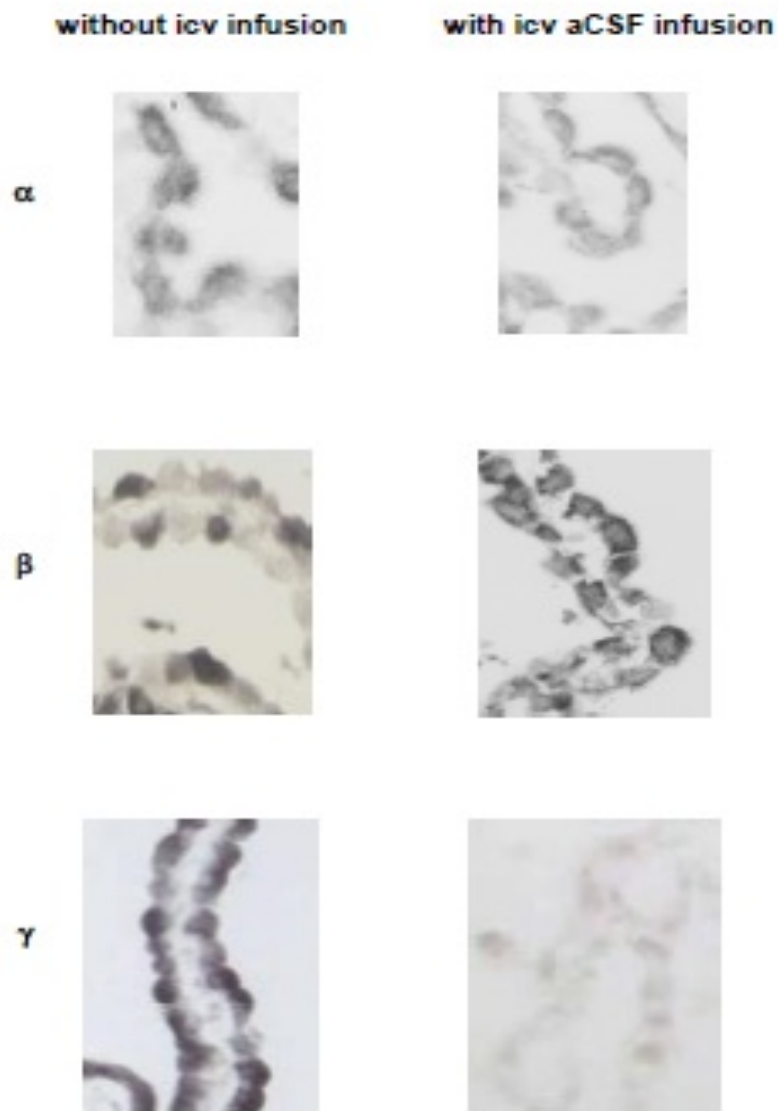


Figure 3.3-S1: ENaC α , β and γ subunit immunostaining in the choroid plexus of rats with out an icv cannula (left panels) and of rats with icv cannula and icv infusion of aCSF (right panel).

Figure S2

Choroid Plexus

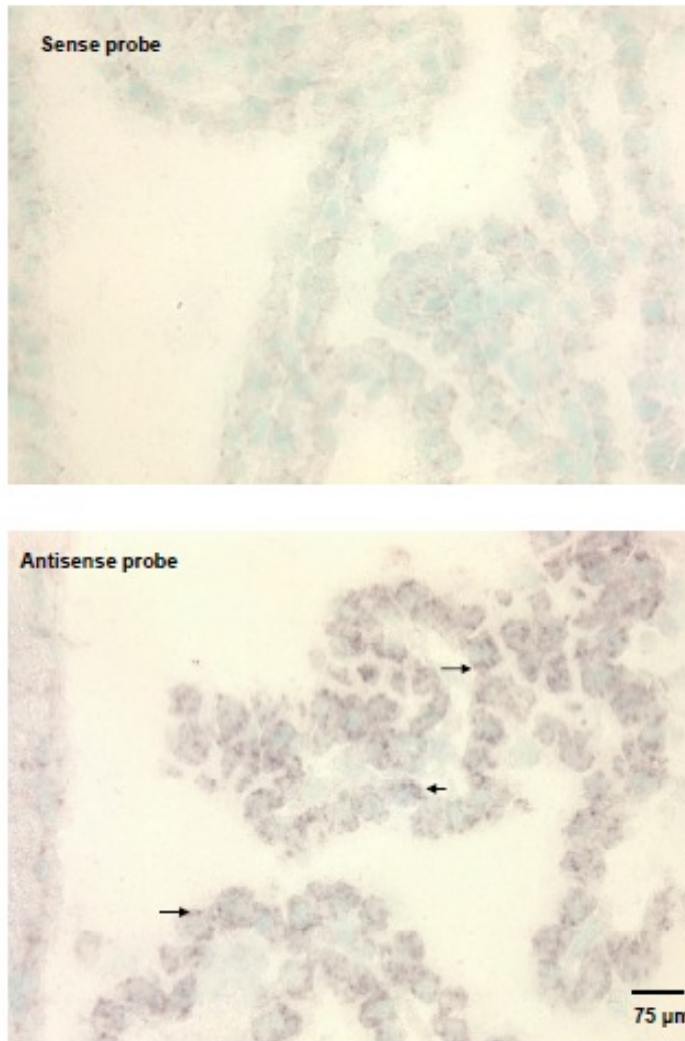


Figure 3.3-S2: *In situ* hybridization of ENaC α -subunit in the choroid plexus. Images represent nonradioactive *in situ* hybridization with specific ENaC α -subunit riboprobes in representative sections of the choroid plexus. Top panel: brain section hybridized using sense riboprobes as negative control. Lower panel: brain section hybridized using

antisense riboprobes for localization. Arrows indicate the positive cells with purple staining of the cytoplasm after nuclear counterstaining with methyl-green.

Figure S3

Supraoptic Nucleus

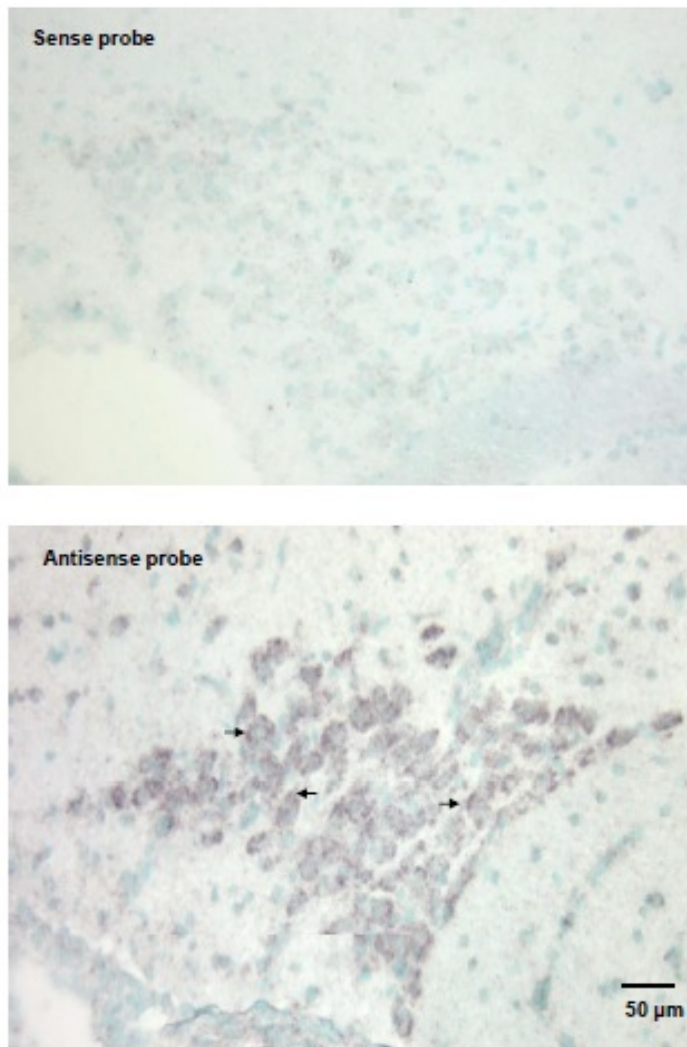


Figure 3.3-S3: In situ hybridization of ENaC α -subunit in the supraoptic nucleus. Top panel: brain section hybridized using sense riboprobes as negative control. Lower panel: antisense riboprobe hybridization for localization. Arrows indicate the positive magnocellular neurons with purple staining of the cytoplasm after nuclear counterstaining with methyl-green.

Figure S4

Supraoptic Nucleus

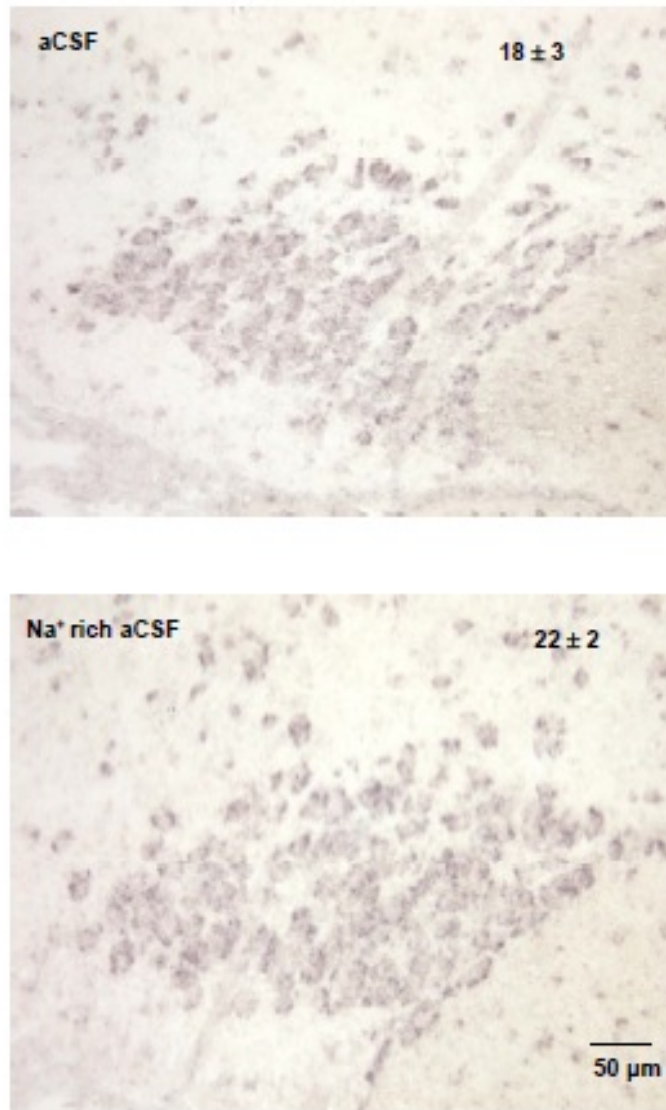


Figure 3.3-S4: Effects of 2-week icv infusion of Na⁺ rich aCSF on α ENaC mRNA staining in the supraoptic nucleus by in situ hybridization. Insets show means \pm SEM for percent staining (%) (fraction of area that was stained).

Figure S5

Paraventricular Nucleus

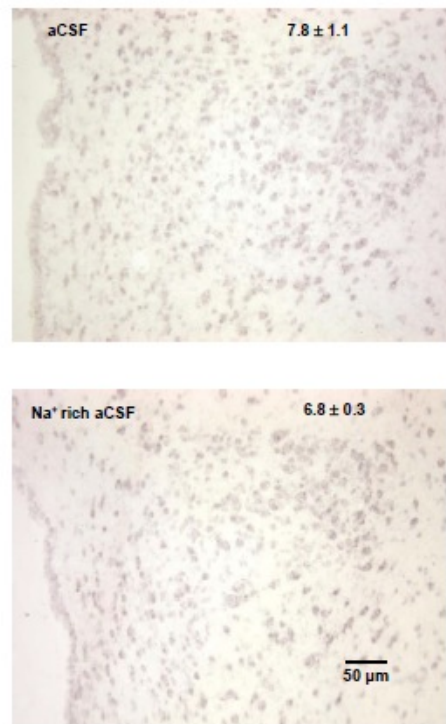


Figure 3.3-S5: Effects of 2-week icv infusion of Na⁺-rich aCSF on α ENaC mRNA staining in the paraventricular nucleus by in situ hybridization. Insets show means \pm SEM for percent staining (%) (fraction of area that was stained).

Table 3.3-S2: (Next page) Relative mRNA abundance of ENaC subunits, MR, SGK1, Nedd4L, CYP11B1 and B2 in different brain areas after 2-week icv infusion of aCSF or Na⁺-rich aCSF alone or combined with spironolactone (Spir.) Data for the 2 groups without spironolactone are also shown in table 3.2-1. Values are Mean \pm SEM ($n=6$ /group). By two-way ANOVA, there is a significant effect of Na⁺-rich aCSF on β ENaC mRNA levels ($F=5.15$, * $p<0.05$ versus aCSF groups) with no effect of

spironolactone on this increase. Whole nuclei were punched from the brain and homogenized for total RNA extraction. BD: below detection.

	aCSF	aCSF + Spir.	Na ⁺ -CSF	Na ⁺ -CSF+Spir.
α/PGK1 ($\times 10^{-3}$)				
Choroid plexus	2.1 \pm 0.2	2.4 \pm 0.4	2.6 \pm 0.7	1.9 \pm 0.5
Supraoptic nucleus	1.8 \pm 0.2	1.8 \pm 0.2	1.5 \pm 0.1	1.9 \pm 0.2
Paraventricular nucleus	1.4 \pm 0.2	1.2 \pm 0.1	1.3 \pm 0.2	1.4 \pm 0.2
Subfornical organ	4.1 \pm 0.6	3.5 \pm 0.3	3.7 \pm 0.3	3.2 \pm 0.2
β/PGK1 ($\times 10^{-3}$)				
Choroid plexus	0.9 \pm 0.2	1.5 \pm 0.3	1.9 \pm 0.3*	2.5 \pm 0.7*
Supraoptic nucleus	0.9 \pm 0.2	1.4 \pm 0.3	1.3 \pm 0.1	1.5 \pm 0.3
Paraventricular nucleus	1.0 \pm 0.1	1.1 \pm 0.2	0.9 \pm 0.1	1.1 \pm 0.1
Subfornical organ	2.0 \pm 0.4	3.0 \pm 0.7	2.3 \pm 0.3	3.1 \pm 0.6
γ/PGK1 ($\times 10^{-4}$)				
Choroid plexus	0.9 \pm 0.2	0.9 \pm 0.1	0.8 \pm 0.1	1.5 \pm 0.3
Supraoptic nucleus	1.1 \pm 0.1	1.2 \pm 0.1	1.1 \pm 0.2	1.3 \pm 0.1
Paraventricular nucleus	0.8 \pm 0.1	0.7 \pm 0.1	0.8 \pm 0.1	0.7 \pm 0.1
Subfornical organ	3.7 \pm 0.4	4.8 \pm 1.6	3.1 \pm 0.8	3.6 \pm 0.3
MR/PGK1 ($\times 10^{-2}$)				
Choroid plexus	2.0 \pm 0.1	2.9 \pm 0.5	3.3 \pm 0.3	2.8 \pm 0.6
Supraoptic nucleus	1.8 \pm 0.1	2.1 \pm 0.2	1.8 \pm 0.1	1.8 \pm 0.1
Paraventricular nucleus	1.3 \pm 0.1	1.6 \pm 0.1	1.3 \pm 0.1	1.4 \pm 0.2
Subfornical organ	2.2 \pm 0.5	2.5 \pm 0.2	2.0 \pm 0.2	2.0 \pm 0.4
Sgk1/PGK1 ($\times 10^{-1}$)				
Choroid plexus	3.4 \pm 0.4	3.8 \pm 0.5	3.4 \pm 0.4	3.7 \pm 0.5

Supraoptic nucleus	1.1 ± 0.1	1.0 ± 0.1	1.0 ± 0.1	1.2 ± 0.1
Paraventricular nucleus	0.9 ± 0.2	0.9 ± 0.1	1.0 ± 0.2	1.1 ± 0.3
Subfornical organ	3.4 ± 0.2	3.8 ± 0.4	3.8 ± 0.3	4.6 ± 0.3
<i>Nedd4L/PGK1</i> (×10 ⁻²)				
Choroid plexus	7.4 ± 0.6	8.8 ± 1.4	9.7 ± 1.5	10.0 ± 2.6
Supraoptic nucleus	6.7 ± 0.6	8.2 ± 0.7	9.5 ± 3.4	8.9 ± 2.7
Paraventricular nucleus	7.0 ± 0.5	6.2 ± 0.4	5.8 ± 0.6	6.0 ± 0.4
Subfornical organ	9.7 ± 0.8	9.8 ± 0.6	8.7 ± 0.6	9.3 ± 0.9
<i>CYP11B1/PGK1</i> (×10 ⁻³)				
Choroid plexus	1.7 ± 0.4	2.5 ± 0.7	2.0 ± 0.3	2.0 ± 0.2
Supraoptic nucleus	1.1 ± 0.1	1.6 ± 0.4	1.3 ± 0.2	1.7 ± 0.4
Paraventricular nucleus	0.7 ± 0.07	0.6 ± 0.04	0.5 ± 0.04	0.6 ± 0.1
Subfornical organ	0.3 ± 0.06	0.4 ± 0.08	0.4 ± 0.08	0.5 ± 0.04
<i>CYP11B2/PGK1</i> (×10 ⁻⁴)				
Choroid plexus	BD	BD	BD	BD
Supraoptic nucleus	1.1 ± 0.1	1.2 ± 0.2	1.3 ± 0.2	1.4 ± 0.2
Paraventricular nucleus	1.0 ± 0.1	0.9 ± 0.1	0.7 ± 0.1	1.0 ± 0.1
Subfornical organ	0.2 ± 0.04	0.3 ± 0.05	0.2 ± 0.03	0.3 ± 0.05

Data for the 2 groups without spironolactone are also shown in table 1 of the main paper. Values are Mean ± SEM (n=6/group). By two-way ANOVA, there is a significant effect of Na⁺-rich aCSF on βENaC mRNA levels (F=5.15, * p<0.05 versus aCSF groups) with no effect of spironolactone on this increase. Whole nuclei were punched from the brain and homogenized for total RNA extraction. BD: below detection.

3.3.8 **DISCUSSION**

The main new findings of the present study are that, in Wistar rats, chronic icv infusion of Na⁺-rich aCSF increases βENaC mRNA and immunoreactivity in the choroid plexus and α- and β-ENaC immunoreactivities in the ependyma. Icv infusion of Na⁺-rich aCSF increases α- and β-ENaC particles in the apical microvilli of the choroid plexus and in the basolateral membrane of the ependyma. In contrast, Na⁺-rich aCSF has no effect on ENaC expression in the supraoptic nucleus, paraventricular nucleus, and subfornical organ. Blockade of ENaC by icv infusion of benzamil increases CSF [Na⁺] in rats infused icv with aCSF but lowers hypothalamic [Na⁺].

3.3.8.1 CSF [Na⁺] and ENaC Expression in the Brain

In Dahl S and SHR, high salt intake increases CSF [Na⁺] (Huang et al. 2001b, Huang et al. 2004). It is well established that an increase in CSF [Na⁺] *per se* – by icv infusion of Na⁺-rich aCSF – causes sympathetic hyperactivity and hypertension (Bunag & Miyajima 1984, Kawano et al. 1991, Huang et al. 2001b, Huang et al. 2008). In this experimental approach, icv infusion of Na⁺-rich aCSF does not affect plasma [Na⁺] (Bunag & Miyajima 1984, Gomez-Sanchez & Gomez-Sanchez 1994) and tends to increase water intake (Gomez-Sanchez & Gomez-Sanchez 1994, Imaizumi et al. 1994). There is functional evidence that the sympatho-excitatory and pressor response to CSF [Na⁺] are mediated by an aldosterone-MR-ENaC pathway (Huang et al. 2006b, Wang & Leenen 2003). The present study evaluated the impact of a chronic increase in CSF [Na⁺] on this pathway in both Na⁺-transporting epithelia and in neurons in the central nervous system.

3.3.8.1.1 *Choroid Plexus*

In the brain ventricles, the epithelial cells of the choroid plexus are the major site for the production of CSF (Brown et al. 2004). The CSF is not an ultrafiltrate of the plasma but is actively secreted by the choroid plexus. The epithelium of the choroid plexus mediates the secretion of Na^+ , Cl^- and HCO_3^- into the CSF as well as the net absorption of K^+ from the CSF into the blood (Brown et al. 2004). Na^+K^+ ATPase is located in the apical membrane of choroid plexus cells and plays a pivotal role in the active ouabain-sensitive transport of Na^+ from epithelial cells to CSF and of K^+ from CSF to the choroid plexus cells (Brown et al. 2004, Masuzawa et al. 1984). We recently showed by electron microscopy that ENaC is located in both the apical and basolateral membranes of the choroid plexus cells, with a greater number of ENaC subunits on the microvilli than on the basolateral membrane (Amin et al. 2009). This pattern of localization is similar to that in the ciliary body of the rat eye (Mirshahi et al. 1999) and suggests that ENaC may contribute to Na^+ influx into choroid plexus cells from both the CSF and the blood, with influx of Na^+ from the CSF into the choroid epithelial cells possibly dominating. Indeed in control (aCSF) rats, icv infusion of benzamil increased CSF $[\text{Na}^+]$ by 8 mmol/L, suggesting that ENaC plays a major role in Na^+ re-uptake from the CSF. Consistent with this concept, in the present study, a chronic increase in CSF $[\text{Na}^+]$ increased α and β ENaC particles particularly in the apical membranes of the choroid plexus cells at the CSF side. The increase in α ENaC particles in the microvilli may reflect enhanced protein trafficking or posttranscriptional or posttranslational regulation in the choroid plexus because the abundance of α ENaC mRNA did not change. Conversely, for β ENaC, both mRNA and protein abundance increased suggesting that enhanced gene expression and

de novo protein synthesis contributed. Taking these results together, one may speculate that an increase in CSF $[Na^+]$ may further enhance Na^+ entry from the CSF side into the choroid plexus by increasing α and β ENaC particles in the microvilli of the choroid plexus. However, in contrast to its effects in control rats, in rats infused with Na^+ -rich aCSF, blockade of ENaC with icv infusion of benzamil did not cause a significant further increase in CSF $[Na^+]$ (Fig.3.3-6), suggesting that in this setting other factors may play a role. For example, inhibition of Na^+ efflux from the choroid plexus into the CSF by inhibition of the Na^+ -pump (Huang et al. 2004) may have increased intracellular Na^+ (Amin et al. 2009), thereby decreasing Na^+ influx via ENaC.

The mechanisms involved in regulation of ENaC in the choroid plexus have not yet been studied. Classically, the aldosterone-MR-SGK1 pathway is a major regulator of ENaC expression and trafficking in peripheral epithelial cells (Pearce & Kleyman 2007). In the kidney, aldosterone increases α ENaC surface expression and activity via MR by increasing α ENaC mRNA and it may regulate ENaC trafficking independent of MR (Asher et al. 1996, Masilamani et al. 1999, Nielsen et al. 2007). In the colon, aldosterone upregulates transcription of β and γ but not α ENaC (Amasheh et al. 2000). These findings indicate that in transport epithelia in the periphery, MR activation differentially regulates expression of ENaC subunits in a tissue specific manner. MR are present in the choroid plexus and MR mRNA was not affected by Na^+ -rich aCSF. Expression of the *CYP11B2* gene encoding for aldosterone synthase in the choroid plexus cells could not be substantiated. Icv infusion of Na^+ -rich aCSF does not alter plasma aldosterone but increases hypothalamic aldosterone (Huang et al. 2006b), and this aldosterone may via the CSF bind MR in choroid plexus cells and possibly contribute to the regulation of

ENaC by Na⁺-rich aCSF. In the present study, Na⁺-rich aCSF increased αENaC particles without altering αENaC mRNA and immunoreactivity in the choroid plexus. Concomitant infusion of spironolactone did not affect αENaC mRNA but lowered αENaC immunostaining in the Na⁺-rich aCSF treated group. Na⁺-rich aCSF increased βENaC mRNA and immunoreactivity and did not affect γENaC mRNA in the choroid plexus. Spironolactone did not affect the increase in βENaC mRNA but prevented the increase in protein by Na⁺-rich aCSF. These findings suggest that the regulation of ENaC subunits in the choroid plexus by an increase in CSF [Na⁺] is quite unique and may involve several mechanisms, one of them posttranscriptional regulation via MR. The effect of spironolactone on α and βENaC immunostaining is consistent with MR blockade. Alternatively its anti-androgen property could play a role. In the kidney of male Wistar rats, testosterone significantly upregulates αENaC mRNA through androgen receptors (Quinkler et al. 2005), but no change in mRNA was noted in the present study. Regarding other mechanisms, vasopressin may play a role. In the kidney, chronic infusion of a vasopressin V2 receptor agonist or water restriction markedly increases abundances of β and γENaC mRNA (Nicco et al. 2001). Vasopressin and vasopressin V1b receptor transcripts are found in the choroid plexus (Zemo & McCabe 2001). Vasopressin may also be released from the hypothalamus into the CSF, to act on vasopressin V1-receptors in the choroid plexus. Vasopressin expression increased 10 fold in the choroid plexus and hypothalamus of Sprague-Dawley rats after 5 days of 2% NaCl in drinking water with an increase in CSF osmolality from 295 to 309 mOsm/kg H₂O (Szmydynger-Chodobska et al. 2006). The 10 mmol/L [Na⁺] increase by icv infusion of

Na⁺-rich aCSF increases osmolality by 24 mOsm/kg H₂O and a resulting vasopressin release may contribute to the upregulation of βENaC expression.

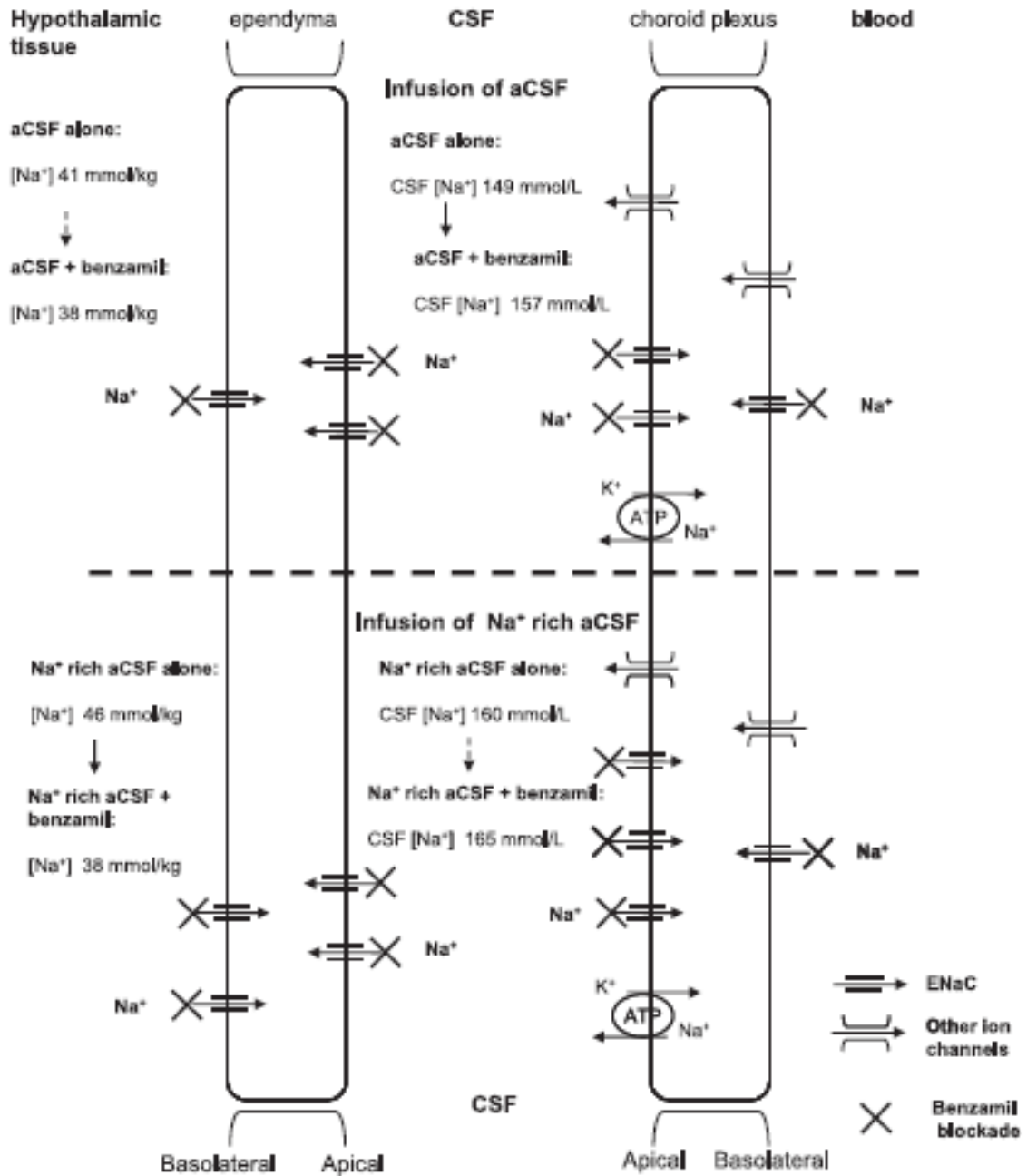


Figure 3.3–6: Schematic outline of location of ENaC in the choroid plexus and ependymal cells and their possible role in Na⁺ transport across the choroid plexus and ependyma in Wistar rats. Under control conditions, ENaC predominates at the apical

membrane of the choroid plexus and ependymal cells, presumably leading to net Na^+ transport into epithelial cells of the choroid plexus or into brain tissue. Consistent with this localization, benzamil increases CSF $[\text{Na}^+]$ but lowers hypothalamic tissue $[\text{Na}^+]$ (top). Infusion of Na^+ rich aCSF increases ENaC at the apical membrane of the choroid plexus, presumably to increase Na transport from the CSF into epithelial cells of the choroid plexus. ENaC also increases at the basolateral membrane of the ependyma, presumably to allow more Na^+ out of the brain tissue back into the CSF (bottom).

3.3.8.1.2 Ependyma

The ependyma is a layer of specialized cells lining the wall of the brain's ventricles. The ependymal cells are interconnected by gap junctions and may facilitate diffusion of K^+ from the extracellular space of the hypothalamus (Del Bigio 1995a, Bruni 1998, Jarvis & Andrew 1988). Whether or not the ependyma actively regulates $[\text{Na}^+]$ in the interstitial space has not yet been studied. In ependymal cells in the area of the anteroventral third ventricle the higher abundance of ENaC subunits on the apical than on the basolateral membranes is suggestive for net transport of Na^+ from CSF into brain tissue (Fig 3.3-6). Indeed, in control (aCSF) rats, benzamil caused an increase in CSF $[\text{Na}^+]$ without an associated increase in $[\text{Na}^+]$ in the hypothalamic tissue. Moreover, icv infusion of benzamil prevented the increase in tissue $[\text{Na}^+]$ by Na^+ rich aCSF despite an even higher CSF $[\text{Na}^+]$. Benzamil blockade appears therefore to prevent transport of Na^+ from the CSF into the brain tissue consistent with an important role for apical ENaC in transporting Na^+ into brain tissue. The Na^+ in the hypothalamic tissue includes both extracellular and intracellular sodium. The increase in tissue $[\text{Na}^+]$ by icv Na^+ rich aCSF

likely reflects primarily an increase in extracellular $[\text{Na}^+]$, followed by some increase in intracellular $[\text{Na}^+]$.

Infusion of Na^+ -rich aCSF increased the immunoreactivities for and gold-particle labeling of α and β ENaC in the basal membranes. Such increases may enhance Na^+ transport from brain tissue back into the CSF to maintain tissue $[\text{Na}^+]$. Consistent with this concept, Na^+ rich aCSF increased tissue $[\text{Na}^+]$ by ~ 5 mmol/kg less compared to the increase in CSF $[\text{Na}^+]$ by ~ 10 mmol/L (Fig. 3.3-5 and 3.3-6). Regarding the mechanisms involved in regulation of ENaC in the ependyma, spironolactone did not prevent the increase in immunoreactivity of α ENaC but lowered immunoreactivity of β ENaC in both the aCSF and Na^+ -rich aCSF treated groups. The ependyma and choroid plexus may therefore both show posttranscriptional regulation via MR as one of several mechanisms involved in regulation of ENaC subunits by CSF $[\text{Na}^+]$.

3.3.8.1.3 Hypothalamic nuclei

The supraoptic nucleus, paraventricular nucleus and subfornical organ were studied representing three important nuclei involved in different aspects of signaling in response to an increase in CSF and tissue $[\text{Na}^+]$. Central infusion of a MR blocker or of benzamil prevents the increase in hypothalamic “ouabain” and the sympatho-excitatory and pressor responses to an increase in CSF $[\text{Na}^+]$ or aldosterone (Huang et al. 2006b, Wang & Leenen 2003). It is not yet clear where in the hypothalamus the MR and benzamil sensitive sodium channels involved in these responses are actually located, and studies in specific nuclei may give further insights in this regard. Located within close proximity to the ependyma of the third ventricle, Na^+ -sensitive neurons in the subfornical organ may sense changes in CSF $[\text{Na}^+]$ and project to the paraventricular nucleus and supraoptic

nucleus (Denton et al. 1996, Noda 2006), possibly leading to production of aldosterone in magnocellular neurons (Huang et al. 2008, Takahashi et al. 1987a). In the present study, the transcription of aldosterone synthase or 11 β -hydroxylase was not affected by Na⁺-rich aCSF in these three nuclei, but enzymatic activity was not assessed. Icv infusion of Na⁺-rich aCSF increases hypothalamic aldosterone and corticosterone content (Huang et al. 2008), suggesting that the regulation of aldosterone and corticosterone production by Na⁺ may involve early steps in the steroid biosynthetic pathway.

In situ hybridization and immunohistochemistry show that ENaC transcripts and protein are most prominently present in the magnocellular neurons of the paraventricular nucleus and supraoptic nucleus. ENaC in these neurons may possibly mediate aldosterone induced increases in “ouabain” which can be blocked by benzamil (Wang et al. 2003a). However, in contrast to brain epithelial cells, Na⁺-rich aCSF infusion did not alter ENaC mRNA and protein expression in either nucleus. Subcellular distribution of ENaC in response to Na⁺-rich aCSF infusion was not evaluated. mRNA levels of MR, SGK1 and Nedd4L were also unaffected by Na⁺-rich aCSF. Phosphorylated SGK1 tended to be decreased by Na⁺-rich aCSF. Such a decrease may lower membrane channel abundance and activity (Pearce & Kleyman 2007). The functional relevance of these findings requires further studies.

3.3.8.2 Limitations of this study

Several possible limitations should be considered. Firstly, direct measures of ENaC activity were not obtained in the present study. Blockade by benzamil at 4 μ g/kg/day infusion rate may suggest that the changes of one or two ENaC subunits are indeed associated with parallel changes of ENaC activity in the choroid plexus or ependyma.

This infusion rate is similar to the one used by others (Gomez-Sanchez & Gomez-Sanchez 1994). For a baseline CSF production rate ~ 6 ml/day and total CSF volume of ~ 0.5 ml in rats of $\sim 250 - 300$ g body weight (Harnish & Samuel 1988), icv infusion of benzamil at $4 \mu\text{g/kg/day}$ would result in a concentration of $\sim 10 \mu\text{M/L}$ in the CSF, but is likely lower since benzamil will also distribute into brain tissue. Thus, one may expect maximal inhibition of ENaC but inhibition of other sodium channels or transporters cannot be excluded (Kleyman & Cragoe 1988a).

Secondly, icv infusion of Na^+ -rich aCSF increased osmolality by $24 \text{ mOsm/kg H}_2\text{O}$ and which may influence expression of ENaC subunits in the brain epithelial cells. A control group for osmolality was not included and further studies are obviously required to evaluate whether a local increase in osmolality influences ENaC expression in the brain.

Thirdly, icv infusion of control aCSF *per se* did not change γ ENaC mRNA but decreased immunoreactivity to low levels in the choroid plexus as well as other brain areas. Immunoreactivity to α and β ENaC was not affected, and immuno-electron microscopy showed that abundance of γ and β ENaC particles were comparable. The decrease in γ ENaC immunoreactivity by icv infusion of aCSF may reflect a change in the γ ENaC protein that affects its immunoreactivity rather than the protein being actually decreased.

3.3.8.3 Perspectives

All three ENaC subunits are distributed on both apical and basal membranes of choroid plexus and ependymal cells. This pattern of localization is quite unique in comparison with renal tubule or colon epithelial cells where ENaC is only present in the apical membrane at the luminal surface (Duc et al. 1994). In the brain, regulation of CSF and brain interstitium $[\text{Na}^+]$ cannot depend on parallel changes in water transport, and may

require movement of Na^+ via ENaC in either direction. When CSF $[\text{Na}^+]$ increases, enhanced α and β ENaC in the apical microvilli of the choroid plexus may facilitate Na^+ entry into the choroid plexus cells from the CSF. Similarly, when hypothalamic tissue $[\text{Na}^+]$ increases, higher α and β ENaC immunoreactivities on the basal surface of the ependyma may reflect a mechanism to attenuate the increase in tissue $[\text{Na}^+]$ by transporting Na^+ out of tissue into the CSF. Further studies need to explore whether dysregulation of ENaC in the choroid plexus and/or ependyma contributes to sympatho-excitatory and pressor responses to high salt diet in Dahl S or SHR.

In conclusion, in Wistar rats, a chronic increase in CSF $[\text{Na}^+]$ by icv infusion of Na^+ -rich aCSF increases expression of β ENaC in the epithelial cells of the choroid plexus and α and β ENaC in the ependyma. In contrast, Na^+ -rich aCSF has no effect on expression of ENaC subunits in the supraoptic nucleus, paraventricular nucleus and subfornical organ. Spironolactone only prevents the increase in β ENaC protein by Na^+ -rich aCSF in the choroid plexus and ependyma, suggesting that the regulation of ENaC expression occurs via several mechanisms distinctly different from its regulation in the kidney or colon. Upregulation of ENaC expression in response to an increase in CSF $[\text{Na}^+]$ in brain epithelia may be one of the key determinants for Na^+ transport from the CSF into the choroid plexus and from brain tissue into the CSF.

3.3.9 ACKNOWLEDGEMENTS

The authors would like to acknowledge the assistance of Ms. Li Bi, Ms. Roselyn White and Mr. Peter Ripstein for technical assistance and Ms. Danielle Oja for formatting assistance. Dr. Leenen holds the Pfizer Chair in Hypertension Research, an endowed chair supported by Pfizer Canada, University of Ottawa Heart Institute Foundation and Canadian Institutes of Health Research.

3.3.10 SOURCES OF FUNDING

This research was supported by operating grant FRN-74432 from the Canadian Institutes of Health Research (CIHR) (to FHH Leenen). Md Shahrir Amin was supported by a Pfizer/CIHR/Canadian Hypertension Society doctoral research award and program grant PRG5275 from the Heart and Stroke Foundation of Ontario.

**3.4 MANUSCRIPT # 4: EXPRESSION OF
EPITHELIAL SODIUM CHANNELS AND
REGULATORY GENES IN THE BRAIN OF DAHL
S AND R RATS.**

Md Shahrier Amin^{1,2}, Erona Reza^{1,2}, Hong Wei Wang¹, Esraa-el-Shahat¹, Roselyn White¹, Bing S Huang¹, Frederique Tesson³ and Frans HH Leenen^{1,2}.

¹Hypertension Unit, University of Ottawa Heart Institute, Ottawa, Ontario, Canada

²Department of Cellular and Molecular Medicine, University of Ottawa, Ottawa, Ontario, Canada

³Faculty of Health Sciences, University of Ottawa, Ottawa, Ontario, Canada

CONCISE TITLE

ENaC and regulatory genes in the brain of Dahl rats

STATUS

Prepared for submission.

3.4.1 RELEVANCE TO OVERALL PROJECT

In this study we tested our hypothesis #4, second part, that high salt diet upregulates ENaC expression in the brain of Dahl S rats. We evaluated the expression of ENaC subunits in the brain of Dahl R versus Dahl S rats. In previous studies expression of SGK1 was found to be paradoxically regulated by salt in the kidneys of Dahl S rats. We therefore also sequenced the coding and noncoding regulatory areas of the SGK1 gene for possible polymorphisms between Dahl S and R rats.

3.4.2 CONTRIBUTION

Responsible for the overall project and performed the following:

1. Design and planning of most of the initial experiments.
2. Setting up the methods for punching of specific brain areas for initial RT-PCR experiments.
3. Performed the experiments and studied protein distribution by immunohistochemistry.
4. Studied sub-cellular distribution by EM.
5. Set up the methods for measuring CSF $[\text{Na}^+]$.
6. Sequenced the SGK1 gene.
7. Compilation of all of the data and preparation of the manuscript.

3.4.3 ABSTRACT

Blockade of mineralocorticoid receptors (MR), epithelial sodium channels (ENaC) or 'ouabain' in the brain prevents the increase in BP in Dahl salt sensitive (S) rats on high salt diet. In order to identify possible molecular mechanisms involved, we evaluated mRNA and protein expression of ENaC subunits and mRNA expression of MR, SGK1 and 11 β HSD2 in cardiovascular regulatory centers and epithelia in the brain of Dahl S and salt-resistant (R) rats. Young, male, S and R rats were placed on regular (0.3%) or high (8%) salt for 2 or 4 weeks. Expression of the genes of interest in the SON, PVN and choroid plexus was studied by RT-PCR, Western blots and immunohistochemistry.

On regular salt, S rats had greater abundance of the ENaC proteins in the choroid plexus. At the subcellular level there was increased abundance of β ENaC in all subcellular compartments. On high salt diet the higher abundance of ENaC subunits persisted in S rats. Immunoreactivity to β and γ ENaC was higher in the SON of S versus R rats on regular salt. High salt increased β and γ ENaC mRNA expression and membranous staining in the SON, associated with an increase of SGK1 and 11 β HSD2 mRNA only in S rats. ENaC expression was similar in the PVN of both strains and not affected by high salt diet. The increased neuronal ENaC in the SON of S rats may reflect increased local aldosterone and contribute to enhanced production of 'ouabain' on high salt diet.

3.4.4 INTRODUCTION

Increased transport of Na^+ into the central nervous system (CNS) and enhanced responses to $[\text{Na}^+]$ appear to contribute to sympathetic hyperactivity and hypertension in salt sensitive models such as the Dahl salt sensitive (S) rat (Simchon et al. 1999, Huang & Leenen 1995a, Huang et al. 2004, Huang et al. 2001b, Wang & Leenen 2003). Intracerebroventricular (icv) infusion of low doses of benzamil – a potent blocker of the epithelial sodium channel (ENaC) (Kleyman & Cragoe 1988a) – prevents sympathetic hyperactivity and hypertension in Dahl S rats on high salt diet (Nishimura et al. 1998, Gomez-Sanchez & Gomez-Sanchez 1995, Wang & Leenen 2002), or to an increase in CSF $[\text{Na}^+]$ by icv infusion of Na^+ rich aCSF (Huang & Leenen 2002, Wang & Leenen 2003), suggesting that ENaC in the CNS plays a major role.

ENaC is a member of the DEG/ENaC family of cation selective ion channels and is composed of three subunits α , β and γ (Firsov et al. 1998). All three ENaC subunits are expressed in the brain in the choroid plexus, ependyma and mainly magnocellular neurons of the paraventricular (PVN) and supraoptic (SON) nuclei, and to a lesser extent in other nuclei (Amin et al. 2005). In the choroid plexus ENaC subunits are more abundant in the apical microvilli (Amin et al. 2009), and icv infusion of benzamil increases CSF $[\text{Na}^+]$, suggesting that ENaC contributes to re-uptake of Na^+ from the CSF into the choroid plexus and blood. In the PVN, the enhanced pressor response to aldosterone in the presence of increased $[\text{Na}^+]$ is prevented by benzamil suggesting that aldosterone mediated activation of ENaC may be involved in translating increased $[\text{Na}^+]$ to enhanced neuronal activity (Gabor & Leenen 2009a). Otherwise, the role of ENaC in regulation of neuronal function in the CNS has not yet been studied.

Aldosterone acting through MR is a major regulator of ENaC expression and activity. The serum and glucocorticoid regulated kinase 1 (SGK1) an aldosterone induced protein, increases expression of ENaC subunits and prevents their removal from the cell membrane by phosphorylation of neural precursor cells expressed developmentally down regulated 4-like gene (Nedd4L) (Loffing et al. 2001b). The ENaC genes are similar in Dahl S and R rats (Shehata et al. 2007) whereas the complete sequences of the SGK1 (Farjah et al. 2003) and NEDD4L genes (Umemura et al. 2006) have not yet been evaluated in Dahl R and S rats. However expression of ENaC subunits as well as of SGK1 (Aoi et al. 2007, Farjah et al. 2003) is paradoxically enhanced by high salt diet in the kidneys of Dahl S rats versus no changes or a decrease in R rats (Aoi et al. 2007, Kakizoe et al. 2009, Amin et al. 2011) indicating dysfunctional regulation in Dahl S rats. In the CNS, expression of β and γ ENaC was higher in the choroid cells of Dahl SS/MCW rats, but benzamil-blockable Na^+ influx into choroid cells in vitro was similar in Dahl SS/MCW versus SS.BN13 rats (Amin et al. 2009). On high salt, this pattern persisted. This dissociation between activity and expression may relate to an altered subcellular localization of the subunits or the presence of inactive channels. Effects of high salt on expression of ENaC and its regulators in hypothalamic neurons of Dahl rats have not yet been evaluated.

We hypothesized that dysregulation of ENaC in Dahl S rats extends to the CNS and thereby contributes to enhanced Na^+ transport into or out of the CSF and/or enhanced neuronal responses to increased $[\text{Na}^+]$. We therefore assessed the effects of 2 and 4 weeks of high salt diet on ENaC expression by measuring mRNA and protein abundance and subcellular distribution of ENaC subunits and mRNA abundance of MR, SGK1 and

NEDD4L in the choroid plexus, SON and PVN in Dahl S and R rats and screened for possible polymorphisms in the coding and regulatory regions of the NEDD4L and the SGK1 genes. To assess the functional role of ENaC in the choroid plexus of Dahl S versus R rats, the effects of icv infusion of benzamil on CSF $[Na^+]$ was assessed.

3.4.5 MATERIALS AND METHODS

Male 4 weeks old Dahl salt sensitive (SS/Jr-Hsd: S) and Dahl salt resistant (SR/Jr-Hsd: R) rats were purchased from Harlan Sprague-Dawley (Indianapolis, Indiana). The rats were housed two per cage under standard conditions on a 12 hour light-dark cycle at 24°C and were allowed a 5 days acclimatization period on normal rat chow and tap water before entering the study. All procedures were performed according to the guidelines of the Canadian Council on Animal Care and were approved by the University of Ottawa Animal Care Committee.

3.4.5.1 Experimental protocols

Molecular biology studies: Two sets of experiments were performed. In each set, Dahl S and R rats (5-7 rats/group) were assigned randomly to either regular (120 $\mu\text{mol Na}^+/\text{gm}$) or high (1,370 $\mu\text{mol Na}^+/\text{gm}$) salt diet for 2 or 4 weeks. At the end of 2 or 4 weeks, under isoflurane anesthesia a cannula was inserted into the right carotid artery and the next morning blood pressure (BP) and heart rate were recorded in conscious unstressed animals using Data Acquisition system and Acqknowledge III software. For real-time PCR and Western blot, under pentobarbital anesthesia, rats were perfused transcardially with RNase free cold PBS (pH 7.4). Brains were removed immediately and snap frozen in liquid nitrogen and preserved at -80°C .

Distribution and subcellular localization: Two sets of Dahl S and R rats (4-7 rats/group) were assigned randomly to either regular (120 $\mu\text{mol Na}^+/\text{gm}$) or high (1,370 $\mu\text{mol Na}^+/\text{gm}$) salt diet for 12-14 days. The rats were perfused transcardially with chilled normal saline followed by 4% paraformaldehyde and 0.05% glutaraldehyde in phosphate

buffer (pH 7.4) for immunohistochemistry and in sodium cacodylate buffer (pH 7.4) for immunoEM.

Biochemical measurements: Dahl S and R rats on regular salt diet (6-10 rats/group) were implanted with icv cannulas connected to osmotic minipumps delivering aCSF + vehicle (15% propylene glycol) or aCSF + benzamil (@ 25 $\mu\text{g}\cdot\text{day}^{-1}$ in vehicle) for 12-14 days. At the end of the experiment, in the early afternoon under halothane anesthesia, each rat was placed in a stereotaxic frame, and 100–200 μl of CSF was withdrawn from the cisterna magna, as described previously (Huang et al. 2004). Rats were then decapitated, and brains were collected and stored at -80°C for measurement of tissue $[\text{Na}^+]$. The dose of benzamil was based on preliminary experiments in Wistar rats treated with vehicle or different doses of benzamil for 2 weeks (CSF $[\text{Na}^+]$ with vehicle = 156 ± 3 mmol/L; Benzamil 10 $\mu\text{g}\cdot\text{day}^{-1}$ = 155 ± 3 mmol/L; Benzamil 20 $\mu\text{g}\cdot\text{day}^{-1}$ = 161 ± 3 mmol/L; Benzamil 30 $\mu\text{g}\cdot\text{day}^{-1}$ 173 ± 2 mmol/L; n=6 rats/group).

3.4.5.2 Real-Time Quantitative RT-PCR

Rats were perfused with chilled diethyl pyrocarbonate (DEPC, Sigma-Aldrich Canada Ltd, Oakville, ON, Canada) treated phosphate-buffered saline (PBS, pH 7.4) under isoflurane anesthesia. After perfusion, the brains were removed and snap-frozen in liquid nitrogen and then stored at -80°C . Brains were serially cryosectioned into 80- μm -thick coronal slices and brain punches of specific areas were taken with pre-chilled, 25- μl Drummond microdispensers (Drummond Scientific). The tissue pellet was homogenized in 0.2-ml Trizol reagent by using a pestle (Bel-Art-Product, Pequannock, NJ) driven by a pellet pestle motor, and 0.3ml Trizol reagent was then added. Total RNA was extracted from homogenized tissues according to the manufacturer's instructions.

1 µg of total RNA was used for cDNA synthesis by QuantiTect Reverse Transcription kit with elimination of genomic DNA (Qiagen Inc., Mississauga, Ontario, Canada). Sequences of the specific primers for α , β and γ ENaC, MR and SGK1 were same as described previously (Wang et al. 2010b) and are listed in Table 3.4-S1. For 11 β HSD2 (gb U22424.1), a 326bp PCR fragment corresponding to positions 767-1092 was amplified and then was subcloned into pCRII TA vector (Invitrogen, Burlington, ON, Canada) followed by restriction endonuclease and sequencing analysis. The concentration of plasmid was quantified by UV absorbance at 260nm. Serial 10-fold dilutions of plasmid (100pg/µl to 0.001pg/µl) were used to generate an external standard with the PCR condition as follow: an initial denaturation step at 94°C for 3 min to activate Taq polymerase (Genescript Inc), followed by 30 cycles of denaturation at 94°C for 40 sec, annealing at 56°C for 40 sec and extension at 72°C for 45sec.

Real-time PCR was performed with a Roche Light Cycler using Fast Start DNA Master SYBR Green I dye (Roche Diagnostics, Lava, QC, Canada). The real-time qPCR conditions and external standards for α , β and γ ENaC subunits, MR, SGK1 and the reference gene phosphor-glycerate kinase 1 (PGK1) were the same as previously described (Amin et al. 2005, Wang et al. 2010). The real-time PCR condition for 11 β HSD2 were set as follow: initial at 95 °C for 10 min followed by 40 cycles of denaturation at 95 °C for 5 sec; annealing at 62 °C for 5 sec ; extension at 72 °C for 11 sec. Expression was normalized to PGK1 levels as an endogenous reference. Normalization was achieved by dividing the amount of cDNA of each gene by the PGK1 quantity.

Table 3.4-S1: Primer sequences used in qRT-PCR analysis of expression of the ENaC subunits, MR, SGK1 and 11 β HSD2.

Gene	Primer	Sequence	Amplicon length
α ENaC	F	5'-GTTCTGTGACTACCGAAAGCAGAG -3'	429 bp
	R	5'- CGTAGGCAGCATGAGAAGTGTGATG-3	
β ENaC	F	5'-TGGATCACTGTCATCAAGCTAGTG-3'	440 bp
	R	5'-TGGTACCAGCATCTTGACCCTATG-3'	
γ ENaC	F	5'- CGTCAGTGGCACAAAGCCAA - 3'	301 bp
	R	5'-GAGAGCCTCCTCAAACCATG -3'	
MR	F	5'- GCTCAACATTGTCCAGTACA - 3'	263 bp
	R	5'- GCACAGGTGGTCCTAAGATT- 3'	
SGK1	F	5'- GCGCAATGTTCTGTTGAAGA - 3'	314 bp
	R	5'- TGTGCTCGATGTTCTCCTTG - 3'	
11 β HSD2	F	5'-CGTCACTCAAGGGGACGTAT-3'	326 bp
	R	5'-TACAACGGGGCTAAGGTCAG-3'	
PGK	F	5'- GCTGCAGAACTCAAATCTCT - 3'	263 bp
	R	5'-TGTGTGCAGTCCCAAAGCA - 3'	

3.4.5.3 Western Blotting

Whole protein was isolated from brain punches of specific nuclei using ice-cold isolation solution containing 300 mM sucrose / 10 mM Trithanolamine buffer pH 7.5 and 1% of protease inhibitor cocktail (Sigma). The homogenate was spun at 4000 g for 10 minutes at 4°C, the supernatant was collected and protein concentration measured using BCA assay (Pierce, Rockford, IL). 40 μ g of protein from each area was separated on precast 4-12% bis-tris gels, transferred to PVDF membranes (Biorad, Reinach, Switzerland) and probed with antibodies against the ENaC subunits prepared as described previously (Amin et al. 2011) (α ENaC -1:10,000, β and γ ENaC - 1:5000). β -actin (1:5000, Sigma) was used as internal control. Details regarding the quality and specificity of the ENaC antibodies were recently published (Amin et al. 2011). The signal was developed with the ECL⁺ system (Perkin Elmer) and visualized using an Alpha Ease image system. Band

densities were quantitated by Alpha Ease software. The results are expressed in arbitrary units (percent change of normalized densitometry of target gene versus β actin from control).

3.4.5.4 Immunohistochemistry

Different areas were studied by immunohistochemical staining of 5- μ m coronal sections of the perfused frozen brains. The slides were incubated with primary antibodies against α , β and γ ENaC (α ENaC -1:500, β and γ ENaC - 1:250) (Amin et al. 2011) and developed with Vectastain Elite ABC and diaminobenzidine kits (Vector Laboratories, Burlington, ON, Canada). Images were captured using Spot digital camera attached to a high resolution bright-field transmitted light microscope (Olympus BX60). Distribution of the staining in the membrane and cytoplasm was assessed blindly and scored as: 1 (<30%), 2 (30-70%) and 3 (>70%) based on the number of cells stained. Intensity of the staining was scored as nil (0), mild (1), moderate (2) or strong (3). The two scores were multiplied to obtain a single composite score ranging from 0 to 9, for the membrane and cytoplasm. In the SON and PVN, only the magnocellular neurons showed positive immunostaining for ENaC subunits on frozen sections. The parvocellular neurons in PVN showed only background staining and were not evaluated.

3.4.5.5 Immunoelectron Microscopy (EM)

Subcellular distribution of ENaC subunits was assessed by immunoelectron microscopy of microdissected choroid plexus of the lateral ventricle. After incubation with the primary antibodies against ENaC subunits, 15-nm gold particle-conjugated secondary antibodies (EY Laboratories, San Mateo, CA) were used to demarcate subcellular localization of the proteins. A minimum of 5 intact choroid epithelial cells was evaluated

from each rat. Total area studied was measured from the scanning (1000x) images and the numbers of gold-labeled particles in each subcellular compartment were counted from the magnified (>6000x) images. The results are expressed as number per 100 μm^2 .

3.4.5.6 Assessment of CSF and Tissue $[\text{Na}^+]$

$[\text{Na}^+]$ in the CSF and hypothalamic tissue were measured using an ion-selective electrode (model MI-425, Microelectrodes, Bedford, NH) as described previously (Wang et al. 2010b). The electrode was connected to a standard pH meter (VWR, West Chester, PA), and relative millivolt readings were recorded for the standards and samples. $[\text{Na}^+]$ was measured using a range of standards of NaCl in aCSF or the solvent used for solubilizing hypothalamic tissue for measuring CSF or hypothalamic tissue $[\text{Na}^+]$ respectively. Log standard $[\text{Na}^+]$ was plotted against the relative millivolt readings, and unknowns were calculated from the appropriate standard curve.

3.4.5.7 Sequencing

DNA was extracted from blood leucocytes (Qiagen, Mississauga, ON, Canada). The 2000 bp upstream the transcription start site, 2000 bp downstream the last exon and entire coding region of rat SGK1 (ENSRNOT00000016121Ensembl release 4.3, Feb 2007; NM 019232 Nov2004 assembly of UCSC) and the coding region of Nedd4L (BC086371) were amplified by PCR. PCR conditions for SGK1 included initial denaturation at 95°C for 5 min followed by 35 cycles (denaturation at 95°C for 1 min, annealing at 56°-64° for different primer pairs for 1 min and extension at 60°C for 1 min) and final extension at 72°C for 1 min. The following protocols were followed for sequencing Nedd4L with optimizations for each segment: initial denaturation at 95°C for 5 min followed by 30 cycles of denaturation at 95°C for 1 min, annealing at 56°C for all exons (except for

exons 18, 21 for which the annealing temperature was 60°C) for 1 min and final extension at 72°C for 1 min. Sequencing was performed using the Big-Dye Terminator v.3.0 chemistry (ABI, Foster city, CA) according to the instructions provided by the manufacturer (PE Applied Biosystems, Foster City, CA). Sequencing products were purified on DyeEx 2.0 spin kit columns (Qiagen Canada, Mississauga, ON, Canada) and analyzed on 3100 DNA analyzer (Applied Biosystems, Foster City, CA). The obtained sequences were compared to the published SGK1 and Nedd4L gene sequences of the Brown-Norway rat.

3.4.5.8 Statistical Analysis

Values are presented as mean \pm standard error of the mean (SEM). All comparisons between groups were determined by two way analysis of variance (ANOVA) followed by the Student-Newman-Keuls test where applicable. $p < 0.05$ was considered statistically significant. The effect was considered 'appears to be' or 'tended to' for p values between 0.05 - 0.08.

3.4.6 RESULTS

3.4.6.1 Blood Pressure

On regular salt, resting mean arterial pressure (MAP) tended ($p=0.08$) to be higher in S (119 ± 4 at 7, 134 ± 4 mm Hg at 9 weeks of age) compared to R (114 ± 5 at 7 and 121 ± 3 mm Hg at 9 weeks of age) rats. High salt intake did not affect BP in R (125 ± 4 mm Hg at 9 weeks of age) but caused a moderate increase in MAP after 2 weeks (148 ± 2 mmHg, $p<0.05$) and a marked increase after 4 weeks (192 ± 10 mm Hg, $p<0.05$) in S rats.

3.4.6.2 Expression of ENaC subunits

3.4.6.2.1 **Choroid plexus (Tables 3.4-1, Figure 3.4-1 and 3.4-2):**

On regular salt intake, the abundance of α ENaC mRNA was similar in both strains but the levels of the α ENaC protein was higher at 9 weeks in Dahl S versus R. High salt diet did not affect mRNA and protein abundance in either strain. By EM, 25-30% of α ENaC were in the microvilli and ~5-10% in the basal membrane. The subcellular localization of α ENaC was similar in Dahl R and S rats and not affected by high salt diet.

On regular salt intake, β ENaC mRNA abundance was similar but protein higher in Dahl S compared to Dahl R rats at both 7 and 9 weeks of age. Staining as well as number of β ENaC labeled gold particles in all subcellular compartments was significantly higher in Dahl S, with 2 fold more particles in both the apical and basolateral membrane of Dahl S versus Dahl R. High salt intake did not affect β ENaC mRNA abundance in either strain and the higher protein abundance in Dahl S persisted.

On regular salt intake, γ ENaC mRNA abundance was similar in the CP of Dahl S and R rats. Abundance of both the 90 and 70 kDa proteins was higher in Dahl S than R at 9

Table 3.4–1: Effect of high salt diet on expression of ENaC subunits in the choroid plexus of Dahl R and S rats.

			Dahl R		Dahl S	
			Reg Salt	High Salt	Reg Salt	High Salt
Alpha ENaC	<i>mRNA</i>	2 wks	0.9 ± 0.1	1.0 ± 0.1	1.0 ± 0.05	0.9 ± 0.03
	<i>(x10⁻³)</i>	4 wks	3.5 ± 0.6	2.6 ± 0.5	2.0 ± 0.4	2.5 ± 0.2
	<i>80 kDa</i>	2 wks	100±21	124±24	95±5	88±5
	<i>Protein</i>	4 wks	100±8	103±12	148±18 [#]	120±13 [#]
Beta ENaC	<i>mRNA</i>	2 wks	1.6 ± 0.3	1.5 ± 0.2	0.7 ± 0.1	0.7± 0.05
	<i>(x10⁻⁴)</i>	4 wks	1.0 ± 0.3	0.9 ± 0.2	0.8 ± 0.1	0.9 ± 0.1
	<i>85 kDa</i>	2 wks	100±7	101±10	135±11 [#]	125±16 [#]
	<i>Protein</i>	4 wks	100±5	89±18	130±8 [#]	153±12 [#]
	<i>Immuno</i>	Cytop	4.5±0.5	4.3±0.6	4.2±1.1	4.8±0.5
		Apic	3.3±0.4	3.3±0.7	4.8±1.3 [#]	4.7±0.6 [#]
Gamma ENaC	<i>mRNA</i>	2 wks	2.5±0.3	1.8±0.3	2.7±0.1	1.5±0.2
	<i>(x10⁻³)</i>	4 wks	3.1±0.7	4.6±1.2	2.8±0.7	4.2±0.1
	<i>90 kDa</i>	2 wks	100±11	77±10	86±11	86±16
	<i>Protein</i>	4 wks	100±7	101±15	120±8 [#]	141±14 [#]
	<i>70 kDa</i>	2 wks	100±21	81±21	90±19	88±15
	<i>Protein</i>	4 wks	100±4	111±24	159±30 [#]	162±29 [#]
	<i>Immuno</i>	Cytop	5.0±0.4	5.9±0.8	6.5±0.5 [#]	6.9±0.6 [#]
		Apic	3.7±0.8	4.4±0.7	6.2±0.7 [#]	6.9±0.6 [#]

Values are mean ± SEM (n=4-6 rats / group)

* p<0.05, Reg vs High salt

[#] p<0.05, Dahl R vs Dahl S

mRNA expression was measured versus PGK1

Protein abundance was measured versus βactin and normalized to Dahl R Reg Salt as 100%

Cytop = Cytoplasmic immunoreactivity

Apic = Apical immunoreactivity

Immunoreactivity for αENaC was low in the CP and not quantified.

weeks on either diet. Both cytoplasmic and apical immuno-reactivity were also higher in Dahl S than R on regular salt diet. Relative subcellular distribution of γ ENaC in different compartments was similar in the two strains on regular salt, whereas high salt diet increased number of γ ENaC labeled particles in the microvilli of both strains and only in the basal membrane in Dahl S.

Fig 3.4-1: Abundance of ENaC subunits in the choroid plexus

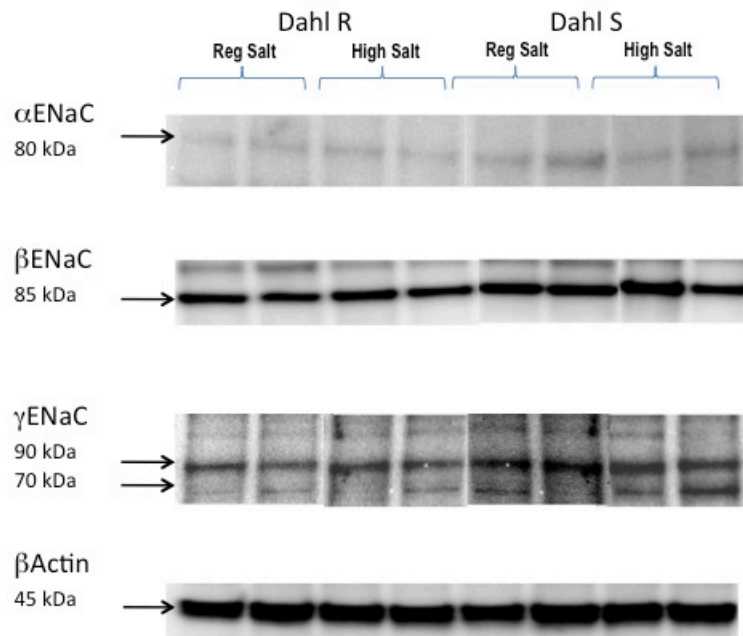


Figure 3.4-1: Protein abundance of ENaC subunits in the choroid plexus after 4 weeks on regular or high salt diet. α and β ENaC protein abundance was higher in Dahl S versus R rats, and this increase persisted on high salt diet. Abundance of 90 and 70 kDa fraction of γ ENaC was also higher in Dahl S on both diets

Fig 3.4-2: Immunoreactivity to β ENaC in the choroid plexus

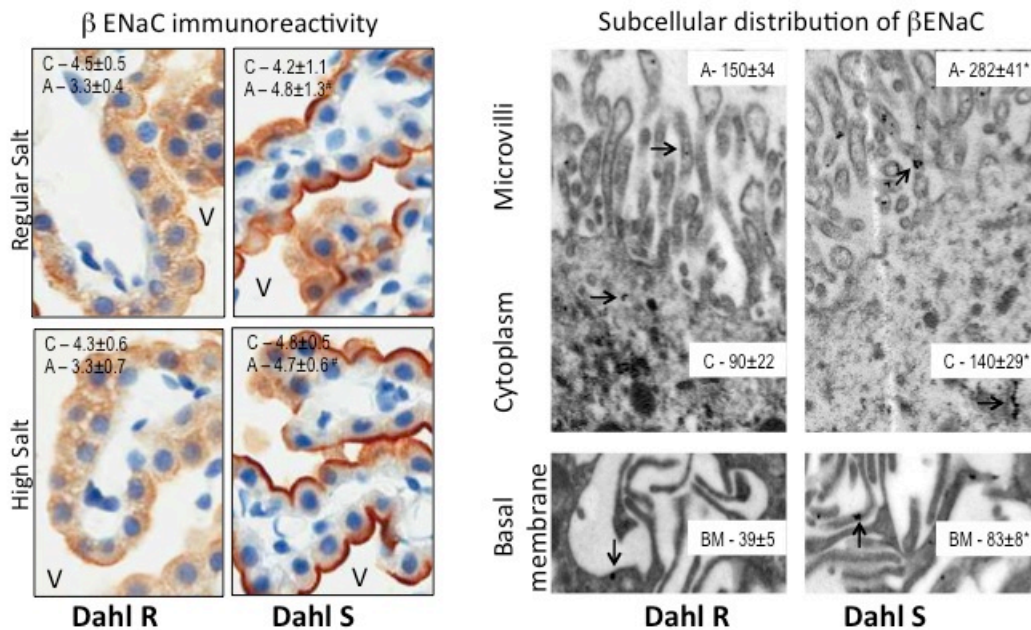


Figure 3.4-2 : Immunoreactivity and subcellular distribution of β ENaC in the choroid plexus of Dahl S and R rats. Dahl S shows greater apical immunoreactivity (left panels) and greater abundance of β ENaC in all subcellular compartments (right panels). The higher immunoreactivity and abundance in Dahl S persists on a high salt diet. Insets show mean \pm SEM for cytoplasmic (C) and apical (A) immunoreactivity (n=4-6 rats/group). * $p < 0.05$, Reg vs High salt; # $p < 0.05$, Dahl R vs Dahl S. BM = Basal membrane, V= Ventricle.

Table 3.4–2: Subcellular localization of ENaC subunits in the choroid cells of Dahl R and S rats on regular or high salt diet for 12-14 days.

		α ENaC		β ENaC		γ ENaC	
		Reg Salt	High salt	Reg Salt	High salt	Reg Salt	High salt
Apical microvilli	Dahl R	35±7	33±8	150±34	82±12*	11±1	21±3*
	Dahl S	42±2	39±2	282±41 [#]	221±21 [#]	14±1	23±5*
Cytoplasm	Dahl R	46±9	32±8	90±22	46±11	14±3	15±2
	Dahl S	60±19	53±19	140±29 [#]	114±27 [#]	11±2	10±3
Basolateral membrane	Dahl R	10±3	10±1	39±5	13±4	5±1	5±0.1
	Dahl S	13±3	14±5	83±8 [#]	96±32 [#]	4±1	8±1 [@]

Values are mean ± SEM (n=3-4 / group) of number of gold particles per 100 sq micron

* p<0.05, Regular versus High salt

[#] p<0.05, Dahl S versus Dahl R

[@] p <0.05, interaction of strain and salt

3.4.6.2.2 SON (Table 3-4, Figures 3-4 and 3-5)

On regular salt, expression of α ENaC mRNA tended to (p=0.08) be higher in Dahl S than R rats at both ages. Expression of the α ENaC protein was weak, and was not quantified. High salt diet did not appear to cause a change in the mRNA and protein abundance of α ENaC in either strain.

Expression of β ENaC mRNA was similar in the two strains on regular salt. The 85 kDa band of β ENaC was faint in the SON and not quantified. Cytoplasmic and membranous immunoreactivity was detectable in the magnocellular cells and was more intense in Dahl S than R rats. High salt increased β ENaC mRNA levels only in Dahl S associated with persistence of the higher cytoplasmic and membranous immunoreactivity.

Table 3.4–3: Effect of high salt diet on expression of ENaC subunits in the supraoptic nucleus of Dahl R and S rats.

			Dahl R		Dahl S	
			Reg Salt	High Salt	Reg Salt	High Salt
Alpha ENaC	<i>mRNA</i>	2 wks	1.7±0.3	2.5±0.3	2.5±0.4	3.3±0.7
	<i>(x10⁻³)</i>	4 wks	2.0±0.4	1.3±0.3	2.8±0.7	3.2±0.5
	<i>80 kDa</i>	2 wks	100±4	82±7	84±8	92±7
	<i>Protein</i>	4 wks	100±19	81±16	115±34	102±12
Beta ENaC	<i>mRNA</i>	2 wks	3.4±0.7	3.6±1.3	4.6±0.9	9.5±0.9*
	<i>(x10⁻⁵)</i>	4 wks	1.8±0.3	1.8±0.4	2.0±0.4	3.7±0.8
	<i>Immuno</i>	Cytop	2.7±0.7	2.8±0.5	4.7±1.3 [#]	4.0±0.7 [#]
		Memb	1.7±0.3	1.8±0.2	3.3±1.3 [#]	2.8±0.5 [#]
Gamma ENaC	<i>mRNA</i>	2 wks	1.0±0.1	2.4±0.6*	1.7±0.3	3.0±0.2*
	<i>(x10⁻⁴)</i>	4 wks	1.3±0.8	2.0±0.3	1.6±0.3	3.0±0.5*
	<i>90 kDa</i>	2 wks	100±12	166±35	144±19	133±35
	<i>Protein</i>	4 wks	100±11	109±23	55±10	93±5
	<i>70 kDa</i>	2 wks	100±14	144±47	104±19	74±13
	<i>Protein</i>	4 wks	100±20	87±34	31±11	73±18
	<i>Immuno</i>	Cytop	5.3±0.4	6.0±0.5	7.0±0.4 [#]	5.1±0.4
Memb		4.0±1.2	4.7±0.6	5.3±0.4 [#]	6.6±0.7*	

Values are mean ± SEM (n=4-6 / group)

* p<0.05, Reg vs High salt

[#] p<0.05, Dahl R vs Dahl S

mRNA expression was measured versus PGK1

Protein abundance was measured versus beta actin and normalized to DR Reg Salt as 100%

Cytop = Cytoplasmic immunoreactivity

Memb = Membranous immunoreactivity

Immunoreactivity for αENaC was low in the magnocellular neurons and not quantified.

Figure 3.4- 3: Protein abundance of ENaC subunits in the SON and PVN

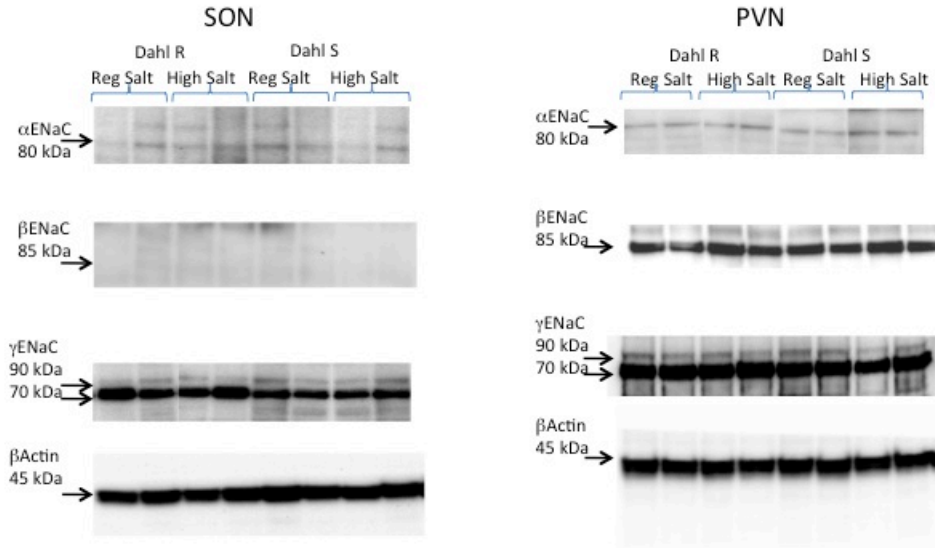


Figure 3.4–3: Protein abundance of the ENaC subunits in the SON and PVN after 4 weeks on regular versus high salt diet. The arrows show the specific bands that were quantified. Abundance of protein is similar in Dahl R and S rats, and is not affected by a high salt diet. βENaC protein was not detectable in the SON by Western blot.

On regular salt diet, γ ENaC mRNA expression was similar in S and R rats. On regular salt, higher cytoplasmic and membranous immunoreactivity was noted in magnocellular cells of Dahl S than of R rats. High salt for 2 weeks increased abundance of the mRNA in both strains, but after high salt for 4 weeks only in S rats. This was associated with a further increase in membranous staining in Dahl S.

Figure 3.4-4: Immunoreactivity to β and γ ENaC in the SON

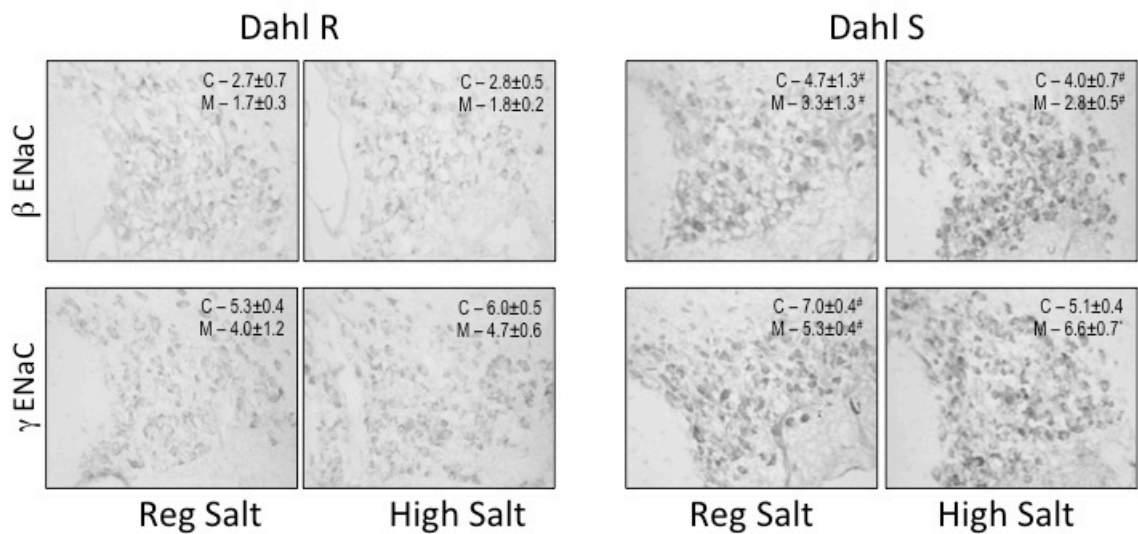


Figure 3.4-4: Immunoreactivity to β and γ ENaC in the SON of Dahl R and S rats on regular or high salt diet. Immunoreactivity to both β and γ ENaC protein was higher in the SON of Dahl S rats, and remained elevated or further increased with high salt diet. Insets show mean \pm SEM for cytoplasmic (C) and membranous (M) immunoreactivity ($n=4-6$ rats/group). * $p<0.05$, Reg vs High salt; # $p<0.05$, Dahl R vs Dahl S.

3.4.6.2.3 PVN (Table 3-5, Figure 3-4)

Abundance of α ENaC mRNA and protein was similar in Dahl R and S at both 7 and 9 weeks. High salt diet did not significantly affect protein abundance in the PVN.

Immunoreactivity to α ENaC was also weak in the PVN.

Table 3.4–4: Effect of high salt diet on expression of ENaC subunits in the paraventricular nucleus of Dahl R and S rats.

			Dahl R		Dahl S		
			Reg Salt	High Salt	Reg Salt	High Salt	
Alpha ENaC	<i>mRNA</i>	2 wks	1.1±0.2	1.3±0.1	1.2±0.2	1.1±0.1	
	<i>(x10⁻³)</i>	4 wks	3.1±0.2	2.8±0.4	3.2±0.2	2.9±0.4	
	<i>80 kDa</i>	2 wks	100±3	107±13	128±19	124±21	
	<i>Protein</i>	4 wks	100±4	111±9	137±10	115±16	
Beta ENaC	<i>mRNA</i>	2 wks	1.5±0.2	1.5±0.3	1.6±0.2	1.7±0.2	
	<i>(x10⁻⁵)</i>	4 wks	1.7±0.3	1.5±0.3	1.5±0.2	1.2±0.1	
	<i>85 kDa</i>	2 wks	100±19	148±18	93±23	84±15	
	<i>Protein</i>	4 wks	100±13	104±10	110±9	89±11	
	<i>Immuno</i>	Cytop		3.3±0.7	2.3±0.6	1.7±0.3	2.3±0.9
		Memb		1.3±0.6	1.5±0.3	1.3±0.3	2.0±1.0
Gamma ENaC	<i>mRNA</i>	2 wks	1.0±0.1	1.1±0.1	0.9±0.1	0.8±0.1	
	<i>(x10⁻⁴)</i>	4 wks	1.3±0.1	1.4±0.1	1.2±0.2	1.3±0.1	
	<i>90 kDa</i>	2 wks	100±10	140±4	168±16	132±10	
	<i>Protein</i>	4 wks	100±5	93±4	118±6	108±10	
	<i>70 kDa</i>	2 wks	100±29	83±26	119±33	82±30	
		<i>Protein</i>	4 wks	100±8	112±7	124±5	94±6
	<i>Immuno</i>	Cytop		4.7±0.4	4.4±0.4	5.4±1.0	5.3±0.5
		Memb		3.7±0.4	4.8±0.5	4.4±0.4	5.3±0.5

Values are mean ± SEM (n=4-6 rats / group)

mRNA expression was measured versus PGK1

Protein abundance was measured versus β actin and normalized to Dahl R Reg Salt as 100%

Cytop = Cytoplasmic immunoreactivity

Memb = Membranous immunoreactivity

Immunoreactivity for α ENaC was low in the PVN and not quantified.

On regular salt intake, β and γ ENaC mRNA, protein abundance and immunoreactivity in magnocellular neurons were similar in Dahl R and S. High salt diet did not affect β and γ ENaC mRNA and protein abundance or distribution in either strain.

Table 3.4–5: Effect of high salt diet on mRNA expression of MR, SGK1 and 11 β HSD2 in the choroid plexus, SON and PVN of Dahl R and S rats.

			Dahl R		Dahl S	
			Reg Salt	High Salt	Reg Salt	High Salt
Choroid plexus	MR ($\times 10^{-2}$)	2 wks	1.1 \pm 0.2	1.3 \pm 0.2	1.2 \pm 0.1	1.0 \pm 0.03
		4 wks	2.8 \pm 0.3	2.3 \pm 0.2	2.2 \pm 0.2	2.4 \pm 0.3
	SGK1 ($\times 10^{-1}$)	2 wks	3.3 \pm 0.3	4.0 \pm 0.5*	3.3 \pm 0.5	4.9 \pm 0.4*
		4 wks	3.6 \pm 0.3	4.1 \pm 0.4	4.6 \pm 0.7	5.2 \pm 0.7
	11 β HSD2 ($\times 10^{-3}$)	2 wks	2.1 \pm 0.2	1.8 \pm 0.1	1.9 \pm 0.1	1.6 \pm 0.1
		4 wks	2.0 \pm 0.2	2.2 \pm 0.2	2.2 \pm 0.2	1.6 \pm 0.1
SON	MR ($\times 10^{-2}$)	2 wks	2.3 \pm 0.2	3.1 \pm 0.6	4.0 \pm 0.7	3.7 \pm 0.6
		4 wks	1.0 \pm 0.2	0.7 \pm 0.2	1.1 \pm 0.2	0.9 \pm 0.1
	SGK1 ($\times 10^{-1}$)	2 wks	2.0 \pm 0.04	2.2 \pm 0.04	2.9 \pm 0.1	6.1 \pm 0.1*
		4 wks	1.9 \pm 0.3	2.0 \pm 0.4	1.5 \pm 0.2	3.1 \pm 0.7
	11 β HSD2 ($\times 10^{-3}$)	2 wks	1.3 \pm 0.1	2.7 \pm 0.7*	2.4 \pm 0.3	3.0 \pm 0.3*
		4 wks	1.5 \pm 0.1	1.3 \pm 0.1	1.6 \pm 0.2	2.2 \pm 0.2
PVN	MR ($\times 10^{-2}$)	2 wks	0.6 \pm 0.2	0.8 \pm 0.1	0.8 \pm 0.2	0.7 \pm 0.1
		4 wks	1.0 \pm 0.1	0.9 \pm 0.1	0.8 \pm 0.1	0.6 \pm 0.1
	SGK1 ($\times 10^{-1}$)	2 wks	0.9 \pm 0.2	1.1 \pm 0.2	0.8 \pm 0.1	2.2 \pm 0.3*
		4 wks	1.1 \pm 0.2	1.3 \pm 0.2	1.2 \pm 0.2	1.8 \pm 0.4
	11 β HSD2 ($\times 10^{-3}$)	2 wks	1.7 \pm 0.1	1.4 \pm 0.2	1.5 \pm 0.1	1.8 \pm 0.1
		4 wks	1.8 \pm 0.2	1.7 \pm 0.1	1.6 \pm 0.1	1.4 \pm 0.3

Values are mean \pm SEM (n=4-6 rats / group)

* p<0.05, Reg vs High salt

mRNA expression was measured versus PGK1

3.4.6.3 Expression of regulators of ENaC (Table 3.4-6)

3.4.6.3.1 Choroid plexus

MR and 11 β HSD2 mRNA levels were similar in the CP of Dahl S and R rats on regular salt intake and not affected by high salt diet. SGK1 expression was also similar in the CP of Dahl S and R rats on regular salt at both 7 and 9 weeks of age. High salt for 2 weeks increased SGK1 mRNA levels irrespective of strain, but no longer after 4 weeks.

3.4.6.3.2 SON

On regular salt, expression of MR and SGK1 mRNA were similar in both strains while 11 β HSD2 tended to be higher in S rats. High salt for 2 weeks significantly increased the mRNA abundance of SGK1 and 11 β HSD2 in S but not in R rats and this increase tended ($p=0.06$) to persist after 4 weeks of high salt. No effect of salt was noted in R rats.

3.4.6.3.3 PVN

MR, SGK1 and 11 β HSD2 mRNA abundance in the PVN was similar in S and R rats. High salt for 2 weeks significantly increased SGK1 mRNA levels in the PVN of Dahl S rats and this effect tended to ($p=0.07$) persist in S rats after 4 weeks.

3.4.6.4 Effect of regular or high salt diet on CSF [Na⁺] (Figure 3.4-6)

CSF [Na⁺] was similar in Dahl R and S rats on regular salt diet. Icv infusion of benzamil significantly increased CSF [Na⁺], by ~5 mmol/L in Dahl R rats and somewhat less in Dahl S. High salt diet for 12-14 days did not affect CSF [Na⁺] in Dahl R, but significantly increased CSF [Na⁺] by ~5-6 mmol/L in Dahl S rats. Infusion of benzamil did not affect CSF [Na⁺] in either strain on high salt diet. Hypothalamic tissue [Na⁺] was also similar in Dahl R and S rats (Dahl R vehicle 38 \pm 1 mmol/L, Dahl S vehicle 36 \pm 1 mmol/L) and not

affected by icv infusion of benzamil (Dahl R benzamil 37 ± 1 mmol/L, Dahl S benzamil 36 ± 1 mmol/L).

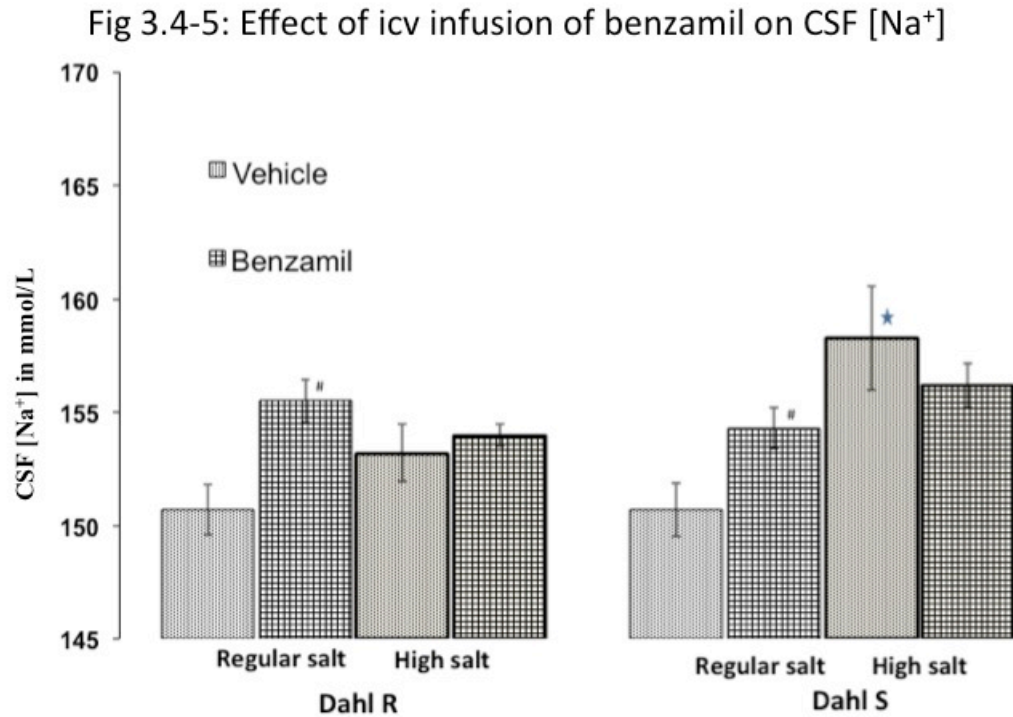


Figure 3.4–5: Effect of icv infusion of benzamil on CSF $[Na^+]$ in Dahl R and S rats on regular or high salt diet. On regular salt, icv benzamil increases CSF $[Na^+]$, somewhat more in Dahl R than Dahl S rats. High salt increases CSF $[Na^+]$ in Dahl S by ~ 7 mmol/L, but not in R rats. Icv benzamil does not affect CSF $[Na^+]$ on high salt in either strain. Values are mean \pm SEM ($n=4-10$ rats/group). $*p<0.05$, Reg vs High salt; $\#p<0.05$, Veh vs Benz.

3.4.6.5 Sequencing for Nedd4L and SGK1

No differences were found in the complete coding sequence and 2000 bp upstream exon 1 of the Nedd4L gene between Wistar, R and S rats. There were 4 synonymous SNPs

(C258, C323, C675 and C293) in Wistar, R and S rats that were different from the published sequence of the Brown Norway strain.

No differences in sequence were noted in the 2000 bp of the 5'-flanking region of the SGK1 gene, introns, exons and the 2000 bp of the 3'-flanking region of the gene between Dahl R, Dahl S, Wistar and the published Brown Norway sequence.

3.4.7 DISCUSSION

This study evaluated the effects of high salt diet on the expression of ENaC subunits and their regulators in brain epithelia and nuclei of Dahl R and S rats. Abundance of the ENaC subunits (α ENaC: protein, β ENaC: protein and immunoreactivity and γ ENaC: 90 and 70 kDa protein and immunoreactivity) is higher in the choroid plexus of Dahl S versus R rats and these increases persist on high salt diet. On regular salt diet, β and γ ENaC immunoreactivity is higher in the SON of Dahl S rats. High salt increases β and γ ENaC mRNA expression associated with an increase of SGK1 and 11 β HSD2 mRNA and the increased membranous staining persists in the SON of Dahl S rats.

3.4.7.1 Choroid plexus

The epithelium of the choroid plexus is the major site for the production of CSF (Brown et al. 2004, Keep et al. 1997, Praetorius 2007). Apical Na⁺K⁺ATPase in the choroid cells generates the electrochemical gradient for secretion of Na⁺ into the CSF followed by passive transport of Na⁺ into the cells from the basolateral surface (Brown et al. 2004, Keep et al. 1997, Praetorius 2007). In recent studies (Amin et al. 2005, Amin et al. 2009, Wang et al. 2010b), we demonstrated the presence of both the mRNA and protein of the ENaC subunits in the choroid plexus. By EM, the subcellular distribution shows about 30% of α ENaC and 40-50% of β and γ ENaC labeled gold particles on the apical microvilli, and only 5-10% in the basolateral membrane. Similar to our previous studies comparing Dahl SS/Mcw with Dahl SS/BN13 controls (Amin et al. 2009), the mRNA abundance of the 3 subunits was not significantly different, but protein abundance higher in Dahl SS/JrHSD (S) compared to SR/JrHSD (R) rats. Consistent with our previous study (Amin et al. 2009), immunoreactivity at the apical membrane was significantly

higher for β and γ ENaC in S versus R rats. By EM, β ENaC abundance was greater in all 3 subcellular compartments and particularly in the apical microvilli. High salt diet had no effects on ENaC mRNA, protein and immunoreactivity in the choroid plexus of Dahl R rats and by EM, β ENaC clearly decreased in the apical microvilli. In Dahl S, high salt diet also did not affect ENaC mRNA expression and the higher abundance of protein and immunoreactivity persisted. Qualitatively this pattern of ENaC expression is similar to the pattern in the renal medulla: increased protein expression is present on regular salt diet, which is not decreased, even further enhanced in Dahl S by high salt diet (Amin et al. 2011).

A variety of factors may contribute to this dysregulation of ENaC in the choroid plexus of Dahl S rats. The absence of differences in the regulatory and coding sequences of the ENaC genes between S and R rats (Shehata et al. 2007) and similar mRNA levels suggests differential regulation mainly at the protein level. In the present study, we show that regulatory and coding sequences for two important regulators of ENaC protein – SGK1 and Nedd4L – also show no differences. At the mRNA level, MR, SGK1 and 11 β HSD2 transcripts are clearly present in the choroid plexus and similar in Dahl S and R rats. Protein and activity have not yet been assessed. Plasma aldosterone levels markedly decrease in response to high salt diet in both S and R rats (Amin et al. 2011). However, tissue aldosterone levels may actually increase in Dahl S rats on high salt diet, as shown in the kidneys (Bayorh et al. 2005, Zhu et al. 2009) and recently in the hypothalamus (Gomez-Sanchez et al. 2010, Huang et al. 2009b). Whether aldosterone via MR contributes to dysregulation of ENaC in the choroid plexus requires further studies.

In vitro, 20 to 30% of the influx of Na^+ into the choroid cells is inhibited by benzamil presumably reflecting the role of ENaC in Na^+ influx. As most of the ENaC in the CP is on apical microvilli facing the CSF, it appears that ENaC particularly contributes to Na^+ reuptake from the CSF into the choroid plexus. Indeed, icv infusion of benzamil increases CSF $[\text{Na}^+]$ in Wistar and Dahl rats on regular salt diet. Despite higher abundance of β and γ ENaC in the apical and basolateral membrane of Dahl S versus R rats, no significant differences were noted in the ENaC mediated influx of Na^+ into the choroid cells of Dahl SS/MCW versus Dahl SS/BN13 rats (Amin et al. 2009) and in the present study the effect of icv benzamil on CSF $[\text{Na}^+]$ was somewhat less in Dahl S versus R rats. Moreover, benzamil did not have a significant effect on CSF $[\text{Na}^+]$ in both strains on high salt diet despite persistent higher protein expression in S rats. ENaC at the cell surface can be of two types – active channels that have already undergone proteolytic cleavage and silent channels that have bypassed the cleavage steps and directly inserted into the membrane (Palmer 1992). A number of factors such as concentration of ions especially Na^+ or activity of second messengers regulate proteolytic activity and open probability (P_o) of the channels at the membrane (Eaton et al. 2009, Rossier & Stutts 2009). Mechanisms that decrease P_o of the channels in the choroid cells of Dahl S may explain the diminished rather than enhanced response to benzamil and by negative feedback cause increased expression (Rauh et al. 2010). On high salt diet, Na^+K^+ ATPase activity may decrease to inhibit further increases in CSF Na^+ , and a resultant increase in intracellular $[\text{Na}^+]$ may inhibit P_o of the sodium channels (Amin et al. 2009).

3.4.7.2 Magnocellular neurons in PVN and SON

Expression of ENaC subunits was similar in the magnocellular neurons in the PVN of Dahl R and S rats, and not affected by high salt diet. In contrast, in the SON Dahl S showed similar mRNA abundance on regular salt, but greater immunoreactivity to β and γ ENaC. High salt enhanced abundance of β and γ ENaC mRNA and membranous expression in the SON of Dahl S rats versus no changes in Dahl R. In addition, high salt diet increased SGK1 and 11 β HSD2 mRNA in the SON of Dahl S rats. Considering that high salt diet increases hypothalamic aldosterone in Dahl S rats compared to a decrease in Dahl R rats (Huang et al. 2009b), one may speculate that aldosterone through SGK1 causes enhanced expression of β and γ ENaC in the SON.

Functional studies suggest that the increase in CSF $[\text{Na}^+]$ in Dahl S rats on high salt diet activates a central pathway involving aldosterone-MR-ENaC that leads to an increase in ‘ouabain’ and angiotensinergic activity in the PVN and downstream pathways (Leenen 2010, Huang et al. 2006a). High salt increased expression and membrane abundance of ENaC subunits in the magnocellular neurons of the SON in Dahl S but not R rats. These neurons produce vasopressin, oxytocin and possibly aldosterone and ‘ouabain’ (Takahashi et al. 1987a, Yamada et al. 1992) as well. One may speculate that increased aldosterone via MR and ENaC increases intracellular $[\text{Na}^+]$ and this may represent a stimulus for increased production of ‘ouabain’. The role of magnocellular neurons in the PVN appears to be different in this regard.

3.4.8 Limitations of study

One of the major limitations of our study is the lack of functional studies that could confirm possibly enhanced activity of magnocellular neurons in the SON. Studying

intracellular $[Na^+]$ using dyes such as sodium green (Amin et al. 2009) may confirm the increased activity of ENaC. Further biochemical and electrophysiological studies are required to assess whether increased activity of the magnocellular neurons in the SON in Dahl S rats on high salt diet indeed contributes to increased 'ouabain' release.

3.4.9 Conclusion

On regular salt Dahl S rats exhibit enhanced expression of ENaC subunits in the renal medulla (Amin et al. 2011), choroid plexus (Amin et al. 2009) and SON, which persists or further increases on high salt diet. The mechanisms responsible for the enhanced expression in Dahl S rats on regular salt are not yet known. The increase in CSF $[Na^+]$ and CNS aldosterone on high salt diet may contribute to the enhanced expression in the choroid plexus and SON. In the SON, this increase may lead to enhanced neuronal activity and secretion of 'ouabain' causing sympathoexcitation and hypertension.

3.4.10 Acknowledgement

The authors would like to acknowledge Ms. Danielle Oja for her excellent skills in assisting in the preparation and formatting of this article. Dr. Leenen holds the Pfizer Chair in Hypertension Research, an endowed chair supported by Pfizer Canada, University of Ottawa Heart Institute Foundation and Canadian Institutes of Health Research.

3.4.11 Sources of Funding

This research was supported by operating grant FRN: MOP-74432 from the Canadian Institutes of Health Research. Md Shahrier Amin was supported by a Pfizer/CIHR/Canadian Hypertension Society doctoral research award and program grant PRG5275 from the Heart and Stroke Foundation of Ontario.

**3.5 MANUSCRIPT # 5: SODIUM TRANSPORT IN
THE CHOROID PLEXUS AND SALT SENSITIVE
HYPERTENSION.**

Md Shahrier Amin^{1,2}, Erona Reza^{1,2}, Hongwei Wang¹, Frans H H Leenen^{1,2}

¹ Hypertension Unit, University of Ottawa Heart Institute, Ottawa, Ontario, Canada

² Department of Cellular and Molecular Medicine, University of Ottawa, Ottawa,
Ontario, Canada

SHORT TITLE

Sodium transport in choroid plexus

STATUS

This article was published in Hypertension, 2009; Volume 54, Issue 4: Pages 860-867.

3.5.1 Relevance

No previous studies had evaluated the functional role of ENaC in the choroid plexus. Here we studied the role of ENaC in Na⁺ transport by the choroid plexus and evaluated the effect of high salt diet, in order to identify mechanism in the CP that contribute to the increase in CSF [Na⁺] on a high salt diet in Dahl S rats.

3.5.2 CONTRIBUTION

Responsible for the overall project and performed the following:

1. Design and planning of the experiments
2. Tissue collection and processing in most of the experiments.
3. Performed and analyzed all the immunoblots, immunohistochemistry and EM experiments.
4. Performed all the functional experiments of Na⁺ transport.
5. Compilation of all the data and preparation of the final manuscript.

3.5.3 ABSTRACT

To elucidate the role of epithelial Na channels (ENaC) and Na⁺K⁺ATPase in Na transport by the choroid plexus (CP) we studied ENaC expression and Na transport in the CP. Lateral ventricle CPs were obtained from 5-6 week old, male Wistar, Dahl R and Dahl S rats on regular (0.3%) or high (8.0%) salt diet. The effects of ENaC blocker benzamil and Na⁺K⁺ATPase blocker ouabain on Na transport were evaluated by measuring the amount of retained ²²Na (cpm/100 μg) and by evaluating intracellular [Na] ([Na]_i) with Sodium Green fluorescence. In Wistar rats ENaC distribution was: microvilli 10-30%, cytoplasm 60-80% and basolateral membrane 5-10%. Benzamil (10⁻⁸M) decreased ²²Na retention by 20%; ouabain (10⁻³ M) increased retention by 40%, whereas ouabain and benzamil combined caused no change. Similar changes were noted in [Na]_i. In Dahl rats on regular salt diet, [Na]_i was similar but the amount of retained ²²Na was less in S versus R rats. High salt did not affect ENaC mRNA or protein neither the benzamil induced decreases in retained ²²Na or [Na]_i in either strain. However, high salt increased [Na]_i and attenuated the increase in uptake of ²²Na by ouabain in R but not S rats suggesting inhibition of Na⁺K⁺ATPase activity only in R rats. These findings suggest that both ENaC and Na⁺K⁺ATPase regulate Na transport in the CP. Aberrant regulation of Na transport and of Na⁺K⁺ATPase activity, but not of ENaC, might contribute to the increase in CSF [Na] in S rats on high salt diet.

KEYWORDS

Sodium, Choroid plexus, ENaC, Na⁺K⁺ATPase, Dahl rats, Hypertension

3.5.4 INTRODUCTION

Strict regulation of [Na] in the cerebrospinal fluid (CSF) and thus the central nervous system is crucial for normal functioning of neurons. An increase in CSF [Na] by as little as 2 mM can increase firing rate of neurons (Honda et al. 1990a, Honda et al. 1990b). A chronic 5 mM increase in CSF [Na] causes sympathetic hyperactivity and hypertension (Huang et al. 2004). Such a subtle increase in CSF [Na] might be a primary abnormality in salt induced hypertension. CSF [Na] increases by up to 5 mM in Dahl salt-sensitive (S) rats and SHR on high salt diet and this increase appears to precede the increase in BP while CSF [Na] shows minimal changes in “salt-resistant” strains such as WKY and Dahl salt-resistant (R) rats (Huang et al. 2004, Simchon et al. 1999).

The epithelium of the choroid plexus (CP) is the major site for production of CSF, which is later absorbed by arachnoid granulations (Praetorius 2007, Brown et al. 2004). Net transport of Na between plasma and CSF is a balance of Na influx into and efflux out of the CP cells which is accomplished by selective distribution and activity of a variety of enzymes and transporters (Mathew 2007, Keep et al. 1987). An increase in CSF [Na] in Dahl S rats on high salt diet may thus be due to increased efflux of Na into the CSF, decreased re-uptake of Na from the CSF or both. However the actual mechanisms contributing to the increase in CSF [Na] in Dahl S rats or SHR on high salt diet have not yet been studied.

A number of Na transporters mediate Na influx into the CP. Based on their distribution either on the apical or the basolateral surface they contribute to transport of Na from CSF or plasma into the CP cells along a prevailing electrochemical gradient. The Na channel blocker, amiloride decreases Na transport into the CP and CSF (Murphy & Johanson

1989a, Murphy & Johanson 1989b, Wright 1972b). Blockade of the sodium hydrogen exchanger (NHE) was first thought to be responsible for this, but NHE proteins are almost undetectable in the CP of rats (Kalaria et al. 1998, Praetorius 2007). Amiloride also blocks epithelial sodium channels (ENaC), which we recently reported to be present in the CP of rats (Amin et al. 2005). ENaC are members of the amiloride sensitive Na channels with three subunits α , β & γ forming a hetero-multimeric Na channel in many transporting epithelia (Canessa et al. 1993a, Canessa et al. 1994b, Duc et al. 1994).

Na^+K^+ ATPase forms the major pathway for active Na efflux from the CP. The predominant isoform in the choroid cells is the $\alpha 1$ Na^+K^+ ATPase while all three α isoforms are abundant in the brain micro-vessels (Praetorius & Nielsen 2006, Pollay et al. 1985, Masuzawa et al. 1984). Its predominant location on the ventricular surface of the epithelium provides the driving force for directional transport of Na into the CSF against an electro-chemical gradient (Johansson et al. 2008, Pollay et al. 1985, Masuzawa et al. 1984). The Na^+K^+ ATPase inhibitor, ouabain, at 6.7×10^{-5} M has no effect on the flux of ^{22}Na from ventricle to blood but reduces the flux from blood to ventricle by 33% in CP of frogs (Wright 1972b). Similarly 10^{-6} M ouabain added to the artificial CSF used for ventriculo-cisternal perfusion of rabbits reduces transport of ^{22}Na from blood to CSF by 50-60% (Davson & Segal 1971). Icv infusion of ouabain at 10 $\mu\text{g}/\text{day}$, decreases CSF [Na] by 6-8 mM in Wistar rats on high salt diet (Huang et al. 2004).

Considering that the role of ENaC in Na transport by the CP has not yet been studied at all, the first objective of the current study was to assess in Wistar rats the expression and sub-cellular distribution of ENaC in the CP and the effects of blockers of ENaC and Na^+K^+ ATPase on parameters of Na transport by the CP in vitro. This first set of

experiments demonstrated that both ENaC and Na⁺K⁺ATPase contribute to Na transport by the CP. As second objective we then evaluated whether aberrant regulation of ENaC or Na⁺K⁺ATPase may contribute to the salt induced increase in CSF [Na] in Dahl S rats and assessed the above parameters in Dahl S versus Dahl R rats on regular or high salt diet.

3.5.5 METHODS

3.5.5.1 Animals and protocols

Young 5-6 weeks old, male Wistar, Dahl S and Dahl R rats received regular (0.3%, 120 μ M Na/gm) or high (8%, 1370 μ M Na/gm) salt diet for 7-14 days. For details of methods, see <http://hyper.ahajournals.org>.

3.5.5.2 Quantitative RT-PCR

The CP of the lateral ventricles was micro-punched for total RNA isolation as described previously (Amin et al. 2005). Genomic DNA was removed by DNase I (Ambion, Austin, TX) and cDNAs were synthesized by Superscript II RNase H⁻ Reverse Transcriptase (Invitrogen, Burlington, Ontario, Canada). The mRNA abundance of α , β and γ ENaC was measured by quantitative real-time PCR. Phospho-glycerate kinase 1 (PGK1) was used as the house keeping gene. The PCR conditions and external standard for PGK1, α , β and γ ENaC were the same as previously described (Amin et al. 2005).

3.5.5.3 Immunoblotting

5 μ g CP protein extracts were run on a 4-12% gradient gel (Bio-rad) by SDS-PAGE, and transferred onto a PVDF membrane (Bio-Rad). The membrane was probed with the primary antibodies to α ENaC (1:500), β ENaC or γ ENaC (1:1000) (Masilamani et al. 1999) overnight at 4°C, followed by goat anti-rabbit secondary antibody (1:5000, Santa Cruz). β actin (1:10000) was used as an internal standard to compare band density.

3.5.5.4 Immunohistochemistry

Immunohistochemistry was performed as previously described (Amin et al. 2005) using the primary antibodies (Masilamani et al. 1999) diluted in blocking solution (1:250 - α &

γ ENaC, 1:500 - β ENaC) and processed using the Vectastain Elite ABC kit (Vector Laboratories). Antigen-antibody reactions were developed with Vector DAB kit with Nickel enhancement. Intensity of the staining was assessed using Image Pro (Version 6.2). In addition distribution of the staining in the apical membranes and cytoplasm was assessed blindly by two individuals and scored 1 (<30%), 2 (30-70%) and 3 (>70%) based on the area stained.

3.5.5.5 Immuno electron microscopy

Immuuno EM was done following standard protocols with the primary antibodies diluted in 0.1% BSA in PBS (1:100). Number of gold particles (per $100\mu\text{m}^2$) in the cytoplasm, apical or basal membrane was counted in cells having intact morphology (4-8 per rat). ~4000 EM fields were quantified.

3.5.5.6 Studies with isolated CP

The CP of lateral ventricles was quickly removed after decapitation and stored on individual snap well inserts (Corning) of 6 well culture plates. The insert and well were filled with 500 and 2000 μl respectively of aCSF or aCSF⁺drug.

3.5.5.6.1 Uptake of ^{22}Na

From each rat one CP was bathed in aCSF as control and the contralateral CP bathed in aCSF containing drugs: Benzamil (1, 10 or 100 nM), Ouabain (1 mM or 1 μM), Ethyl Iso-Propyl Amiloride (EIPA) (1 mM) or both Benzamil and Ouabain for 2 hours. Each CP was then put in 0.5 ml eppendorf tubes containing 250 μl of the same incubation solution with 1 $\mu\text{Ci/ml}$ of ^{22}Na and incubated for 30 sec. Activity of ^{22}Na was assessed on a liquid scintillation counter (1219 Rackbeta) and is expressed as cpm/100 μg of CP.

Retention of ^{22}Na was negligible in CP briefly dipped in aCSF containing ^{22}Na . The amount of retained ^{22}Na increased with increasing duration of incubation and approached a steady state V_d within 1 min (Fig 3.5-S1), with no further uptake beyond 1 min.

3.5.5.6.2 Measurement of intracellular [Na] ($[\text{Na}]_i$)

The CPs were first loaded with 10 μM Sodium Green (Molecular probes). After 3 washes in aCSF the CPs were divided into 3-5 pieces and put in aCSF or aCSF containing drugs as above for 2 hours. After the incubation period, each piece was transferred to glass cover slips and viewed in an inverted epi-fluorescence microscope. Sodium Green was excited by an Argon Laser at 488 nm and emissions between 500-560 nm were assessed. Fluorescence intensity of Sodium Green was calibrated to the [Na] by incubation in the presence of Gramicidin (5 μM) and varying the [Na] in aCSF by replacing Na with NMDG. Intensity of Sodium Green fluorescence increased when the CSF [Na] was increased. The change in fluorescence intensity with varying [Na] was used to generate a calibration curve for measurement of $[\text{Na}]_i$ (Fig 3.5-S2).

3.5.5.7 Statistical analysis

Data are expressed as means \pm SEM. Effects of individual drugs on Na transport in Wistar rats were assessed by paired t-test. The effects of diet and strain on gene expression and parameters of Na transport were evaluated by two way ANOVA. Effects were considered statistically significant at $p < 0.05$.

3.5.6 Supplementary Methods

3.5.6.1 Animals and protocols

Young, (3-4 weeks old) male Wistar, Dahl S and Dahl R rats were purchased from Charles River Canada Inc (Montreal, Canada). Rats were housed two per cage under standard conditions on a 12 hr light – dark cycle at 24°C. All procedures were approved by the Animal Care Committee of the University of Ottawa. After an acclimatization period of ~1 week the animals were placed on regular (0.3%, 120 µM Na/gm) or high (8%, 1370 µM Na/gm) salt diet for 7-14 days. The 7-day time point was used for activity assays to identify early changes in Na transport. The 14 day time point was used for expression profiling to elucidate more stable changes in expression. At the end, the CPs were dissected under a microscope and were processed for ²²Na uptake and sodium green studies. In separate groups of rats, the brains were used for RNA extraction, immunohistochemistry and EM studies.

3.5.6.2 Quantitative RT-PCR

After perfusion with chilled diethyl pyrocarbonate (DEPC, Sigma, St. Louis, MO) treated phosphate-buffered saline (PBS, pH 7.4), the brains were removed and snap-frozen in liquid nitrogen and then stored at –80° C. Serial 80 µm thick coronal slices were cryosectioned. The CP of the lateral ventricles was micro-punched for total RNA isolation as described previously (Amin et al. 2005). Genomic DNA was removed by DNase I (Ambion, Austin, TX) and cDNAs were synthesized by Superscript II RNase H⁻ Reverse Transcriptase (Invitrogen, Burlington, ON, Canada).

mRNA abundance of α , β and γ ENaC subunits was measured by quantitative real-time PCR. Supplement table 1 shows the primers used. Phospho-glycerate kinase 1 (PGK1)

was used as the house keeping gene. The PCR conditions and external standard for PGK1, α , β and γ ENaC subunits were the same as previously described (Amin et al. 2005).

3.5.6.3 Immunoblotting

Isolated whole CPs and macroscopically dissected renal cortex were homogenized in ice-cold isolation solution containing 300 mM sucrose and 10 mM triethanolamine, pH 7.5, containing 1% of protease inhibitor cocktail (Sigma, St. Louis, MO). The homogenate was spun at 1000 g for 20 minutes at 4°C, the supernatant was collected and protein concentration was measured using BCA assay (Pierce biotechnology, Rockford, IL). 5 (CP of Dahl rats) or 25 (CP of Wistar rats) μ g protein were run on a 4-12% gradient gel (Bio-rad) by SDS-PAGE, and the proteins were transferred onto a PVDF membrane (Bio-Rad, Hercules, CA). After blocking with BSA in Tris-buffered saline-Tween (TBST), the membrane was probed with the primary antibodies to α ENaC (1:500), β ENaC or γ ENaC (1:1000) (Masilamani et al. 1999) overnight at 4°C, followed by goat anti-rabbit secondary antibody (1:5000, Santa Cruz). The antibodies detected bands at ~80 and ~37 kDa for α ENaC, ~85 kDa for β ENaC and ~90 & ~70 kDa for γ ENaC; which were abolished by co-incubation with the immunizing peptide. The stripped membrane was re-probed with mouse anti β actin (1:10000) and sheep anti-mouse (1:10000) as an internal control. The signal was developed with the ECL⁺ system (Perkin Elmer, Shelton, CT) and visualized by an Alpha Innotech imager. Band densities were quantified by Alpha Ease software (Alpha Innotech, San Leandro, CA).

3.5.6.4 Immunohistochemistry

Brains were perfusion-fixed with 4% paraformaldehyde and 0.05% glutaraldehyde in PBS (pH 7.4). 5 μm coronal slices were collected on superfrost plus slides. Immunohistochemistry was performed as previously described (Amin et al. 2005). Briefly, slides were incubated in 1% sodium-borohydride in PBS for 20 minutes, 0.5% H_2O_2 in 20% methanol for 30 minutes, followed by incubation in blocking solution (1% BSA & 3% goat serum in PBS). Sections were then incubated with the primary antibodies (Masilamani et al. 1999) diluted in blocking solution (1:250 for α , γ or 1:500 for βENaC) overnight and processed using the Vectastain Elite ABC kit (Vector Laboratories, Burlington, ON, Canada) by incubating with the biotinylated secondary antibody for 1 hour and with biotinylated horseradish peroxidase for another 1 hour. Antigen-antibody reactions were developed with Vector DAB kit with Nickel enhancement. Complete labeling of a section was confirmed by the presence of uniform DAB label intensity in most parts.

For semi-quantification, images were captured in *.tiff* format using Spot digital camera and Spot software with a high resolution bright field transmitted light microscope (Olympus B \times 60). Assessment was done for intensity and percent area of staining as well as relative cellular distribution. Intensity and percent area of staining were assessed by Image Pro (6.02). The cutoff for measurement was adjusted to include positive staining but exclude the background and was kept constant for all sections. Mean intensity of staining was not different between groups. Cellular distribution in the apical membranes or in the cytoplasm was assessed blindly by two individuals. Abundance of staining was graded as 1 if <30% , 2 if 30-70% and 3 if >70% of cells in each area showed prominent

immunoreactivity in the area assessed. The averages of at least 6 individual measurements from different sections in each rat were used.

3.5.6.5 Immuno electron microscopy

Brains were perfusion-fixed with 4% paraformaldehyde and 0.05% glutaraldehyde in 0.1 M Na-cacodylate buffer, post-fixed for 30 min, dissected under a stereomicroscope and the CP stored in 0.1 M Na-Cacodaylate buffer at 4°C. Tissues were dehydrated in a series of graded alcohols (60, 80, 95%), infiltrated with LR White resin and polymerized at 50° C. Thin sections were mounted on Formvar coated nickel grids and placed onto drops of 1% BSA for 30 min. Without rinsing, the grids were then placed onto drops of primary antibodies diluted in 0.1% BSA in PBS (1:100) and incubated overnight at 4°C. Subsequent to rinsing in PBS the grids were incubated at room temperature for 1 hour on drops of secondary goat anti-rabbit IgG conjugated to 15 nm gold particles (1:100, EY Laboratories, San Mateo, CA). Grids were counterstained with 3% uranyl acetate and lead citrate.

Sections were imaged in a Jeol 1230 TEM using AMT software. Low magnification (1000×) images were used for area calculation by Image Pro. No gold particles could be seen when primary antibody was omitted. Number of gold particles (per 100µm²) in the cytoplasm, apical or basal membrane were counted from highly magnified images (8000-20000×) using ACDSee software in cells having intact morphology (4-8 per rat). A total of ~4000 EM fields were quantified.

3.5.6.6 Studies with isolated CP

Pilot experiments showed that in male rats effects of drugs were most consistent in the afternoon between 2:00-4:00 pm. This time frame was therefore chosen for tissue

collections. Briefly the rats were decapitated, the brains removed quickly and kept in cold aCSF. The CP of lateral ventricles was then removed quickly under a microscope and stored on individual snap well inserts (Corning Inc., Corning, NY) in 6 well culture plates. The insert and well were filled with 500 and 2000 μ l respectively of aCSF or aCSF⁺ drug. In preliminary experiments >70% CP cells were found to be alive for upto 6 hours after isolation in viability assessments on a Beckman-Coulter cell counter. All experiments were performed within 2-3 hours during which the oxygenation and pH (7.3-7.4) was maintained by constant bubbling of the well solution with 5% CO₂ and 95% O₂. Temperature was maintained at 37° C with a slide warmer or chamber heater.

3.5.6.7 Uptake of ²²Na⁺

Procedures were adapted from Murphy and Johanson [4]. From each rat one CP was bathed in aCSF as control and the other in aCSF containing drugs: Benzamil (1, 10 or 100 nM), Ouabain (1 mM or 1 μ M), Ethyl Iso-Propyl Amiloride (EIPA, 1 mM) or both Benzamil (10 nM) and Ouabain (1 μ M) for ~2 hours. Each CP was then put in 0.5 ml eppendorf tubes containing 250 μ l of the same incubation solution with 1 μ Ci/ml of ²²Na. In initial studies samples were incubated for 0, 15, 30, 45, 60, 90 or 120 sec to assess the time course of uptake (see Fig 3.5-S1). The CP was briefly rinsed in excess volumes of aCSF, stretched 5 cm on a glass slide to remove as much as possible of the adherent ²²Na and then transferred onto pre-weighed aluminium foils. The samples were air-dried, weighed and transferred to scintillation vials containing 7.5 ml of scintillation fluid (CytoScint, IGN). Activity of ²²Na (counts per minute) was assessed on a liquid scintillation counter (1219 Rackbeta) and expressed as cpm/100 μ g of CP. In all subsequent experiments the 30 sec. incubation time was used.

3.5.6.8 Measurement of intracellular [Na] ($[Na]_i$)

The CPs were loaded with 10 μ M Sodium Green (Molecular Probes, Invitrogen Corp., Carlsbad, CA) in aCSF containing 10 μ M pluronic (Molecular Probes) for 1 hour at 37° C. The CPs were then washed 3 times with aCSF, divided into 3-5 pieces and put in control aCSF or aCSF containing drugs as above for 2 hours. Negative controls consisted of CP not loaded with Sodium Green or CP loaded with Sodium Green but incubated in aCSF where Na was replaced with equimolar NMDG (Sigma). Sodium Green was excited by an Argon Laser at 488 nm and emissions between 500-560 nm were quantified. The same settings were used throughout the experiments. Areas of the CP encompassing 8-10 cells at midsection, with uniform loading and clear outlines were selected for quantification. Cell outline was assessed from the parallel images obtained under bright field optics. Mean fluorescence intensity and percent area were calculated using Image Pro. Photobleaching was minimized by conducting all experiments in minimal light. After the incubation period, the CPs were transferred to glass cover slips and viewed in an inverted epifluorescence microscope with a digital camera linked to a PC running Fluoviewmax software.

To calibrate intracellular [Na], CP from Wistar rats were incubated with aCSF containing Gramicidin (1 mg/ml, Molecular probes) to equilibrate extra- and intracellular [Na] and varying concentrations of Na – 0, 30, 45, 60 and 75 mmol (n=4 to 6). Osmolarity was maintained by replacing Na with equimolar NMDG. $[Na]_i$ was calculated, assuming a 1:1 binding stoichiometry between Na and Sodium Green, i.e. when the concentration of the fluorophore is not excessive and is uniform, the emitted fluorescence is directly proportional to intracellular [Na]. The average fluorescence intensity was calculated as F

= $(I - I_{bg})$, where I is the measured intensity and I_{bg} the average background intensity.

Figure S2 shows the calibration curve obtained by incubating the CPs in different concentrations of Na.

3.5.6.9 Statistical analysis

Data are expressed as means \pm SEM. In Wistar rats the effects of individual drugs on ^{22}Na retention and intracellular $[\text{Na}]_i$ were compared to values in control CP parts from the same rat by paired t-tests. The magnitude of the effect of different doses of the drugs was compared by ANOVA. The effects of strain and diet on expression of the mRNA abundance, protein abundance and immunoreactivity were evaluated by two way ANOVA. The effects of salt diet, strain and drugs on retention of ^{22}Na and $[\text{Na}]_i$ were also evaluated by two way ANOVA. Effects were considered statistically significant at $p < 0.05$.

3.5.7 RESULTS

3.5.7.1 Expression and sub-cellular distribution of ENaC in the CP

Both mRNA and protein of all three ENaC subunits were expressed in the CP of all three rat strains studied. Fig 3.5-1a shows the major bands detected by the antibodies in the kidney (as positive control) and the CP of Wistar rats: ~80 and 37 kDa for α ENaC, ~85 kDa for β ENaC and ~90 and 70 kDa for γ ENaC. Immunoreactivity was present in >70% of CP cells and was most prominent in the apical membranes and cytoplasm (Fig 3.5-1b). Similarly, at the sub-cellular level ~35% of α ENaC and ~15-20% of β and γ ENaC were in the apical microvilli, only ~5-10% in the basolateral membranes and the remainder in the cytoplasm (Fig 3.5-1b).

3.5.7.2 Na^+ transport in the CP

Fig 2 shows the effect of various drugs on the retention of ^{22}Na by the CP in Wistar rats on regular salt diet. 1 μM ouabain which blocks α_2 and α_3 $\text{Na}^+\text{K}^+\text{ATPase}$ did not affect the amount of ^{22}Na retained, whereas 1 mM ouabain which blocks all α isoforms increased retention by ~40%. 1 nM benzamil did not have a significant effect, but there was a dose dependent decrease in the amount of retained ^{22}Na with 10 and 100 nM benzamil. In order to minimize the possible involvement of other channels further experiments were continued using only the lowest effective dose of benzamil (10 nM). This dose of benzamil decreased retained ^{22}Na in the CP at 30, 45 & 60 sec by 18%, 20% and 25% respectively (Fig 3.5-S1). 1 mM ouabain and 10 nM benzamil together caused no overall change in the amount of retained ^{22}Na (Fig 3.5-2). The NHE blocker EIPA at 1 μM had minimal effect (~10% decrease) on retained ^{22}Na .

Table 3.5–1 Abundance of mRNA and protein and cellular distribution of ENaC subunits in the CP of S and R rats on regular or high salt diet for 2 weeks.

			Dahl R		Dahl S	
			Reg salt	High salt	Reg salt	High salt
ENaC α	mRNA abundance	x 10 ⁻³	0.9 ± 0.1	1.0 ± 0.1	1.0 ± 0.05	0.9 ± 0.03
	Protein abundance	80 kDa	0.11 ± 0.01	0.11 ± 0.002	0.14 ± 0.006*	0.14 ± 0.007*
		37 kDa	0.11 ± 0.01	0.12 ± 0.002	0.15 ± 0.002*	0.15 ± 0.009*
Immuno.	Apical Cytop.		1.0 ± 0.01	1.0 ± 0.01	1.0 ± 0.01	1.0 ± 0.01
			1.0 ± 0.01	1.0 ± 0.01	1.0 ± 0.01	1.0 ± 0.01
ENaC β	mRNA abundance	x 10 ⁻⁴	1.6 ± 0.3	1.5 ± 0.2	0.7 ± 0.1*	0.7 ± 0.05*
	Protein abundance	85 kDa	0.41 ± 0.01	0.38 ± 0.02	0.40 ± 0.05	0.35 ± 0.04
	Immuno.	Per area	16 ± 5	29 ± 4	41 ± 4*	42 ± 11*
		Apical Dist Cytop Dist	1.3 ± 0.3 2.0 ± 0.6	1.0 ± 0.01 3.0 ± 0.01	3.0 ± 0.01* 2.3 ± 0.3	2.7 ± 0.9* 2.7 ± 0.3
ENaC γ	mRNA abundance	x 10 ⁻⁵	2.5 ± 0.3	1.8 ± 0.3	2.7 ± 0.1	1.5 ± 0.2
	Protein abundance	90 kDa	0.3 ± 0.003	0.3 ± 0.004	0.3 ± 0.006	0.2 ± 0.002
		70 kDa	0.5 ± 0.003	0.5 ± 0.006	0.5 ± 0.009	0.4 ± 0.005
	Immuno.	Per area	32 ± 8	36 ± 5	65 ± 3*	67 ± 4*
		Apical Dist Cytop Dist	1.3 ± 0.3 2.3 ± 0.3	2 ± 0.01 2.3 ± 0.3	3 ± 0.01* 3 ± 0.01*	2.7 ± 0.3* 3 ± 0.6*

Values are mean ± SEM, n = 4-6/group;

* p<0.05 vs Dahl R

mRNA abundance versus PGK

Protein abundance versus β actin

Units for apical and cytoplasmic (cytop) distribution (Dist) are arbitrary (see Methods). Minimal distribution was found at the basolateral membranes and was not further quantified.

% area: % of the CP showing staining

Figure 1a

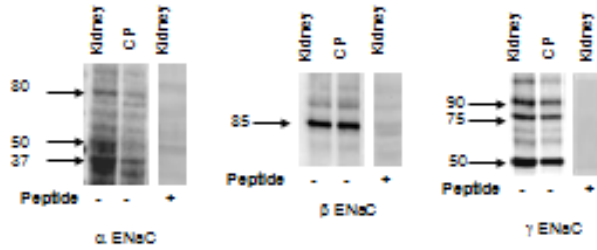


Figure 1b

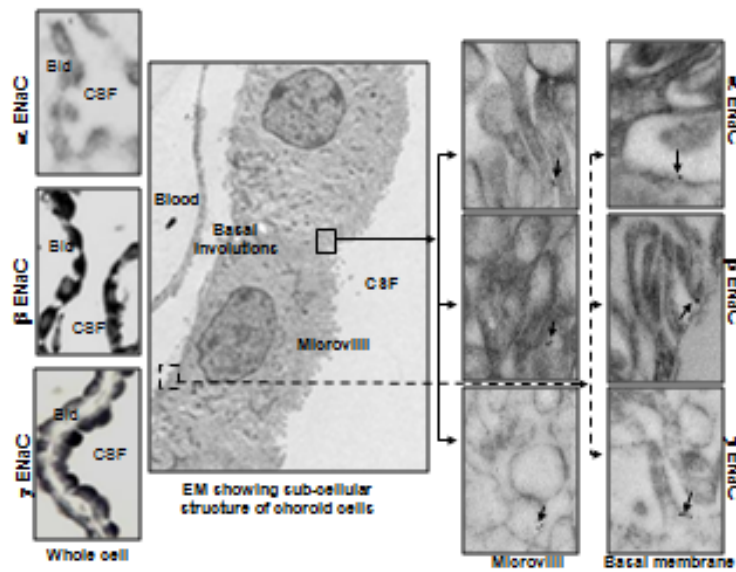


Figure 3.5–1: Presence of ENaC subunits in the choroid plexus of Wistar rats on regular salt diet. Fig 1a shows Western blots. The antibodies detected bands at ~80 and 37 kDa for α ENaC, ~85 kDa for β ENaC and ~90 kDa and 70 kDa for γ ENaC. No bands were detected in the presence of the immunizing peptides. Fig 1b shows ENaC immunoreactivity and subcellular localization in the choroid plexus of Wistar rats: Both the microvilli and cytoplasm show strong positive reaction. EM quantification shows 20-40% of subunits on the microvilli and 5-10% on the basolateral membrane.

Intensity of the Sodium Green (Fig 3.5-S3) was low under basal conditions with a calculated $[Na]_i$ of 35 ± 3 mM. Fluorescence intensity was much lower in the presence of 10 nM benzamil with $[Na]_i$ 16 ± 2 mmol and higher in the presence of 1 mM ouabain with $[Na]_i$ 60 ± 3 mM. Fluorescence intensity was similar to controls in the presence of both ouabain and benzamil with a calculated $[Na]_i$ of 39 ± 2 mM.

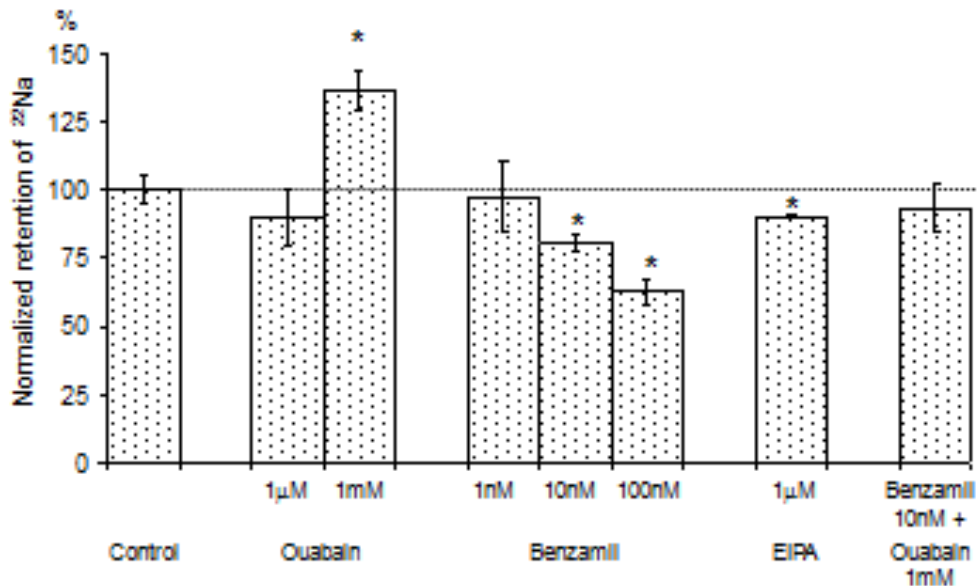


Figure 3.5–2: Effect of drugs on retained ^{22}Na by the choroid plexus of Wistar rats: 1 mM ouabain increased ^{22}Na content by ~40% ($n=5-8$). 1 nM benzamil did not have a significant effect but higher doses decreased ^{22}Na content in a dose dependent manner ($n=8-14$). The benzamil induced decrease was not seen in the presence of ouabain ($n=7$). 1 μ M EIPA caused a minimal decrease in ^{22}Na content ($n=3$). Values are means \pm SEM as percent changes versus control. * $p < 0.05$ vs control.

3.5.7.2.1 Effect of high salt diet on ENaC expression in Dahl rats

Abundance of α ENaC mRNA was similar in Dahl R and S but abundance of both 80 and 37 kDa protein fractions of α ENaC was higher in Dahl S than R. Relative abundance of

the 37 and 80 kDa fraction of α ENaC was similar in S and R rats (Table 3.5-1, Fig 3.5-3). Immunoreactivity to α ENaC showed low staining intensity and was similar in R and S rats. High salt diet did not affect α ENaC mRNA abundance, protein quantity and immunodensity in either strain (Table 3.5-1, Fig 3.5-3).

β ENaC mRNA was ~ 2 fold less whereas β ENaC protein abundance was similar and immunoreactivity greater in the apical membrane in the CP of S versus R rats (Table 3.5-1, Fig 3.5-3). High salt diet did not affect β ENaC mRNA or protein abundance in R and S rats and the higher immunoreactivity in the S rats persisted on high salt diet (Table 3.5-1, Fig 3.5-3).

Abundance of the mRNA, 90 kDa and 70 kDa bands of γ ENaC were similar whereas immunoreactivity to γ ENaC was higher in both apical membranes and cytoplasm of CPs of S versus R rats. High salt diet tended to lower ($p=0.08$) γ ENaC mRNA but did not affect protein abundance or distribution (Table 3.5-1, Fig 3.5-3). Figure 3.5-S4 shows the actual Western blots in Dahl rats on regular and high salt.

3.5.7.2.2 Effect of high salt diet on Na transport in the CP

On regular salt, the amount of retained ^{22}Na (Fig 3.5-4) was lower in the CP of Dahl S than Dahl R rats whereas $[\text{Na}]_i$ (Fig 3.5-5) was similar. Benzamil decreased retention of ^{22}Na and $[\text{Na}]_i$ to the same extent in both strains (Fig 3.5-4 and 3.5-5). Ouabain increased the amount of retained ^{22}Na by $\sim 40\%$ (Fig 3.5-4) in rats on regular salt diet but increased $[\text{Na}]_i$ only in Dahl R rats (Fig 3.5-5). High salt diet significantly increased $[\text{Na}]_i$ (Fig 3.5-5) and lowered the amount of retained ^{22}Na in R rats only (Fig 3.5-4). The decrease in retention of ^{22}Na and in $[\text{Na}]_i$ by benzamil was not affected by high salt diet in either strain. However, high salt attenuated the ouabain induced increase in ^{22}Na retention by

~50% in Dahl R and – if anything – enhanced the effect in S rats (Fig 3.5-4). The ouabain induced increase in $[Na]_i$ was also less in Dahl R on high salt, whereas in Dahl S this response remained absent (Fig 3.5-5). Dahl R and Wistar rats showed the same pattern of responses to high salt (Fig 3.5-S5).

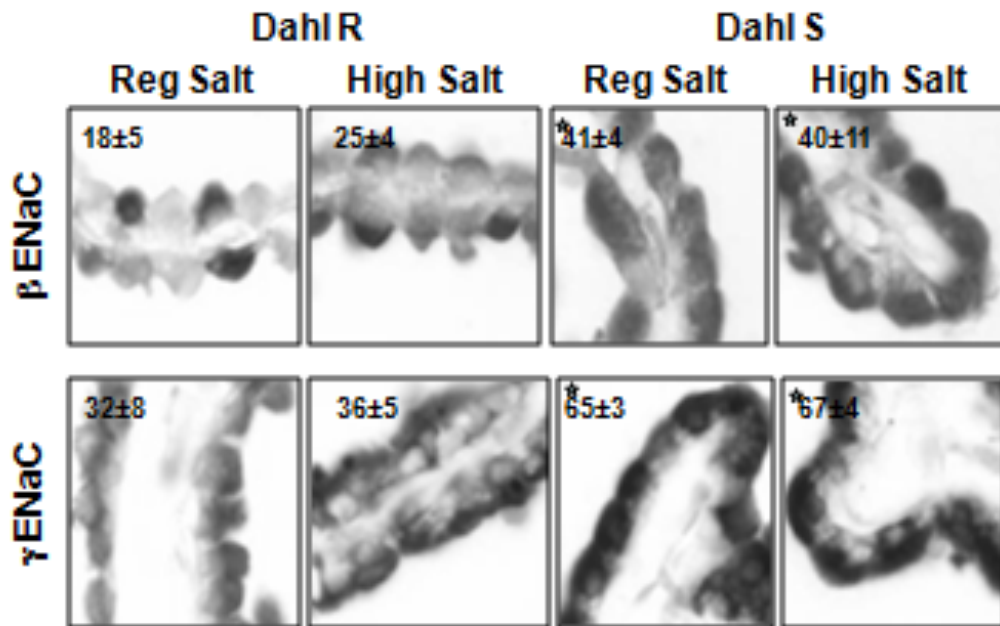


Figure 3.5–3: Immunoreactivity to β and γ ENaC in the choroid plexus of S and R rats on regular or high salt diet for 2 weeks: Immunoreactivity is greater in both the apical membrane and cytoplasm in S than R rats. High salt does not affect immunoreactivity in either strain ($n=3-5$). Insets show means \pm SEM for % of CP area stained. * $p<0.05$ S versus R rats. Immuno reactivity to α ENaC was low (see Table 3.5-1) and is not shown.

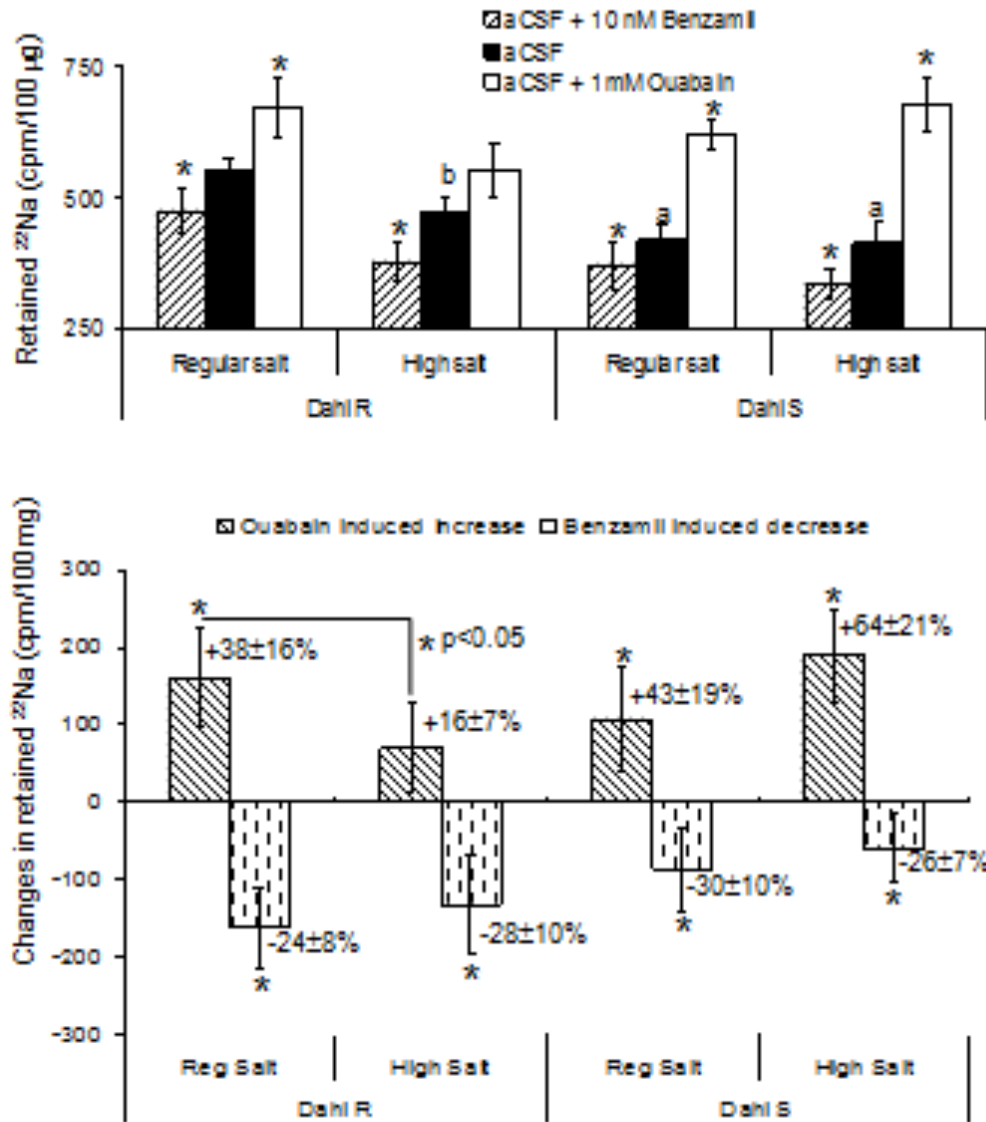


Figure 3.5-4: Effects ouabain and benzamil on ^{22}Na retention in the choroid plexus of Dahl R and S rats on regular or high salt diet. Top panel shows the absolute values, and the lower panel the absolute and percent changes (in brackets) by ouabain and benzamil. Values are means \pm SEM ($n=6-14/\text{group}$). * $p<0.05$ Benzamil or ouabain vs aCSF; ^a: $p<0.05$ aCSF Dahl S vs Dahl R; ^b: $p<0.05$ aCSF Dahl R, regular vs high salt

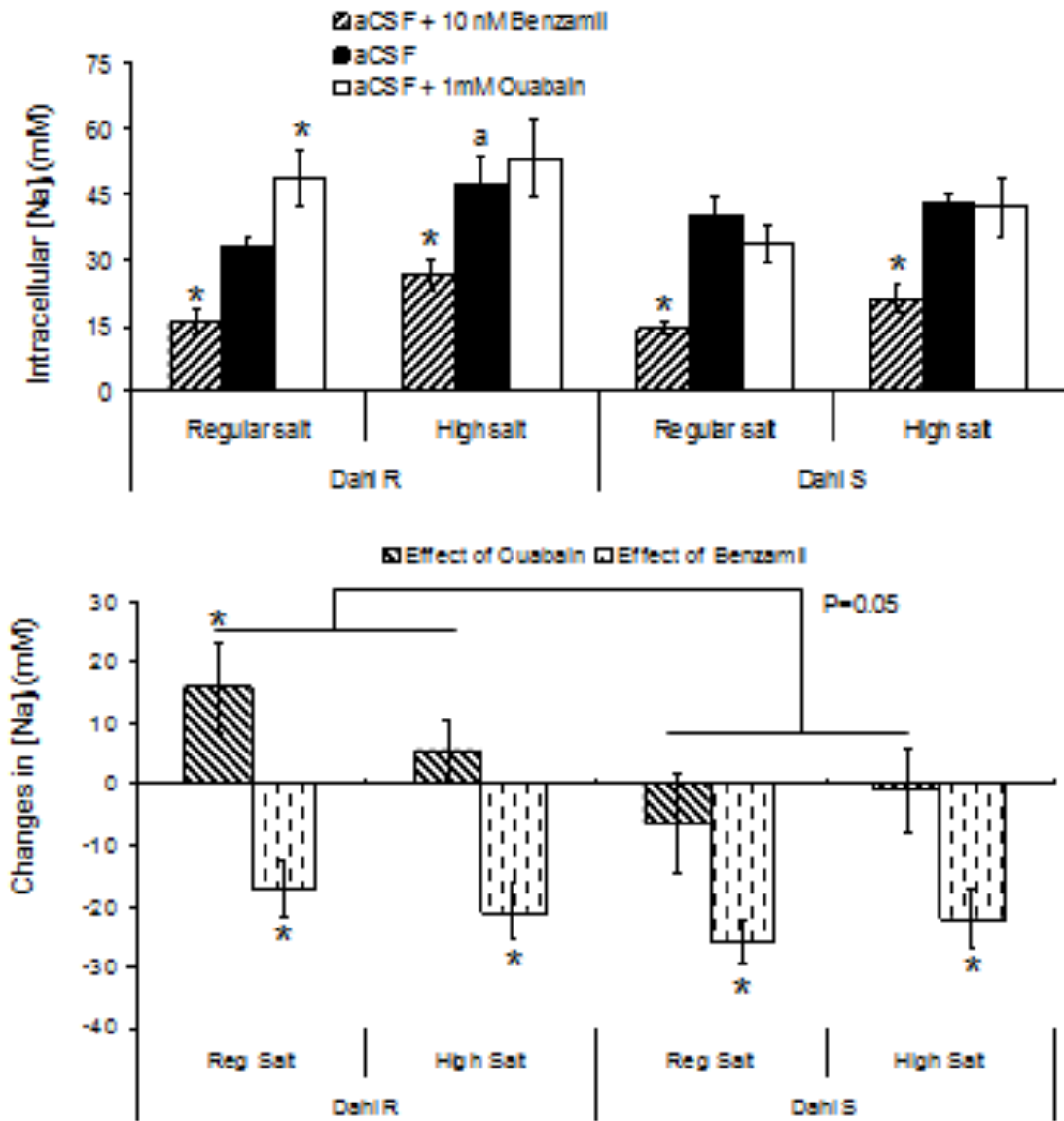


Figure 3.5-5: Effects of ouabain and benzamil on intracellular [Na⁺] ([Na_i]) in the choroid plexus of R and S rats on regular or high salt diet. Top panel shows the absolute values and the lower panel the absolute changes by ouabain and benzamil. Values are means ± SEM (n=5). *p < 0.05 Benzamil vs aCSF or ouabain vs aCSF ^ap < 0.05 Dahl R aCSF, high vs regular salt

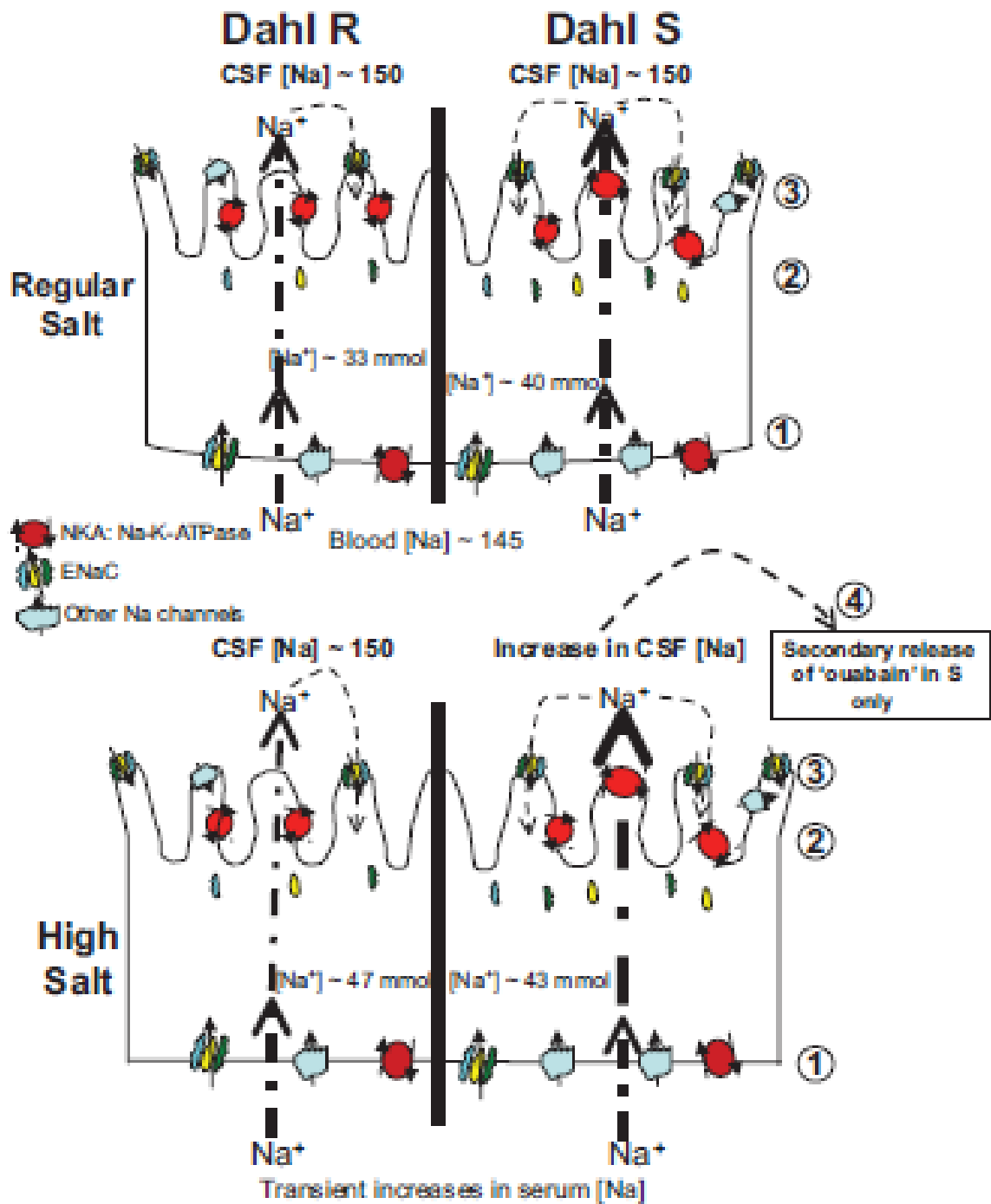


Figure 3.5–6: Schematic outline of the location of ENaC and $\text{Na}^+\text{K}^+\text{ATPase}$ in CP cells and their possible role in Na^+ transport across the CP in Dahl S and R rats on regular or high-salt diet. Top, CP of Dahl S and R rats on regular salt: (1) enhanced basal Na^+

influx and apical efflux in S vs R; (2) similar apical Na^+ efflux by Na^+K^+ ATPase into CSF in S and R rats; and (3) greater apical ENaC expression and activity (?) in S vs R rats. Bottom, Dahl S and R rats on high salt: (1) enhanced basal Na influx persists in S vs R rats; (2) apical Na^+K^+ ATPase activity persists in S but decreases in R rats; (3) ENaC expression and activity do not further increase in S rats despite increase in CSF $[\text{Na}^+]$ on high-salt diet; and (4) release of ouabain increases in S vs R rats to inhibit Na-K-ATPase in vivo and to attenuate further increases in CSF $[\text{Na}^+]$.

Figure S1

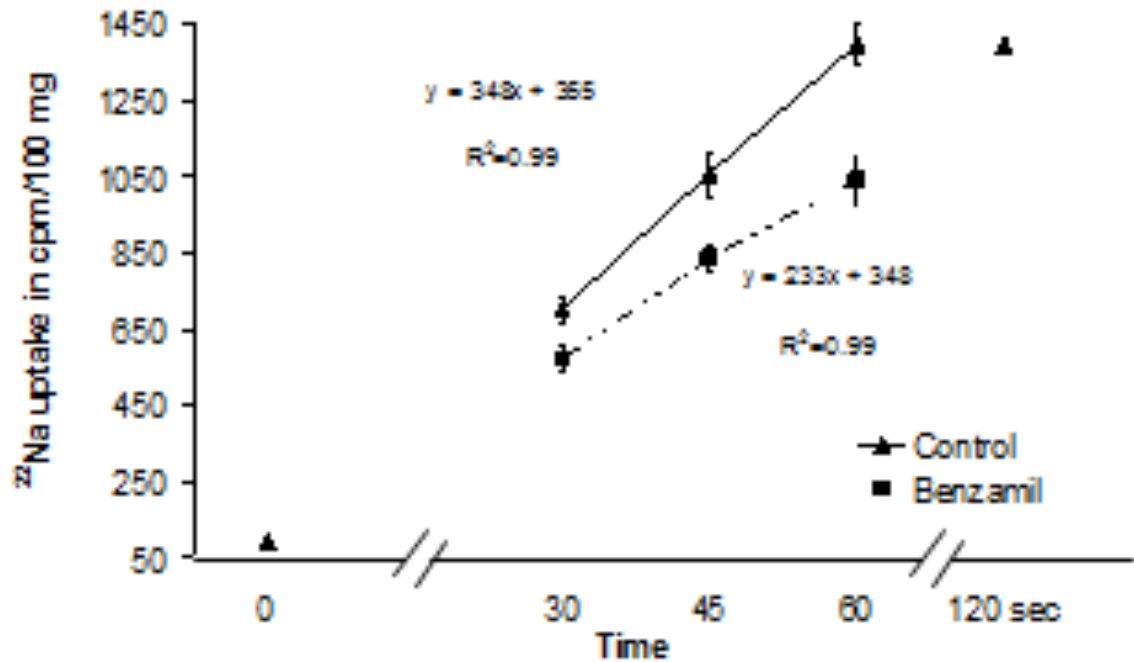


Figure 3.5-S1: Evaluation of ^{22}Na content in the choroid plexus (CP) over time: ^{22}Na content in CP increases with the duration of incubation and reaches a steady-state by 1 min. 10 nM benzamil decreases ^{22}Na content in the CP by ~25% suggesting that ENaC mediate Na influx into the CP. Values are mean \pm SEM ($n=7-8$ / time point) * $p < 0.05$ at each time point.

Figure S2

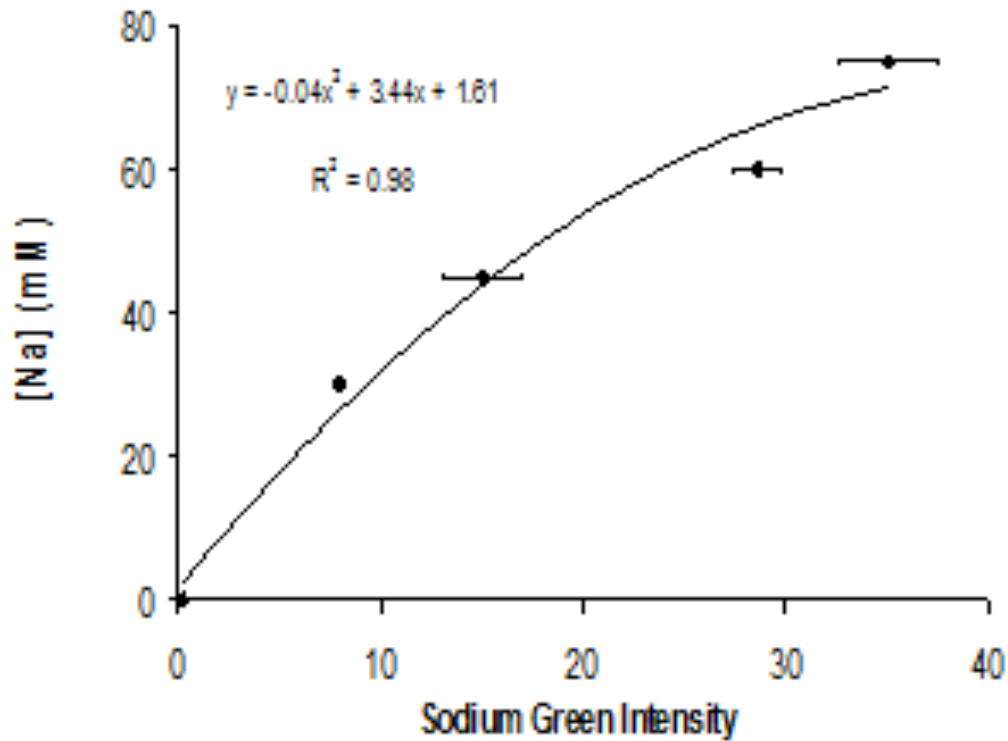
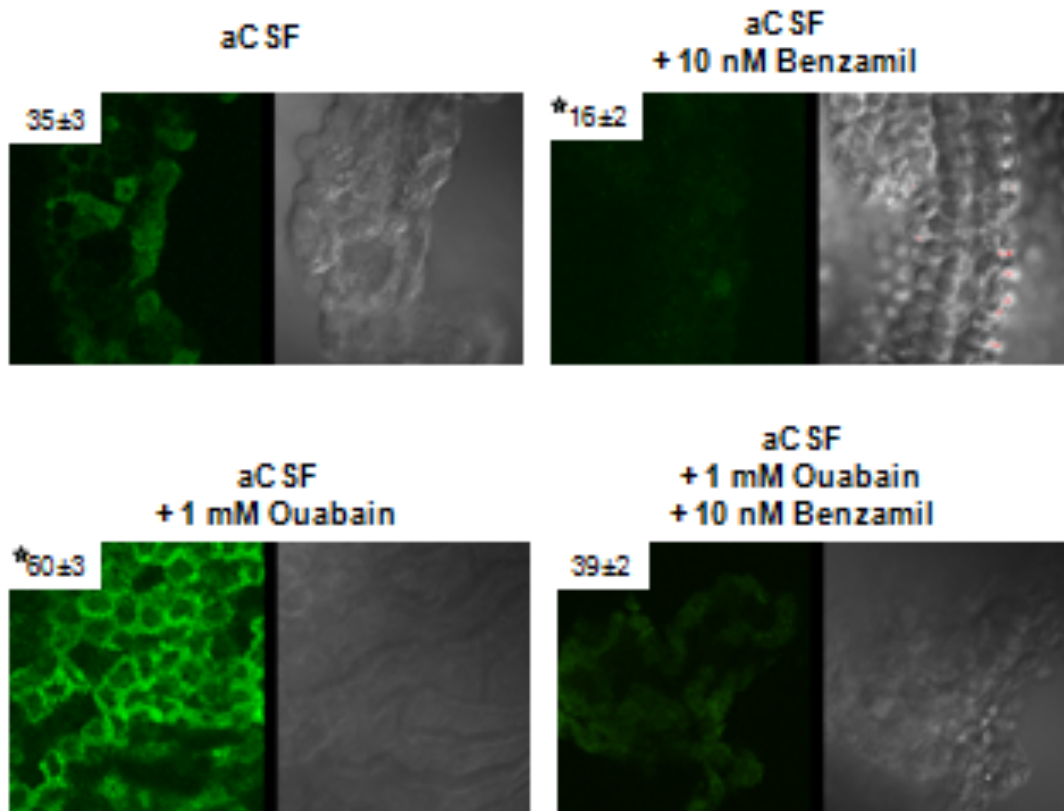


Figure 3.5-S2: Measurement of intracellular [Na] using Sodium Green fluorescence intensity: Intracellular [Na] increases in choroid cells incubated with Gramicidin according to the [Na] in the aCSF calibrating solutions with varying concentrations of Na. The polynomial equation thus derived was used to calculate $[Na]_i$. Values are mean \pm SEM ($n=4-6$ /sodium concentration).

Figure S3



*Figure 3.5-S3: Effect of drugs on Sodium Green fluorescence in the choroid plexus of Wistar rats: 10 nM benzamil decreased fluorescence to background levels. 1 mM ouabain increased fluorescence and offset the benzamil induced decrease. Brightfield images shown in the second and fourth panels demonstrate outline of the cells in the field ($n=6$). Calculated $[Na]_i$ in mM are shown in the insets. * $p < 0.05$ versus aCSF alone.*

3.5.8 DISCUSSION

The major findings of the current study are that in the epithelial cells of the CP ENaC is prominent on the apical microvilli and contributes to Na transport. Both benzamil blockable Na influx and ouabain-blockable efflux contribute to Na transport across the CP. On regular salt, the amount of retained ^{22}Na and ouabain induced increase in $[\text{Na}]_i$ are both lower in S rats. High salt diet increases $[\text{Na}]_i$ and decreases the amount of retained ^{22}Na and ouabain-blockable efflux only in R rats. The effects of benzamil were not dependent on strain or dietary salt. Figure 3.5-6 provides a schematic outline of the main locations of ENaC and $\text{Na}^+\text{K}^+\text{ATPase}$ in CP cells and their possible role in Na^+ transport across the CP in S versus R rats, as will discussed in detail.

3.5.8.1 Sodium transport in the CP

Benzamil dose dependently blocks a number of channels including ENaC, ASIC, NHE and NCX (Kleyman & Cragoe 1990). However, it has the highest potency for ENaC (Kleyman & Cragoe 1990). At the nanomolar concentration used in the current experiments, the benzamil blockade can be assumed to be limited to ENaC (Kleyman & Cragoe 1990). The specific NHE blocker EIPA at a high concentration of 1 μM decreased retained ^{22}Na only by ~10%, while benzamil at 10 nM caused a 25% decrease suggesting that a significant portion of the previously (Murphy & Johanson 1989b, Murphy & Johanson 1989a, Wright 1972b) reported inhibition of Na influx by amiloride is ENaC mediated. Inhibition of this ENaC mediated influx of Na^+ – while efflux continues – caused a marked decrease in $[\text{Na}]_i$, as measured by Sodium Green fluorescence.

The choroid cells in CP express the $\alpha 1$, $\beta 1$ and $\beta 3$ subunits of the $\text{Na}^+\text{K}^+\text{ATPase}$, while the blood vessels express all of the $\alpha 1$ - $\alpha 3$ and $\beta 1$ -3 subunits (Zlokovic et al. 1993a,

Zlokovic et al. 1993b). In the current study, 1 μ M ouabain which blocks the α 2 and α 3 subunits did not have a significant effect on retained ^{22}Na but 1 mM ouabain increased retention by 40%, and increased $[\text{Na}]_i$ by \sim 50%. This finding indicates that ouabain inhibits the efflux by blockade of the α 1 subunit of $\text{Na}^+\text{K}^+\text{ATPase}$ predominantly in the CP cells. Blockade of the enzyme by ouabain together with blockade of ENaC by benzamil resulted in unchanged ^{22}Na retention and $[\text{Na}]_i$ indicating that similar to renal epithelia (Loffing et al. 2001a) ENaC mediated influx and $\text{Na}^+\text{K}^+\text{ATPase}$ dependent efflux jointly contribute to Na transport across the choroid epithelial cells.

3.5.8.2 ENaC localization and expression in the CP

In absorbing epithelia of the kidneys and colon ENaC is expressed on the luminal surface where it mediates the final steps of Na re-absorption (Duc et al. 1994). The basolateral $\text{Na}^+\text{K}^+\text{ATPase}$ generates the electrochemical gradient required for ENaC mediated Na transport (Loffing et al. 2001a, Kunzelmann & Mall 2002). In the CP, $\text{Na}^+\text{K}^+\text{ATPase}$ is localized mainly on the microvilli and contributes to Na secretion into the CSF and its blockade clearly lowers CSF $[\text{Na}]$ (Huang et al. 2004). However, in contrast to the pattern in renal epithelia, we demonstrate by EM that in Wistar rats only 5-10% of ENaC is localized on the basolateral membrane and 15-30% are expressed on the microvilli. This pattern is similar to that in the ciliary body of the eye where ENaC appears to contribute to Na reabsorption from the aqueous humor (Civan et al. 1997, Mirshahi et al. 1999, Rauz et al. 2003a). Therefore ENaC might contribute to Na influx into choroid cells primarily from the CSF and to a less extent from the blood. Further studies are clearly required to elucidate the mechanisms that regulate cellular distribution and

function of ENaC in the CP, which may involve other functions (Brockway et al. 2005, Drummond et al. 2001, Jernigan et al. 2008) besides Na-transport.

Dahl and Wistar rats showed a similar pattern for ENaC localization. On regular salt diet, components of ENaC expression appeared to be higher in S versus R rats, i.e. higher protein abundance for α and higher staining intensity for β and γ subunits. This pattern was not influenced by high salt diet, and may indicate a higher ENaC activity in S versus R rats.

3.5.8.3 Na transport in the CP of Dahl R and S rats

Most interestingly, on regular salt retention of ^{22}Na was lower but $[\text{Na}]_i$ was similar in the CP of S versus R rats. Considering also that CSF uptake of iv ^{22}Na is enhanced in vivo in S versus R rats (Simchon et al. 1999), these findings may reflect enhanced Na transport across the CP. Such enhanced transport may be due to increased activity of $\text{Na}^+\text{K}^+\text{ATPase}$ associated with increased influx through Na-channels such as ENaC in S rats. However, the benzamil induced decreases in ^{22}Na uptake and in $[\text{Na}]_i$ were similar between the two strains. It appears that the higher abundance of ENaC at the apical membranes in S versus R rats does not lead to significantly higher activity and Na influx. Alternatively, blockade by benzamil of higher ENaC dependent influx at the apical membrane may be offset by a larger non-ENaC dependent influx at the basolateral membranes of S rats. Ouabain also similarly increased ^{22}Na retention in S and R rats, consistent with a similar role for $\text{Na}^+\text{K}^+\text{ATPase}$ in efflux in the two strains. However, ouabain increased $[\text{Na}]_i$ only in R rats and not at all in S rats. The increase in ^{22}Na retention but absence of an increase in $[\text{Na}]_i$ by ouabain in S rats may therefore reflect enhanced turnover of Na_i i.e. larger influx and efflux, the latter, not dependent on

$\text{Na}^+\text{K}^+\text{ATPase}$. Further studies are required to elucidate the actual mechanisms for this enhanced influx efflux.

3.5.8.4 High salt lowers $\text{Na}^+\text{K}^+\text{ATPase}$ mediated efflux in R but not S rats

High salt diet increased $[\text{Na}]_i$ by ~30% and decreased retained ^{22}Na by ~20% in R rats but caused no changes in S rats. In renal epithelia an increase in $[\text{Na}]_i$ would be compensated by greater activity of $\text{Na}^+\text{K}^+\text{ATPase}$ to maintain $[\text{Na}]_i$, cell volume and osmolarity. In the CP of Dahl R rats on high salt the opposite appears to occur. High salt diet markedly decreased the ouabain sensitive component of efflux and the further increase in $[\text{Na}]_i$. Such a decrease in $\text{Na}^+\text{K}^+\text{ATPase}$ activity in the CP of R rats on high salt diet might be a mechanism to prevent increases in CSF $[\text{Na}]$ and resultant sympatho-excitation and hypertension. The mechanism(s) responsible for this decrease in activity still need to be explored, and these studies may lead to new insights into the salt resistance of e.g. R rats, and by extension humans. In the current experimental design, any endogenous inhibitor of enzyme activity should have dissociated by the ~2 hours pre-incubation. Mechanisms causing a decrease in expression appear to be more likely.

In contrast to Dahl R, in S rats high salt failed to inhibit ouabain dependent Na transport and if anything caused a moderate increase. This enhanced activity or increased expression of the pump may reflect a primary abnormality of mechanisms regulating the pump in Dahl S rats, as compared to R or Wistar rats (Abdelrahman et al. 1995, Zicha et al. 2001). A persistent high activity of the pump would contribute to an increase in CSF $[\text{Na}^+]$, resulting in increased release of ouabain like compounds (“ouabain”) (Wang & Leenen 2002) to inhibit this increase in pump activity (Abdelrahman et al. 1995) and to blunt the increase in CSF $[\text{Na}^+]$ (Huang et al. 2004). Alternatively, CSF $[\text{Na}^+]$ may

increase through other mechanisms, and the resultant increase in concentration of “ouabain” would also inhibit the pump but also enhance $\text{Na}^+\text{K}^+\text{ATPase}$ expression in the CP through negative feedback (Hosoi et al. 1997). In the current experimental design, any endogenous ‘ouabain’ should have dissociated by the ~2 hours pre-incubation (Kent et al. 2004) thereby exposing the un-inhibited pump activity. In support of this second possibility, despite the somewhat larger inhibition of efflux by ouabain in S rats on high salt, ouabain still did not increase $[\text{Na}]_i$. This pattern of changes is consistent with this second possibility and the above stated conclusion of enhanced efflux of Na (into the CSF) in S rats, not dependent on $\text{Na}^+\text{K}^+\text{ATPase}$. Further studies including molecular biology approaches will provide further insights in this regard.

The present studies on Na-transport in the CP of Dahl rats appear to point to mechanisms contributing to an increase in CSF $[\text{Na}]^+$ and thereby possibly to hypertension in Dahl S on high salt diet. Dahl S clearly differed from Dahl R, whereas the latter responded similar to Wistar rats as another control strain. Further studies in congenic or consomic strains are needed to assess whether these CP mechanisms indeed track the CSF $[\text{Na}]$ and hypertension.

3.5.8.5 Perspectives

Being the prime source of CSF, Na transport mechanisms in the CP are important in the regulation of CSF $[\text{Na}]$. The current study suggests aberrant regulation of Na transport and of $\text{Na}^+\text{K}^+\text{ATPase}$ in the CP of S rats, that may contribute to the increase in CSF $[\text{Na}^+]$ in this strain on high salt diet. Future studies using microarrays and tissue-arrays in the early phase of high salt diet might elucidate the possible mediators of this abnormal Na

transport and identify new candidate genes causing the increase in CSF [Na] and hypertension in S rats on high salt diet, as well the salt resistance of Dahl R rats.

3.5.9 ACKNOWLEDGEMENTS

The authors are thankful to Dr Mark A. Knepper (National Institutes for Health) and Dr Lawrence G. Palmer (Cornell University) for generous gift of ENaC antibodies. We also thank Dr Bing Huang, Mr. Peter Ripstein, Ms Roselyn White, Ms Li Bi and Ms Junhui Tan for technical assistance and Ms Danielle Oja for her formatting assistance.

3.5.10 DISCLOSURES

M S Amin was supported by a Pfizer/Canadian Institutes of Health Research/Canadian Hypertension Society doctoral research award and an Ontario Graduate Scholarship in Science and Technology.

F. H. H. Leenen holds the Pfizer Chair in Hypertension Research, an endowed chair supported by Pfizer Canada, the University of Ottawa Heart Institute Foundation, and the Canadian Institutes of Health Research.

3.5.11 SOURCE OF FUNDING

This work was supported by Canadian Institutes of Health Research Operating Grant MT-13182.

3.6 MANUSCRIPT # 6: THE CENTRAL ROLE OF THE BRAIN IN SALT-SENSITIVE HYPERTENSION.

Bing S. Huang, Md Shahrier Amin and Frans H. H. Leenen

Right running title

The brain in salt-sensitive hypertension

Running title

Hypertension

3.6.1 Relevance to overall project

This publication was a review of the current literature regarding neural mechanisms of salt sensitive hypertension. The possible mechanisms were discussed and based on that we identified genes whose mutation could possibly contribute to salt induced hypertension in Dahl S rats.

3.6.2 Contribution

Responsible for writing the genetic mechanisms section of the review.

3.6.3 Abstract

Purpose of review: To integrate recent studies showing that abnormal Na^+ transport in the central nervous system plays a pivotal role in genetic models of salt-sensitive hypertension.

Recent findings: Na^+ transport–regulating mechanisms classically considered to reflect renal control of the blood pressure, i.e. aldosterone – mineralocorticoid receptors – epithelial sodium channels – NaKATPase have now been demonstrated to be present in the central nervous system contributing to regulation of cerebrospinal fluid $[\text{Na}^+]$ by the choroid plexus and to neuronal responsiveness of cerebrospinal fluid / brain $[\text{Na}^+]$. Dysfunction of either or both can activate central nervous system pathways involving ‘ouabain’ and angiotensin 1 (AT1) receptor stimulation. The latter causes sympathetic hyperactivity and adrenal release of marinobufagenin – a digitalis-like inhibitor of the α_1 Na^+K^+ ATPase isoform – both contributing to hypertension on high salt intake. Conversely, specific central nervous system blockade of mineralocorticoid receptors or ENaC prevents the development of hypertension on high salt intake, irrespective of the presence of a ‘salt-sensitive kidney’. Variants in the coding regions of some of the genes involved in Na^+ transport have been identified, but sodium sensitivity may be mainly determined by abnormal regulation of expression, pointing to primary abnormalities in regulation of transcription.

Summary: Looking beyond the kidney is providing new insights into mechanisms contributing to salt-sensitive hypertension, which will help to dissect the genetic factors involved and to discover novel strategies to prevent and treat salt-sensitive hypertension.

Keywords

Central nervous system, blood pressure, dietary salt, genetics, mineralocorticoid receptors
– epithelial sodium channels, ouabain

3.6.4 Introduction

High salt intake causes hypertension in salt-sensitive animals and humans. Classically, it is assumed that the hypertension enables abnormally functioning kidneys to excrete the high salt load. In genetically determined salt sensitivity, it is assumed that intrinsic changes in renal function lead to a defect in the kidneys' ability to excrete salt and an increase in blood pressure until sodium balance is restored. A rarely quoted, carefully conducted study by Morgan *et al.* (Morgan *et al.* 1990), however, demonstrated as long as 15 years ago that Dahl salt-sensitive rats with a salt-resistant kidney develop as severe hypertension on high salt intake as do Dahl salt-sensitive rats with a salt-sensitive kidney. Moreover, for some years it also has been clear that blockade in the central nervous system (CNS) of mechanisms leading to sympathetic hyperactivity prevent / reverse the hypertension in Dahl salt-sensitive rats on high salt intake without associated problems such as edema, indicating that the Dahl salt-sensitive kidney can maintain sodium and water homeostasis without hypertension and that perhaps the CNS is a primary determinant of salt-sensitive hypertension. How can high salt intake activate CNS mechanisms leading to hypertension? In the present review, we first discuss recent studies demonstrating the presence of Na⁺ transport regulation in the CNS by aldosterone–mineralocorticoid receptors (MR) – epithelial sodium channels (ENaC)–NaKATPase similar to that present in the kidneys. Secondly we report that this pathway in the CNS in genetic models of salt-sensitive hypertension is upregulated and mediates salt-sensitive hypertension; and thirdly we focus on recent animal studies evaluating variations in genes involved in Na⁺ transport mechanisms and their expression in the CNS.

3.6.5 Central nervous system mechanisms contributing to salt-sensitive hypertension

Central nervous system mechanisms discussed include high salt intake and $[\text{Na}^+]$ in plasma and cerebrospinal fluid (CSF); aldosterone–MR–epithelial sodium channels (ENaC) in the CNS; the activation of Na^+ -sensitive pathways in the CNS; and the role of CNS aldosterone, MR, and ENaC in salt sensitive hypertension.

3.6.5.1 High salt intake and $[\text{Na}^+]$ in plasma and cerebrospinal fluid

3.6.5.1.1 Plasma $[\text{Na}^+]$

High salt intake may cause small increases in plasma $[\text{Na}^+]$ that may (Fang et al. 2000) or may not (Huang et al. 2004) be detectable depending on the extent of water intake and timing of blood sampling relative to high salt intake. Sampling frequently over a 24-hour period, Fang and co-workers (Fang et al. 2000) showed that after a 4-day exposure to an 8% high-salt diet, plasma $[\text{Na}^+]$ increased by 3–4 mmol/l, similarly in spontaneously hypertensive rats (SHRs) and Wistar–Kyoto (WKY) rats during both awake and sleep periods. In young normotensive subjects, increasing salt intake from 10 to 250 mmol/day over 5 days increased plasma $[\text{Na}^+]$ by 3 mmol/l, and in both hypertensive and normotensive subjects changing salt intake from 350 to 10–20 mmol/day lowered plasma $[\text{Na}^+]$ to a similar extent by 3–4 mmol/l (He et al. 2005). Plasma $[\text{Na}^+]\uparrow$ may activate osmoreceptors located mainly in the gut and in circumventricular organs such as the organum vasculosum laminae terminalis and subfornical organ (McKinley & Johnson 2004) and thereby stimulate thirst and vasopressin release. Recent studies suggest that $[\text{Na}^+]\uparrow$ may also activate a sodium sensor, Na_x , a member of the subfamily of voltage-sensitive Na^+ channels located in the subfornical organ, and thereby control salt-intake

behaviour (Hiyama et al. 2004). No studies so far have shown involvement of the Na_x in sympathoexcitation or blood pressure regulation.

3.6.5.1.2 Cerebrospinal fluid $[\text{Na}^+]$

Recently we showed that a high-salt diet does not affect CSF $[\text{Na}^+]$ in ‘salt-resistant’ strains such as Wistar, WKY, and Dahl salt-resistant rats, but it increases CSF $[\text{Na}^+]$ by up to 5 mmol/l in Dahl salt-sensitive rats and SHR. This increase in CSF $[\text{Na}^+]$ preceded the increases in blood pressure and heart rate (Huang et al. 2004). In contrast, CSF $[\text{Na}^+]$ increased similarly by 2–3 mmol/l in patients with both salt-sensitive and non-salt-sensitive hypertension after 7 days on a high-salt diet (16–18 g/day) vs. a low-salt diet (1–3 g/day (Kawano et al. 1992). Increases in CSF $[\text{Na}^+]$ by 2 mmol/l or more are sufficient to increase firing rate of neurons in (e.g.) the paraventricular nucleus or supraoptic nucleus (Paxinos & Watson 1998a). A chronic 5-mmol/l increase in CSF $[\text{Na}^+]$ is more than sufficient to cause sympathetic hyperactivity and hypertension. In Wistar and Dahl salt-resistant rats, such an increase in CSF $[\text{Na}^+]$ increases blood pressure by ~15 mmHg (Huang et al. 1998, Huang et al. 2001b), but in Dahl salt-sensitive rats by ~35 mmHg (Huang et al. 2001b). Thus, whereas high salt intake increases plasma $[\text{Na}^+]$ similarly (if at all) in normotensive and hypertensive animals or humans, both Na^+ entry into the CSF on high salt intake and neuronal responsiveness to brain Na^+ can be enhanced in models of salt-sensitive hypertension but not in salt-resistant control strains (Fig. 3.6-1) (Huang et al. 2004, Huang et al. 2001b). Enhanced neuronal responsiveness was postulated for the patients with salt-sensitive essential hypertension mentioned above (Kawano et al. 1992).

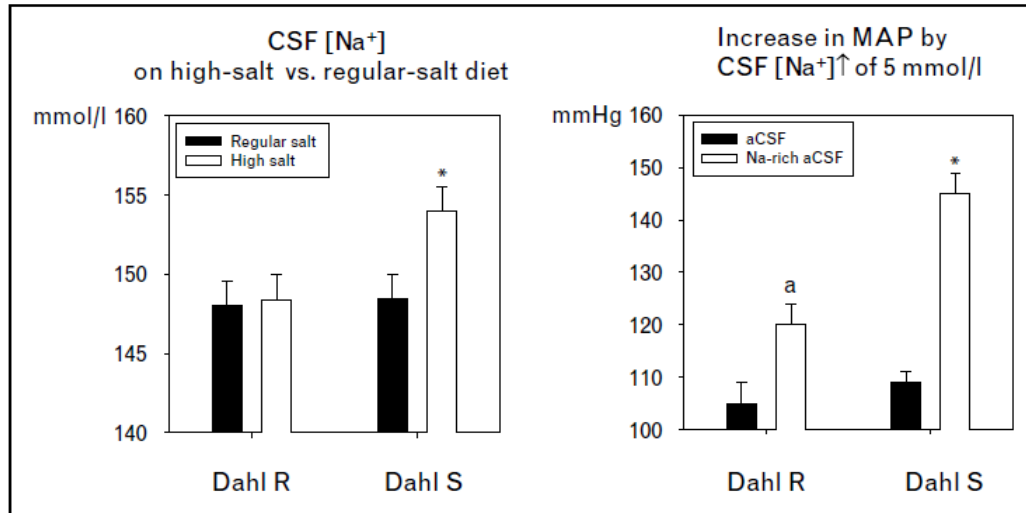


Figure 3.6–1: Response of CSF [Na⁺] to high salt diet and response of BP to a 5 mmol/L increase in CSF [Na⁺] in Dahl S versus R rats. Left panel: Cerebrospinal fluid (CSF) [Na⁺] in Dahl salt-sensitive (S) and salt-resistant (R) rats on high-salt or regular salt intake for 5–7 days. Right panel: Resting mean arterial pressure (MAP) in Dahl S and R rats on regular salt intake after intracerebroventricular infusion of aCSF or Na⁺-rich aCSF for 2 weeks. **P* < 0.05, vs. others. a: *P* < 0.05, vs. Dahl R with intracerebroventricular aCSF (Huang et al. 2001a, Huang et al. 2004).

3.6.5.2 Aldosterone–mineralocorticoid receptors–epithelial sodium channels in the central nervous system

Recent studies indicate that the MR–ENaC Na⁺ transport-regulating mechanism is also present in the brain, and binding of aldosterone to the MR in the CNS activates ENaC, which favours Na⁺ entry into the CSF and brain interstitium and may increase excitability of neurons involved in cardiovascular regulation (Fig. 3.6-2) (Huang et al. 2004, Huang et al. 2001b).

Mineralocorticoid receptors are abundantly present in different brain areas such as the choroid plexus, ventricular ependyma, and neurons in nuclei involved in cardiovascular regulation such as the paraventricular nucleus and the median preoptic nucleus (Amin et al. 2005). All the enzymes needed for aldosterone biosynthesis exist in the brain (Stromstedt & Waterman 1995) and aldosterone remains present in the brain after adrenalectomy (Gomez-Sanchez et al. 2005a). In general MR are not selective for aldosterone, and both aldosterone and corticosterone can bind to MR. Specificity can be conferred by ligand-specific activators as well as by 11 β -hydroxysteroid dehydrogenase type 2 (11 β -HSD2). The latter is found in (e.g.) periventricular tissue (Hughey et al. 2004b).

Recently we demonstrated that ENaC is also abundantly present in different brain areas and is coexpressed with MR in the choroid plexus and neurons in (e.g.) the paraventricular nucleus, supraoptic nucleus, and median preoptic nucleus (Amin et al. 2005). The choroid plexus is a major regulator of CSF production as well as CSF [Na⁺], which tends to be 2–3 mmol/l higher than plasma [Na⁺] (Huang et al. 2004). An increase in ENaC activity in the choroid plexus may favour Na⁺ entry into CSF and increase CSF [Na⁺]. Na⁺ transport into the CSF also appears to depend on the NaKATPase activity at the CSF side of the choroid plexus. Central infusion of ouabain in Wistar rats to inhibit the Na⁺K⁺ATPase decreases CSF [Na⁺] markedly (Huang et al. 2004). Recent studies suggest that endogenous ouabain-like compounds (OLCs) are one of the regulators of CSF [Na⁺] (see ‘Role of central nervous system, aldosterone, mineralocorticoid receptors, and epithelial sodium channels in salt sensitive hypertension’). As a steroid, OLC is present in the mammalian brain. Hauptert and coworkers (Murrell et al. 2005) recently

examined expression of genes possibly involved in OLC synthesis pathways and demonstrated the existence of a unique steroid synthesis circuit in the hypothalamus for local synthesis of OLCs. Adducin is a ubiquitously expressed tetrameric cytoskeletal protein composed of α / β or α / γ heterodimers and stimulates NaKATPase activity by increasing the apparent ATP affinity to Na⁺K⁺ATPase (Ferrandi et al. 1999). Besides being present in the kidney, all three adducin subunits are also present in the hypothalamus (Sakai et al. 2000). Whether adducin regulates NaKATPase in the CNS has not yet been studied, but this is possible considering that γ -adducin coimmunoprecipitates with $\alpha_{2/3}$ Na⁺K⁺ATPase from neurons of both SHR and WKY rats (Sakai et al. 2000).

3.6.5.3 Activation of Na⁺-sensitive pathways in the central nervous system

The increase in CSF [Na⁺] by high salt intake in Dahl salt-sensitive rats can be mimicked by intracerebroventricular infusion of Na⁺-rich artificial cerebrospinal fluid (aCSF). Na⁺-rich aCSF administered intracerebroventricularly (Macleod et al. 2003, Huang et al. 1998) or into nuclei such as the paraventricular nucleus (Jin et al. 2001) increases sympathetic activity and blood pressure. The sympathetic and blood pressure responses are elicited by the increased CSF [Na⁺] *per se*, and not the associated increase in osmolarity, because the same increase in CSF osmolality by (e.g.) mannitol does not induce sympathetic and pressor responses (Jin et al. 2001). Intracerebroventricular infusion of aldosterone enhances the sympathoexcitatory and pressor responses to a small increase in CSF [Na⁺] (Huang et al. 2005, Wang et al. 2003a). Central infusion of benzamil to block ENaC (Wang et al. 2003a) or of an MR antagonist (Macleod et al. 2003) prevents the excitatory responses to increased CSF [Na⁺] and aldosterone. These

findings indicate that both MR activation and ENaC mediate excitatory responses to CSF $[\text{Na}^+]_{\uparrow}$ and that MR activation activates the CNS pathways through ENaC.

Modulating the $\text{Na}^+\text{K}^+\text{ATPase}$ in the CNS by an endogenous regulator may affect (on the one hand) Na^+ transport across the choroid plexus and thereby CSF $[\text{Na}^+]_{\uparrow}$ with (de)activation of the Na^+ -sensitive pathways in the CNS, and (on the other hand) affect Na^+ and Ca^{2+} transport across neuronal membranes and thereby neuronal excitability. Indeed, central infusion of ouabain to inhibit the $\text{Na}^+\text{K}^+\text{ATPase}$ decreases CSF $[\text{Na}^+]_{\uparrow}$ and in parallel causes sympathoexcitation and hypertension (Huang et al. 2004). An increase in CSF $[\text{Na}^+]_{\uparrow}$ by intracerebroventricular infusion of Na^+ -rich aCSF or by high salt intake in Dahl salt-sensitive rats or SHR increases hypothalamus OLC. This increase in OLC appears to be a physiological response to prevent a further increase in CSF $[\text{Na}^+]_{\uparrow}$ (see ‘Role of central nervous system, aldosterone, mineralocorticoid receptors, and epithelial sodium channels in salt sensitive hypertension’). In parallel, OLC plays an essential role in the CNS pathways activated by CSF $[\text{Na}^+]_{\uparrow}$, because blockade of OLC with intracerebroventricular antibody Fab fragments binding OLC with high affinity (Macleod et al. 2003) prevents the sympathetic hyperactivity and hypertension. CSF $[\text{Na}^+]_{\uparrow}$ increases OLC in the hypothalamus through MR–ENaC, given that the response is blocked by intracerebroventricular infusion of spironolactone (Macleod et al. 2003) or benzamil (Wang & Leenen 2003). These MR and ENaC may be located on OLC-producing neurons in (e.g.) the supraoptic or paraventricular nucleus.

Downstream to the activation of MR–ENaC–OLC by CSF $[\text{Na}^+]_{\uparrow}$, angiotensin type 1 receptor stimulation appears to mediate these responses, because intracerebroventricular infusion of losartan prevents sympathoexcitatory and pressor responses induced by CSF

[Na⁺]↑ or ouabain (Huang & Leenen 1999, Huang et al. 1998). In addition, in Wistar rats, intracerebroventricular infusion of Na⁺-rich aCSF increases angiotensin-converting enzyme and angiotensin 1 receptor densities in several nuclei implicated in cardiovascular regulation. These increases are prevented by blockade of brain OLC with intracerebroventricular antibody Fab fragments (Macleod et al. 2003). Recent studies suggest that responses to angiotensin II in the CNS are mediated by intracellular mechanisms involving superoxide (O₂⁻) as a signalling intermediate. In mouse neuroblastoma, neuro-2A cells or cultured neurons of circumventricular organs, angiotensin II increases intracellular O₂⁻ production and [Ca²⁺], which are prevented by overexpression of cytoplasm-targeted superoxide dismutase or losartan (Yau et al. 1999, Ruiz-Arribas et al. 1995). Intracerebroventricular infusion of angiotensin II increases renal efferent sympathetic nerve activity, blood pressure, and norepinephrine secretion from the posterior hypothalamus, and these responses are all prevented by intracerebroventricular infusion of superoxide dismutase mimetics (Ruiz-Arribas et al. 1995, Sanchez del Pino et al. 1995).

3.6.6 Role of central nervous system aldosterone, mineralocorticoid receptors, and epithelial sodium channels in salt-sensitive hypertension

In Dahl salt-sensitive but not salt-resistant rats, high salt intake increases CSF [Na⁺] (Huang et al. 2004), OLC in the hypothalamus (Wang & Leenen 2002), sympathetic activity, and blood pressure (Huang & Leenen 1999, Wang & Leenen 2002). In Dahl salt-sensitive rats on high salt, blockade of brain OLC by intracerebroventricular infusion of Fab fragments un-inhibits the NaKATPase, thereby facilitates Na⁺ transport into the

CSF, and causes a further increase in CSF $[Na^+]$ (Huang et al. 2004) (Fig. 3.6-2). It appears that as a negative feedback, an increase in brain OLC following high salt intake in Dahl salt-sensitive rats attenuates the increase in CSF $[Na^+]$ due to abnormal Na^+ transport across the choroid plexus. Despite this further increase in CSF $[Na^+]$, central infusion of Fab fragments also prevents the sympathoexcitation and hypertension in Dahl salt-sensitive rats on high salt intake (Huang & Leenen 1998), substantiating the dual role of OLC in the CNS. The cellular mechanisms for these functional abnormalities in Na^+ transport by the choroid plexus have not yet been clarified. In Dahl salt-sensitive rats on high salt intake, blockade of ENaC by intracerebroventricular infusion of benzamil prevents the increase in CSF $[Na^+]$ (Huang BS, Leenen FHH, unpublished data), implicating increased ENaC activity in the choroid plexus of Dahl salt-sensitive rats. In parallel, benzamil prevents the increases in blood pressure and heart rate (Wang & Leenen 2002).

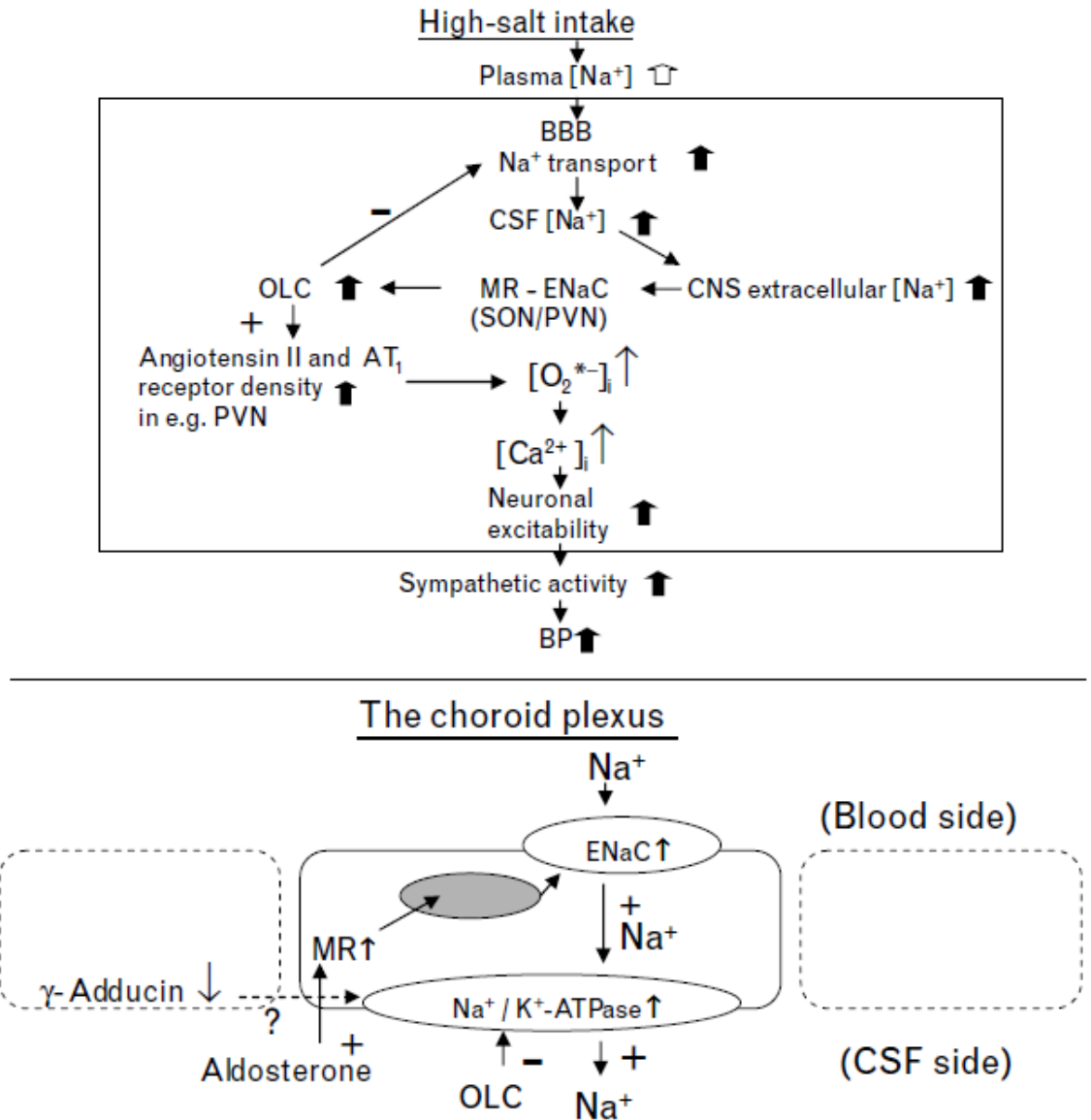


Figure 3.6–2: Outline of putative $[Na^+]$ transport mechanisms in the central nervous system (CNS) contributing to sympathetic hyperactivity and hypertension in salt-sensitive rats on high-salt intake. In these genetic strains on high-salt intake, Na^+ transport into cerebrospinal fluid (CSF) is enhanced and $[Na^+]$ in CSF and brain interstitium is increased. For unknown reasons, binding of locally produced mineralocorticoid (MR) (e.g. aldosterone) to MR activates endothelial sodium channels (ENaC) as well as the $Na^+K^+ATPase$ activity in the choroid plexus; ENaC in neurons in (e.g.) the

paraventricular (PVN) and supraoptic (SON) nuclei, resulting in an increase in intracellular $[Na^+]$ and $[Ca^{2+}]$; the latter increases neuronal excitability. Both lead to an increase in ouabain-like compound (OLC) release possibly from the SON. OLC inhibits the $Na^+K^+ATPase$ activity in the choroid plexus and prevents a further increase in CSF $[Na^+]$ and activates the renin–angiotensin system. As a result, in spontaneously hypertensive rats and Dahl salt-sensitive rats, high-salt intake increases sympathetic outflow and blood pressure (BP) (Huang et al. 2001a, Huang et al. 2004).

No studies so far have assessed aldosterone synthesis and release in specific brain nuclei or CSF in Dahl salt-sensitive vs. salt-resistant rats. As a steroid, aldosterone synthesis requires 3β -steroid dehydrogenase to convert pregnenolone to progesterone. Gomez-Sanchez *et al.* (Gomez-Sanchez et al. 2005b) recently showed that intracerebroventricular infusion of trilosan, an inhibitor of 3β -steroid dehydrogenase, prevents as well as reverses salt-sensitive hypertension in Dahl salt-sensitive rats. Intracerebroventricular infusion of the specific MR blocker RU28318 also prevents the development of hypertension in Dahl salt-sensitive rats on high salt intake (Gomez-Sanchez et al. 1992). Similarly, intracerebroventricular injection of RU28318 decreases blood pressure in a dose-dependent manner in SHRs on high salt intake (Rahmouni et al. 2001). These findings suggest that increased local production of an MR agonist – likely aldosterone – in the CNS contributes to central mechanisms of salt-sensitive hypertension.

Altogether, the above studies support the concept that increased MR–ENaC activity in the CNS contributes to salt-sensitive hypertension. This response appears opposite to MR–ENaC regulation in the kidneys, where high salt intake lowers ENaC activity. How

and where in the CNS MR and ENaC increase in response to high salt intake in Dahl salt-sensitive rats have not yet been studied.

On regular salt, hypothalamus OLC content is higher in SHR vs. WKY rats (Leenen et al. 1993a) as well as in Milan hypertensive vs. normotensive rats (Ferrandi et al. 1997). In SHRs on regular salt intake, the OLC appears to be of little functional consequence given that blockade of OLC by intracerebroventricular infusion of antibody-Fab fragments has no effects on blood pressure (Huang & Leenen 1996). On high salt intake in Dahl salt-sensitive rats or SHRs but not in Dahl salt-resistant or WKY rats, hypothalamus OLC content increases (Leenen et al. 1993a, Wang & Leenen 2002), and blockade of OLC with intracerebroventricular Fab fragments blocks the sympathetic hyperactivity and hypertension in both strains (Huang & Leenen 1996, Huang & Leenen 1998). In Dahl salt-sensitive rats on high salt, the increase in hypothalamic OLC is prevented by blockade of ENaC with intracerebroventricular infusion of benzamil (Wang & Leenen 2002). These studies indicate that in Dahl salt-sensitive rats, high salt intake increases OLC in the CNS through ENaC-dependent pathways either in the choroid plexus or OLC-producing neurons. The possible involvement of OLC in Na⁺ transport pathways in the CNS of Milan hypertensive rats on regular or high salt intake has not yet been explored.

Recent studies suggest that OLC is involved in CNS pathways leading to sympathetic hyperactivity as well as to adrenal synthesis and release of marinobufagenin, an endogenous bufadienolide digitalis-like inhibitor of the α_1 -NaKATPase isoform (Fedorova et al. 2005). In rats, marinobufagenin causes both natriuresis and vasoconstriction. Peripheral administration of an anti-marinobufagenin antibody lowers

blood pressure in Dahl salt-sensitive rats on high salt (Fedorova et al. 2002). In Dahl salt-sensitive rats, acute Na⁺ loading increases blood pressure, pituitary OLC, plasma norepinephrine, and marinobufagenin excretion (Fedorova et al. 2005). Intravenous administration of OLC antibody prevents these responses, suggesting that OLC contributes to both sympathoexcitation and marinobufagenin release (Fedorova et al. 2005).

Regarding possible other regulators of Na⁺-sensitive pathways in the CNS, the role of adducin for salt-sensitive hypertension in e.g. Dahl salt-sensitive or Milan hypertensive rats has not yet been assessed. Perfusion with a γ -adducin-specific antibody increases neuronal firing rate in hypothalamus and brainstem neuronal cultures. Incubation with angiotensin II increases firing associated with decreased endogenous γ -adducin (Sakai et al. 2000). Hypothalamic γ -adducin is ~70% lower in hypertension induced by subcutaneous infusion of angiotensin II or by DOCA salt (Yang et al. 2004). Hypothalamic and brainstem γ -adducin expression is ~50% lower in SHR vs. WKY rats (Sakai et al. 2000). Altogether, these findings suggest that increased activity of brain renin–angiotensin system (RAS) may cause a decrease in γ -adducin in the hypothalamus, possibly resulting in decreased NaKATPase activity and thereby enhanced basal firing rates in neurons involved in cardiovascular regulation.

3.6.7 Genetic determinants of salt sensitivity with focus on the mineralocorticoid receptor – epithelial sodium channels – renin-angiotensin system pathway

To date variants in several genes have been identified, which can be related to the pathogenesis of salt-sensitive hypertension (Beeks et al. 2004) – most along the

mineralocorticoid–RAS pathway. One of the recent strategies in discovering genetic variants has been the integrated genomic-transcriptomic approach in which it is assumed that genes that are both differentially expressed in a relevant tissue and that map to a hypertension-related quantitative trait locus (QTL) are likely to contribute to the hypertension. For salt-induced hypertension, these studies have so far focused only on expression in the kidneys. Evaluation of genes that are both differentially expressed in the CNS and map to a QTL for salt-induced hypertension may provide new insights. Here we focus mainly on recent animal studies evaluating variations in genes involved in Na⁺ transport mechanisms that could alter the neural setpoint of blood pressure on high salt intake.

3.6.7.1 Cytochrome P450 enzymes

The protein products of the genes *CYP11B1* (11- β -hydroxylase) and *CYP11B2* (aldosterone synthase) mediate the final steps of aldosterone synthesis. Both are located on chromosome 7 with similar (95%) intron / exon structure but different 5' upstream promoters. A QTL in this region of the chromosome harboring *CYP11B1* (but excluding *CYP11B2*) is associated with a 23-mmHg systolic blood pressure variation between Dahl salt-sensitive and salt-resistant rats on 2% NaCl diet (Cicila et al. 2001). The Dahl salt-sensitive rats have the same alleles for these genes as the Sprague–Dawley parent rat strain, whereas Dahl salt-resistant rats have mutations that cause five-amino-acid and two-amino-acid substitutions in 11- β -hydroxylase and aldosterone synthase, respectively. These decrease the effectiveness of 11- β -hydroxylase to produce 18-OH-deoxycorticosterone (DOC) by twofold (Matsukawa et al. 1993) and increase the rate of conversion of 11-DOC to aldosterone by aldosterone synthase almost 1000-fold

(Matsukawa et al. 1993). Low-salt diet increases and high-salt diet decreases aldosterone synthase mRNA in the adrenals to the same extent in Dahl salt-sensitive and salt-resistant rats, without affecting 11- β -hydroxylase (Matsukawa et al. 1993). The enzymes are also expressed in the brain. Low sodium increased aldosterone synthase expression in the adrenal, but dietary salt had no effect on the mRNA expression in the hypothalamus or brainstem of WKY rats (Ye et al. 2003). This does not exclude changes in expression in specific nuclei, however. Regulatory sequences in the genes' upstream regions regulating expression of the enzymes have not yet been studied. The increasing evidence for extra-adrenal aldosterone production and its significant nonclassic actions in (e.g.) heart and brain calls for evaluation of the regulation of 11- β -hydroxylase and aldosterone synthase in these tissues.

3.6.7.2 Other steroid-metabolizing enzymes

Identification of other steroid-metabolizing enzymes such as those involved in the synthesis of endogenous OLC is gaining new focus. Using bioinformatics, a putative biosynthetic pathway for ouabain was constructed recently and the candidate genes encoding enzymes in this pathway identified from sequence databases (Murrell et al. 2005). cRNA of seven of the enzymes could be detected by microarray chips. Two of these, encoding P450 side-chain cleavage and Δ 5-3 β -hydroxysteroid dehydrogenase isomerase – which act in early steps of steroid biosynthesis – showed fourfold to fivefold increased expression in the hypothalamus of Milan hypertensive compared with the Milan normotensive strain on a regular salt diet. Milan hypertensive rats also have 10-fold higher levels of OLC in the hypothalamus (Ferrandi et al. 1992). In response to high salt, OLC levels in the hypothalamus increase twofold in Dahl salt-sensitive but not salt-

resistant rats (Wang & Leenen 2002). Regulation of these genes, particularly in response to a high-salt diet, and possible genetic variants have not yet been studied.

3.6.7.3 Salt-inducible kinase

A serine / threonine protein kinase – salt-inducible kinase (SIK) – was recently identified from adrenals of Sprague–Dawley rats on a high-salt diet (Wang et al. 1999). A QTL on chromosome 20p12 includes the SIK gene and in congenic SHR–Lewis rats contributes 20–30 mmHg to the increase in blood pressure on a high-salt diet (Rapp 2000), (Kunes & Zicha 1994) SIK phosphorylates the transducer of regulated CRE (cAMP response element) binding protein (CREB) activity (TORC2) – a coactivator of CREB – which then loses its binding capacity to CREB. This represses CREB activity and adrenocorticotropin-dependent expression of steroidogenic enzymes. CREs are located in promoter regions of (e.g.) *CYP11B2*, where SIK prevents cAMP-dependent expression of reporter gene (Okamoto et al. 2005), (Katoh et al. 2004). Its regulation and possible genetic variants have not yet been studied.

3.6.7.4 Mineralocorticoid receptor

Rat chromosome 19 harbors two relevant genes – *MR* (19q11) and *11 β HSD2* (19q11-12). A Y73C substitution of *MR* has been reported in the Brown-Norway rat that increases transactivation of MR by aldosterone twofold (Marissal-Arvy et al. 2004). The blood pressure response to aldosterone or high-salt diet was not studied in these rats. Whether similar mutations of *MR* are present in other strains has not yet been reported, nor whether genetic variants exist in *11 β HSD2*.

3.6.7.5 Serum and glucocorticoid regulated kinase 1

The SGK1 locus on chromosome 1p12 maps to blood pressure QTL region 2 deduced from (Dahl S × Lewis) rats (Farjah et al. 2003). The full-length SGK1 cDNA sequences of Dahl salt-sensitive rats are the same as those of the parental Sprague–Dawley. In Dahl salt-sensitive rats, however, a high-salt diet causes a twofold rise in renal SGK1 levels, in contrast to the 50% decrease in Sprague–Dawley (Farjah et al. 2003). Aldosterone increased SGK1 mRNA by threefold in Dahl salt-resistant but not in Dahl salt-sensitive rats (Aoi et al. 2006), suggesting impaired regulation by aldosterone in Dahl salt-sensitive rats. It is therefore possible that the glucocorticoid response elements and transcription factor binding sites upstream the SGK1 start codon harbor mutations imparting abnormal regulation in Dahl salt-sensitive rats. SGK1 expression is abundant in the brain, but its response to high-salt diet has not yet been studied.

3.6.7.6 Epithelial sodium channel

In Liddle's syndrome truncations, frameshift or missense mutations affecting ENaC β and γ prevent interaction with the Nedd4 proteins, leading to enhanced surface expression and activity. The genes for ENaC are located on chromosomes 4q42 (α) and 1q36-q41 (β and γ). The latter overlies known blood pressure QTLs (Rapp 2000). Sequence analyses, however, did not reveal relevant mutations in the coding regions of the three ENaC genes in genetically hypertensive rat strains including Dahl salt-sensitive rats (Grunder et al. 1997, Huang et al. 1995, Kreutz et al. 1997). In contrast, ENaC subunits are abnormally regulated in kidneys of Dahl salt-sensitive rats and SBH (Sabra hypertensive) rats. In kidneys of Sprague–Dawley or Wistar rats, low-salt diet increases mRNA abundance of ENaC α but has no effect on ENaC β or γ mRNA (Stokes & Sigmund 1998). High

sodium, conversely, decreases ENaC α mRNA in the kidney without affecting ENaC β or γ (Lim et al. 2004, Stokes & Sigmund 1998). Conversely, in the kidneys of Dahl salt-sensitive rats, high-salt diet for 4 weeks increased ENaC α mRNA by 2.5-fold; ENaC β and γ were not studied (Aoi et al. 2004). Aldosterone increased ENaC α mRNA in both Dahl salt-sensitive and salt-resistant rats by threefold but decreased ENaC β and γ mRNA levels in Dahl salt-sensitive rats with no effect in Dahl salt-resistant rats (Aoi et al. 2006). Expression of upstream kinases such as phosphatidylinositol-dependent kinase 1 or extracellular signal related kinase 1 / 2, which might affect SGK1 activity and thereby ENaC expression, was not altered. In kidneys of Sabra salt-resistant rats, expression of ENaC β and γ was not altered by high-sodium diet but was decreased in SBH rats; ENaC α levels were not affected in either strain (Nicco et al. 2003). Na^+ transport in renal inner medullary cells and across the choroid plexus is enhanced in Dahl salt-sensitive vs. salt-resistant rats (Husted et al. 1996, Simchon et al. 1999), which may relate to intrinsically higher ENaC activity in Dahl salt-sensitive rats. Considering the pivotal role of ENaC in the CNS for salt-sensitive hypertension, regulation of ENaC in the CNS needs to be studied.

3.6.7.7 Nedd4

The ubiquitin ligase – Nedd4L family of proteins interacts with PPxY motifs of ENaC subunits through their WW domains and decreases ENaC cell surface abundance. The gene on chromosome 8q24 lies in blood pressure QTL cluster 8 in several rat strains including (DS \times Lewis) with a systolic blood pressure differential of \sim 20 mmHg (Rapp 2000, Garrett et al. 1998). Whereas 8% NaCl diet increased Nedd4L expression nearly twofold in Dahl salt-resistant kidney, no such effect was seen in Dahl salt-sensitive rats

(Umemura et al. 2006). Variations in regulatory sequences of the Nedd4 gene might be responsible. Nedd4 isoforms are also highly expressed in the brain, but their role in regulation of ENaC in the CNS and neural regulation of blood pressure has not yet been assessed.

3.6.7.8 Na⁺K⁺ATPASE

Na⁺K⁺ATPase subunits are coded from different chromosomal segments, some of which (α 1–2q34; α 3–1q21; β 3–8q31) lie on important blood pressure QTLs (Wang et al. 1999). The α 1 locus was found to be associated with as much as 40% of the salt-sensitive blood pressure variation in transgenic Dahl salt-sensitive rats carrying the R gene (Herrera et al. 1998). The A1079T substitution was detected in α 1 Na⁺K⁺ATPase gene of Dahl salt-sensitive rats (Herrera & Ruiz-Opazo 1990), but this was not confirmed by others (Barnard et al. 2001). Recently Kaneko *et al.* (Kaneko et al. 2005) suggested that the A1079T nucleotide substitution induces a more thermodynamically stable 4-basepair hairpin loop structure compared with the wild type (A1079), resulting in a bias towards A1079 whenever DNA amplification precedes detection of this mutation. The Dahl salt-sensitive variant showed lower affinity for Na but higher affinity for K and similar affinity for ouabain compared with the wild type in Dahl salt-resistant rats.

3.6.7.9 Adducin

Mutations in all three adducin subunits (α – Chr 14, β – Chr 4, and γ – Chr 1) are present in MHS; but only the adducin α MHS allele cosegregates with blood pressure in an F2 (MHS \times MNS) population. The adducin β and γ polymorphisms epistatically interact with that of the adducin α in modulating blood pressure levels (Bianchi et al. 1994).

Adducin α and γ are abundant in the kidney and brain. Interaction of adducin with $\text{Na}^+\text{K}^+\text{ATPase}$ and other channel proteins such as ENaC in the brain still needs to be studied (Yang et al. 2002).

3.6.7.10 Angiotensin II / arginine vasopressin receptor

The angiotensin II / arginine vasopressin receptor gene maps to rat chromosome 1q41, in a QTL region associated with a 10-mmHg to 13-mmHg increased blood pressure on high-salt diet in a (DS \times DR) F2 male cohort. Molecular characterization of cDNAs from Dahl salt-sensitive and salt-resistant rats revealed two amino acid substitutions (N119S, C163R) in the Dahl salt-sensitive angiotensin II / arginine vasopressin receptor. Ligand binding assays demonstrated fivefold and twofold higher affinity of the Dahl salt-sensitive receptor for ^{125}I -angiotensin II and ^3H -arginine vasopressin, respectively (Ruiz-Opazo et al. 2002). The receptor is extensively expressed in neurons and epithelia in the CNS (Hurbin et al. 2000), but its role in salt-sensitive hypertension remains to be studied.

3.6.8 Conclusion

Functional studies indicate that in genetic models of salt-sensitive hypertension such as Dahl salt-sensitive rats and SHRs, dysregulation of $[\text{Na}^+]$ homeostasis leads to an increase in CSF $[\text{Na}^+]$ on high salt intake as well as enhanced neuronal responsiveness to CSF Na^+ , which can both contribute to increases in sympathetic outflow and blood pressure. Enhanced activity of the aldosterone –MR – ENaC – OLC pathway both in the choroid plexus and in neurons may explain both components of CNS-mediated salt sensitivity. It is not yet known what causes the paradoxical response of MR – ENaC to high $[\text{Na}^+]$ in the brain. We have discussed a few genes whose regulation is impaired in salt-sensitive rats, and a few whose expression and function have not yet been determined

in central regulatory pathways, as summarized in Table 1. Many of them may be part of a central Na^+ transport–regulating gene network that finetunes neuronal responses to environmental triggers such as high-salt diet through small changes in neuronal excitability. A major barrier in detecting changes in expression in specific brain areas has been the use of suboptimal methods. Most studies on mRNA expression have used whole hypothalamus or brainstem, which may mask localized changes in specific nuclei. Laser capture microdissection, punches, in-situ hybridization, and immunohistochemical methods are better suited to identify subtle changes in gene and protein expression.

Many of these genes may also contribute to salt sensitivity in humans (Beeks et al. 2004). The phenotype for a polymorphic variant often differs across different populations and may change with age, gender, or concomitant use of antihypertensive medications. Better definitions of salt-sensitive phenotypes are needed to dissect the genetics of salt-sensitive hypertension in humans. Evaluation of candidate genes for salt sensitivity and their contribution to neural mechanisms controlling blood pressure can move us beyond the classic paradigm putting the kidney at the center of all hypertension and open new avenues to discover novel strategies to prevent or treat salt-sensitive hypertension.

Table 3.6–1: Components of the Na⁺ transport regulating gene network: known polymorphisms and expression in response to high salt diet in salt sensitive rats. NS, not studied or not studied in salt-sensitive rats on high-salt diet; Dahl R, Dahl salt-resistant rats; SIK, salt-inducible kinase; MHS, Milan Hypertensive rat; OLC, ouabain-like compound; BN, Brown Norway rat; ENaC, epithelial sodium channels; Dahl S, Dahl salt-sensitive rats; AVP, arginine vasopressin.

	Mutations in coding regions	Mutations in regulatory regions	Kidney expression	Brain expression	Activity
11-β-hydroxylase	<i>R127C</i> , <i>V351A</i> , <i>V381L</i> , <i>I384L</i> , and <i>V443M</i> substitutions in Dahl R	NS	NS	Dahl rats not studied	Decreased in Dahl R
Aldosterone synthase	<i>E136D</i> and <i>Q251R</i> substitutions in Dahl R	NS	NS	Dahl rats not studied	Increased in Dahl R
SIK	NS	NS	NS	NS	NS

	Mutations in coding regions	Mutations in regulatory regions	Kidney expression	Brain expression	Activity
Side-chain cleavage enzyme	NS	NS	NS	Increased in MHS hypothalamus	Increased OLC in Dahl S and MHS hypothalamus
HSD isomerase	NS	NS	NS	Increased in MHS hypothalamus	Increased OLC in Dahl S and MHS hypothalamus
Mineralocorticoid receptor	<i>Y73C</i> substitution in BN	NS	NS	NS	Enhanced transactivation by aldosterone in BN

	Mutations in coding regions	Mutations in regulatory regions	Kidney expression	Brain expression	Activity
ENaC	None found	NS	Increased ENaC α in Dahl S	NS	Increased in Dahl S
Nedd4L	NS	NS	Increased in Dahl R; no change in Dahl S	NS	NS
Angiotensin II / AVP receptor	<i>N119S</i> and <i>C163R</i> substitutions in Dahl S	NS	NS	NS	Increased affinity for AVP and angiotensin II in Dahl S
Na⁺K⁺ATPase	<i>Q276L</i> substitution in $\alpha 1$ subunit in Dahl S	NS	NS	NS	Increased Na:K coupling in Dahl S

3.6.9 Acknowledgements

Research by the authors discussed in this review was supported by operating grants from the Canadian Institute of Health Research (CIHR). Dr. Amin is supported by a Pfizer / CIHR / CHS doctoral research award and Program grant PRG5275 from the Heart and Stroke Foundation of Ontario. Dr. Leenen holds the Pfizer Chair in Hypertension Research, an endowed chair supported by Pfizer Canada, University of Ottawa Heart Institute Foundation, and CIHR.

GENERAL DISCUSSION

In Wistar rats, both mRNA and protein of all three ENaC subunits are expressed in brain epithelia and magnocellular neurons in the SON and PVN. ENaC subunits are more abundant on the apical microvilli versus basolateral membrane of choroid cells. Benzamil decreases Na^+ influx into choroid cells by ~20-30% and increases CSF $[\text{Na}^+]$ by ~8 mmol/L in Wistar rats. Icv infusion of Na^+ rich aCSF increases apical membrane expression of βENaC in the choroid cells and of α and βENaC in basolateral membrane of ependymal cells, but has no effect on neuronal expression of ENaC.

Although the SGK1 gene is identical in Dahl R and S rats, expression of SGK1 is enhanced by high salt diet in e.g. the kidneys and SON of Dahl S rats on high salt diet. The mRNA expression and membranous immunoreactivity to ENaC subunits is higher in the IMCDs of kidney, choroid cells and SON of Dahl S versus R rats. In Dahl R rats, high salt attenuates the ouabain blockable efflux of Na^+ from choroid cells and CSF $[\text{Na}^+]$ remains unchanged. In contrast, in Dahl S rats, the ouabain blockable efflux of $^{22}\text{Na}^+$ is not attenuated with high salt and if anything somewhat increases, causing CSF $[\text{Na}^+]$ to rise. Expression of SGK1 and $11\beta\text{HSD2}$ is enhanced by high salt diet in the SON of Dahl S rats but not Dahl R rats. This may cause the increased expression and membranous immunoreactivity to ENaC subunits in the magnocellular neurons.

4.1 ENaC EXPRESSION IN THE CHOROID PLEXUS

4.1.1 ENaC Expression in Wistar rats

Both the mRNA and protein of all three subunits of ENaC were found to be expressed in the choroid plexus. mRNA abundance of α ENaC was relatively higher than that of β and γ ENaC, while protein abundance of β and γ ENaC were more, suggesting that post-transcriptional and post-translational mechanisms regulate protein abundance. Although the immunoreactivity appeared to be predominantly apical, electron microscopy showed that ENaC subunits are expressed on both the apical and basolateral membranes, with dissimilar distribution. Abundance of the subunits was several folds higher (~20-40%) in the apical microvilli than on the basolateral membrane (~5-10%). Since the Na^+K^+ ATPase in the choroid plexus is predominantly expressed on the apical membrane, the apical-predominant localization of ENaC was in sharp contrast to most other Na^+ reabsorbing epithelia, such as the renal tubules and colonic epithelium, but somewhat similar to the distribution in e.g. ciliary epithelium of the eye. Mechanisms in the choroid cells that regulate preferential transfer of the proteins to either of the membranes may play an important role in Na^+ transport through ENaC in the choroid plexus.

4.1.2 Factors affecting ENaC expression in the choroid plexus

Many factors can affect the abundance, distribution and P_o of ENaC in the choroid plexus. Among major hormonal regulators are both circulating and locally produced aldosterone, corticosteroids, vasopressin, insulin and AngII. We partially studied regulation of ENaC expression by aldosterone, Na^+ and high salt. Specifically we showed

that rat choroid plexus also shows abundant expression of MR. Our studies showed an effect of MR blockade mostly on distribution of the subunits. Chronic infusion of Na⁺ rich aCSF caused a clear increase in abundance of α and β ENaC protein in the apical microvilli of choroid cells. Moreover we noted decreased expression of γ ENaC in the choroid cells following icv infusion alone. The local CSF microenvironment in the ventricles appears to be an important regulator of ENaC expression and membrane abundance. Further studies on post-transcriptional and post-translational regulation of ENaC subunits should be able to shed more light on regulation of ENaC function in the choroid plexus and its role in regulation of CSF [Na⁺].

4.1.3 ENaC expression in Dahl rats

The mRNA abundance of individual subunits was not significantly different between age matched Dahl R and S rats and more or less similar in distribution to Wistar rats. We used different antibodies in our studies between Dahl and Wistar rats, which may explain somewhat lower immunoreactivity to α ENaC in the CP of Dahl rats. Nevertheless α EnaC labeled gold particles could still be detected by immuno EM.

Interestingly the ratio of the 90 to 70 kDa fraction of γ ENaC in the choroid plexus of both Dahl R and S rats was found to be higher at 9 weeks. We had not done a similar study in Wistar rats and the significance of this observation at this point remains uncertain. However, it may suggest either an increased production of nascent subunits or, decreased proteolytic cleavage with maturation of the rats. More importantly, in the context of our studies, it was not significantly different between Dahl S and Dahl R. In our previous studies, Dahl SS/MCW rats compared to Dahl SS/BN13 controls also showed similar higher immunoreactivity to β and γ ENaC in the choroid cells, suggesting that the gene

responsible for this higher expression may be located on Chromosome 13. We did not find any differences in the sequence of the SGK1 gene between Dahl R, Dahl S and Wistar rats. Further studies are required to elucidate the factors that are responsible for increased expression of β and γ ENaC in the choroid cells of Dahl S rats.

4.1.4 Effect of high salt diet on ENaC expression in the choroid plexus

In age matched Dahl R and S rats, high salt diet for 2 or 4 weeks did not significantly affect expression of ENaC subunits in the choroid plexus. Considering that expression of ENaC subunits was already higher on regular salt in the choroid plexus of Dahl S versus R rats, it appears that the expression of ENaC in the choroid plexus of Dahl S is already at its maximum and cannot be further upregulated by high salt to for example prevent the increasing $[\text{Na}^+]$ on high salt diet. Persistence of the higher abundance of β ENaC in the basolateral membrane in Dahl S rats may contribute to increased influx and through apical Na^+K^+ ATPase increases in CSF $[\text{Na}^+]$.

In the ependyma however, we noted increased membranous immunoreactivity to γ ENaC in Dahl S versus R rats on high salt diet. Studies in rat CCD show that over-expression of γ ENaC is sufficient to increase Na^+ transport (Volk et al. 2005). How the higher γ ENaC contributes to regulation of hypothalamic tissue $[\text{Na}^+]$ remains to be studied.

4.1.5 ENaC function in the choroid plexus

We showed that ENaC in the choroid plexus is indeed functional and contributes to ~20-30% influx of Na^+ into the choroid cells in both Wistar and Dahl rats. As expected, this inwardly flux of Na^+ through ENaC into the choroid cells was found to be dependent on the Na^+K^+ ATPase mediated efflux. It would appear that Na^+ flows into the cell through ENaC both from the blood at the basolateral membrane and from the CSF at the apical

membrane. However, since the net flow of Na^+ in the choroid plexus is from blood to CSF, apical ENaC in the choroid cells possibly play a role in reabsorption of Na^+ from the CSF, maybe as a mechanism for fine tuning CSF $[\text{Na}^+]$.

Our assays could not differentiate between ENaC activity in the two surfaces of the choroid cells. Specific blockade of ENaC by application of e.g. benzamil to either the apical or basal compartments in cultures of choroid cells grown on semi-permeable membranes may be able to answer the question. In our experience, growing these cells on semipermeable membranes was very difficult and expression of ENaC in choroid cells grown in culture was relatively lower than in vivo expression. Indirect evidence from functional studies however suggests that ENaC in both the basolateral and apical membranes is indeed functional. Intravenous administration of amiloride was found to inhibit Na^+ transport into the CSF by ~ 20-25% (Murphy & Johanson 1989b, Murphy & Johanson 1990), suggesting blockade of basolateral ENaC. We did not repeat the experiments with i.v. benzamil.

Interestingly, on regular salt retention of ^{22}Na was lower but $[\text{Na}]_i$ was similar in the choroid plexus of S versus R rats. Considering also that CSF uptake of iv ^{22}Na is enhanced in vivo in S versus R rats these findings may reflect enhanced Na transport across the choroid plexus. Such enhanced transport may be due to increased activity of $\text{Na}^+\text{K}^+\text{ATPase}$ associated with increased influx through Na-channels such as ENaC in S rats. However, the benzamil induced decreases in ^{22}Na uptake and in $[\text{Na}]_i$ were similar between the two strains. It appears that the higher abundance of ENaC at the apical membranes in S versus R rats does not lead to significantly higher activity and Na^+ influx. Icv infusion of benzamil was also found to increase CSF $[\text{Na}^+]$, more so in Wistar

rats (~5-8 mmol/L), but also in Dahl R rats, and negligibly in Dahl S rats. Alternatively, blockade by benzamil of higher ENaC dependent influx at the apical membrane may be offset by a larger non-ENaC dependent influx at the basolateral membranes of S rats. Ouabain also similarly increased ^{22}Na retention in S and R rats, consistent with a similar role for $\text{Na}^+\text{K}^+\text{ATPase}$ in Na^+ efflux in the two strains. However, ouabain increased $[\text{Na}]_i$ only in R rats and not at all in S rats. The increase in ^{22}Na retention but absence of an increase in $[\text{Na}]_i$ by ouabain in S rats may therefore reflect enhanced turnover of Na_i i.e. larger influx and efflux, the latter, not dependent on $\text{Na}^+\text{K}^+\text{ATPase}$. Further studies are required to elucidate the actual mechanisms for this enhanced influx efflux and identify possible factors that regulate P_o of the channels in the choroid plexus.

4.1.6 Effect of high salt on CSF $[\text{Na}^+]$, ENaC function and Na^+ transport in the choroid plexus

CSF $[\text{Na}^+]$ increases in salt sensitive strains such as Dahl S but not in salt resistant strains such as Dahl R or Wistar rats (Huang et al. 2004, Nakamura & Cowley 1989). In the current study we saw a similar trend. We had hypothesized that this increase in CSF $[\text{Na}^+]$ is due to enhanced ENaC mediated Na^+ transport into the CSF. However, ENaC was found to be predominantly apically located, which was against the hypothesis. EM studies then showed that ~10% of the subunits are actually inserted into the basolateral membrane and these may play a role in Na^+ influx into the cell, which would then be secreted into the CSF by the apical $\text{Na}^+\text{K}^+\text{ATPase}$. We did note slightly higher percentage of βENaC on the basolateral membrane in Dahl S rats, but this might be due to the generally higher expression in this strain and was not affected by high salt diet.

Interestingly, high salt diet was found to increase $[Na]_i$ by ~30% and decrease retained ^{22}Na by ~20% in Dahl R (SS/BN13) rats but caused no changes in the Dahl S rats. In renal epithelia an increase in $[Na]_i$ would be compensated by greater activity of $Na^+K^+ATPase$ to maintain $[Na]_i$, cell volume and osmolarity. In the CP of Dahl R rats, and also Wistar rats, on high salt the opposite appears to occur. High salt diet markedly decreased the ouabain sensitive component of efflux and the further increase in $[Na]_i$. Such a decrease in $Na^+K^+ATPase$ activity in the CP of R rats on high salt diet might be a mechanism to prevent increases in CSF $[Na^+]$ and resultant sympatho-excitation and hypertension. The mechanism(s) responsible for this decrease in activity still need to be explored, and these studies may lead to new insights into the salt resistance of e.g. R rats, and by extension humans. In our experimental setup, any endogenous inhibitor of enzyme activity should have dissociated by the ~2 hours pre-incubation and mechanisms causing a decrease in expression appear to be more likely.

In contrast to Dahl R, in S rats high salt failed to inhibit ouabain dependent Na^+ transport and if anything caused a moderate increase. This enhanced activity or increased expression of the pump may reflect a primary abnormality of mechanisms regulating the pump in Dahl S rats, as compared to R or Wistar rats (Abdelrahman et al. 1995, Zicha et al. 2001) and may be responsible for the increase in CSF $[Na^+]$ on high salt diet.

4.2 ENaC EXPRESSION IN THE EPENDYMA

The ependyma and tanycytes in the AV3V lining form the functional barrier to the free flow of solutes between the CSF and brain ISF (Jarvis & Andrew 1988). Ependymal cells and tanycytes are intimately associated with both the CSF and hypothalamic neurons, and have an extensive array of gap junctions. We did not use any specific method to

differentiate between ependymal cells and tanycytes and ENaC subunits were found to be expressed on both the apical and basal membrane of most cells lining the AV3V cavity.

4.2.1 Effect of Na⁺ on ENaC expression in ependyma

Considering its location again on the apical and basolateral membranes of ependymal cells, ENaC may act in Na⁺ transport into or out of the interstitium. Our study in Wistar rats showed that infusion of Na⁺ rich aCSF not only increases hypothalamic [Na⁺] but preferentially increases the number of α and β ENaC labelled gold particles on the basolateral membrane of ependymal cells too (Wang et al. 2010b). This suggests that increased ENaC on the basolateral membrane may be a mechanism to decrease the higher hypothalamic tissue [Na⁺].

4.3 ENaC EXPRESSION IN MAGNOCELLULAR NEURONS

Combining our studies in Wistar rats and Dahl rats, it appears that stoichiometry of the channels formed may be different in different parts of the brain. ENaC are also known to form functional channels with other members of the DEG/ENaC family and in different tissues, ENaC subunits assemble to form channels that differ with respect to regulation, Na⁺ selectivity, P_o and function (Eaton et al. 2009, Palmer 1992). We focused our studies on expression of ENaC in the hypothalamic neurons, especially the magnocellular SON and PVN, both of which showed prominent ENaC expression and immunoreactivity, and are thought to mediate the sympathetic hyperactivity in response to increases in CSF [Na⁺].

Despite relatively lower abundance of the β and γ ENaC mRNA in the magnocellular SON and PVN compared to α ENaC mRNA, protein abundance and immunoreactivity were both detectable, indicating differences in translational efficiency of the proteins between the epithelia and neurons. The similar level of mRNA and protein expression on regular salt diet between Dahl S and Dahl R suggests that mechanisms of regulation and expression in the neurons are not different between these two strains. In Wistar rats, infusion of Na^+ rich aCSF also did not affect expression of ENaC subunits in the magnocellular neurons (Wang et al. 2010b). Altogether it appears that on regular salt intake ENaC in neurons is minimally affected by changes of extracellular $[\text{Na}^+]$.

4.3.1 Effect of high salt on expression of ENaC subunits and their regulators in the SON

Interestingly, high salt diet enhanced abundance of the mRNA and membranous expression of ENaC subunits in the SON of Dahl S rats versus no changes in Dahl R. Parallel functional studies in our lab have also shown that high versus regular salt diet increases hypothalamic aldosterone by ~35% in Dahl S rats versus decreases in Dahl R rats (Huang et al. 2009b). Other groups have also reported similar findings that indeed aldosterone production is enhanced in the brain of Dahl S versus R rats (Gomez-Sanchez et al. 2010). We noted increased abundance of 11β HSD2 and SGK1 with high salt diet in the SON of Dahl S rats only. This increased expression of ENaC in the SON of Dahl S, may be secondary to the increased brain aldosterone (Gomez-Sanchez et al. 2010). Moreover increased expression of 11β HSD2 in the SON on high salt in Dahl S rats, also may confer increased selectivity to aldosterone. Acting through increased SGK1, aldosterone may cause this enhanced expression of β and γ ENaC in the SON. Alternately,

increases in vasopressin (Wainford & Kapusta 2010) may also contribute to the increased expression of β and γ ENaC in SON.

4.3.2 Functional implications

Increased $[\text{Na}^+]$ in the CSF of Dahl S rats on high salt diet appears to be the triggering factor for the subsequent increase in sympathetic hyperactivity. An increase in CSF $[\text{Na}^+]$ *per se*, by icv infusion of Na^+ -rich aCSF also causes sympathetic hyperactivity and hypertension in otherwise normotensive strains (Huang et al. 2006b, Huang et al. 1998). The mechanisms linking the increase in CSF $[\text{Na}^+]$ and the increase in sympathetic activity are poorly understood. Functional studies in our lab and by others suggest that the increase in CSF $[\text{Na}^+]$ activates a central pathway involving aldosterone-MR-ENaC that causes increases in ‘ouabain’ and angiotensinergic activity (Huang et al. 2006a, Leenen 2010, Leenen et al. 2002). In the current studies we show that on regular salt membrane abundance of β and γ ENaC subunits in the magnocellular neurons in the SON is higher in Dahl S versus R rats and this increase persists on a high salt diet. Increases in CSF $[\text{Na}^+]$ may activate Na_x channels in the SFO and other mechanisms in e.g. the AV3V, which have extensive projections to the magnocellular neurons. The latter are thought to respond primarily by secretion of peptide hormones such as vasopressin and oxytocin but there is evidence supporting the fact that they may also produce mediators such as ‘ouabain’ (Yoshika et al. 2011, Takahashi et al. 1987b) and aldosterone (Huang et al. 2010). It has been generally presumed that the magnocellular neurons primarily act by axonal release of their peptide products in the pituitary. However, it is now established that release of peptides also occurs at the dendritic terminals of the magnocellular neurons thereby affecting the activity of surrounding glia, pre-synaptic axon terminals

ending on these dendrites and adjacent brain areas especially the AV3V (Monteiro et al. 2011, Ludwig et al. 2005, Widmer et al. 2003, Wotjak et al. 2002, Wotjak et al. 1994, Landgraf & Ludwig 1991, Ludwig et al. 1996). The released products are further dissipated by bulk flow into the CSF and hence to other parts of the brain (Leng & Ludwig 2008) causing autocrine and paracrine effects and providing feedback control to upstream neurons and epithelia. As discussed in a recent review, ‘neurotransmitters carry messages that matter only at particular time and place ... while peptides are public announcements, the messages endure at least for a while; they are messages not from one cell to another, but from one population of neurons to another’ (Leng & Ludwig 2006, Leng & Ludwig 2008). Whether or not ‘ouabain’ and aldosterone act in a fashion similar to peptide hormones and whether or not they are released from the SON and the dendritic terminals remains to be studied. In the context of the current studies, persistent higher expression and presumably increased P_o of ENaC in neurons in Dahl S rats on high salt may decrease their threshold for excitability in response to changes in extracellular $[Na^+]$. The increase in neuronal activity may result in greater frequency of neuronal spikes and thereby greater release of e.g. ‘ouabain’. Such sustained slow release of ‘ouabain’ may contribute to sympathetic hyperactivity and hypertension in Dahl S rats on a high salt diet.

4.4 CONCLUSION

Hypertension is a major cause of morbidity and mortality worldwide. As a major risk factor for hypertension - salt sensitivity, can be either inherited or acquired. Understanding the pathways and molecular mechanisms that contribute to the increase in BP is a prerequisite to formulating better strategies to combat the disease. We studied the epithelial sodium channel (ENaC) - which is an important regulator of the body's sodium balance and have identified the specific sites in the kidneys where ENaC is up-regulated in salt sensitive Dahl S rats. No mutations in the SGK1 gene that could be responsible for the increased expression of ENaC or SGK1 in Dahl S rats on high salt diet were found, suggesting that other regulators need to be studied. We are the first to show that ENaC subunits are expressed in the CNS and that expression of ENaC and its regulators such as SGK1 and MR is modulated by Na^+ , either from the diet or through direct infusion into the brain. Compared to Wistar rats and Dahl SS/BN13 where only the chromosome 13 in Dahl S had been substituted with that from BN rats, salt sensitive Dahl S rats did not downregulate mechanisms in brain epithelia that pump Na^+ into the brain. Such a lack of inhibition may be responsible for the increase in CSF $[\text{Na}^+]$ in these genetically salt sensitive rats and the trigger for subsequent increase in sympathetic hyperactivity and hypertension. Moreover, high salt diet enhanced expression of ENaC subunits in the SON, which is thought to secrete 'ouabain' - one of the key mediators of Na^+ induced hypertension. Figure 4.4-1 summarizes possible mechanisms in Dahl S rats that may lead to increases in BP on high salt diet. Our findings enhance our understanding of the

mechanisms by which Na^+ enters the CNS and activates key areas in the hypothalamus leading to sympathetic hyperactivity and hypertension on high salt diet.

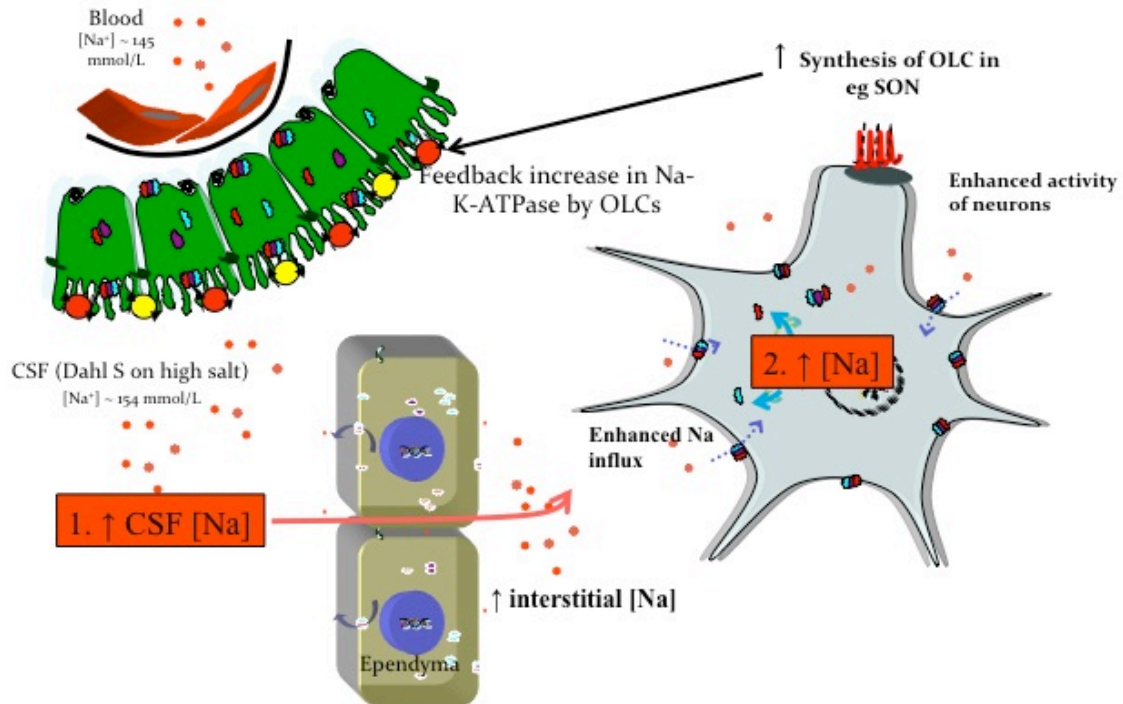


Figure 4.4–1: Mechanisms in Dahl S rats that may lead to sympathetic hyperactivity and hypertension. High salt decreases ouabain blockable efflux of $[\text{Na}^+]$ presumably into CSF in salt resistant strains, but not in Dahl S rats and causes persistent increases in CSF $[\text{Na}^+]$. Higher $[\text{Na}^+]$ alongwith the greater expression of ENaC in e.g. the magnocellular SON neurons may increase the excitability of these cells and enhance production of mediators such as ‘ouabain’ and vasopressin. The persistence of higher CSF $[\text{Na}^+]$ may be responsible for continuous production of ‘ouabain’ in Dahl S and activation of sympathoexcitatory pathways causing hypertension.

REFERENCES

- Abbott, N. J. (2004) Evidence for bulk flow of brain interstitial fluid: significance for physiology and pathology. *Neurochemistry international*, **45**, 545-552.
- Abdelrahman, A. M., Harmsen, E. and Leenen, F. H. (1995) Dietary sodium and Na,K-ATPase activity in Dahl salt-sensitive versus salt-resistant rats. *Journal of hypertension*, **13**, 517-522.
- Abe, K., Tsunoda, K., Sato, M., Omata, K., Yasujima, M. and Yoshinaga, K. (1987) Interactions of renal prostaglandins, renin-angiotensin system and renal kallikrein-kinin system in human hypertension. *Agents and actions*, **22**, 215-220.
- Ackermann, U. (1975) On the regulation of the renal response blood volume expansion by vascular parameters in the rat. *Pflugers Arch*, **355**, 151-164.
- Ackermann, U. and Azizi, N. (2000) Increased central AT(1)-receptor activation, not systemic vasopressin, sustains hypertension in ANP knockout mice. *American journal of physiology*, **278**, R1441-1445.
- Aguilera, G., Kiss, A., Lu, A. and Camacho, C. (1996) Regulation of adrenal steroidogenesis during chronic stress. *Endocrine research*, **22**, 433-443.
- Ahima, R., Krozowski, Z. and Harlan, R. (1991) Type I corticosteroid receptor-like immunoreactivity in the rat CNS: distribution and regulation by corticosteroids. *The Journal of comparative neurology*, **313**, 522-538.
- Ahima, R. S. and Harlan, R. E. (1991) Differential corticosteroid regulation of type II glucocorticoid receptor-like immunoreactivity in the rat central nervous system: topography and implications. *Endocrinology*, **129**, 226-236.

- Albiston, A. L., Obeyesekere, V. R., Smith, R. E. and Krozowski, Z. S. (1994) Cloning and tissue distribution of the human 11 beta-hydroxysteroid dehydrogenase type 2 enzyme. *Molecular and cellular endocrinology*, **105**, R11-17.
- Alper, S. L., Stuart-Tilley, A., Simmons, C. F., Brown, D. and Drenckhahn, D. (1994) The fodrin-ankyrin cytoskeleton of choroid plexus preferentially colocalizes with apical Na⁺K⁺-ATPase rather than with basolateral anion exchanger AE2. *The Journal of clinical investigation*, **93**, 1430-1438.
- Althaus, M., Bogdan, R., Clauss, W. G. and Fronius, M. (2007) Mechano-sensitivity of epithelial sodium channels (ENaCs): laminar shear stress increases ion channel open probability. *Faseb J*, **21**, 2389-2399.
- Alvarez de la Rosa, D., Canessa, C. M., Fyfe, G. K. and Zhang, P. (2000) Structure and regulation of amiloride-sensitive sodium channels. *Annual review of physiology*, **62**, 573-594.
- Alvarez de la Rosa, D., Coric, T., Todorovic, N., Shao, D., Wang, T. and Canessa, C. M. (2003) Distribution and regulation of expression of serum- and glucocorticoid-induced kinase-1 in the rat kidney. *The Journal of physiology*, **551**, 455-466.
- Alvarez de la Rosa, D., Paunescu, T. G., Els, W. J., Helman, S. I. and Canessa, C. M. (2004) Mechanisms of regulation of epithelial sodium channel by SGK1 in A6 cells. *The Journal of general physiology*, **124**, 395-407.
- Amasheh, S., Epple, H. J., Mankertz, J., Detjen, K., Goltz, M., Schulzke, J. D. and Fromm, M. (2000) Differential regulation of ENaC by aldosterone in rat early and late distal colon. *Annals of the New York Academy of Sciences*, **915**, 92-94.

- Amin, M. S., Reza, E., El-Shahat, E., Wang, H. W., Tesson, F. and Leenen, F. H. (2011) Enhanced expression of epithelial sodium channels in the renal medulla of Dahl S rats. *Canadian Journal of Physiology and Pharmacology*, **89**, 159-168.
- Amin, M. S., Reza, E., Wang, H. and Leenen, F. H. (2009) Sodium transport in the choroid plexus and salt-sensitive hypertension. *Hypertension*, **54**, 860-867.
- Amin, M. S., Wang, H. W., Reza, E., Whitman, S. C., Tuana, B. S. and Leenen, F. H. (2005) Distribution of epithelial sodium channels and mineralocorticoid receptors in cardiovascular regulatory centers in rat brain. *American journal of physiology*, **289**, R1787-1797.
- Anan, T., Nagata, Y., Koga, H. et al. (1998) Human ubiquitin-protein ligase Nedd4: expression, subcellular localization and selective interaction with ubiquitin-conjugating enzymes. *Genes Cells*, **3**, 751-763.
- Aoi, W., Niisato, N., Miyazaki, H. and Marunaka, Y. (2004) Flavonoid-induced reduction of ENaC expression in the kidney of Dahl salt-sensitive hypertensive rat. *Biochemical and biophysical research communications*, **315**, 892-896.
- Aoi, W., Niisato, N., Sawabe, Y., Miyazaki, H. and Marunaka, Y. (2006) Aldosterone-induced abnormal regulation of ENaC and SGK1 in Dahl salt-sensitive rat. *Biochemical and biophysical research communications*, **341**, 376-381.
- Aoi, W., Niisato, N., Sawabe, Y., Miyazaki, H., Tokuda, S., Nishio, K., Yoshikawa, T. and Marunaka, Y. (2007) Abnormal expression of ENaC and SGK1 mRNA induced by dietary sodium in Dahl salt-sensitively hypertensive rats. *Cell biology international*, **31**, 1288-1291.

- Asher, C., Chigayev, A. and Garty, H. (2001) Characterization of interactions between Nedd4 and beta and gammaENaC using surface plasmon resonance. *Biochemical and biophysical research communications*, **286**, 1228-1231.
- Asher, C., Sinha, I. and Garty, H. (2003) Characterization of the interactions between Nedd4-2, ENaC, and sgk-1 using surface plasmon resonance. *Biochimica et biophysica acta*, **1612**, 59-64.
- Asher, C., Wald, H., Rossier, B. C. and Garty, H. (1996) Aldosterone-induced increase in the abundance of Na⁺ channel subunits. *The American journal of physiology*, **271**, C605-611.
- Awayda, M. S., Ismailov, II, Berdiev, B. K. and Benos, D. J. (1995) A cloned renal epithelial Na⁺ channel protein displays stretch activation in planar lipid bilayers. *The American journal of physiology*, **268**, C1450-1459.
- Awayda, M. S. and Subramanyam, M. (1998) Regulation of the epithelial Na⁺ channel by membrane tension. *The Journal of general physiology*, **112**, 97-111.
- Baker, E. H., Dong, Y. B., Sagnella, G. A. et al. (1998) Association of hypertension with T594M mutation in beta subunit of epithelial sodium channels in black people resident in London. *Lancet*, **351**, 1388-1392.
- Baker, E. H., Duggal, A., Dong, Y., Ireson, N. J., Wood, M., Markandu, N. D. and MacGregor, G. A. (2002) Amiloride, a specific drug for hypertension in black people with T594M variant? *Hypertension*, **40**, 13-17.
- Banasikowska, K., Post, M., Cutz, E., O'Brodivich, H. and Otulakowski, G. (2004) Expression of epithelial sodium channel alpha-subunit mRNAs with alternative

- 5'-untranslated regions in the developing human lung. *Am J Physiol Lung Cell Mol Physiol*, **287**, L608-615.
- Bangel-Ruland, N., Sobczak, K., Christmann, T., Kentrup, D., Langhorst, H., Kusche-Vihrog, K. and Weber, W. M. (2010) Characterization of the epithelial sodium channel delta-subunit in human nasal epithelium. *Am J Respir Cell Mol Biol*, **42**, 498-505.
- Bankir, L., Bichet, D. G. and Bouby, N. (2010) Vasopressin V2 receptors, ENaC, and sodium reabsorption: a risk factor for hypertension? *American journal of physiology*, **299**, F917-928.
- Bankir, L., Fernandes, S., Bardoux, P., Bouby, N. and Bichet, D. G. (2005) Vasopressin-V2 receptor stimulation reduces sodium excretion in healthy humans. *J Am Soc Nephrol*, **16**, 1920-1928.
- Barbry, P. and Lazdunski, M. (1996) Structure and regulation of the amiloride-sensitive epithelial sodium channel. *Ion channels*, **4**, 115-167.
- Barker, P. M., Nguyen, M. S., Gatzky, J. T., Grubb, B., Norman, H., Hummler, E., Rossier, B., Boucher, R. C. and Koller, B. (1998) Role of gammaENaC subunit in lung liquid clearance and electrolyte balance in newborn mice. Insights into perinatal adaptation and pseudohypoaldosteronism. *The Journal of clinical investigation*, **102**, 1634-1640.
- Barnard, R., Kelly, G., Manzetti, S. O. and Harris, E. L. (2001) Neither the New Zealand genetically hypertensive strain nor Dahl salt-sensitive strain has an A1079T transversion in the alpha1 isoform of the Na(+),K(+)-ATPase gene. *Hypertension*, **38**, 786-792.

- Baxendale-Cox, L. M. and Duncan, R. L. (1999) Insulin increases sodium (Na⁺) channel density in A6 epithelia: implications for expression of hypertension. *Biol Res Nurs*, **1**, 20-29.
- Bayorh, M. A., Ganafa, A. A., Emmett, N., Socci, R. R., Eatman, D. and Fridie, I. L. (2005) Alterations in aldosterone and angiotensin II levels in salt-induced hypertension. *Clin Exp Hypertens*, **27**, 355-367.
- Beeks, E., Kessels, A. G., Kroon, A. A., van der Klauw, M. M. and de Leeuw, P. W. (2004) Genetic predisposition to salt-sensitivity: a systematic review. *Journal of hypertension*, **22**, 1243-1249.
- Beevers, D. G. (2002) The epidemiology of salt and hypertension. *Clin Auton Res*, **12**, 353-357.
- Bell, P. D., Lapointe, J. Y. and Peti-Peterdi, J. (2003a) Macula densa cell signaling. *Annual review of physiology*, **65**, 481-500.
- Bell, P. D., Lapointe, J. Y., Sabirov, R., Hayashi, S., Peti-Peterdi, J., Manabe, K., Kovacs, G. and Okada, Y. (2003b) Macula densa cell signaling involves ATP release through a maxi anion channel. *Proceedings of the National Academy of Sciences of the United States of America*, **100**, 4322-4327.
- Benos, D. J. (2004) Sensing tension: recognizing ENaC as a stretch sensor. *Hypertension*, **44**, 616-617.
- Benos, D. J. and Stanton, B. A. (1999) Functional domains within the degenerin/epithelial sodium channel (Deg/ENaC) superfamily of ion channels. *The Journal of physiology*, **520 Pt 3**, 631-644.

- Bens, M., Vallet, V., Cluzeaud, F., Pascual-Letallec, L., Kahn, A., Rafestin-Oblin, M. E., Rossier, B. C. and Vandewalle, A. (1999) Corticosteroid-dependent sodium transport in a novel immortalized mouse collecting duct principal cell line. *J Am Soc Nephrol*, **10**, 923-934.
- Berdiev, B. K. and Benos, D. J. (2006) Epithelial sodium channel in planar lipid bilayers. *Methods in molecular biology (Clifton, N.J)*, **337**, 89-99.
- Berger, S., Bleich, M., Schmid, W. et al. (1998) Mineralocorticoid receptor knockout mice: pathophysiology of Na⁺ metabolism. *Proceedings of the National Academy of Sciences of the United States of America*, **95**, 9424-9429.
- Bertram, C., Trowern, A. R., Copin, N., Jackson, A. A. and Whorwood, C. B. (2001) The maternal diet during pregnancy programs altered expression of the glucocorticoid receptor and type 2 11beta-hydroxysteroid dehydrogenase: potential molecular mechanisms underlying the programming of hypertension in utero. *Endocrinology*, **142**, 2841-2853.
- Betz, A. L. (1983) Sodium transport in capillaries isolated from rat brain. *J Neurochem*, **41**, 1150-1157.
- Betz, A. L. and Goldstein, G. W. (1978) Polarity of the blood-brain barrier: neutral amino acid transport into isolated brain capillaries. *Science (New York, N.Y)*, **202**, 225-227.
- Betz, A. L. and Goldstein, G. W. (1980) The basis for active transport at the blood-brain barrier. *Advances in experimental medicine and biology*, **131**, 5-16.
- Betz, A. L. and Goldstein, G. W. (1986) Specialized properties and solute transport in brain capillaries. *Annual review of physiology*, **48**, 241-250.

- Beutler, K. T., Masilamani, S., Turban, S., Nielsen, J., Brooks, H. L., Ageloff, S., Fenton, R. A., Packer, R. K. and Knepper, M. A. (2003) Long-term regulation of ENaC expression in kidney by angiotensin II. *Hypertension*, **41**, 1143-1150.
- Bhargava, A., Fullerton, M. J., Myles, K., Purdy, T. M., Funder, J. W., Pearce, D. and Cole, T. J. (2001) The serum- and glucocorticoid-induced kinase is a physiological mediator of aldosterone action. *Endocrinology*, **142**, 1587-1594.
- Bianchi, G., Baer, P. G., Fox, U. and Guidi, E. (1977) The role of the kidney in the rat with genetic hypertension. *Postgraduate medical journal*, **53 Suppl 2**, 123-138.
- Bianchi, G., Fox, U., Di Francesco, G. F., Bardi, U. and Radice, M. (1973) The hypertensive role of the kidney in spontaneously hypertensive rats. *Clinical science and molecular medicine*, **45 Suppl 1**, 135s-139.
- Bianchi, G., Fox, U., Pagetti, D., Caravaggi, A. M., Baer, P. G. and Baldoli, E. (1975) Mechanisms involved in renal hypertension. *Kidney Int Suppl*, S165-173.
- Bianchi, G., Tripodi, G., Casari, G. et al. (1994) Two point mutations within the adducin genes are involved in blood pressure variation. *Proceedings of the National Academy of Sciences of the United States of America*, **91**, 3999-4003.
- Bize, V. and Horisberger, J. D. (2007) Sodium self-inhibition of human epithelial sodium channel: selectivity and affinity of the extracellular sodium sensing site. *American journal of physiology*, **293**, F1137-1146.
- Bjerregaard, P., Dewailly, E., Young, T. K., Blanchet, C., Hegele, R. A., Ebbesson, S. E., Risica, P. M. and Mulvad, G. (2003) Blood pressure among the Inuit (Eskimo) populations in the Arctic. *Scandinavian journal of public health*, **31**, 92-99.

- Bjerregaard, P., Young, T. K., Dewailly, E. and Ebbesson, S. O. (2004) Indigenous health in the Arctic: an overview of the circumpolar Inuit population. *Scandinavian journal of public health*, **32**, 390-395.
- Blazer-Yost, B. L., Butterworth, M., Hartman, A. D., Parker, G. E., Faletti, C. J., Els, W. J. and Rhodes, S. J. (2001) Characterization and imaging of A6 epithelial cell clones expressing fluorescently labeled ENaC subunits. *Am J Physiol Cell Physiol*, **281**, C624-632.
- Blazer-Yost, B. L., Liu, X. and Helman, S. I. (1998) Hormonal regulation of ENaCs: insulin and aldosterone. *The American journal of physiology*, **274**, C1373-1379.
- Bonny, O., Chraïbi, A., Loffing, J., Jaeger, N. F., Grunder, S., Horisberger, J. D. and Rossier, B. C. (1999) Functional expression of a pseudohypoaldosteronism type I mutated epithelial Na⁺ channel lacking the pore-forming region of its alpha subunit. *The Journal of clinical investigation*, **104**, 967-974.
- Bonvalet, J. P. (1998) Regulation of sodium transport by steroid hormones. *Kidney Int Suppl*, **65**, S49-56.
- Booth, R. E. and Stockand, J. D. (2003) Targeted degradation of ENaC in response to PKC activation of the ERK1/2 cascade. *American journal of physiology*, **284**, F938-947.
- Booth, R. E., Tong, Q., Medina, J., Snyder, P. M., Patel, P. and Stockand, J. D. (2003) A region directly following the second transmembrane domain in gamma ENaC is required for normal channel gating. *The Journal of biological chemistry*, **278**, 41367-41379.

- Boucher, R. C., Stutts, M. J., Knowles, M. R., Cantley, L. and Gatzky, J. T. (1986) Na⁺ transport in cystic fibrosis respiratory epithelia. Abnormal basal rate and response to adenylate cyclase activation. *The Journal of clinical investigation*, **78**, 1245-1252.
- Boulkroun, S., Ruffieux-Daidie, D., Vitagliano, J. J., Poirot, O., Charles, R. P., Lagnaz, D., Firsov, D., Kellenberger, S. and Staub, O. (2008) Vasopressin-inducible ubiquitin-specific protease 10 increases ENaC cell surface expression by deubiquitylating and stabilizing sorting nexin 3. *American journal of physiology*, **295**, F889-900.
- Bourque, C. W. (2008) Central mechanisms of osmosensation and systemic osmoregulation. *Nat Rev Neurosci*, **9**, 519-531.
- Bourque, C. W. and Oliet, S. H. (1997) Osmoreceptors in the central nervous system. *Annual review of physiology*, **59**, 601-619.
- Bowman, P. D., Ennis, S. R., Rarey, K. E., Betz, A. L. and Goldstein, G. W. (1983) Brain microvessel endothelial cells in tissue culture: a model for study of blood-brain barrier permeability. *Annals of neurology*, **14**, 396-402.
- Brier, M. E. and Luft, F. C. (1994) Sodium kinetics in white and black normotensive subjects: possible relevance to salt-sensitive hypertension. *The American journal of the medical sciences*, **307 Suppl 1**, S38-42.
- Brockway, L. M., Benos, D. J., Keyser, K. T. and Kraft, T. W. (2005) Blockade of amiloride-sensitive sodium channels alters multiple components of the mammalian electroretinogram. *Visual neuroscience*, **22**, 143-151.

- Brockway, L. M., Zhou, Z. H., Bubien, J. K., Jovov, B., Benos, D. J. and Keyser, K. T. (2002) Rabbit retinal neurons and glia express a variety of ENaC/DEG subunits. *Am J Physiol Cell Physiol*, **283**, C126-134.
- Brooks, H. L., Allred, A. J., Beutler, K. T., Coffman, T. M. and Knepper, M. A. (2002) Targeted proteomic profiling of renal Na⁽⁺⁾ transporter and channel abundances in angiotensin II type 1a receptor knockout mice. *Hypertension*, **39**, 470-473.
- Brooks, V. L., Haywood, J. R. and Johnson, A. K. (2005) Translation of salt retention to central activation of the sympathetic nervous system in hypertension. *Clinical and experimental pharmacology & physiology*, **32**, 426-432.
- Brooks, V. L., Scrogin, K. E. and McKeogh, D. F. (2001) The interaction of angiotensin II and osmolality in the generation of sympathetic tone during changes in dietary salt intake. An hypothesis. *Annals of the New York Academy of Sciences*, **940**, 380-394.
- Brown, P. D., Davies, S. L., Speake, T. and Millar, I. D. (2004) Molecular mechanisms of cerebrospinal fluid production. *Neuroscience*, **129**, 957-970.
- Brown, P. N., Jackson, P. C., Staddon, G. E., Richardson, R. B. and Griffith, H. B. (1985) Compartmental analysis of cerebrospinal fluid transfer and absorption in simulated hydrocephalus. *Physics in medicine and biology*, **30**, 1113-1121.
- Bruni, J. E. (1998) Ependymal development, proliferation, and functions: a review. *Microsc Res Tech*, **41**, 2-13.
- Bruni, J. E., Del Bigio, M. R. and Clattenburg, R. E. (1985) Ependyma: normal and pathological. A review of the literature. *Brain research*, **356**, 1-19.

- Bruns, J. B., Carattino, M. D., Sheng, S., Maarouf, A. B., Weisz, O. A., Pilewski, J. M., Hughey, R. P. and Kleyman, T. R. (2007) Epithelial Na⁺ channels are fully activated by furin- and prostaticin-dependent release of an inhibitory peptide from the gamma-subunit. *The Journal of biological chemistry*, **282**, 6153-6160.
- Bubien, J. K. (2010) Epithelial Na⁺ channel (ENaC), hormones, and hypertension. *The Journal of biological chemistry*, **285**, 23527-23531.
- Budzikowski, A. S. and Leenen, F. H. (1997) Brain 'ouabain' in the median preoptic nucleus mediates sodium-sensitive hypertension in spontaneously hypertensive rats. *Hypertension*, **29**, 599-605.
- Bugaj, V., Pochynyuk, O. and Stockand, J. D. (2009) Activation of the epithelial Na⁺ channel in the collecting duct by vasopressin contributes to water reabsorption. *American journal of physiology*, **297**, F1411-1418.
- Bunag, R. D. and Miyajima, E. (1984) Baroreflex impairment precedes hypertension during chronic cerebroventricular infusion of hypertonic sodium chloride in rats. *The Journal of clinical investigation*, **74**, 2065-2073.
- Burch, L. H., Talbot, C. R., Knowles, M. R., Canessa, C. M., Rossier, B. C. and Boucher, R. C. (1995) Relative expression of the human epithelial Na⁺ channel subunits in normal and cystic fibrosis airways. *The American journal of physiology*, **269**, C511-518.
- Burt, V. L., Cutler, J. A., Higgins, M., Horan, M. J., Labarthe, D., Whelton, P., Brown, C. and Roccella, E. J. (1995a) Trends in the prevalence, awareness, treatment, and control of hypertension in the adult US population. Data from the health examination surveys, 1960 to 1991. *Hypertension*, **26**, 60-69.

- Burt, V. L., Whelton, P., Roccella, E. J., Brown, C., Cutler, J. A., Higgins, M., Horan, M. J. and Labarthe, D. (1995b) Prevalence of hypertension in the US adult population. Results from the Third National Health and Nutrition Examination Survey, 1988-1991. *Hypertension*, **25**, 305-313.
- Busjahn, A., Aydin, A., Uhlmann, R. et al. (2002) Serum- and glucocorticoid-regulated kinase (SGK1) gene and blood pressure. *Hypertension*, **40**, 256-260.
- Busjahn, A. and Luft, F. C. (2003) Twin studies in the analysis of minor physiological differences between individuals. *Cell Physiol Biochem*, **13**, 51-58.
- Butterworth, M. B., Edinger, R. S., Frizzell, R. A. and Johnson, J. P. (2009) Regulation of the epithelial sodium channel by membrane trafficking. *American journal of physiology*, **296**, F10-24.
- Butterworth, M. B., Edinger, R. S., Johnson, J. P. and Frizzell, R. A. (2005) Acute ENaC stimulation by cAMP in a kidney cell line is mediated by exocytic insertion from a recycling channel pool. *The Journal of general physiology*, **125**, 81-101.
- Caldwell, R. A., Boucher, R. C. and Stutts, M. J. (2004) Serine protease activation of near-silent epithelial Na⁺ channels. *Am J Physiol Cell Physiol*, **286**, C190-194.
- Caldwell, R. A., Boucher, R. C. and Stutts, M. J. (2005) Neutrophil elastase activates near-silent epithelial Na⁺ channels and increases airway epithelial Na⁺ transport. *Am J Physiol Lung Cell Mol Physiol*, **288**, L813-819.
- Campese, V. M. and Park, J. (2006) The kidney and hypertension: over 70 years of research. *Journal of nephrology*, **19**, 691-698.
- Canessa, C. M., Horisberger, J. D. and Rossier, B. C. (1993a) Epithelial sodium channel related to proteins involved in neurodegeneration. *Nature*, **361**, 467-470.

- Canessa, C. M., Horisberger, J. D., Schild, L. and Rossier, B. C. (1995) Expression cloning of the epithelial sodium channel. *Kidney international*, **48**, 950-955.
- Canessa, C. M., Merillat, A. M. and Rossier, B. C. (1994a) Membrane topology of the epithelial sodium channel in intact cells. *The American journal of physiology*, **267**, C1682-1690.
- Canessa, C. M., Schild, L., Buell, G., Thorens, B., Gautschi, I., Horisberger, J. D. and Rossier, B. C. (1994b) Amiloride-sensitive epithelial Na⁺ channel is made of three homologous subunits. *Nature*, **367**, 463-467.
- Canessa, M., Romero, J. R., Ruiz-Opazo, N. and Herrera, V. L. (1993b) The alpha 1 Na(+)-K⁺ pump of the Dahl salt-sensitive rat exhibits altered Na⁺ modulation of K⁺ transport in red blood cells. *The Journal of membrane biology*, **134**, 107-122.
- Carattino, M. D., Edinger, R. S., Grieser, H. J., Wise, R., Neumann, D., Schlattner, U., Johnson, J. P., Kleyman, T. R. and Hallows, K. R. (2005) Epithelial sodium channel inhibition by AMP-activated protein kinase in oocytes and polarized renal epithelial cells. *The Journal of biological chemistry*, **280**, 17608-17616.
- Carattino, M. D., Hill, W. G. and Kleyman, T. R. (2003) Arachidonic acid regulates surface expression of epithelial sodium channels. *The Journal of biological chemistry*, **278**, 36202-36213.
- Carattino, M. D., Hughey, R. P. and Kleyman, T. R. (2008) Proteolytic processing of the epithelial sodium channel gamma subunit has a dominant role in channel activation. *The Journal of biological chemistry*, **283**, 25290-25295.

- Carattino, M. D., Liu, W., Hill, W. G., Satlin, L. M. and Kleyman, T. R. (2007) Lack of a role of membrane-protein interactions in flow-dependent activation of ENaC. *American journal of physiology*, **293**, F316-324.
- Carattino, M. D., Sheng, S., Bruns, J. B., Pilewski, J. M., Hughey, R. P. and Kleyman, T. R. (2006) The epithelial Na⁺ channel is inhibited by a peptide derived from proteolytic processing of its alpha subunit. *The Journal of biological chemistry*, **281**, 18901-18907.
- Carithers, J., Bealer, S. L., Brody, M. J. and Johnson, A. K. (1980) Fine structural evidence of degeneration in supraoptic nucleus and subfornical organ of rats with lesions in the anteroventral third ventricle. *Brain research*, **201**, 1-12.
- Carlson, S. H., Roysomutti, S., Peng, N. and Wyss, J. M. (2001) The role of the central nervous system in NaCl-sensitive hypertension in spontaneously hypertensive rats. *American journal of hypertension*, **14**, 155S-162S.
- Chakfe, Y. and Bourque, C. W. (2001) Peptidergic excitation of supraoptic nucleus neurons: involvement of stretch-inactivated cation channels. *Experimental neurology*, **171**, 210-218.
- Chalfant, M. L., Denton, J. S., Langloh, A. L., Karlson, K. H., Loffing, J., Benos, D. J. and Stanton, B. A. (1999) The NH₂ terminus of the epithelial sodium channel contains an endocytic motif. *The Journal of biological chemistry*, **274**, 32889-32896.
- Chang, S. S., Grunder, S., Hanukoglu, A. et al. (1996) Mutations in subunits of the epithelial sodium channel cause salt wasting with hyperkalaemic acidosis, pseudohypoaldosteronism type 1. *Nature genetics*, **12**, 248-253.

- Chen, L., Reif, M. C. and Schafer, J. A. (1991) Clonidine and PGE₂ have different effects on Na⁺ and water transport in rat and rabbit CCD. *The American journal of physiology*, **261**, F126-136.
- Chen, L., Williams, S. K. and Schafer, J. A. (1990) Differences in synergistic actions of vasopressin and deoxycorticosterone in rat and rabbit CCD. *The American journal of physiology*, **259**, F147-156.
- Chen, Q. H. and Toney, G. M. (2001) AT(1)-receptor blockade in the hypothalamic PVN reduces central hyperosmolality-induced renal sympathoexcitation. *American journal of physiology*, **281**, R1844-1853.
- Chen, S. Y., Bhargava, A., Mastroberardino, L., Meijer, O. C., Wang, J., Buse, P., Firestone, G. L., Verrey, F. and Pearce, D. (1999) Epithelial sodium channel regulated by aldosterone-induced protein sgk. *Proceedings of the National Academy of Sciences of the United States of America*, **96**, 2514-2519.
- Chen, X. J., Eaton, D. C. and Jain, L. (2002) Beta-adrenergic regulation of amiloride-sensitive lung sodium channels. *Am J Physiol Lung Cell Mol Physiol*, **282**, L609-620.
- Chou, S. Y., Spitalewitz, S., Faubert, P. F., Park, I. Y. and Porush, J. G. (1984) Inner medullary hemodynamics in chronic salt-depleted dogs. *The American journal of physiology*, **246**, F146-154.
- Cicila, G. T., Garrett, M. R., Lee, S. J., Liu, J., Dene, H. and Rapp, J. P. (2001) High-resolution mapping of the blood pressure QTL on chromosome 7 using Dahl rat congenic strains. *Genomics*, **72**, 51-60.

- Cirillo, M., Capasso, G., Di Leo, V. A. and De Santo, N. G. (1994) A history of salt. *American journal of nephrology*, **14**, 426-431.
- Civan, M. M., Peterson-Yantorno, K., Sanchez-Torres, J. and Coca-Prados, M. (1997) Potential contribution of epithelial Na⁺ channel to net secretion of aqueous humor. *The Journal of experimental zoology*, **279**, 498-503.
- Collier, D. M. and Snyder, P. M. (2009a) Extracellular chloride regulates the epithelial sodium channel. *The Journal of biological chemistry*, **284**, 29320-29325.
- Collier, D. M. and Snyder, P. M. (2009b) Extracellular protons regulate human ENaC by modulating Na⁺ self-inhibition. *The Journal of biological chemistry*, **284**, 792-798.
- Collier, D. M. and Snyder, P. M. (2010) Identification of ENaC inter-subunit Cl⁻ inhibitory residues suggests a trimeric {alpha}{gamma}{beta} channel architecture. *The Journal of biological chemistry*.
- Condon, J. C., Pezzi, V., Drummond, B. M., Yin, S. and Rainey, W. E. (2002) Calmodulin-dependent kinase I regulates adrenal cell expression of aldosterone synthase. *Endocrinology*, **143**, 3651-3657.
- Couloigner, V., Fay, M., Djelidi, S., Farman, N., Escoubet, B., Runembert, I., Sterkers, O., Friedlander, G. and Ferrary, E. (2001) Location and function of the epithelial Na channel in the cochlea. *American journal of physiology*, **280**, F214-222.
- Cover, C. M., Wang, J. M., St Lezin, E., Kurtz, T. W. and Mellon, S. H. (1995) Molecular variants in the P450c11AS gene as determinants of aldosterone synthase activity in the Dahl rat model of hypertension. *The Journal of biological chemistry*, **270**, 16555-16560.

- Cowley, A. W., Jr. (1997) Role of the renal medulla in volume and arterial pressure regulation. *The American journal of physiology*, **273**, R1-15.
- Crone, C. and Olesen, S. P. (1982) Electrical resistance of brain microvascular endothelium. *Brain research*, **241**, 49-55.
- Crowley, S. D. and Coffman, T. M. (2007) In hypertension, the kidney rules. *Current hypertension reports*, **9**, 148-153.
- Crowley, S. D., Gurley, S. B. and Coffman, T. M. (2007) AT(1) receptors and control of blood pressure: the kidney and more. *Trends in cardiovascular medicine*, **17**, 30-34.
- Crowley, S. D., Gurley, S. B., Oliverio, M. I. et al. (2005) Distinct roles for the kidney and systemic tissues in blood pressure regulation by the renin-angiotensin system. *The Journal of clinical investigation*, **115**, 1092-1099.
- Cui, Y., Su, Y. R., Rutkowski, M., Reif, M., Menon, A. G. and Pun, R. Y. (1997) Loss of protein kinase C inhibition in the beta-T594M variant of the amiloride-sensitive Na⁺ channel. *Proceedings of the National Academy of Sciences of the United States of America*, **94**, 9962-9966.
- Curtis, J. J., Luke, R. G., Dustan, H. P., Kashgarian, M., Whelchel, J. D., Jones, P. and Diethelm, A. G. (1983) Remission of essential hypertension after renal transplantation. *The New England journal of medicine*, **309**, 1009-1015.
- Dahl, L. K. and Heine, M. (1975) Primary role of renal homografts in setting chronic blood pressure levels in rats. *Circulation research*, **36**, 692-696.
- Dahl, L. K., Heine, M. and Tassinari, L. (1962a) Effects of chronic excess salt ingestion. Evidence that genetic factors play an important role in susceptibility to

- experimental hypertension. *The Journal of experimental medicine*, **115**, 1173-1190.
- Dahl, L. K., Heine, M. and Tassinari, L. (1962b) Role of genetic factors in susceptibility to experimental hypertension due to chronic excess salt ingestion. *Nature*, **194**, 480-482.
- Dahl, L. K., Heine, M. and Thompson, K. (1972) Genetic influence of renal homografts on the blood pressure of rats from different strains. *Proceedings of the Society for Experimental Biology and Medicine. Society for Experimental Biology and Medicine (New York, N.Y.*, **140**, 852-856.
- Dahl, L. K., Heine, M. and Thompson, K. (1974) Genetic influence of the kidneys on blood pressure. Evidence from chronic renal homografts in rats with opposite predispositions to hypertension. *Circulation research*, **40**, 94-101.
- Davson, H. and Segal, M. (1996) *The secretion of cerebrospinal fluid. In: Physiology of the Cerebrospinal Fluid and Blood Brain Barriers* CRC, Boca Raton, FL.
- Davson, H. and Segal, M. B. (1971) Secretion and drainage of the cerebrospinal fluid. *Acta neurologica latinoamericana*, **1**, Suppl 1:99-118.
- De Kloet, E. R. (2004) Hormones and the stressed brain. *Annals of the New York Academy of Sciences*, **1018**, 1-15.
- Debonneville, C., Flores, S. Y., Kamynina, E. et al. (2001) Phosphorylation of Nedd4-2 by Sgk1 regulates epithelial Na(+) channel cell surface expression. *The EMBO journal*, **20**, 7052-7059.

- DeFronzo, R. A., Cooke, C. R., Andres, R., Faloona, G. R. and Davis, P. J. (1975) The effect of insulin on renal handling of sodium, potassium, calcium, and phosphate in man. *The Journal of clinical investigation*, **55**, 845-855.
- Del Bigio, M. R. (1995a) The ependyma: a protective barrier between brain and cerebrospinal fluid. *Glia*, **14**, 1-13.
- Del Bigio, M. R. (1995b) Ependymal reactions to injury. A review. *Journal of neuropathology and experimental neurology*, **54**, 405-406.
- Del Bigio, M. R. and Bruni, J. E. (1986) Reaction of rabbit lateral periventricular tissue to shunt tubing implants. *Journal of neurosurgery*, **64**, 932-940.
- DeLong, J. and Civan, M. M. (1984) Apical sodium entry in split frog skin: current-voltage relationship. *The Journal of membrane biology*, **82**, 25-40.
- Denton, D. A., McKinley, M. J. and Weisinger, R. S. (1996) Hypothalamic integration of body fluid regulation. *Proceedings of the National Academy of Sciences of the United States of America*, **93**, 7397-7404.
- Diakov, A. and Korbmacher, C. (2004) A novel pathway of epithelial sodium channel activation involves a serum- and glucocorticoid-inducible kinase consensus motif in the C terminus of the channel's alpha-subunit. *The Journal of biological chemistry*, **279**, 38134-38142.
- DiBona, G. F. (1986) Neural mechanisms in body fluid homeostasis. *Federation proceedings*, **45**, 2871-2877.
- DiBona, G. F. and Kopp, U. C. (1997) Neural control of renal function. *Physiological reviews*, **77**, 75-197.

- Djelidi, S., Fay, M., Cluzeaud, F., Escoubet, B., Eugene, E., Capurro, C., Bonvalet, J. P., Farman, N. and Blot-Chabaud, M. (1997) Transcriptional regulation of sodium transport by vasopressin in renal cells. *The Journal of biological chemistry*, **272**, 32919-32924.
- Dong, Y. B., Zhu, H. D., Baker, E. H., Sagnella, G. A., MacGregor, G. A., Carter, N. D., Wicks, P. D., Cook, D. G. and Cappuccio, F. P. (2001) T594M and G442V polymorphisms of the sodium channel beta subunit and hypertension in a black population. *Journal of human hypertension*, **15**, 425-430.
- Drummond, H. A. (2009) Yes, no, maybe so: ENaC proteins as mediators of renal myogenic constriction. *Hypertension*, **54**, 962-963.
- Drummond, H. A., Abboud, F. M. and Welsh, M. J. (2000) Localization of beta and gamma subunits of ENaC in sensory nerve endings in the rat foot pad. *Brain research*, **884**, 1-12.
- Drummond, H. A., Gebremedhin, D. and Harder, D. R. (2004) Degenerin/epithelial Na⁺ channel proteins: components of a vascular mechanosensor. In: *Hypertension*, Vol. 44, pp. 643-648.
- Drummond, H. A., Grifoni, S. C. and Jernigan, N. L. (2008a) A new trick for an old dogma: ENaC proteins as mechanotransducers in vascular smooth muscle. *Physiology (Bethesda, Md)*, **23**, 23-31.
- Drummond, H. A., Jernigan, N. L. and Grifoni, S. C. (2008b) Sensing tension: epithelial sodium channel/acid-sensing ion channel proteins in cardiovascular homeostasis. *Hypertension*, **51**, 1265-1271.

- Drummond, H. A., Price, M. P., Welsh, M. J. and Abboud, F. M. (1998) A molecular component of the arterial baroreceptor mechanotransducer. *Neuron*, **21**, 1435-1441.
- Drummond, H. A., Welsh, M. J. and Abboud, F. M. (2001) ENaC subunits are molecular components of the arterial baroreceptor complex. *Annals of the New York Academy of Sciences*, **940**, 42-47.
- Duc, C., Farman, N., Canessa, C. M., Bonvalet, J. P. and Rossier, B. C. (1994) Cell-specific expression of epithelial sodium channel alpha, beta, and gamma subunits in aldosterone-responsive epithelia from the rat: localization by in situ hybridization and immunocytochemistry. *The Journal of cell biology*, **127**, 1907-1921.
- Dyka, F. M., May, C. A. and Enz, R. (2005) Subunits of the epithelial sodium channel family are differentially expressed in the retina of mice with ocular hypertension. *J Neurochem*, **94**, 120-128.
- Eaton, D. C., Chen, J., Ramosevac, S., Matalon, S. and Jain, L. (2004) Regulation of Na⁺ channels in lung alveolar type II epithelial cells. *Proceedings of the American Thoracic Society*, **1**, 10-16.
- Eaton, D. C., Helms, M. N., Koval, M., Bao, H. F. and Jain, L. (2009) The contribution of epithelial sodium channels to alveolar function in health and disease. *Annual review of physiology*, **71**, 403-423.
- Eaton, D. C., Malik, B., Saxena, N. C., Al-Khalili, O. K. and Yue, G. (2001) Mechanisms of aldosterone's action on epithelial Na⁺ transport. *The Journal of membrane biology*, **184**, 313-319.

- Ecelbarger, C. A., Kim, G. H., Terris, J., Masilamani, S., Mitchell, C., Reyes, I., Verbalis, J. G. and Knepper, M. A. (2000) Vasopressin-mediated regulation of epithelial sodium channel abundance in rat kidney. *American journal of physiology*, **279**, F46-53.
- Ecelbarger, C. A., Kim, G. H., Wade, J. B. and Knepper, M. A. (2001) Regulation of the abundance of renal sodium transporters and channels by vasopressin. *Experimental neurology*, **171**, 227-234.
- Edelfors, S. (1975) Distribution of sodium, potassium and lithium in the brain of lithium-treated rats. *Acta Pharmacol Toxicol (Copenh)*, **37**, 387-392.
- Elliott, P., Dyer, A. and Stamler, R. (1989) The INTERSALT study: results for 24 hour sodium and potassium, by age and sex. INTERSALT Co-operative Research Group. *Journal of human hypertension*, **3**, 323-330.
- Elliott, P., Stamler, J., Nichols, R., Dyer, A. R., Stamler, R., Kesteloot, H. and Marmot, M. (1996) Intersalt revisited: further analyses of 24 hour sodium excretion and blood pressure within and across populations. Intersalt Cooperative Research Group. *BMJ (Clinical research ed)*, **312**, 1249-1253.
- Ennis, S. R., Ren, X. D. and Betz, A. L. (1996) Mechanisms of sodium transport at the blood-brain barrier studied with in situ perfusion of rat brain. *J Neurochem*, **66**, 756-763.
- Ergonul, Z., Frindt, G. and Palmer, L. G. (2006) Regulation of maturation and processing of ENaC subunits in the rat kidney. *American journal of physiology*, **291**, F683-693.

- Erinoff, L., Heller, A. and Oparil, S. (1975) Prevention of hypertension in the SH rat: effects of differential central catecholamine depletion. *Proceedings of the Society for Experimental Biology and Medicine. Society for Experimental Biology and Medicine (New York, N.Y.* **150**, 748-754.
- Escoubet, B., Coureau, C., Blot-Chabaud, M., Bonvalet, J. P. and Farman, N. (1996) Corticosteroid receptor mRNA expression is unaffected by corticosteroids in rat kidney, heart, and colon. *The American journal of physiology*, **270**, C1343-1353.
- Escoubet, B., Coureau, C., Bonvalet, J. P. and Farman, N. (1997) Noncoordinate regulation of epithelial Na channel and Na pump subunit mRNAs in kidney and colon by aldosterone. *The American journal of physiology*, **272**, C1482-1491.
- Fang, Z., Carlson, S. H., Peng, N. and Wyss, J. M. (2000) Circadian rhythm of plasma sodium is disrupted in spontaneously hypertensive rats fed a high-NaCl diet. *American journal of physiology*, **278**, R1490-1495.
- Farjah, M., Roxas, B. P., Geenen, D. L. and Danziger, R. S. (2003) Dietary salt regulates renal SGK1 abundance: relevance to salt sensitivity in the Dahl rat. *Hypertension*, **41**, 874-878.
- Farman, N., Talbot, C. R., Boucher, R., Fay, M., Canessa, C., Rossier, B. and Bonvalet, J. P. (1997) Noncoordinated expression of alpha-, beta-, and gamma-subunit mRNAs of epithelial Na⁺ channel along rat respiratory tract. *The American journal of physiology*, **272**, C131-141.
- Fedorova, O. V., Agalakova, N. I., Talan, M. I., Lakatta, E. G. and Bagrov, A. Y. (2005) Brain ouabain stimulates peripheral marinobufagenin via angiotensin II signalling in NaCl-loaded Dahl-S rats. *Journal of hypertension*, **23**, 1515-1523.

- Fedorova, O. V., Talan, M. I., Agalakova, N. I., Lakatta, E. G. and Bagrov, A. Y. (2002) Endogenous ligand of alpha(1) sodium pump, marinobufagenin, is a novel mediator of sodium chloride--dependent hypertension. *Circulation*, **105**, 1122-1127.
- Ferrandi, M., Manunta, P., Balzan, S., Hamlyn, J. M., Bianchi, G. and Ferrari, P. (1997) Ouabain-like factor quantification in mammalian tissues and plasma: comparison of two independent assays. *Hypertension*, **30**, 886-896.
- Ferrandi, M., Minotti, E., Salardi, S., Florio, M., Bianchi, G. and Ferrari, P. (1992) Ouabainlike factor in Milan hypertensive rats. *The American journal of physiology*, **263**, F739-748.
- Ferrandi, M., Salardi, S., Tripodi, G. et al. (1999) Evidence for an interaction between adducin and Na(+)-K(+)-ATPase: relation to genetic hypertension. *The American journal of physiology*, **277**, H1338-1349.
- Findling, J. W., Raff, H., Hansson, J. H. and Lifton, R. P. (1997) Liddle's syndrome: prospective genetic screening and suppressed aldosterone secretion in an extended kindred. *The Journal of clinical endocrinology and metabolism*, **82**, 1071-1074.
- Fink, G. D. and Bryan, W. J. (1982) Influence of forebrain periventricular lesions on the development of renal hypertension in rabbits. *Hypertension*, **4**, 155-160.
- Firestone, G. L., Giampaolo, J. R. and O'Keefe, B. A. (2003) Stimulus-dependent regulation of serum and glucocorticoid inducible protein kinase (SGK) transcription, subcellular localization and enzymatic activity. *Cell Physiol Biochem*, **13**, 1-12.

- Firsov, D., Gautschi, I., Merillat, A. M., Rossier, B. C. and Schild, L. (1998) The heterotetrameric architecture of the epithelial sodium channel (ENaC). *The EMBO journal*, **17**, 344-352.
- Firsov, D., Robert-Nicoud, M., Gruender, S., Schild, L. and Rossier, B. C. (1999) Mutational analysis of cysteine-rich domains of the epithelium sodium channel (ENaC). Identification of cysteines essential for channel expression at the cell surface. *The Journal of biological chemistry*, **274**, 2743-2749.
- Firsov, D., Schild, L., Gautschi, I., Merillat, A. M., Schneeberger, E. and Rossier, B. C. (1996) Cell surface expression of the epithelial Na channel and a mutant causing Liddle syndrome: a quantitative approach. *Proceedings of the National Academy of Sciences of the United States of America*, **93**, 15370-15375.
- Flament-Durand, J. and Brion, J. P. (1985) Tanycytes: morphology and functions: a review. *Int Rev Cytol*, **96**, 121-155.
- Franco, V. and Oparil, S. (2006) Salt sensitivity, a determinant of blood pressure, cardiovascular disease and survival. *Journal of the American College of Nutrition*, **25**, 247S-255S.
- Fricke, B., Lints, R., Stewart, G., Drummond, H., Dodt, G., Driscoll, M. and von Düring, M. (2000) Epithelial Na⁺ channels and stomatin are expressed in rat trigeminal mechanosensory neurons. *Cell and tissue research*, **299**, 327-334.
- Friedman, R., Tassinari, L. M., Heine, M. and Iwai, J. (1979) Differential development of salt-induced and renal hypertension in Dahl hypertension-sensitive rats after neonatal sympathectomy. *Clin Exp Hypertens*, **1**, 779-799.

- Friedrich, B., Feng, Y., Cohen, P., Risler, T., Vandewalle, A., Broer, S., Wang, J., Pearce, D. and Lang, F. (2003) The serine/threonine kinases SGK2 and SGK3 are potent stimulators of the epithelial Na⁺ channel alpha,beta,gamma-ENaC. *Pflugers Arch*, **445**, 693-696.
- Friedrich, B., Warntges, S., Klingel, K. et al. (2002) Up-regulation of the human serum and glucocorticoid-dependent kinase 1 in glomerulonephritis. *Kidney & blood pressure research*, **25**, 303-307.
- Frindt, G. and Burg, M. B. (1972) Effect of vasopressin on sodium transport in renal cortical collecting tubules. *Kidney international*, **1**, 224-231.
- Frindt, G., Ergonul, Z. and Palmer, L. G. (2007) Na channel expression and activity in the medullary collecting duct of rat kidney. *American journal of physiology*, **292**, F1190-1196.
- Frindt, G., Ergonul, Z. and Palmer, L. G. (2008) Surface expression of epithelial Na channel protein in rat kidney. *The Journal of general physiology*, **131**, 617-627.
- Fronius, M., Bogdan, R., Althaus, M., Morty, R. E. and Clauss, W. G. (2010) Epithelial Na⁺ channels derived from human lung are activated by shear force. *Respiratory physiology & neurobiology*, **170**, 113-119.
- Fronius, M. and Clauss, W. G. (2008) Mechano-sensitivity of ENaC: may the (shear) force be with you. *Pflugers Arch*, **455**, 775-785.
- Fuller, P. J., Brennan, F. E. and Burgess, J. S. (2000) Acute differential regulation by corticosteroids of epithelial sodium channel subunit and Nedd4 mRNA levels in the distal colon. *Pflugers Arch*, **441**, 94-101.

- Gabor, A. and Leenen, F. H. (2009a) Mechanisms in the PVN mediating local and central sodium-induced hypertension in Wistar rats. *American journal of physiology. Regulatory, integrative and comparative physiology*, **296**, R618-630.
- Gabor, A. and Leenen, F. H. (2009b) Mechanisms in the PVN mediating local and central sodium-induced hypertension in Wistar rats. *American journal of physiology*, **296**, R618-630.
- Gadallah, M. F., Abreo, K. and Work, J. (1995) Liddle's syndrome, an underrecognized entity: a report of four cases, including the first report in black individuals. *Am J Kidney Dis*, **25**, 829-835.
- Gaillard, E. A., Kota, P., Gentzsch, M., Dokholyan, N. V., Stutts, M. J. and Tarran, R. (2010) Regulation of the epithelial Na⁺ channel and airway surface liquid volume by serine proteases. *Pflugers Arch*, **460**, 1-17.
- Garcia-Caballero, A., Rasmussen, J. E., Gaillard, E., Watson, M. J., Olsen, J. C., Donaldson, S. H., Stutts, M. J. and Tarran, R. (2009) SPLUNC1 regulates airway surface liquid volume by protecting ENaC from proteolytic cleavage. *Proceedings of the National Academy of Sciences of the United States of America*, **106**, 11412-11417.
- Gardner, D. S., Jackson, A. A. and Langley-Evans, S. C. (1997) Maintenance of maternal diet-induced hypertension in the rat is dependent on glucocorticoids. *Hypertension*, **30**, 1525-1530.
- Garrett, M. R., Dene, H., Walder, R., Zhang, Q. Y., Cicila, G. T., Assadnia, S., Deng, A. Y. and Rapp, J. P. (1998) Genome scan and congenic strains for blood pressure QTL using Dahl salt-sensitive rats. *Genome research*, **8**, 711-723.

- Garty, H. and Palmer, L. G. (1997) Epithelial sodium channels: function, structure, and regulation. *Physiological reviews*, **77**, 359-396.
- Gauthier, P., Reis, D. J. and Nathan, M. A. (1981) Arterial hypertension elicited either by lesions or by electrical stimulations of the rostral hypothalamus in the rat. *Brain research*, **211**, 91-105.
- Geerling, J. C. and Loewy, A. D. (2008) Central regulation of sodium appetite. *Experimental physiology*, **93**, 177-209.
- Gesing, A., Bilanz-Bleuel, A., Droste, S. K., Linthorst, A. C., Holsboer, F. and Reul, J. M. (2001) Psychological stress increases hippocampal mineralocorticoid receptor levels: involvement of corticotropin-releasing hormone. *J Neurosci*, **21**, 4822-4829.
- Gibbs, C. R., Lip, G. Y. and Beevers, D. G. (2000) Salt and cardiovascular disease: clinical and epidemiological evidence. *Journal of cardiovascular risk*, **7**, 9-13.
- Glorioso, N., Filigheddu, F., Troffa, C., Soro, A., Parpaglia, P. P., Tsikoudakis, A., Myers, R. H., Herrera, V. L. and Ruiz-Opazo, N. (2001) Interaction of alpha(1)-Na,K-ATPase and Na,K,2Cl-cotransporter genes in human essential hypertension. *Hypertension*, **38**, 204-209.
- Glorioso, N., Herrera, V. L., Bagamasbad, P., Filigheddu, F., Troffa, C., Argiolas, G., Bulla, E., Decano, J. L. and Ruiz-Opazo, N. (2007) Association of ATP1A1 and deaer single-nucleotide polymorphism haplotypes with essential hypertension: sex-specific and haplotype-specific effects. *Circulation research*, **100**, 1522-1529.
- Goldstein, G. W. and Betz, A. L. (1986) The blood-brain barrier. *Scientific American*, **255**, 74-83.

- Golestaneh, N., De Kozak, Y., Klein, C. and Mirshahi, M. (2001) Epithelial sodium channel and the mineralocorticoid receptor in cultured rat Muller glial cells. *Glia*, **33**, 160-168.
- Golestaneh, N., Nicolas, C., Picaud, S., Ferrari, P. and Mirshahi, M. (2000) The epithelial sodium channel (ENaC) in rodent retina, ontogeny and molecular identity. *Current eye research*, **21**, 703-709.
- Golestaneh, N., Picaud, S. and Mirshahi, M. (2002) The mineralocorticoid receptor in rodent retina: ontogeny and molecular identity. *Molecular vision*, **8**, 221-225.
- Gomez-Sanchez, C. E., Zhou, M. Y., Cozza, E. N., Morita, H., Foecking, M. F. and Gomez-Sanchez, E. P. (1997) Aldosterone biosynthesis in the rat brain. *Endocrinology*, **138**, 3369-3373.
- Gomez-Sanchez, E. P., Ahmad, N., Romero, D. G. and Gomez-Sanchez, C. E. (2005a) Is aldosterone synthesized within the rat brain? *Am J Physiol Endocrinol Metab*, **288**, E342-346.
- Gomez-Sanchez, E. P., Fort, C. and Thwaites, D. (1992) Central mineralocorticoid receptor antagonism blocks hypertension in Dahl S/JR rats. *The American journal of physiology*, **262**, E96-99.
- Gomez-Sanchez, E. P. and Gomez-Sanchez, C. E. (1994) Effect of central amiloride infusion on mineralocorticoid hypertension. *The American journal of physiology*, **267**, E754-758.
- Gomez-Sanchez, E. P. and Gomez-Sanchez, C. E. (1995) Effect of central infusion of benzamil on Dahl S rat hypertension. *The American journal of physiology*, **269**, H1044-1047.

- Gomez-Sanchez, E. P., Gomez-Sanchez, C. E. and Fort, C. (1994) Immunization of Dahl SS/jr rats with an ouabain conjugate mitigates hypertension. *American journal of hypertension*, **7**, 591-596.
- Gomez-Sanchez, E. P., Gomez-Sanchez, C. M., Plonczynski, M. and Gomez-Sanchez, C. E. (2010) Aldosterone synthesis in the brain contributes to Dahl salt-sensitive rat hypertension. *Experimental physiology*, **95**, 120-130.
- Gomez-Sanchez, E. P., Samuel, J., Vergara, G. and Ahmad, N. (2005b) Effect of 3beta-hydroxysteroid dehydrogenase inhibition by trilostane on blood pressure in the Dahl salt-sensitive rat. *American journal of physiology*, **288**, R389-393.
- Gomez-Sanchez, E. P., Zhou, M. and Gomez-Sanchez, C. E. (1996) Mineralocorticoids, salt and high blood pressure. *Steroids*, **61**, 184-188.
- Gonzalez-Nicolini, V. and McGinty, J. F. (2002) Gene expression profile from the striatum of amphetamine-treated rats: a cDNA array and in situ hybridization histochemical study. *Brain Res Gene Expr Patterns*, **1**, 193-198.
- Gordon, F. J., Haywood, J. R., Brody, M. J. and Johnson, A. K. (1982) Effect of lesions of the anteroventral third ventricle (AV3V) on the development of hypertension in spontaneously hypertensive rats. *Hypertension*, **4**, 387-393.
- Gotoh, H., Okumura, A., Nagai, K. and Okumura, N. (2008) Localization of phosphotyrosine489-beta-adducin immunoreactivity in the hypothalamic tanycytes and its involvement in energy homeostasis. *Brain research*, **1228**, 97-106.
- Goulet, C. C., Volk, K. A., Adams, C. M., Prince, L. S., Stokes, J. B. and Snyder, P. M. (1998) Inhibition of the epithelial Na⁺ channel by interaction of Nedd4 with a PY

- motif deleted in Liddle's syndrome. *The Journal of biological chemistry*, **273**, 30012-30017.
- Greig, E. R., Baker, E. H., Mathialahan, T., Boot-Handford, R. P. and Sandle, G. I. (2002) Segmental variability of ENaC subunit expression in rat colon during dietary sodium depletion. *Pflugers Arch*, **444**, 476-483.
- Grifoni, S. C., Chiposi, R., McKey, S. E., Ryan, M. J. and Drummond, H. A. Altered whole kidney blood flow autoregulation in a mouse model of reduced beta-ENaC. *American journal of physiology*, **298**, F285-292.
- Grim, C. E., Miller, J. Z., Luft, F. C., Christian, J. C. and Weinberger, M. H. (1979) Genetic influences on renin, aldosterone, and the renal excretion of sodium and potassium following volume expansion and contraction in normal man. *Hypertension*, **1**, 583-590.
- Grob, M., Drolet, G. and Mougnot, D. (2004) Specific Na⁺ sensors are functionally expressed in a neuronal population of the median preoptic nucleus of the rat. *J Neurosci*, **24**, 3974-3984.
- Grossmann, C. and Gekle, M. (2009) New aspects of rapid aldosterone signaling. *Molecular and cellular endocrinology*, **308**, 53-62.
- Grunder, S., Muller, A. and Ruppertsberg, J. P. (2001) Developmental and cellular expression pattern of epithelial sodium channel alpha, beta and gamma subunits in the inner ear of the rat. *The European journal of neuroscience*, **13**, 641-648.
- Grunder, S., Zagato, L., Yagil, C., Yagil, Y., Sassard, J. and Rossier, B. C. (1997) Polymorphisms in the carboxy-terminus of the epithelial sodium channel in rat models for hypertension. *Journal of hypertension*, **15**, 173-179.

- Guan, Z., Pollock, J. S., Cook, A. K., Hobbs, J. L. and Inscho, E. W. (2009) Effect of epithelial sodium channel blockade on the myogenic response of rat juxtamedullary afferent arterioles. *Hypertension*, **54**, 1062-1069.
- Guidi, E., Menghetti, D., Milani, S., Montagnino, G., Palazzi, P. and Bianchi, G. (1996) Hypertension may be transplanted with the kidney in humans: a long-term historical prospective follow-up of recipients grafted with kidneys coming from donors with or without hypertension in their families. *J Am Soc Nephrol*, **7**, 1131-1138.
- Guipponi, M., Vuagniaux, G., Wattenhofer, M. et al. (2002) The transmembrane serine protease (TMPRSS3) mutated in deafness DFNB8/10 activates the epithelial sodium channel (ENaC) in vitro. *Human molecular genetics*, **11**, 2829-2836.
- Guyton, A. C. (1990a) Long-term arterial pressure control: an analysis from animal experiments and computer and graphic models. *The American journal of physiology*, **259**, R865-877.
- Guyton, A. C. (1990b) Renal function curves and control of body fluids and arterial pressure. *Acta physiologica Scandinavica*, **591**, 107-113.
- Guyton, A. C. (1990c) The surprising kidney-fluid mechanism for pressure control--its infinite gain! *Hypertension*, **16**, 725-730.
- Gyurko, R., Wielbo, D. and Phillips, M. I. (1993) Antisense inhibition of AT1 receptor mRNA and angiotensinogen mRNA in the brain of spontaneously hypertensive rats reduces hypertension of neurogenic origin. *Regulatory peptides*, **49**, 167-174.
- Hager, H., Kwon, T. H., Vinnikova, A. K., Masilamani, S., Brooks, H. L., Frokiaer, J., Knepper, M. A. and Nielsen, S. (2001) Immunocytochemical and immunoelectron

- microscopic localization of alpha-, beta-, and gamma-ENaC in rat kidney. *American journal of physiology*, **280**, F1093-1106.
- Hall, J. E. (1986) Control of sodium excretion by angiotensin II: intrarenal mechanisms and blood pressure regulation. *The American journal of physiology*, **250**, R960-972.
- Hall, J. E., Brands, M. W. and Shek, E. W. (1996) Central role of the kidney and abnormal fluid volume control in hypertension. *Journal of human hypertension*, **10**, 633-639.
- Hall, J. E., Guyton, A. C., Coleman, T. G., Mizelle, H. L. and Woods, L. L. (1986) Regulation of arterial pressure: role of pressure natriuresis and diuresis. *Federation proceedings*, **45**, 2897-2903.
- Hall, J. E., Guyton, A. C. and Mizelle, H. L. (1990) Role of the renin-angiotensin system in control of sodium excretion and arterial pressure. *Acta physiologica Scandinavica*, **591**, 48-62.
- Hallows, K. R., Wang, H., Edinger, R. S. et al. (2009) Regulation of epithelial Na⁺ transport by soluble adenylyl cyclase in kidney collecting duct cells. *The Journal of biological chemistry*, **284**, 5774-5783.
- Han, F., Ozawa, H., Matsuda, K., Nishi, M. and Kawata, M. (2005) Colocalization of mineralocorticoid receptor and glucocorticoid receptor in the hippocampus and hypothalamus. *Neuroscience research*, **51**, 371-381.
- Hanneman, R. L. (1996) Intersalt: hypertension rise with age revisited. *BMJ (Clinical research ed)*, **312**, 1283-1284; discussion 1284-1287.

- Hano, T., Jeng, Y. and Rho, J. (1989) Norepinephrine overflow and re-uptake in perfused mesenteric arteries of Dahl salt-sensitive and salt-resistant rats. *Journal of hypertension*, **7**, 43-49.
- Hansson, J. H., Nelson-Williams, C., Suzuki, H. et al. (1995a) Hypertension caused by a truncated epithelial sodium channel gamma subunit: genetic heterogeneity of Liddle syndrome. *Nature genetics*, **11**, 76-82.
- Hansson, J. H., Schild, L., Lu, Y., Wilson, T. A., Gautschi, I., Shimkets, R., Nelson-Williams, C., Rossier, B. C. and Lifton, R. P. (1995b) A de novo missense mutation of the beta subunit of the epithelial sodium channel causes hypertension and Liddle syndrome, identifying a proline-rich segment critical for regulation of channel activity. *Proceedings of the National Academy of Sciences of the United States of America*, **92**, 11495-11499.
- Hanwell, D., Ishikawa, T., Saleki, R. and Rotin, D. (2002) Trafficking and cell surface stability of the epithelial Na⁺ channel expressed in epithelial Madin-Darby canine kidney cells. *The Journal of biological chemistry*, **277**, 9772-9779.
- Harnish, P. P. and Samuel, K. (1988) Reduced cerebrospinal fluid production in the rat and rabbit by diatrizoate. Ventriculocisternal perfusion. *Investigative radiology*, **23**, 534-536.
- Harris, E. L. and Barnard, R. (2006a) A1079T transversion in the gene for the alpha1 isophorm of the Na⁺/K⁺ ATPase in the Dahl S rat. *Journal of hypertension*, **24**, 1209-1210; author reply 1210-1203.

- Harris, E. L. and Barnard, R. (2006b) Reply to Herrera and Ruiz-Opazo's letter published in the June 2006 issue. *Journal of hypertension*, **24**, 2312-2313; author reply 2313-2316.
- Harris, M., Garcia-Caballero, A., Stutts, M. J., Firsov, D. and Rossier, B. C. (2008) Preferential assembly of epithelial sodium channel (ENaC) subunits in *Xenopus* oocytes: role of furin-mediated endogenous proteolysis. *The Journal of biological chemistry*, **283**, 7455-7463.
- Harvey, K. F., Dinudom, A., Cook, D. I. and Kumar, S. (2001) The Nedd4-like protein KIAA0439 is a potential regulator of the epithelial sodium channel. *The Journal of biological chemistry*, **276**, 8597-8601.
- Harvey, K. F., Dinudom, A., Komwatana, P., Jolliffe, C. N., Day, M. L., Parasivam, G., Cook, D. I. and Kumar, S. (1999) All three WW domains of murine Nedd4 are involved in the regulation of epithelial sodium channels by intracellular Na⁺. *The Journal of biological chemistry*, **274**, 12525-12530.
- Haywood, J. R., Buggy, J., Fink, G. D., DiBona, G. F., Johnson, A. K. and Brody, M. J. (1984) Alterations in cerebrospinal fluid sodium and osmolality in rats during one-kidney, one-wrap renal hypertension. *Clinical and experimental pharmacology & physiology*, **11**, 545-549.
- He, F. J., Markandu, N. D., Sagnella, G. A., de Wardener, H. E. and MacGregor, G. A. (2005) Plasma sodium: ignored and underestimated. *Hypertension*, **45**, 98-102.
- Helms, M. N., Chen, X. J., Ramosevac, S., Eaton, D. C. and Jain, L. (2006a) Dopamine regulation of amiloride-sensitive sodium channels in lung cells. *Am J Physiol Lung Cell Mol Physiol*, **290**, L710-L722.

- Helms, M. N., Self, J., Bao, H. F., Job, L. C., Jain, L. and Eaton, D. C. (2006b) Dopamine activates amiloride-sensitive sodium channels in alveolar type I cells in lung slice preparations. *Am J Physiol Lung Cell Mol Physiol*, **291**, L610-618.
- Herrera, V. L., Chobanian, A. V. and Ruiz-Opazo, N. (1988) Isoform-specific modulation of Na⁺, K⁺-ATPase alpha-subunit gene expression in hypertension. *Science (New York, N.Y.*, **241**, 221-223.
- Herrera, V. L., Cova, T., Sassoon, D. and Ruiz-Opazo, N. (1994) Developmental cell-specific regulation of Na⁽⁺⁾-K⁽⁺⁾-ATPase alpha 1-, alpha 2-, and alpha 3-isoform gene expression. *The American journal of physiology*, **266**, C1301-1312.
- Herrera, V. L., Emanuel, J. R., Ruiz-Opazo, N., Levenson, R. and Nadal-Ginard, B. (1987) Three differentially expressed Na,K-ATPase alpha subunit isoforms: structural and functional implications. *The Journal of cell biology*, **105**, 1855-1865.
- Herrera, V. L., Lopez, L. V. and Ruiz-Opazo, N. (2001) Alpha1 Na,K-ATPase and Na,K,2Cl-cotransporte/D3mit3 loci interact to increase susceptibility to salt-sensitive hypertension in Dahl S(HSD) rats. *Molecular medicine (Cambridge, Mass*, **7**, 125-134.
- Herrera, V. L. and Ruiz-Opazo, N. (1990) Alteration of alpha 1 Na⁺,K⁽⁺⁾-ATPase 86Rb⁺ influx by a single amino acid substitution. *Science (New York, N.Y.*, **249**, 1023-1026.
- Herrera, V. L., Xie, H. X., Lopez, L. V., Schork, N. J. and Ruiz-Opazo, N. (1998) The alpha1 Na,K-ATPase gene is a susceptibility hypertension gene in the Dahl salt-sensitiveHSD rat. *The Journal of clinical investigation*, **102**, 1102-1111.

- Hicke, L. (1997) Ubiquitin-dependent internalization and down-regulation of plasma membrane proteins. *Faseb J*, **11**, 1215-1226.
- Hicke, L. (2001) Protein regulation by monoubiquitin. *Nat Rev Mol Cell Biol*, **2**, 195-201.
- Hiyama, T. Y., Matsuda, S., Fujikawa, A., Matsumoto, M., Watanabe, E., Kajiwara, H., Niimura, F. and Noda, M. (2010) Autoimmunity to the sodium-level sensor in the brain causes essential hypernatremia. *Neuron*, **66**, 508-522.
- Hiyama, T. Y., Watanabe, E., Okado, H. and Noda, M. (2004) The subfornical organ is the primary locus of sodium-level sensing by Na(x) sodium channels for the control of salt-intake behavior. *J Neurosci*, **24**, 9276-9281.
- Hiyama, T. Y., Watanabe, E., Ono, K., Inenaga, K., Tamkun, M. M., Yoshida, S. and Noda, M. (2002) Na(x) channel involved in CNS sodium-level sensing. *Nature neuroscience*, **5**, 511-512.
- Honda, K., Negoro, H., Dyball, R. E., Higuchi, T. and Takano, S. (1990a) The osmoreceptor complex in the rat: evidence for interactions between the supraoptic and other diencephalic nuclei. *The Journal of physiology*, **431**, 225-241.
- Honda, K., Negoro, H., Higuchi, T. and Takano, S. (1990b) Activation of supraoptic neurosecretory cells by osmotic stimulation of the median preoptic nucleus. *Neuroscience letters*, **119**, 167-170.
- Hong, G., Lockhart, A., Davis, B. et al. (2003) PPARgamma activation enhances cell surface ENaCalpha via up-regulation of SGK1 in human collecting duct cells. *Faseb J*, **17**, 1966-1968.

- Hosoi, R., Matsuda, T., Asano, S., Nakamura, H., Hashimoto, H., Takuma, K. and Baba, A. (1997) Isoform-specific up-regulation by ouabain of Na⁺,K⁺-ATPase in cultured rat astrocytes. *Journal of neurochemistry*, **69**, 2189-2196.
- Hou, J., Speirs, H. J., Seckl, J. R. and Brown, R. W. (2002) Sgk1 gene expression in kidney and its regulation by aldosterone: spatio-temporal heterogeneity and quantitative analysis. *J Am Soc Nephrol*, **13**, 1190-1198.
- Hsieh, K., Lalouschek, W., Schillinger, M. et al. (2005) Impact of alphaENaC polymorphisms on the risk of ischemic cerebrovascular events: a multicenter case-control study. *Clin Chem*, **51**, 952-956.
- Huang, B. S., Ahmadi, S., Ahmad, M., White, R. A. and Leenen, F. H. (2010) Central neuronal activation and pressor responses induced by circulating ANG II: role of the brain aldosterone-"ouabain" pathway. *American journal of physiology*, **299**, H422-430.
- Huang, B. S., Amin, M. S. and Leenen, F. H. (2006a) The central role of the brain in salt-sensitive hypertension. *Current opinion in cardiology*, **21**, 295-304.
- Huang, B. S., Cheung, W. J., Wang, H., Tan, J., White, R. A. and Leenen, F. H. (2006b) Activation of brain renin-angiotensin-aldosterone system by central sodium in Wistar rats. *American journal of physiology*, **291**, H1109-1117.
- Huang, B. S., Ganten, D. and Leenen, F. H. (2001a) Responses to central Na⁽⁺⁾ and ouabain are attenuated in transgenic rats deficient in brain angiotensinogen. *Hypertension*, **37**, 683-686.

- Huang, B. S., Harmsen, E., Yu, H. and Leenen, F. H. (1992) Brain ouabain-like activity and the sympathoexcitatory and pressor effects of central sodium in rats. *Circulation research*, **71**, 1059-1066.
- Huang, B. S. and Leenen, F. H. (1995a) Brain 'ouabain,' sodium, and arterial baroreflex in spontaneously hypertensive rats. *Hypertension*, **25**, 814-817.
- Huang, B. S. and Leenen, F. H. (1995b) Brain 'ouabain' and desensitization of arterial baroreflex by high sodium in Dahl salt-sensitive rats. *Hypertension*, **25**, 372-376.
- Huang, B. S. and Leenen, F. H. (1996) Blockade of brain "ouabain" prevents sympathoexcitatory and pressor responses to high sodium in SHR. *The American journal of physiology*, **271**, H103-108.
- Huang, B. S. and Leenen, F. H. (1998) Both brain angiotensin II and "ouabain" contribute to sympathoexcitation and hypertension in Dahl S rats on high salt intake. *Hypertension*, **32**, 1028-1033.
- Huang, B. S. and Leenen, F. H. (1999) Brain renin-angiotensin system and ouabain-induced sympathetic hyperactivity and hypertension in Wistar rats. *Hypertension*, **34**, 107-112.
- Huang, B. S. and Leenen, F. H. (2002) Brain amiloride-sensitive Phe-Met-Arg-Phe-NH₂--gated Na⁽⁺⁾ channels and Na⁽⁺⁾-induced sympathoexcitation and hypertension. *Hypertension*, **39**, 557-561.
- Huang, B. S. and Leenen, F. H. (2005) Blockade of brain mineralocorticoid receptors or Na⁺ channels prevents sympathetic hyperactivity and improves cardiac function in rats post-MI. *American journal of physiology*, **288**, H2491-2497.

- Huang, B. S., Van Vliet, B. N. and Leenen, F. H. (2004) Increases in CSF [Na⁺] precede the increases in blood pressure in Dahl S rats and SHR on a high-salt diet. *American journal of physiology*, **287**, H1160-1166.
- Huang, B. S., Veerasingham, S. J. and Leenen, F. H. (1998) Brain "ouabain," ANG II, and sympathoexcitation by chronic central sodium loading in rats. *The American journal of physiology*, **274**, H1269-1276.
- Huang, B. S., Wang, H. and Leenen, F. H. (2001b) Enhanced sympathoexcitatory and pressor responses to central Na⁺ in Dahl salt-sensitive vs. -resistant rats. *American journal of physiology*, **281**, H1881-1889.
- Huang, B. S., Wang, H. and Leenen, F. H. (2005) Chronic central infusion of aldosterone leads to sympathetic hyperreactivity and hypertension in Dahl S but not Dahl R rats. *American journal of physiology*, **288**, H517-524.
- Huang, B. S., White, R. A., Ahmad, M., Jeng, A. Y. and Leenen, F. H. (2008) Central infusion of aldosterone synthase inhibitor prevents sympathetic hyperactivity and hypertension by central Na⁺ in Wistar rats. *American journal of physiology*, **295**, R166-172.
- Huang, B. S., White, R. A., Ahmad, M., Tan, J., Jeng, A. Y. and Leenen, F. H. (2009a) Central infusion of aldosterone synthase inhibitor attenuates left ventricular dysfunction and remodelling in rats after myocardial infarction. *Cardiovascular research*, **81**, 574-581.
- Huang, B. S., White, R. A., Jeng, A. Y. and Leenen, F. H. (2009b) Role of central nervous system aldosterone synthase and mineralocorticoid receptors in salt-

- induced hypertension in Dahl salt-sensitive rats. *American journal of physiology*, **296**, R994-R1000.
- Huang, D. Y., Boini, K. M., Friedrich, B. et al. (2006c) Blunted hypertensive effect of combined fructose and high-salt diet in gene-targeted mice lacking functional serum- and glucocorticoid-inducible kinase SGK1. *American journal of physiology*, **290**, R935-944.
- Huang, H., Pravenec, M., Wang, J. M., Kren, V., St Lezin, E., Szpirer, C., Szpirer, J. and Kurtz, T. W. (1995) Mapping and sequence analysis of the gene encoding the beta subunit of the epithelial sodium channel in experimental models of hypertension. *Journal of hypertension*, **13**, 1247-1251.
- Hughey, R. P., Bruns, J. B., Kinlough, C. L., Harkleroad, K. L., Tong, Q., Carattino, M. D., Johnson, J. P., Stockand, J. D. and Kleyman, T. R. (2004a) Epithelial sodium channels are activated by furin-dependent proteolysis. *The Journal of biological chemistry*, **279**, 18111-18114.
- Hughey, R. P., Bruns, J. B., Kinlough, C. L. and Kleyman, T. R. (2004b) Distinct pools of epithelial sodium channels are expressed at the plasma membrane. *The Journal of biological chemistry*, **279**, 48491-48494.
- Hughey, R. P., Carattino, M. D. and Kleyman, T. R. (2007) Role of proteolysis in the activation of epithelial sodium channels. *Current opinion in nephrology and hypertension*, **16**, 444-450.
- Hughey, R. P., Mueller, G. M., Bruns, J. B., Kinlough, C. L., Poland, P. A., Harkleroad, K. L., Carattino, M. D. and Kleyman, T. R. (2003) Maturation of the epithelial

- Na⁺ channel involves proteolytic processing of the alpha- and gamma-subunits. *The Journal of biological chemistry*, **278**, 37073-37082.
- Hummler, E., Barker, P., Gatzky, J., Beermann, F., Verdumo, C., Schmidt, A., Boucher, R. and Rossier, B. C. (1996) Early death due to defective neonatal lung liquid clearance in alpha-ENaC-deficient mice. *Nature genetics*, **12**, 325-328.
- Hummler, E., Barker, P., Talbot, C. et al. (1997) A mouse model for the renal salt-wasting syndrome pseudohypoaldosteronism. *Proceedings of the National Academy of Sciences of the United States of America*, **94**, 11710-11715.
- Hurbin, A., Orcel, H., Ferraz, C., Moos, F. C. and Rabie, A. (2000) Expression of the genes encoding the vasopressin-activated calcium-mobilizing receptor and the dual angiotensin II/vasopressin receptor in the rat central nervous system. *J Neuroendocrinol*, **12**, 677-684.
- Hussy, N., Bres, V., Rochette, M., Duvoid, A., Alonso, G., Dayanithi, G. and Moos, F. C. (2001) Osmoregulation of vasopressin secretion via activation of neurohypophysial nerve terminals glycine receptors by glial taurine. *J Neurosci*, **21**, 7110-7116.
- Hussy, N., Deleuze, C., Desarmenien, M. G. and Moos, F. C. (2000) Osmotic regulation of neuronal activity: a new role for taurine and glial cells in a hypothalamic neuroendocrine structure. *Prog Neurobiol*, **62**, 113-134.
- Hussy, N., Deleuze, C., Pantaloni, A., Desarmenien, M. G. and Moos, F. (1997) Agonist action of taurine on glycine receptors in rat supraoptic magnocellular neurones: possible role in osmoregulation. *The Journal of physiology*, **502 (Pt 3)**, 609-621.

- Husted, R. F., Matsushita, K. and Stokes, J. B. (1994) Induction of resistance to mineralocorticoid hormone in cultured inner medullary collecting duct cells by TGF-beta 1. *The American journal of physiology*, **267**, F767-775.
- Husted, R. F., Takahashi, T. and Stokes, J. B. (1996) IMCD cells cultured from Dahl S rats absorb more Na⁺ than Dahl R rats. *The American journal of physiology*, **271**, F1029-1036.
- Husted, R. F., Takahashi, T. and Stokes, J. B. (1997) The basis of higher Na⁺ transport by inner medullary collecting duct cells from Dahl salt-sensitive rats: implicating the apical membrane Na⁺ channel. *The Journal of membrane biology*, **156**, 9-18.
- Imaizumi, K., Tsuda, M., Wanaka, A., Tohyama, M. and Takagi, T. (1994) Differential expression of sgk mRNA, a member of the Ser/Thr protein kinase gene family, in rat brain after CNS injury. *Brain Res Mol Brain Res*, **26**, 189-196.
- Inoue, T., Okauchi, Y., Matsuzaki, Y. et al. (1998) Identification of a single cytosine base insertion mutation at Arg-597 of the beta subunit of the human epithelial sodium channel in a family with Liddle's disease. *Eur J Endocrinol*, **138**, 691-697.
- INTERSALT (1986) INTERSALT Study an international co-operative study on the relation of blood pressure to electrolyte excretion in populations. I. Design and methods. The INTERSALT Co-operative Research Group. *Journal of hypertension*, **4**, 781-787.
- INTERSALT (1988) Intersalt: an international study of electrolyte excretion and blood pressure. Results for 24 hour urinary sodium and potassium excretion. Intersalt Cooperative Research Group. *BMJ (Clinical research ed)*, **297**, 319-328.

- Ismailov, II, Berdiev, B. K., Shlyonsky, V. G. and Benos, D. J. (1997) Mechanosensitivity of an epithelial Na⁺ channel in planar lipid bilayers: release from Ca²⁺ block. *Biophysical journal*, **72**, 1182-1192.
- Ito, S., Hiratsuka, M., Komatsu, K., Tsukamoto, K., Kanmatsuse, K. and Sved, A. F. (2003) Ventrolateral medulla AT1 receptors support arterial pressure in Dahl salt-sensitive rats. *Hypertension*, **41**, 744-750.
- Ito, S., Komatsu, K., Tsukamoto, K., Kanmatsuse, K. and Sved, A. F. (2002) Ventrolateral medulla AT1 receptors support blood pressure in hypertensive rats. *Hypertension*, **40**, 552-559.
- Iwai, J., Dahl, L. K. and Knudsen, K. D. (1973) Genetic influence on the renin-angiotensin system: low renin activities in hypertension-prone rats. *Circulation research*, **32**, 678-684.
- Iwai, J., Friedman, R. and Tassinari, L. (1980) Genetic influence on brain catecholamines: high brain noradrenaline in salt-sensitive rats. *Clin Sci (Lond)*, **59** Suppl 6, 263s-265s.
- Iwai, N., Baba, S., Mannami, T., Katsuya, T., Higaki, J., Ogihara, T. and Ogata, J. (2001) Association of sodium channel gamma-subunit promoter variant with blood pressure. *Hypertension*, **38**, 86-89.
- Iwai, N., Baba, S., Mannami, T., Ogihara, T. and Ogata, J. (2002) Association of a sodium channel alpha subunit promoter variant with blood pressure. *J Am Soc Nephrol*, **13**, 80-85.

- Jackson, S. N., Williams, B., Houtman, P. and Trembath, R. C. (1998) The diagnosis of Liddle syndrome by identification of a mutation in the beta subunit of the epithelial sodium channel. *Journal of medical genetics*, **35**, 510-512.
- Jain, L., Chen, X. J., Malik, B., Al-Khalili, O. and Eaton, D. C. (1999) Antisense oligonucleotides against the alpha-subunit of ENaC decrease lung epithelial cation-channel activity. *The American journal of physiology*, **276**, L1046-1051.
- Jain, L., Chen, X. J., Ramosevac, S., Brown, L. A. and Eaton, D. C. (2001) Expression of highly selective sodium channels in alveolar type II cells is determined by culture conditions. *Am J Physiol Lung Cell Mol Physiol*, **280**, L646-658.
- Jain, L. and Eaton, D. C. (2006) Alveolar fluid transport: a changing paradigm. *Am J Physiol Lung Cell Mol Physiol*, **290**, L646-L648.
- Jaitovich, A. and Bertorello, A. M. Intracellular sodium sensing: SIK1 network, hormone action and high blood pressure. *Biochimica et biophysica acta*, **1802**, 1140-1149.
- Jarvis, C. R. and Andrew, R. D. (1988) Correlated electrophysiology and morphology of the ependyma in rat hypothalamus. *J Neurosci*, **8**, 3691-3702.
- Jernigan, N. L. and Drummond, H. A. (2005) Vascular ENaC proteins are required for renal myogenic constriction. *American journal of physiology*, **289**, F891-901.
- Jernigan, N. L. and Drummond, H. A. (2006) Myogenic vasoconstriction in mouse renal interlobar arteries: role of endogenous beta and gammaENaC. *American journal of physiology*, **291**, F1184-1191.
- Jernigan, N. L., LaMarca, B., Speed, J., Galmiche, L., Granger, J. P. and Drummond, H. A. (2008) Dietary salt enhances benzamil-sensitive component of myogenic

- constriction in mesenteric arteries. *American journal of physiology*, **294**, H409-420.
- Jernigan, N. L., Speed, J., LaMarca, B., Granger, J. P. and Drummond, H. A. (2009) Angiotensin II regulation of renal vascular ENaC proteins. *American journal of hypertension*, **22**, 593-597.
- Ji, H. L. and Benos, D. J. (2004) Degenerin sites mediate proton activation of deltatetagamma-epithelial sodium channel. *The Journal of biological chemistry*, **279**, 26939-26947.
- Ji, H. L., Su, X. F., Kedar, S., Li, J., Barbry, P., Smith, P. R., Matalon, S. and Benos, D. J. (2006) Delta-subunit confers novel biophysical features to alpha beta gamma-human epithelial sodium channel (ENaC) via a physical interaction. *The Journal of biological chemistry*, **281**, 8233-8241.
- Jin, Q. H., Ueda, Y., Ishizuka, Y., Kunitake, T. and Kannan, H. (2001) Cardiovascular changes induced by central hypertonic saline are accompanied by glutamate release in awake rats. *American journal of physiology*, **281**, R1224-1231.
- Johanson, C. E. (1984) Differential effects of acetazolamide, benzolamide and systemic acidosis on hydrogen and bicarbonate gradients across the apical and basolateral membranes of the choroid plexus. *The Journal of pharmacology and experimental therapeutics*, **231**, 502-511.
- Johanson, C. E., Duncan, J. A., 3rd, Klinge, P. M., Brinker, T., Stopa, E. G. and Silverberg, G. D. (2008) Multiplicity of cerebrospinal fluid functions: New challenges in health and disease. *Cerebrospinal fluid research*, **5**, 10.

- Johanson, C. E. and Murphy, V. A. (1990) Acetazolamide and insulin alter choroid plexus epithelial cell $[Na^+]$, pH, and volume. *The American journal of physiology*, **258**, F1538-1546.
- Johanson, C. E., Stopa, E. G. and McMillan, P. N. (2011) The blood-cerebrospinal fluid barrier: structure and functional significance. *Methods in molecular biology*, **686**, 101-131.
- Johanson, C. E., Sweeney, S. M., Parmelee, J. T. and Epstein, M. H. (1990) Cotransport of sodium and chloride by the adult mammalian choroid plexus. *The American journal of physiology*, **258**, C211-216.
- Johansson, P., Dziegielewska, K. and Saunders, N. (2008) Low levels of Na, K-ATPase and carbonic anhydrase II during choroid plexus development suggest limited involvement in early CSF secretion. *Neuroscience letters*, **442**, 77-80.
- Johns, E. J. (2002) The autonomic nervous system and pressure-natriuresis in cardiovascular-renal interactions in response to salt. *Clin Auton Res*, **12**, 256-263.
- Johnson, M. D., Bao, H. F., Helms, M. N., Chen, X. J., Tigue, Z., Jain, L., Dobbs, L. G. and Eaton, D. C. (2006) Functional ion channels in pulmonary alveolar type I cells support a role for type I cells in lung ion transport. *Proceedings of the National Academy of Sciences of the United States of America*, **103**, 4964-4969.
- Jones, E. S., Owen, E. P., Davidson, J. S., Van Der Merwe, L. and Rayner, B. L. (2010) The R563Q mutation of the epithelial sodium channel beta-subunit is associated with hypertension. *Cardiovascular journal of Africa*, **21**, 1-4.
- Kadekaro, M., Harris, J., Freeman, S., Terrell, M. L., Koehler, E. and Summy-Long, J. Y. (1995) Water intake and activity of hypothalamoneurohypophysial system during

- osmotic and sodium stimulation in rats. *The American journal of physiology*, **268**, R651-657.
- Kakizoe, Y., Kitamura, K., Ko, T. et al. (2009) Aberrant ENaC activation in Dahl salt-sensitive rats. *Journal of hypertension*.
- Kalaria, R. N., Premkumar, D. R., Lin, C. W., Kroon, S. N., Bae, J. Y., Sayre, L. M. and LaManna, J. C. (1998) Identification and expression of the Na⁺/H⁺ exchanger in mammalian cerebrovascular and choroidal tissues: characterization by amiloride-sensitive [3H]MIA binding and RT-PCR analysis. *Brain Res Mol Brain Res*, **58**, 178-187.
- Kamynina, E. and Staub, O. (2002) Concerted action of ENaC, Nedd4-2, and Sgk1 in transepithelial Na⁽⁺⁾ transport. *American journal of physiology*, **283**, F377-387.
- Kaneko, Y., Cloix, J. F., Herrera, V. L. and Ruiz-Opazo, N. (2005) Corroboration of Dahl S Q276L alpha1Na,K-ATPase protein sequence: impact on affinities for ligands and on E1 conformation. *Journal of hypertension*, **23**, 745-752.
- Kaplan, N. M. (1990) New evidence on the role of sodium in hypertension. The Intersalt Study. *American journal of hypertension*, **3**, 168-169.
- Kapoor, N., Bartoszewski, R., Qadri, Y. J., Bebok, Z., Bubien, J. K., Fuller, C. M. and Benos, D. J. (2009) Knockdown of ASIC1 and epithelial sodium channel subunits inhibits glioblastoma whole cell current and cell migration. *The Journal of biological chemistry*, **284**, 24526-24541.
- Karet, F. E. and Lifton, R. P. (1997) Mutations contributing to human blood pressure variation. *Recent progress in hormone research*, **52**, 263-276; discussion 276-267.

- Katoh, Y., Takemori, H., Min, L., Muraoka, M., Doi, J., Horike, N. and Okamoto, M. (2004) Salt-inducible kinase-1 represses cAMP response element-binding protein activity both in the nucleus and in the cytoplasm. *European journal of biochemistry / FEBS*, **271**, 4307-4319.
- Kawano, Y., Sudo, R. T. and Ferrario, C. M. (1991) Effects of chronic intraventricular sodium on blood pressure and fluid balance. *Hypertension*, **17**, 28-35.
- Kawano, Y., Yoshida, K., Kawamura, M. et al. (1992) Sodium and noradrenaline in cerebrospinal fluid and blood in salt-sensitive and non-salt-sensitive essential hypertension. *Clinical and experimental pharmacology & physiology*, **19**, 235-241.
- Keep, R. F., Cawkwell, R. D. and Jones, H. C. (1987) Choroid plexus structure and function in young rats on a high-potassium diet. *Brain research*, **413**, 45-52.
- Keep, R. F., Xiang, J., Ulanski, L. J., Brosius, F. C. and Betz, A. L. (1997) Choroid plexus ion transporter expression and cerebrospinal fluid secretion. *Acta neurochirurgica*, **70**, 279-281.
- Kellenberger, S., Auberson, M., Gautschi, I., Schneeberger, E. and Schild, L. (2001) Permeability properties of ENaC selectivity filter mutants. *The Journal of general physiology*, **118**, 679-692.
- Kellenberger, S., Gautschi, I. and Schild, L. (1999) A single point mutation in the pore region of the epithelial Na⁺ channel changes ion selectivity by modifying molecular sieving. *Proceedings of the National Academy of Sciences of the United States of America*, **96**, 4170-4175.

- Kellenberger, S. and Schild, L. (2002) Epithelial sodium channel/degenerin family of ion channels: a variety of functions for a shared structure. *Physiological reviews*, **82**, 735-767.
- Kent, M. A., Huang, B. S., Van Huysse, J. W. and Leenen, F. H. (2004) Brain Na⁺,K⁺-ATPase isozyme activity and protein expression in ouabain-induced hypertension. *Brain research*, **1018**, 171-180.
- Kim, S. H., Kim, K. X., Raveendran, N. N., Wu, T., Pondugula, S. R. and Marcus, D. C. (2009) Regulation of ENaC-mediated sodium transport by glucocorticoids in Reissner's membrane epithelium. *Am J Physiol Cell Physiol*, **296**, C544-557.
- Kimura, G., Ashida, T., Abe, H. et al. (1990) Sodium sensitive and sodium retaining hypertension. *American journal of hypertension*, **3**, 854-858.
- Kizer, N., Guo, X. L. and Hruska, K. (1997) Reconstitution of stretch-activated cation channels by expression of the alpha-subunit of the epithelial sodium channel cloned from osteoblasts. *Proceedings of the National Academy of Sciences of the United States of America*, **94**, 1013-1018.
- Kleyman, T. R. and Cragoe, E. J., Jr. (1988a) Amiloride and its analogs as tools in the study of ion transport. *The Journal of membrane biology*, **105**, 1-21.
- Kleyman, T. R. and Cragoe, E. J., Jr. (1988b) The mechanism of action of amiloride. *Seminars in nephrology*, **8**, 242-248.
- Kleyman, T. R. and Cragoe, E. J., Jr. (1990) Cation transport probes: the amiloride series. *Methods in enzymology*, **191**, 739-755.
- Knight, K. K., Olson, D. R., Zhou, R. and Snyder, P. M. (2006) Liddle's syndrome mutations increase Na⁺ transport through dual effects on epithelial Na⁺ channel

- surface expression and proteolytic cleavage. *Proceedings of the National Academy of Sciences of the United States of America*, **103**, 2805-2808.
- Knowles, M., Gatzky, J. and Boucher, R. (1983) Relative ion permeability of normal and cystic fibrosis nasal epithelium. *The Journal of clinical investigation*, **71**, 1410-1417.
- Kobayashi, T., Deak, M., Morrice, N. and Cohen, P. (1999) Characterization of the structure and regulation of two novel isoforms of serum- and glucocorticoid-induced protein kinase. *The Biochemical journal*, **344 Pt 1**, 189-197.
- Kolaj, M. and Renaud, L. P. (2007) Presynaptic alpha-adrenoceptors in median preoptic nucleus modulate inhibitory neurotransmission from subfornical organ and organum vasculosum lamina terminalis. *American journal of physiology*, **292**, R1907-1915.
- Kone, B. C., Wenzhang, Z. and Zhiyuan, Y. (2007) New mechanisms for transcriptional repression of ENaC And iNOS. *Transactions of the American Clinical and Climatological Association*, **118**, 45-56.
- Kopp, U. C., Cicha, M. Z. and Smith, L. A. (2003) Dietary sodium loading increases arterial pressure in afferent renal-denervated rats. *Hypertension*, **42**, 968-973.
- Kosari, F., Sheng, S., Li, J., Mak, D. O., Foskett, J. K. and Kleyman, T. R. (1998) Subunit stoichiometry of the epithelial sodium channel. *The Journal of biological chemistry*, **273**, 13469-13474.
- Kretz, O., Barbry, P., Bock, R. and Lindemann, B. (1999) Differential expression of RNA and protein of the three pore-forming subunits of the amiloride-sensitive

- epithelial sodium channel in taste buds of the rat. *J Histochem Cytochem*, **47**, 51-64.
- Kreutz, R., Struk, B., Rubattu, S., Hubner, N., Szpirer, J., Szpirer, C., Ganten, D. and Lindpaintner, K. (1997) Role of the alpha-, beta-, and gamma-subunits of epithelial sodium channel in a model of polygenic hypertension. *Hypertension*, **29**, 131-136.
- Kudo, L. H., van Baak, A. A. and Rocha, A. S. (1990) Effect of vasopressin on sodium transport across inner medullary collecting duct. *The American journal of physiology*, **258**, F1438-1447.
- Kunes, J. and Zicha, J. (1994) Association of salt sensitivity in rats with genes of the major histocompatibility complex. *Hypertension*, **24**, 645-647.
- Kunzelmann, K. and Mall, M. (2002) Electrolyte transport in the mammalian colon: mechanisms and implications for disease. *Physiological reviews*, **82**, 245-289.
- Kurtz, T. W. and Morris, R. C., Jr. (1983) Dietary chloride as a determinant of "sodium-dependent" hypertension. *Science (New York, N.Y.)*, **222**, 1139-1141.
- Kusche-Vihrog, K., Callies, C., Fels, J. and Oberleithner, H. (2010) The epithelial sodium channel (ENaC): Mediator of the aldosterone response in the vascular endothelium? *Steroids*, **75**, 544-549.
- Kusche-Vihrog, K., Sobczak, K., Bangel, N., Wilhelmi, M., Nechyporuk-Zloy, V., Schwab, A., Schillers, H. and Oberleithner, H. (2008) Aldosterone and amiloride alter ENaC abundance in vascular endothelium. *Pflugers Arch*, **455**, 849-857.

- Landgraf, R. and Ludwig, M. (1991) Vasopressin release within the supraoptic and paraventricular nuclei of the rat brain: osmotic stimulation via microdialysis. *Brain research*, **558**, 191-196.
- Lang, F., Bohmer, C., Palmada, M., Seeböhm, G., Strutz-Seeböhm, N. and Vallon, V. (2006) (Patho)physiological significance of the serum- and glucocorticoid-inducible kinase isoforms. *Physiological reviews*, **86**, 1151-1178.
- Lang, F. and Cohen, P. (2001) Regulation and physiological roles of serum- and glucocorticoid-induced protein kinase isoforms. *Sci STKE*, **2001**, RE17.
- Lang, F., Klingel, K., Wagner, C. A. et al. (2000) Deranged transcriptional regulation of cell-volume-sensitive kinase hSGK in diabetic nephropathy. *Proceedings of the National Academy of Sciences of the United States of America*, **97**, 8157-8162.
- Lapointe, J. Y., Bell, P. D., Sabirov, R. Z. and Okada, Y. (2003) Calcium-activated nonselective cationic channel in macula densa cells. *American journal of physiology. Renal physiology*, **285**, F275-280.
- Lebowitz, J., Edinger, R. S., An, B., Perry, C. J., Onate, S., Kleyman, T. R. and Johnson, J. P. (2004) Ikappab kinase-beta (ikkbeta) modulation of epithelial sodium channel activity. *The Journal of biological chemistry*, **279**, 41985-41990.
- Lechan, R. M. and Fekete, C. (2007) Infundibular tanycytes as modulators of neuroendocrine function: hypothetical role in the regulation of the thyroid and gonadal axis. *Acta Biomed*, **78 Suppl 1**, 84-98.
- Lee, I. H., Campbell, C. R., Cook, D. I. and Dinudom, A. (2008) Regulation of epithelial Na⁺ channels by aldosterone: role of Sgk1. *Clinical and experimental pharmacology & physiology*, **35**, 235-241.

- Lee, M. A., Bohm, M., Paul, M. and Ganten, D. (1993) Tissue renin-angiotensin systems. Their role in cardiovascular disease. *Circulation*, **87**, IV7-13.
- Leenen, F. H. (2010) The central role of the brain aldosterone-"ouabain" pathway in salt-sensitive hypertension. *Biochimica et biophysica acta*, **1802**, 1132-1139.
- Leenen, F. H., Harmsen, E., Yu, H. and Ou, C. (1993a) Effects of dietary sodium on central and peripheral ouabain-like activity in spontaneously hypertensive rats. *The American journal of physiology*, **264**, H2051-2055.
- Leenen, F. H., Huang, B. S. and Harmsen, E. (1993b) Role of brain ouabain-like activity in the central effects of sodium in rats. *Journal of cardiovascular pharmacology*, **22 Suppl 2**, S72-74.
- Leenen, F. H., Ruzicka, M. and Huang, B. S. (2002) The brain and salt-sensitive hypertension. *Current hypertension reports*, **4**, 129-135.
- Leksell, L. G., Denton, D. A., Fei, D. T., McKinley, M. J., Muller, A. F., Weisinger, R. S. and Young, H. (1982) On the importance of CSF Na in the regulation of renal sodium excretion and renin release. *Acta Physiol Scand*, **115**, 141-146.
- Leng, G. and Ludwig, M. (2006) Jacques Benoit Lecture. Information processing in the hypothalamus: peptides and analogue computation. *Journal of neuroendocrinology*, **18**, 379-392.
- Leng, G. and Ludwig, M. (2008) Neurotransmitters and peptides: whispered secrets and public announcements. *The Journal of physiology*, **586**, 5625-5632.
- Liang, X., Butterworth, M. B., Peters, K. W., Walker, W. H. and Frizzell, R. A. (2008) An obligatory heterodimer of 14-3-3beta and 14-3-3epsilon is required for

- aldosterone regulation of the epithelial sodium channel. *The Journal of biological chemistry*, **283**, 27418-27425.
- Liang, X., Peters, K. W., Butterworth, M. B. and Frizzell, R. A. (2006) 14-3-3 isoforms are induced by aldosterone and participate in its regulation of epithelial sodium channels. *The Journal of biological chemistry*, **281**, 16323-16332.
- Liddle, G., Bledsoe, T. and Coppage, W. S., Jr. (1963) A familial renal disorder simulating primary aldosteronism but with negligible aldosterone secretion. *Trans Am Assoc Physicians*, **76**, 199-213.
- Liddle, G. W. (1973) Proceedings: Blueprints for the solution of three endocrinological enigmas. The Sir Henry Dale Lecture for 1973. *The Journal of endocrinology*, **59**, ii-ix.
- Liddle, G. W., Bledsoe, T. and Coppage, W. S., Jr. (1974) Hypertension reviews. *Journal of the Tennessee Medical Association*, **67**, 669.
- Liddle, G. W., Brown, R. D. and Liddle, V. R. (1973) Recognition of curable forms of hypertension. *Journal of the Tennessee Medical Association*, **66**, 221-224.
- Liddle, G. W., Hollifield, J. W., Slaton, P. E. and Wilson, H. M. (1976) Effects of various adrenal inhibitors in low-renin essential hypertension. *Journal of steroid biochemistry*, **7**, 937-940.
- Liebman, B. F., Langford, H. G., Whitescarver, S. A., Ott, C. E., Jackson, B., Kurtz, T. W. and Morris, R. C., Jr. (1985) Hypertension and sodium salts. *Science (New York, N.Y.)*, **228**, 351-353.
- Lim, W., Kim, D., Park, J. B., Kim, S. H. and Lee, Y. (2004) Sodium chloride regulation of the alpha epithelial amiloride-sensitive sodium channel (alphaENaC) gene

- requires syntheses of new protein(s). *The Journal of steroid biochemistry and molecular biology*, **88**, 305-310.
- Lin, W., Finger, T. E., Rossier, B. C. and Kinnamon, S. C. (1999) Epithelial Na⁺ channel subunits in rat taste cells: localization and regulation by aldosterone. *The Journal of comparative neurology*, **405**, 406-420.
- Lindemann, B., Barbry, P., Kretz, O. and Bock, R. (1998) Occurrence of ENaC subunit mRNA and immunocytochemistry of the channel subunits in taste buds of the rat vallate papilla. *Annals of the New York Academy of Sciences*, **855**, 116-127.
- Loffing, J., Flores, S. Y. and Staub, O. (2006) Sgk kinases and their role in epithelial transport. *Annual review of physiology*, **68**, 461-490.
- Loffing, J., Loffing-Cueni, D., Macher, A., Hebert, S. C., Olson, B., Knepper, M. A., Rossier, B. C. and Kaissling, B. (2000a) Localization of epithelial sodium channel and aquaporin-2 in rabbit kidney cortex. *American journal of physiology*, **278**, F530-539.
- Loffing, J., Loffing-Cueni, D., Valderrabano, V., Klausli, L., Hebert, S. C., Rossier, B. C., Hoenderop, J. G., Bindels, R. J. and Kaissling, B. (2001a) Distribution of transcellular calcium and sodium transport pathways along mouse distal nephron. *American journal of physiology*, **281**, F1021-1027.
- Loffing, J., Pietri, L., Aregger, F., Bloch-Faure, M., Ziegler, U., Meneton, P., Rossier, B. C. and Kaissling, B. (2000b) Differential subcellular localization of ENaC subunits in mouse kidney in response to high- and low-Na diets. *American journal of physiology*, **279**, F252-258.

- Loffing, J., Zecevic, M., Feraille, E., Kaissling, B., Asher, C., Rossier, B. C., Firestone, G. L., Pearce, D. and Verrey, F. (2001b) Aldosterone induces rapid apical translocation of ENaC in early portion of renal collecting system: possible role of SGK. *American journal of physiology*, **280**, F675-682.
- Loutzenhiser, R. and Aaronson, P. I. (2010) Role of epithelial sodium channels in the renal myogenic response? *Hypertension*, **55**, e6; author reply e7-9.
- Ludwig, M., Bull, P. M., Tobin, V. A., Sabatier, N., Landgraf, R., Dayanithi, G. and Leng, G. (2005) Regulation of activity-dependent dendritic vasopressin release from rat supraoptic neurones. *The Journal of physiology*, **564**, 515-522.
- Ludwig, M., Williams, K., Callahan, M. F. and Morris, M. (1996) Salt loading abolishes osmotically stimulated vasopressin release within the supraoptic nucleus. *Neuroscience letters*, **215**, 1-4.
- Luft, F. C. (1989) Salt and hypertension: recent advances and perspectives. *The Journal of laboratory and clinical medicine*, **114**, 215-221.
- Luft, F. C. (1995) Salt and hypertension: where things stand. *Nephrol Dial Transplant*, **10**, 1524-1525.
- Luft, F. C. (2004) Present status of genetic mechanisms in hypertension. *The Medical clinics of North America*, **88**, 1-18, vii.
- Luft, F. C., Miller, J. Z., Cohen, S. J., Fineberg, N. S. and Weinberger, M. H. (1988a) Heritable aspects of salt sensitivity. *The American journal of cardiology*, **61**, 1H-6H.

- Luft, F. C., Miller, J. Z., Grim, C. E., Fineberg, N. S., Christian, J. C., Daugherty, S. A. and Weinberger, M. H. (1991) Salt sensitivity and resistance of blood pressure. Age and race as factors in physiological responses. *Hypertension*, **17**, 1102-108.
- Luft, F. C., Miller, J. Z., Weinberger, M. H., Christian, J. C. and Skrabal, F. (1988b) Genetic influences on the response to dietary salt reduction, acute salt loading, or salt depletion in humans. *Journal of cardiovascular pharmacology*, **12 Suppl 3**, S49-55.
- Luft, F. C., Miller, J. Z., Weinberger, M. H., Grim, C. E., Daugherty, S. A. and Christian, J. C. (1987) Influence of genetic variance on sodium sensitivity of blood pressure. *Klinische Wochenschrift*, **65**, 101-109.
- Luft, F. C., Steinberg, H., Ganten, U. et al. (1988c) Effect of sodium chloride and sodium bicarbonate on blood pressure in stroke-prone spontaneously hypertensive rats. *Clin Sci (Lond)*, **74**, 577-585.
- MacKenzie, S. M., Clark, C. J., Fraser, R., Gomez-Sanchez, C. E., Connell, J. M. and Davies, E. (2000) Expression of 11beta-hydroxylase and aldosterone synthase genes in the rat brain. *Journal of molecular endocrinology*, **24**, 321-328.
- Macleod, M. R., Johansson, I. M., Soderstrom, I., Lai, M., Gido, G., Wieloch, T., Seckl, J. R. and Olsson, T. (2003) Mineralocorticoid receptor expression and increased survival following neuronal injury. *The European journal of neuroscience*, **17**, 1549-1555.
- Maiyar, A. C., Leong, M. L. and Firestone, G. L. (2003) Importin-alpha mediates the regulated nuclear targeting of serum- and glucocorticoid-inducible protein kinase

- (Sgk) by recognition of a nuclear localization signal in the kinase central domain. *Molecular biology of the cell*, **14**, 1221-1239.
- Maiyar, A. C., Phu, P. T., Huang, A. J. and Firestone, G. L. (1997) Repression of glucocorticoid receptor transactivation and DNA binding of a glucocorticoid response element within the serum/glucocorticoid-inducible protein kinase (sgk) gene promoter by the p53 tumor suppressor protein. *Molecular endocrinology (Baltimore, Md)*, **11**, 312-329.
- Manger, W. M., Simchon, S., Stokes, M. B., Reidy, J. J., Kumar, A. R., Baer, L., Gallo, G. and Haddy, F. J. (2009) Renal functional, not morphological, abnormalities account for salt sensitivity in Dahl rats. *Journal of hypertension*, **27**, 587-598.
- Manitius, J., Kliz, J. and Krupa-Wojciechowska, B. (1985) The effect of dietary sodium loading on the kinetics of sodium excretion and blood pressure regulation in essential hypertensive men. *Cor et vasa*, **27**, 29-35.
- Marissal-Arvy, N., Lombes, M., Petterson, J., Moisan, M. P. and Mormede, P. (2004) Gain of function mutation in the mineralocorticoid receptor of the Brown Norway rat. *The Journal of biological chemistry*, **279**, 39232-39239.
- Marson, O., Chernicky, C. L., Barnes, K. L., Diz, D. I., Slugg, R. M. and Ferrario, C. M. (1985) The anteroventral third ventricle region. Participation in the regulation of blood pressure in conscious dogs. *Hypertension*, **7**, 180-87.
- Marson, O., Saragoca, M. A., Ribeiro, A. B., Bossolan, D., Tufik, S. and Ramos, O. L. (1983) Anteroventral third ventricle and renin-angiotensin system interaction in the two-kidney, one clip hypertensive rat. *Hypertension*, **5**, V90-93.

- Marunaka, Y. (1997) Hormonal and osmotic regulation of NaCl transport in renal distal nephron epithelium. *The Japanese journal of physiology*, **47**, 499-511.
- Marunaka, Y., Hagiwara, N. and Tohda, H. (1992) Insulin activates single amiloride-blockable Na channels in a distal nephron cell line (A6). *The American journal of physiology*, **263**, F392-400.
- Masilamani, S., Kim, G. H., Mitchell, C., Wade, J. B. and Knepper, M. A. (1999) Aldosterone-mediated regulation of ENaC alpha, beta, and gamma subunit proteins in rat kidney. *The Journal of clinical investigation*, **104**, R19-23.
- Masilamani, S., Wang, X., Kim, G. H., Brooks, H., Nielsen, J., Nielsen, S., Nakamura, K., Stokes, J. B. and Knepper, M. A. (2002) Time course of renal Na-K-ATPase, NHE3, NKCC2, NCC, and ENaC abundance changes with dietary NaCl restriction. *American journal of physiology*, **283**, F648-657.
- Masuzawa, T., Ohta, T., Kawamura, M., Nakahara, N. and Sato, F. (1984) Immunohistochemical localization of Na⁺, K⁺-ATPase in the choroid plexus. *Brain research*, **302**, 357-362.
- Matalon, S., Lazrak, A., Jain, L. and Eaton, D. C. (2002) Invited review: biophysical properties of sodium channels in lung alveolar epithelial cells. *J Appl Physiol*, **93**, 1852-1859.
- Mathew, T. C. (2007) Diversity in the surface morphology of adjacent epithelial cells of the choroid plexus: an ultrastructural analysis. *Molecular and cellular biochemistry*, **301**, 235-239.

- Matsubara, M., Metoki, H., Suzuki, M. et al. (2002) Genotypes of the betaENaC gene have little influence on blood pressure level in the Japanese population. *American journal of hypertension*, **15**, 189-192.
- Matsukawa, N., Nonaka, Y., Higaki, J., Nagano, M., Mikami, H., Ogihara, T. and Okamoto, M. (1993) Dahl's salt-resistant normotensive rat has mutations in cytochrome P450(11 beta), but the salt-sensitive hypertensive rat does not. *The Journal of biological chemistry*, **268**, 9117-9121.
- Matsushita, K., McCray, P. B., Jr., Sigmund, R. D., Welsh, M. J. and Stokes, J. B. (1996) Localization of epithelial sodium channel subunit mRNAs in adult rat lung by in situ hybridization. *The American journal of physiology*, **271**, L332-339.
- Mattson, D. L. (2003) Importance of the renal medullary circulation in the control of sodium excretion and blood pressure. *American journal of physiology*, **284**, R13-27.
- May, A., Puoti, A., Gaeggeler, H. P., Horisberger, J. D. and Rossier, B. C. (1997) Early effect of aldosterone on the rate of synthesis of the epithelial sodium channel alpha subunit in A6 renal cells. *J Am Soc Nephrol*, **8**, 1813-1822.
- McCarthy, J. E. (1998) Posttranscriptional control of gene expression in yeast. *Microbiol Mol Biol Rev*, **62**, 1492-1553.
- McDonald, F. J., Price, M. P., Snyder, P. M. and Welsh, M. J. (1995) Cloning and expression of the beta- and gamma-subunits of the human epithelial sodium channel. *The American journal of physiology*, **268**, C1157-1163.

- McDonald, F. J., Western, A. H., McNeil, J. D., Thomas, B. C., Olson, D. R. and Snyder, P. M. (2002) Ubiquitin-protein ligase WWP2 binds to and downregulates the epithelial Na(+) channel. *American journal of physiology*, **283**, F431-436.
- McDonald, F. J., Yang, B., Hrstka, R. F., Drummond, H. A., Tarr, D. E., McCray, P. B., Jr., Stokes, J. B., Welsh, M. J. and Williamson, R. A. (1999) Disruption of the beta subunit of the epithelial Na⁺ channel in mice: hyperkalemia and neonatal death associated with a pseudohypoaldosteronism phenotype. *Proceedings of the National Academy of Sciences of the United States of America*, **96**, 1727-1731.
- McKinley, M. J. and Johnson, A. K. (2004) The physiological regulation of thirst and fluid intake. *News Physiol Sci*, **19**, 1-6.
- Mihailidou, A. S. (2006) Nongenomic actions of aldosterone: physiological or pathophysiological role? *Steroids*, **71**, 277-280.
- Millar, I. D., Bruce, J. and Brown, P. D. (2007) Ion channel diversity, channel expression and function in the choroid plexuses. *Cerebrospinal fluid research*, **4**, 8.
- Mills, I. H. (1970) Regulation of sodium excretion: intra- and extrarenal mechanisms. *Journal of the Royal College of Physicians of London*, **4**, 335-350.
- Mills, S. E. (2008) *Histology for pathologists*. Lippincott Williams and Wilkins.
- Mirshahi, M., Golestaneh, N., Valamanesh, F. and Agarwal, M. K. (2000) Paradoxical effects of mineralocorticoids on the ion gated sodium channel in embryologically diverse cells. *Biochemical and biophysical research communications*, **270**, 811-815.

- Mirshahi, M., Mirshahi, S., Golestaneh, N. et al. (2001) Mineralocorticoid hormone signaling regulates the 'epithelial sodium channel' in fibroblasts from human cornea. *Ophthalmic research*, **33**, 7-19.
- Mirshahi, M., Nicolas, C., Mirshahi, S., Golestaneh, N., d'Hermies, F. and Agarwal, M. K. (1999) Immunochemical analysis of the sodium channel in rodent and human eye. *Experimental eye research*, **69**, 21-32.
- Moisan, M. P., Edwards, C. R. and Seckl, J. R. (1992) Ontogeny of 11 beta-hydroxysteroid dehydrogenase in rat brain and kidney. *Endocrinology*, **130**, 400-404.
- Mokry, M. and Cuppen, E. (2008) The *Atp1a1* gene from inbred Dahl salt sensitive rats does not contain the A1079T missense transversion. *Hypertension*, **51**, 922-927.
- Mongin, A. A. and Orlov, S. N. (2001) Mechanisms of cell volume regulation and possible nature of the cell volume sensor. *Pathophysiology*, **8**, 77-88.
- Monteiro, O., Wiegand, U. K. and Ludwig, M. (2011) Vesicle degradation in dendrites of magnocellular neurones of the rat supraoptic nucleus. *Neuroscience letters*, **489**, 30-33.
- Morgan, D. A., DiBona, G. F. and Mark, A. L. (1990) Effects of interstrain renal transplantation on NaCl-induced hypertension in Dahl rats. *Hypertension*, **15**, 436-442.
- Morimoto, T., Liu, W., Woda, C., Carattino, M. D., Wei, Y., Hughey, R. P., Apodaca, G., Satlin, L. M. and Kleyman, T. R. (2006) Mechanism underlying flow stimulation of sodium absorption in the mammalian collecting duct. *American journal of physiology*, **291**, F663-669.

- Muders, F., Palkovits, M., Bahner, U., Kirst, I., Elsner, D. and Jandeleit-Dahm, K. (2001) Central inhibition of AT1receptors by eprosartan--in vitro autoradiography in the brain. *Pharmacol Res*, **43**, 251-255.
- Murphy, V. A. and Johanson, C. E. (1989a) Acidosis, acetazolamide, and amiloride: effects on ^{22}Na transfer across the blood-brain and blood-CSF barriers. *J Neurochem*, **52**, 1058-1063.
- Murphy, V. A. and Johanson, C. E. (1989b) Alteration of sodium transport by the choroid plexus with amiloride. *Biochimica et biophysica acta*, **979**, 187-192.
- Murphy, V. A. and Johanson, C. E. (1990) $\text{Na}^{(+)}\text{-H}^{+}$ exchange in choroid plexus and CSF in acute metabolic acidosis or alkalosis. *The American journal of physiology*, **258**, F1528-1537.
- Murrell, J. R., Randall, J. D., Rosoff, J., Zhao, J. L., Jensen, R. V., Gullans, S. R. and Hauptert, G. T., Jr. (2005) Endogenous ouabain: upregulation of steroidogenic genes in hypertensive hypothalamus but not adrenal. *Circulation*, **112**, 1301-1308.
- Mutoh, S., Hirayama, H., Ueda, S., Tsuruta, K., Imafuji, M. and Ikegami, K. (1986) Pseudohyperaldosteronism (Liddle's syndrome): a case report. *The Journal of urology*, **135**, 557-558.
- Myerburg, M. M., Harvey, P. R., Heidrich, E. M., Pilewski, J. M. and Butterworth, M. B. Acute regulation of the epithelial sodium channel in airway epithelia by proteases and trafficking. *Am J Respir Cell Mol Biol*, **43**, 712-719.
- Nakamura, K. and Cowley, A. W., Jr. (1989) Sequential changes of cerebrospinal fluid sodium during the development of hypertension in Dahl rats. *Hypertension*, **13**, 243-249.

- Nakamura, T., Canaani, E. and Croce, C. M. (2007) Oncogenic All1 fusion proteins target Drosha-mediated microRNA processing. *Proceedings of the National Academy of Sciences of the United States of America*, **104**, 10980-10985.
- Naray-Fejes-Toth, A., Canessa, C., Cleaveland, E. S., Aldrich, G. and Fejes-Toth, G. (1999) sgk is an aldosterone-induced kinase in the renal collecting duct. Effects on epithelial Na^+ channels. *The Journal of biological chemistry*, **274**, 16973-16978.
- Nicco, C., Bankir, L. and Bouby, N. (2003) Effect of salt and water intake on epithelial sodium channel mRNA abundance in the kidney of salt-sensitive Sabra rats. *Clinical and experimental pharmacology & physiology*, **30**, 963-965.
- Nicco, C., Wittner, M., DiStefano, A., Jounier, S., Bankir, L. and Bouby, N. (2001) Chronic exposure to vasopressin upregulates ENaC and sodium transport in the rat renal collecting duct and lung. *Hypertension*, **38**, 1143-1149.
- Nielsen, J., Kwon, T. H., Frokiaer, J., Knepper, M. A. and Nielsen, S. (2007) Maintained ENaC trafficking in aldosterone-infused rats during mineralocorticoid and glucocorticoid receptor blockade. *American journal of physiology*, **292**, F382-394.
- Nishida, Y., Nagata, T., Takahashi, Y., Sugahara-Kobayashi, M., Murata, A. and Asai, S. (2004) Alteration of serum/glucocorticoid regulated kinase-1 (sgk-1) gene expression in rat hippocampus after transient global ischemia. *Brain Res Mol Brain Res*, **123**, 121-125.
- Nishimura, M., Ohtsuka, K., Nanbu, A., Takahashi, H. and Yoshimura, M. (1998) Benzamil blockade of brain Na^+ channels averts Na^+ -induced hypertension in rats. *The American journal of physiology*, **274**, R635-644.

- Nkeh, B., Samani, N. J., Badenhorst, D., Libhaber, E., Sareli, P., Norton, G. R. and Woodiwiss, A. J. (2003) T594M variant of the epithelial sodium channel beta-subunit gene and hypertension in individuals of African ancestry in South Africa. *American journal of hypertension*, **16**, 847-852.
- Noda, M. (2006) The subfornical organ, a specialized sodium channel, and the sensing of sodium levels in the brain. *Neuroscientist*, **12**, 80-91.
- O'Shaughnessy, K. M. and Karet, F. E. (2004) Salt handling and hypertension. *The Journal of clinical investigation*, **113**, 1075-1081.
- O'Shaughnessy, K. M. and Karet, F. E. (2006) Salt handling and hypertension. *Annual review of nutrition*, **26**, 343-365.
- Obarzanek, E., Proschan, M. A., Vollmer, W. M., Moore, T. J., Sacks, F. M., Appel, L. J., Svetkey, L. P., Most-Windhauser, M. M. and Cutler, J. A. (2003) Individual blood pressure responses to changes in salt intake: results from the DASH-Sodium trial. *Hypertension*, **42**, 459-467.
- Okamoto, M., Nonaka, Y., Takemori, H. and Doi, J. (2005) Molecular identity and gene expression of aldosterone synthase cytochrome P450. *Biochemical and biophysical research communications*, **338**, 325-330.
- Oliver, W. J., Cohen, E. L. and Neel, J. V. (1975) Blood pressure, sodium intake, and sodium related hormones in the Yanomamo Indians, a "no-salt" culture. *Circulation*, **52**, 146-151.
- Ono, F., Harada, H., Komatsu, K., Saijo, K. and Miyoshi, K. (1975) Two cases of pseudoaldosteronism (Liddle's syndrome) in siblings. *Endocrinologia japonica*, **22**, 163-167.

- Ono, S., Kusano, E., Muto, S., Ando, Y. and Asano, Y. (1997) A low-Na⁺ diet enhances expression of mRNA for epithelial Na⁺ channel in rat renal inner medulla. *Pflugers Arch*, **434**, 756-763.
- Orlov, S. N. and Mongin, A. A. (2007) Salt-sensing mechanisms in blood pressure regulation and hypertension. *American journal of physiology*, **293**, H2039-2053.
- Otulakowski, G., Duan, W., Gandhi, S. and O'Brodivich, H. (2007) Steroid and oxygen effects on eIF4F complex, mTOR, and ENaC translation in fetal lung epithelia. *Am J Respir Cell Mol Biol*, **37**, 457-466.
- Otulakowski, G., Freywald, T., Wen, Y. and O'Brodivich, H. (2001) Translational activation and repression by distinct elements within the 5'-UTR of ENaC alpha-subunit mRNA. *Am J Physiol Lung Cell Mol Physiol*, **281**, L1219-1231.
- Otulakowski, G., Rafii, B., Bremner, H. R. and O'Brodivich, H. (1999) Structure and hormone responsiveness of the gene encoding the alpha-subunit of the rat amiloride-sensitive epithelial sodium channel. *Am J Respir Cell Mol Biol*, **20**, 1028-1040.
- Otulakowski, G., Rafii, B., Harris, M. and O'Brodivich, H. (2006) Oxygen and glucocorticoids modulate alphaENaC mRNA translation in fetal distal lung epithelium. *Am J Respir Cell Mol Biol*, **34**, 204-212.
- Otulakowski, G., Rafii, B. and O'Brodivich, H. (2004) Differential translational efficiency of ENaC subunits during lung development. *Am J Respir Cell Mol Biol*, **30**, 862-870.
- Palmer, L. G. (1982) Ion selectivity of the apical membrane Na channel in the toad urinary bladder. *The Journal of membrane biology*, **67**, 91-98.

- Palmer, L. G. (1985a) Interactions of amiloride and other blocking cations with the apical Na channel in the toad urinary bladder. *The Journal of membrane biology*, **87**, 191-199.
- Palmer, L. G. (1985b) Modulation of apical Na permeability of the toad urinary bladder by intracellular Na, Ca, and H. *The Journal of membrane biology*, **83**, 57-69.
- Palmer, L. G. (1990) Epithelial Na channels: the nature of the conducting pore. *Renal physiology and biochemistry*, **13**, 51-58.
- Palmer, L. G. (1992) Epithelial Na channels: function and diversity. *Annual review of physiology*, **54**, 51-66.
- Palmer, L. G. and Andersen, O. S. (1989) Interactions of amiloride and small monovalent cations with the epithelial sodium channel. Inferences about the nature of the channel pore. *Biophysical journal*, **55**, 779-787.
- Palmer, L. G., Corthesy-Theulaz, I., Gaeggeler, H. P., Kraehenbuhl, J. P. and Rossier, B. (1990) Expression of epithelial Na channels in *Xenopus* oocytes. *The Journal of general physiology*, **96**, 23-46.
- Palmer, L. G., Edelman, I. S. and Lindemann, B. (1980) Current-voltage analysis of apical sodium transport in toad urinary bladder: effects of inhibitors of transport and metabolism. *The Journal of membrane biology*, **57**, 59-71.
- Palmer, L. G. and Frindt, G. (1986) Amiloride-sensitive Na channels from the apical membrane of the rat cortical collecting tubule. *Proceedings of the National Academy of Sciences of the United States of America*, **83**, 2767-2770.

- Palmer, L. G. and Frindt, G. (1988) Conductance and gating of epithelial Na channels from rat cortical collecting tubule. Effects of luminal Na and Li. *The Journal of general physiology*, **92**, 121-138.
- Palmer, L. G. and Frindt, G. (1996) Gating of Na channels in the rat cortical collecting tubule: effects of voltage and membrane stretch. *The Journal of general physiology*, **107**, 35-45.
- Parandoosh, Z. and Johanson, C. E. (1982) Ontogeny of blood-brain barrier permeability to, and cerebrospinal fluid sink action on, [14C]urea. *The American journal of physiology*, **243**, R400-407.
- Paxinos, G. and Watson, C. (1998a) The Rat Brain in Stereotaxic coordinates.
- Paxinos, G. and Watson, C. (1998b) *The rat brain in stereotaxic coordinates*. Academic Press, New York.
- Pearce, D. (2001) The role of SGK1 in hormone-regulated sodium transport. *Trends in endocrinology and metabolism: TEM*, **12**, 341-347.
- Pearce, D. and Kleyman, T. R. (2007) Salt, sodium channels, and SGK1. *The Journal of clinical investigation*, **117**, 592-595.
- Perlewitz, A., Nafz, B., Skalweit, A., Fahling, M., Persson, P. B. and Thiele, B. J. (2010) Aldosterone and vasopressin affect α - and γ -ENaC mRNA translation. *Nucleic acids research*, **38**, 5746-5760.
- Pesole, G., Grillo, G., Larizza, A. and Liuni, S. (2000) The untranslated regions of eukaryotic mRNAs: structure, function, evolution and bioinformatic tools for their analysis. *Briefings in bioinformatics*, **1**, 236-249.

- Pesole, G., Mignone, F., Gissi, C., Grillo, G., Licciulli, F. and Liuni, S. (2001) Structural and functional features of eukaryotic mRNA untranslated regions. *Gene*, **276**, 73-81.
- Peters, K. W., Qi, J., Johnson, J. P., Watkins, S. C. and Frizzell, R. A. (2001) Role of snare proteins in CFTR and ENaC trafficking. *Pflugers Arch*, **443 Suppl 1**, S65-69.
- Peti-Peterdi, J., Warnock, D. G. and Bell, P. D. (2002) Angiotensin II directly stimulates ENaC activity in the cortical collecting duct via AT(1) receptors. *J Am Soc Nephrol*, **13**, 1131-1135.
- Pietranera, L., Saravia, F. E., McEwen, B. S., Lucas, L. L., Johnson, A. K. and De Nicola, A. F. (2001) Changes in Fos expression in various brain regions during deoxycorticosterone acetate treatment: relation to salt appetite, vasopressin mRNA and the mineralocorticoid receptor. *Neuroendocrinology*, **74**, 396-406.
- Poch, E., Gonzalez, D., de la Sierra, A., Giner, V., Bragulat, E., Botey, A., Coca, A. and Rivera, F. (2000) Genetic variation of the gamma subunit of the epithelial Na⁺ channel and essential hypertension. Relationship with salt sensitivity. *American journal of hypertension*, **13**, 648-653.
- Pollay, M., Hisey, B., Reynolds, E., Tomkins, P., Stevens, F. A. and Smith, R. (1985) Choroid plexus Na⁺/K⁺-activated adenosine triphosphatase and cerebrospinal fluid formation. *Neurosurgery*, **17**, 768-772.
- Pondugula, S. R., Raveendran, N. N., Ergonul, Z., Deng, Y., Chen, J., Sanneman, J. D., Palmer, L. G. and Marcus, D. C. (2006) Glucocorticoid regulation of genes in the

- amiloride-sensitive sodium transport pathway by semicircular canal duct epithelium of neonatal rat. *Physiological genomics*, **24**, 114-123.
- Pondugula, S. R., Sanneman, J. D., Wangemann, P., Milhaud, P. G. and Marcus, D. C. (2004) Glucocorticoids stimulate cation absorption by semicircular canal duct epithelium via epithelial sodium channel. *American journal of physiology*, **286**, F1127-1135.
- Praetorius, J. (2007) Water and solute secretion by the choroid plexus. *Pflugers Arch*, **454**, 1-18.
- Praetorius, J. and Nielsen, S. (2006) Distribution of sodium transporters and aquaporin-1 in the human choroid plexus. *Am J Physiol Cell Physiol*, **291**, C59-67.
- Pratt, J. H. (2005) Central role for ENaC in development of hypertension. *J Am Soc Nephrol*, **16**, 3154-3159.
- Qi, J., Peters, K. W., Liu, C., Wang, J. M., Edinger, R. S., Johnson, J. P., Watkins, S. C. and Frizzell, R. A. (1999) Regulation of the amiloride-sensitive epithelial sodium channel by syntaxin 1A. *The Journal of biological chemistry*, **274**, 30345-30348.
- Quinkler, M., Bujalska, I. J., Kaur, K., Onyimba, C. U., Buhner, S., Allolio, B., Hughes, S. V., Hewison, M. and Stewart, P. M. (2005) Androgen receptor-mediated regulation of the alpha-subunit of the epithelial sodium channel in human kidney. *Hypertension*, **46**, 787-798.
- Quinton, P. M., Wright, E. M. and Tormey, J. M. (1973) Localization of sodium pumps in the choroid plexus epithelium. *The Journal of cell biology*, **58**, 724-730.

- Rahmouni, K., Barthelmebs, M., Grima, M., Imbs, J. L. and De Jong, W. (2001) Involvement of brain mineralocorticoid receptor in salt-enhanced hypertension in spontaneously hypertensive rats. *Hypertension*, **38**, 902-906.
- Rahmouni, K., Barthelmebs, M., Grima, M., Imbs, J. L. and Wybren De, J. (1999) Brain mineralocorticoid receptor control of blood pressure and kidney function in normotensive rats. *Hypertension*, **33**, 1201-1206.
- Rapp, J. P. (1982) Dahl salt-susceptible and salt-resistant rats. A review. *Hypertension*, **4**, 753-763.
- Rapp, J. P. (2000) Genetic analysis of inherited hypertension in the rat. *Physiological reviews*, **80**, 135-172.
- Rauh, R., Diakov, A., Tzschoppe, A. et al. (2010) A mutation of the epithelial sodium channel associated with atypical cystic fibrosis increases channel open probability and reduces Na⁺ self inhibition. *The Journal of physiology*, **588**, 1211-1225.
- Rauz, S., Walker, E. A., Hughes, S. V., Coca-Prados, M., Hewison, M., Murray, P. I. and Stewart, P. M. (2003a) Serum- and glucocorticoid-regulated kinase isoform-1 and epithelial sodium channel subunits in human ocular ciliary epithelium. *Investigative ophthalmology & visual science*, **44**, 1643-1651.
- Rauz, S., Walker, E. A., Murray, P. I. and Stewart, P. M. (2003b) Expression and distribution of the serum and glucocorticoid regulated kinase and the epithelial sodium channel subunits in the human cornea. *Experimental eye research*, **77**, 101-108.
- Rayner, B. L., Owen, E. P., King, J. A., Soule, S. G., Vreede, H., Opie, L. H., Marais, D. and Davidson, J. S. (2003) A new mutation, R563Q, of the beta subunit of the

- epithelial sodium channel associated with low-renin, low-aldosterone hypertension. *Journal of hypertension*, **21**, 921-926.
- Record, R. D., Froelich, L. L., Vlahos, C. J. and Blazer-Yost, B. L. (1998) Phosphatidylinositol 3-kinase activation is required for insulin-stimulated sodium transport in A6 cells. *The American journal of physiology*, **274**, E611-617.
- Reddy, M. M., Light, M. J. and Quinton, P. M. (1999) Activation of the epithelial Na⁺ channel (ENaC) requires CFTR Cl⁻ channel function. *Nature*, **402**, 301-304.
- Reddy, M. M. and Quinton, P. M. (2003) Functional interaction of CFTR and ENaC in sweat glands. *Pflugers Arch*, **445**, 499-503.
- Reddy, M. M. and Quinton, P. M. (2005) ENaC activity requires CFTR channel function independently of phosphorylation in sweat duct. *The Journal of membrane biology*, **207**, 23-33.
- Reif, M. C., Troutman, S. L. and Schafer, J. A. (1984) Sustained response to vasopressin in isolated rat cortical collecting tubule. *Kidney international*, **26**, 725-732.
- Reif, M. C., Troutman, S. L. and Schafer, J. A. (1986) Sodium transport by rat cortical collecting tubule. Effects of vasopressin and desoxycorticosterone. *The Journal of clinical investigation*, **77**, 1291-1298.
- Reisenauer, M. R., Anderson, M., Huang, L. et al. (2009) AF17 competes with AF9 for binding to Dot1a to up-regulate transcription of epithelial Na⁺ channel alpha. *The Journal of biological chemistry*, **284**, 35659-35669.
- Renard, S., Voilley, N., Bassilana, F., Lazdunski, M. and Barbry, P. (1995) Localization and regulation by steroids of the alpha, beta and gamma subunits of the amiloride-sensitive Na⁺ channel in colon, lung and kidney. *Pflugers Arch*, **430**, 299-307.

- Rettig, R. and Grisk, O. (2005) The kidney as a determinant of genetic hypertension: evidence from renal transplantation studies. *Hypertension*, **46**, 463-468.
- Rezkalla, L. and Borra, S. (2000) Saline-resistant metabolic alkalosis, severe hypokalemia and hypertension in a 74-year-old woman. *Clinical nephrology*, **53**, 66-70.
- Robert-Nicoud, M., Flahaut, M., Elalouf, J. M. et al. (2001) Transcriptome of a mouse kidney cortical collecting duct cell line: effects of aldosterone and vasopressin. *Proceedings of the National Academy of Sciences of the United States of America*, **98**, 2712-2716.
- Robson, A. C., Leckie, C. M., Seckl, J. R. and Holmes, M. C. (1998) 11 Beta-hydroxysteroid dehydrogenase type 2 in the postnatal and adult rat brain. *Brain Res Mol Brain Res*, **61**, 1-10.
- Rodriguez, E. M., Blazquez, J. L., Pastor, F. E., Pelaez, B., Pena, P., Peruzzo, B. and Amat, P. (2005) Hypothalamic tanycytes: a key component of brain-endocrine interaction. *Int Rev Cytol*, **247**, 89-164.
- Rollins, B. M., Garcia-Caballero, A., Stutts, M. J. and Tarran, R. (2010) SPLUNC1 expression reduces surface levels of the epithelial sodium channel (ENaC) in *Xenopus laevis* oocytes. *Channels*, **4**, 255-259.
- Rose, G. and Stamler, J. (1989) The INTERSALT study: background, methods and main results. INTERSALT Co-operative Research Group. *Journal of human hypertension*, **3**, 283-288.

- Ross, S. B., Fuller, C. M., Bubien, J. K. and Benos, D. J. (2007) Amiloride-sensitive Na⁺ channels contribute to regulatory volume increases in human glioma cells. *Am J Physiol Cell Physiol*, **293**, C1181-1185.
- Rossier, B. C. (1997) Lose salt and gain a friend! A tribute to Gerhard Giebisch. *Wiener klinische Wochenschrift*, **109**, 504-506.
- Rossier, B. C., Pradervand, S., Schild, L. and Hummler, E. (2002) Epithelial sodium channel and the control of sodium balance: interaction between genetic and environmental factors. *Annual review of physiology*, **64**, 877-897.
- Rossier, B. C. and Stutts, M. J. (2009) Activation of the epithelial sodium channel (ENaC) by serine proteases. *Annual review of physiology*, **71**, 361-379.
- Rotin, D., Bar-Sagi, D., O'Brodovich, H., Merilainen, J., Lehto, V. P., Canessa, C. M., Rossier, B. C. and Downey, G. P. (1994) An SH3 binding region in the epithelial Na⁺ channel (alpha rENaC) mediates its localization at the apical membrane. *The EMBO journal*, **13**, 4440-4450.
- Rotin, D., Kanelis, V. and Schild, L. (2001) Trafficking and cell surface stability of ENaC. *American journal of physiology*, **281**, F391-399.
- Rubera, I., Loffing, J., Palmer, L. G. et al. (2003) Collecting duct-specific gene inactivation of alphaENaC in the mouse kidney does not impair sodium and potassium balance. *The Journal of clinical investigation*, **112**, 554-565.
- Ruffieux-Daidie, D. and Staub, O. (2011) Intracellular ubiquitylation of the epithelial Na⁺ channel controls extracellular proteolytic channel activation via conformational change. *The Journal of biological chemistry*, **286**, 2416-2424.

- Ruiz-Arribas, A., Fernandez-Abalos, J. M., Sanchez, P., Garda, A. L. and Santamaria, R. I. (1995) Overproduction, purification, and biochemical characterization of a xylanase (Xys1) from *Streptomyces halstedii* JM8. *Appl Environ Microbiol*, **61**, 2414-2419.
- Ruiz-Opazo, N., Barany, F., Hirayama, K. and Herrera, V. L. (1994) Confirmation of mutant alpha 1 Na,K-ATPase gene and transcript in Dahl salt-sensitive/JR rats. *Hypertension*, **24**, 260-270.
- Ruiz-Opazo, N., Cloix, J. F., Melis, M. G., Xiang, X. H. and Herrera, V. L. (1997a) Characterization of a sodium-response transcriptional mechanism. *Hypertension*, **30**, 191-198.
- Ruiz-Opazo, N. and Herrera, V. L. (1992) Analysis of Na⁺ pump genes. *Hypertension*, **19**, 495-496.
- Ruiz-Opazo, N., Lopez, L. V. and Herrera, V. L. (2002) The dual AngII/AVP receptor gene N119S/C163R variant exhibits sodium-induced dysfunction and cosegregates with salt-sensitive hypertension in the Dahl salt-sensitive hypertensive rat model. *Molecular medicine (Cambridge, Mass)*, **8**, 24-32.
- Ruiz-Opazo, N., Xiang, X. H. and Herrera, V. L. (1997b) Pressure-overload deinduction of human alpha 2 Na,K-ATPase gene expression in transgenic rats. *Hypertension*, **29**, 606-612.
- Rundle, S. E., Smith, A. I., Stockman, D. and Funder, J. W. (1989) Immunocytochemical demonstration of mineralocorticoid receptors in rat and human kidney. *Journal of steroid biochemistry*, **33**, 1235-1242.

- Saavedra, J. M., Del Carmine, R., McCarty, R., Guicheney, P., Weise, V. and Iwai, J. (1983) Increased adrenal catecholamines in salt-sensitive genetically hypertensive Dahl rats. *The American journal of physiology*, **245**, H762-766.
- Sacks, F. M., Svetkey, L. P., Vollmer, W. M. et al. (2001) Effects on blood pressure of reduced dietary sodium and the Dietary Approaches to Stop Hypertension (DASH) diet. DASH-Sodium Collaborative Research Group. *The New England journal of medicine*, **344**, 3-10.
- Saito, Y. and Wright, E. M. (1982) Kinetics of the sodium pump in the frog choroid plexus. *The Journal of physiology*, **328**, 229-243.
- Saito, Y. and Wright, E. M. (1983) Bicarbonate transport across the frog choroid plexus and its control by cyclic nucleotides. *The Journal of physiology*, **336**, 635-648.
- Saito, Y. and Wright, E. M. (1984) Regulation of bicarbonate transport across the brush border membrane of the bull-frog choroid plexus. *The Journal of physiology*, **350**, 327-342.
- Saito, Y. and Wright, E. M. (1987) Regulation of intracellular chloride in bullfrog choroid plexus. *Brain research*, **417**, 267-272.
- Sakai, R. R., McEwen, B. S., Fluharty, S. J. and Ma, L. Y. (2000) The amygdala: site of genomic and nongenomic arousal of aldosterone-induced sodium intake. *Kidney international*, **57**, 1337-1345.
- Sanchez del Pino, M. M., Hawkins, R. A. and Peterson, D. R. (1995) Biochemical discrimination between luminal and abluminal enzyme and transport activities of the blood-brain barrier. *The Journal of biological chemistry*, **270**, 14907-14912.

- Sanchez, E., Vargas, M. A., Singru, P. S., Pascual, I., Romero, F., Fekete, C., Charli, J. L. and Lechan, R. M. (2009) Tanycyte pyroglutamyl peptidase II contributes to regulation of the hypothalamic-pituitary-thyroid axis through glial-axonal associations in the median eminence. *Endocrinology*, **150**, 2283-2291.
- Sanders, B. J., Knardahl, S. and Johnson, A. K. (1989) Lesions of the anteroventral third ventricle and development of stress-induced hypertension in the borderline hypertensive rat. *Hypertension*, **13**, 817-821.
- Sariban-Sohraby, S., Latorre, R., Burg, M., Olans, L. and Benos, D. (1984) Amiloride-sensitive epithelial Na⁺ channels reconstituted into planar lipid bilayer membranes. *Nature*, **308**, 80-82.
- Sarnat, H. B. (1992a) Regional differentiation of the human fetal ependyma: immunocytochemical markers. *Journal of neuropathology and experimental neurology*, **51**, 58-75.
- Sarnat, H. B. (1992b) Role of human fetal ependyma. *Pediatric neurology*, **8**, 163-178.
- Sarnat, H. B. (1998) Histochemistry and immunocytochemistry of the developing ependyma and choroid plexus. *Microsc Res Tech*, **41**, 14-28.
- Sasaki, N. (1962) High blood pressure and the salt intake of the Japanese. *Japanese heart journal*, **3**, 313-324.
- Sasaki, N. (1964) The Relationship of Salt Intake to Hypertension in the Japanese. *Geriatrics*, **19**, 735-744.
- Satlin, L. M., Carattino, M. D., Liu, W. and Kleyman, T. R. (2006) Regulation of cation transport in the distal nephron by mechanical forces. *American journal of physiology*, **291**, F923-931.

- Satlin, L. M., Sheng, S., Woda, C. B. and Kleyman, T. R. (2001) Epithelial Na⁽⁺⁾ channels are regulated by flow. *American journal of physiology*, **280**, F1010-1018.
- Sauter, D., Fernandes, S., Goncalves-Mendes, N., Boulkroun, S., Bankir, L., Loffing, J. and Bouby, N. (2006) Long-term effects of vasopressin on the subcellular localization of ENaC in the renal collecting system. *Kidney international*, **69**, 1024-1032.
- Schafer, J. A., Li, L. and Sun, D. (2000) The collecting duct, dopamine and vasopressin-dependent hypertension. *Acta Physiol Scand*, **168**, 239-244.
- Schild, L. (1996) The ENaC channel as the primary determinant of two human diseases: Liddle syndrome and pseudohypoaldosteronism. *Nephrologie*, **17**, 395-400.
- Schild, L., Canessa, C. M., Shimkets, R. A., Gautschi, I., Lifton, R. P. and Rossier, B. C. (1995) A mutation in the epithelial sodium channel causing Liddle disease increases channel activity in the *Xenopus laevis* oocyte expression system. *Proceedings of the National Academy of Sciences of the United States of America*, **92**, 5699-5703.
- Schild, L., Lu, Y., Gautschi, I., Schneeberger, E., Lifton, R. P. and Rossier, B. C. (1996) Identification of a PY motif in the epithelial Na channel subunits as a target sequence for mutations causing channel activation found in Liddle syndrome. *The EMBO journal*, **15**, 2381-2387.
- Schniepp, R., Kohler, K., Ladewig, T. et al. (2004) Retinal colocalization and in vitro interaction of the glutamate transporter EAAT3 and the serum- and

- glucocorticoid-inducible kinase SGK1 [correction]. *Investigative ophthalmology & visual science*, **45**, 1442-1449.
- Schulz-Baldes, A., Berger, S., Grahammer, F., Warth, R., Goldschmidt, I., Peters, J., Schutz, G., Greger, R. and Bleich, M. (2001) Induction of the epithelial Na⁺ channel via glucocorticoids in mineralocorticoid receptor knockout mice. *Pflugers Arch*, **443**, 297-305.
- Shehata, M. F., Leenen, F. H. and Tesson, F. (2007) Sequence analysis of coding and 3' and 5' flanking regions of the epithelial sodium channel alpha, beta, and gamma genes in Dahl S versus R rats. *BMC genetics*, **8**, 35.
- Shelly, C. and Herrera, R. (2002) Activation of SGK1 by HGF, Rac1 and integrin-mediated cell adhesion in MDCK cells: PI-3K-dependent and -independent pathways. *Journal of cell science*, **115**, 1985-1993.
- Sheng, S., Carattino, M. D., Bruns, J. B., Hughey, R. P. and Kleyman, T. R. (2006) Furin cleavage activates the epithelial Na⁺ channel by relieving Na⁺ self-inhibition. *American journal of physiology*, **290**, F1488-1496.
- Shi, Y., Chan, S. and Martinez-Santibanez, G. (2009) An up-close look at the pre-mRNA 3'-end processing complex. *RNA biology*, **6**, 522-525.
- Shigaev, A., Asher, C., Latter, H., Garty, H. and Reuveny, E. (2000) Regulation of sgk by aldosterone and its effects on the epithelial Na⁽⁺⁾ channel. *American journal of physiology*, **278**, F613-619.
- Shimizu, H., Watanabe, E., Hiyama, T. Y., Nagakura, A., Fujikawa, A., Okado, H., Yanagawa, Y., Obata, K. and Noda, M. (2007) Glial Nax channels control lactate signaling to neurons for brain [Na⁺] sensing. *Neuron*, **54**, 59-72.

- Shimkets, R. A., Lifton, R. and Canessa, C. M. (1998) In vivo phosphorylation of the epithelial sodium channel. *Proceedings of the National Academy of Sciences of the United States of America*, **95**, 3301-3305.
- Shimkets, R. A., Lifton, R. P. and Canessa, C. M. (1997) The activity of the epithelial sodium channel is regulated by clathrin-mediated endocytosis. *The Journal of biological chemistry*, **272**, 25537-25541.
- Shimkets, R. A., Warnock, D. G., Bositis, C. M. et al. (1994) Liddle's syndrome: heritable human hypertension caused by mutations in the beta subunit of the epithelial sodium channel. *Cell*, **79**, 407-414.
- Shivers, R. R., Betz, A. L. and Goldstein, G. W. (1984) Isolated rat brain capillaries possess intact, structurally complex, interendothelial tight junctions; freeze-fracture verification of tight junction integrity. *Brain research*, **324**, 313-322.
- Simchon, S., Manger, W., Golanov, E., Kamen, J., Sommer, G. and Marshall, C. H. (1999) Handling $^{22}\text{NaCl}$ by the blood-brain barrier and kidney: its relevance to salt-induced hypertension in dahl rats. *Hypertension*, **33**, 517-523.
- Simonet, L., St Lezin, E. and Kurtz, T. W. (1991) Sequence analysis of the alpha 1 Na^+, K^+ -ATPase gene in the Dahl salt-sensitive rat. *Hypertension*, **18**, 689-693.
- Sjostrom, M., Stenstrom, K., Eneling, K., Zwiller, J., Katz, A. I., Takemori, H. and Bertorello, A. M. (2007) SIK1 is part of a cell sodium-sensing network that regulates active sodium transport through a calcium-dependent process. *Proceedings of the National Academy of Sciences of the United States of America*, **104**, 16922-16927.

- Snyder, P. M. (2000) Liddle's syndrome mutations disrupt cAMP-mediated translocation of the epithelial Na⁽⁺⁾ channel to the cell surface. *The Journal of clinical investigation*, **105**, 45-53.
- Snyder, P. M. (2002) The epithelial Na⁺ channel: cell surface insertion and retrieval in Na⁺ homeostasis and hypertension. *Endocrine reviews*, **23**, 258-275.
- Snyder, P. M. (2005) Minireview: regulation of epithelial Na⁺ channel trafficking. *Endocrinology*, **146**, 5079-5085.
- Snyder, P. M., Cheng, C., Prince, L. S., Rogers, J. C. and Welsh, M. J. (1998) Electrophysiological and biochemical evidence that DEG/ENaC cation channels are composed of nine subunits. *The Journal of biological chemistry*, **273**, 681-684.
- Snyder, P. M., McDonald, F. J., Stokes, J. B. and Welsh, M. J. (1994) Membrane topology of the amiloride-sensitive epithelial sodium channel. *The Journal of biological chemistry*, **269**, 24379-24383.
- Snyder, P. M., Olson, D. R., Kabra, R., Zhou, R. and Steines, J. C. (2004a) cAMP and serum and glucocorticoid-inducible kinase (SGK) regulate the epithelial Na⁽⁺⁾ channel through convergent phosphorylation of Nedd4-2. *The Journal of biological chemistry*, **279**, 45753-45758.
- Snyder, P. M., Olson, D. R., McDonald, F. J. and Bucher, D. B. (2001) Multiple WW domains, but not the C2 domain, are required for inhibition of the epithelial Na⁺ channel by human Nedd4. *The Journal of biological chemistry*, **276**, 28321-28326.

- Snyder, P. M., Olson, D. R. and Thomas, B. C. (2002) Serum and glucocorticoid-regulated kinase modulates Nedd4-2-mediated inhibition of the epithelial Na⁺ channel. *The Journal of biological chemistry*, **277**, 5-8.
- Snyder, P. M., Price, M. P., McDonald, F. J., Adams, C. M., Volk, K. A., Zeiher, B. G., Stokes, J. B. and Welsh, M. J. (1995) Mechanism by which Liddle's syndrome mutations increase activity of a human epithelial Na⁺ channel. *Cell*, **83**, 969-978.
- Snyder, P. M., Steines, J. C. and Olson, D. R. (2004b) Relative contribution of Nedd4 and Nedd4-2 to ENaC regulation in epithelia determined by RNA interference. *The Journal of biological chemistry*, **279**, 5042-5046.
- Song, J., Hu, X., Riazi, S., Tiwari, S., Wade, J. B. and Ecelbarger, C. A. (2006) Regulation of blood pressure, the epithelial sodium channel (ENaC), and other key renal sodium transporters by chronic insulin infusion in rats. *American journal of physiology*, **290**, F1055-1064.
- Song, Y., Herrera, V. L., Filigheddu, F., Troffa, C., Lopez, L. V., Glorioso, N. and Ruiz-Opazo, N. (2001) Non-association of the thiazide-sensitive Na,Cl-cotransporter gene with polygenic hypertension in both rats and humans. *Journal of hypertension*, **19**, 1547-1551.
- Soundararajan, R., Wang, J., Melters, D. and Pearce, D. (2010) Glucocorticoid-induced Leucine zipper 1 stimulates the epithelial sodium channel by regulating serum- and glucocorticoid-induced kinase 1 stability and subcellular localization. *The Journal of biological chemistry*, **285**, 39905-39913.

- Spindler, B., Mastroberardino, L., Custer, M. and Verrey, F. (1997) Characterization of early aldosterone-induced RNAs identified in A6 kidney epithelia. *Pflugers Arch*, **434**, 323-331.
- Staruschenko, A., Adams, E., Booth, R. E. and Stockand, J. D. (2005) Epithelial Na⁺ channel subunit stoichiometry. *Biophysical journal*, **88**, 3966-3975.
- Staruschenko, A., Nichols, A., Medina, J. L., Camacho, P., Zheleznova, N. N. and Stockand, J. D. (2004) Rho small GTPases activate the epithelial Na⁽⁺⁾ channel. *The Journal of biological chemistry*, **279**, 49989-49994.
- Staub, O., Dho, S., Henry, P., Correa, J., Ishikawa, T., McGlade, J. and Rotin, D. (1996) WW domains of Nedd4 bind to the proline-rich PY motifs in the epithelial Na⁺ channel deleted in Liddle's syndrome. *The EMBO journal*, **15**, 2371-2380.
- Staub, O., Gautschi, I., Ishikawa, T., Breitschopf, K., Ciechanover, A., Schild, L. and Rotin, D. (1997) Regulation of stability and function of the epithelial Na⁺ channel (ENaC) by ubiquitination. *The EMBO journal*, **16**, 6325-6336.
- Stenstrom, K., Takemori, H., Bianchi, G., Katz, A. I. and Bertorello, A. M. (2009) Blocking the salt-inducible kinase 1 network prevents the increases in cell sodium transport caused by a hypertension-linked mutation in human alpha-adducin. *Journal of hypertension*, **27**, 2452-2457.
- Stewart, P. M., Murry, B. A. and Mason, J. I. (1994) Human kidney 11 beta-hydroxysteroid dehydrogenase is a high affinity nicotinamide adenine dinucleotide-dependent enzyme and differs from the cloned type I isoform. *The Journal of clinical endocrinology and metabolism*, **79**, 480-484.

- Stockand, J. D. (2002) New ideas about aldosterone signaling in epithelia. *American journal of physiology*, **282**, F559-576.
- Stockand, J. D., Spier, B. J., Worrell, R. T., Yue, G., Al-Baldawi, N. and Eaton, D. C. (1999) Regulation of Na(+) reabsorption by the aldosterone-induced small G protein K-Ras2A. *The Journal of biological chemistry*, **274**, 35449-35454.
- Stokes, J. B. and Sigmund, R. D. (1998) Regulation of rENaC mRNA by dietary NaCl and steroids: organ, tissue, and steroid heterogeneity. *The American journal of physiology*, **274**, C1699-1707.
- Strautnieks, S. S., Thompson, R. J., Gardiner, R. M. and Chung, E. (1996a) A novel splice-site mutation in the gamma subunit of the epithelial sodium channel gene in three pseudohypoaldosteronism type 1 families. *Nature genetics*, **13**, 248-250.
- Strautnieks, S. S., Thompson, R. J., Hanukoglu, A., Dillon, M. J., Hanukoglu, I., Kuhnle, U., Seckl, J., Gardiner, R. M. and Chung, E. (1996b) Localisation of pseudohypoaldosteronism genes to chromosome 16p12.2-13.11 and 12p13.1-pter by homozygosity mapping. *Human molecular genetics*, **5**, 293-299.
- Stromstedt, M. and Waterman, M. R. (1995) Messenger RNAs encoding steroidogenic enzymes are expressed in rodent brain. *Brain Res Mol Brain Res*, **34**, 75-88.
- Stutts, M. J., Rossier, B. C. and Boucher, R. C. (1997) Cystic fibrosis transmembrane conductance regulator inverts protein kinase A-mediated regulation of epithelial sodium channel single channel kinetics. *The Journal of biological chemistry*, **272**, 14037-14040.
- Su, Y. R. and Menon, A. G. (2001) Epithelial sodium channels and hypertension. *Drug metabolism and disposition: the biological fate of chemicals*, **29**, 553-556.

- Su, Y. R., Rutkowski, M. P., Klanke, C. A., Wu, X., Cui, Y., Pun, R. Y., Carter, V., Reif, M. and Menon, A. G. (1996) A novel variant of the beta-subunit of the amiloride-sensitive sodium channel in African Americans. *J Am Soc Nephrol*, **7**, 2543-2549.
- Sullivan, J. M. (1991) Salt sensitivity. Definition, conception, methodology, and long-term issues. *Hypertension*, **17**, 161-68.
- Svetkey, L. P., Simons-Morton, D. G., Proschan, M. A., Sacks, F. M., Conlin, P. R., Harsha, D. and Moore, T. J. (2004) Effect of the dietary approaches to stop hypertension diet and reduced sodium intake on blood pressure control. *Journal of clinical hypertension (Greenwich, Conn)*, **6**, 373-381.
- Sweadner, K. J., Herrera, V. L., Amato, S., Moellmann, A., Gibbons, D. K. and Repke, K. R. (1994) Immunologic identification of Na⁺,K⁽⁺⁾-ATPase isoforms in myocardium. Isoform change in deoxycorticosterone acetate-salt hypertension. *Circulation research*, **74**, 669-678.
- Swezey, N., Tchepichev, S., Gagnon, S., Fertuck, K. and O'Brodivich, H. (1998) Female gender hormones regulate mRNA levels and function of the rat lung epithelial Na channel. *The American journal of physiology*, **274**, C379-386.
- Swift, P. A. and MacGregor, G. A. (2004) The epithelial sodium channel in hypertension: genetic heterogeneity and implications for treatment with amiloride. *Am J Pharmacogenomics*, **4**, 161-168.
- Szmydynger-Chodobska, J., Chung, I. and Chodobski, A. (2006) Chronic hypernatremia increases the expression of vasopressin and voltage-gated Na channels in the rat choroid plexus. *Neuroendocrinology*, **84**, 339-345.

- Tagawa, T. and Dampney, R. A. (1999) AT(1) receptors mediate excitatory inputs to rostral ventrolateral medulla pressor neurons from hypothalamus. *Hypertension*, **34**, 1301-1307.
- Takahashi, H., Matsuzawa, M., Okabayashi, H. et al. (1987a) Evidence for a digitalis-like substance in the hypothalamopituitary axis in rats: implications in the central cardiovascular regulation associated with an excess intake of sodium. *Japanese circulation journal*, **51**, 1199-1207.
- Takahashi, H., Okabayashi, H., Matsuzawa, M., Suga, K., Ikegaki, I., Yoshimura, M. and Ijichi, H. (1987b) Centrally induced vasopressor responses to ouabain in DOCA-salt hypertensive rats. *Cardiovascular research*, **21**, 439-446.
- Takeda, Y., Zhu, A., Yoneda, T., Usukura, M., Takata, H. and Yamagishi, M. (2007) Effects of aldosterone and angiotensin II receptor blockade on cardiac angiotensinogen and angiotensin-converting enzyme 2 expression in Dahl salt-sensitive hypertensive rats. *American journal of hypertension*, **20**, 1119-1124.
- Takeshita, A., Mark, A. L. and Brody, M. J. (1979) Prevention of salt-induced hypertension in the Dahl strain by 6-hydroxydopamine. *The American journal of physiology*, **236**, H48-52.
- Takeuchi, K. (2002) [Bartter syndrome, Gitelman syndrome, Liddle syndrome]. *Nippon rinsho*, **60 Suppl 1**, 532-540.
- Takeuchi, K., Abe, K., Sato, M., Yasujima, M., Omata, K., Murakami, O. and Yoshinaga, K. (1989) Plasma aldosterone level in a female case of pseudohyperaldosteronism (Liddle's syndrome). *Endocrinologia japonica*, **36**, 167-173.

- Tamura, H., Schild, L., Enomoto, N., Matsui, N., Marumo, F. and Rossier, B. C. (1996) Liddle disease caused by a missense mutation of beta subunit of the epithelial sodium channel gene. *The Journal of clinical investigation*, **97**, 1780-1784.
- Taub, M., Springate, J. E. and Cutuli, F. Targeting of renal proximal tubule Na,K-ATPase by salt-inducible kinase. *Biochemical and biophysical research communications*, **393**, 339-344.
- Teruya, H., Yamazato, M., Muratani, H., Sakima, A., Takishita, S., Terano, Y. and Fukiyama, K. (1997) Role of ouabain-like compound in the rostral ventrolateral medulla in rats. *The Journal of clinical investigation*, **99**, 2791-2798.
- Thome, U. H., Davis, I. C., Nguyen, S. V., Shelton, B. J. and Matalon, S. (2003) Modulation of sodium transport in fetal alveolar epithelial cells by oxygen and corticosterone. *Am J Physiol Lung Cell Mol Physiol*, **284**, L376-385.
- Tomita, K., Pisano, J. J. and Knepper, M. A. (1985) Control of sodium and potassium transport in the cortical collecting duct of the rat. Effects of bradykinin, vasopressin, and deoxycorticosterone. *The Journal of clinical investigation*, **76**, 132-136.
- Trochen, N., Ganapathipillai, S., Ferrari, P., Frey, B. M. and Frey, F. J. (2004) Low prevalence of nonconservative mutations of serum and glucocorticoid-regulated kinase (SGK1) gene in hypertensive and renal patients. *Nephrol Dial Transplant*, **19**, 2499-2504.
- Tsai, K. J., Chen, S. K., Ma, Y. L., Hsu, W. L. and Lee, E. H. (2002) *sgk*, a primary glucocorticoid-induced gene, facilitates memory consolidation of spatial learning

- in rats. *Proceedings of the National Academy of Sciences of the United States of America*, **99**, 3990-3995.
- Turnheim, K. (1991) Intrinsic regulation of apical sodium entry in epithelia. *Physiological reviews*, **71**, 429-445.
- Turnheim, K., Frizzell, R. A. and Schultz, S. G. (1977) Effects of anions on amiloride-sensitive, active sodium transport across rabbit colon, in vitro. Evidence for "trans-inhibition" of the Na entry mechanism. *The Journal of membrane biology*, **37**, 63-84.
- Umemura, M., Ishigami, T., Tamura, K. et al. (2006) Transcriptional diversity and expression of NEDD4L gene in distal nephron. *Biochemical and biophysical research communications*, **339**, 1129-1137.
- Valentijn, J. A., Fyfe, G. K. and Canessa, C. M. (1998) Biosynthesis and processing of epithelial sodium channels in *Xenopus* oocytes. *The Journal of biological chemistry*, **273**, 30344-30351.
- Vallet, V., Chraïbi, A., Gaeggeler, H. P., Horisberger, J. D. and Rossier, B. C. (1997) An epithelial serine protease activates the amiloride-sensitive sodium channel. *Nature*, **389**, 607-610.
- Vallon, V., Huang, D. Y., Grahammer, F., Wyatt, A. W., Osswald, H., Wulff, P., Kuhl, D. and Lang, F. (2005) SGK1 as a determinant of kidney function and salt intake in response to mineralocorticoid excess. *American journal of physiology*, **289**, R395-R401.

- Vallon, V. and Lang, F. (2005) New insights into the role of serum- and glucocorticoid-inducible kinase SGK1 in the regulation of renal function and blood pressure. *Current opinion in nephrology and hypertension*, **14**, 59-66.
- VanLandingham, L. G., Gannon, K. P. and Drummond, H. A. (2009) Pressure-induced constriction is inhibited in a mouse model of reduced betaENaC. *American journal of physiology*, **297**, R723-728.
- Verrey, F. (1995) Transcriptional control of sodium transport in tight epithelial by adrenal steroids. *The Journal of membrane biology*, **144**, 93-110.
- Vigne, P., Champigny, G., Marsault, R., Barbry, P., Frelin, C. and Lazdunski, M. (1989) A new type of amiloride-sensitive cationic channel in endothelial cells of brain microvessels. *The Journal of biological chemistry*, **264**, 7663-7668.
- Vogel, T. and Gruss, P. (2009) Expression of Leukaemia associated transcription factor Af9/Mllt3 in the cerebral cortex of the mouse. *Gene Expr Patterns*, **9**, 83-93.
- Voisin, D. L. and Bourque, C. W. (2002) Integration of sodium and osmosensory signals in vasopressin neurons. *Trends in neurosciences*, **25**, 199-205.
- Volk, K. A., Husted, R. F., Sigmund, R. D. and Stokes, J. B. (2005) Overexpression of the epithelial Na⁺ channel gamma subunit in collecting duct cells: interactions of Liddle's mutations and steroids on expression and function. *The Journal of biological chemistry*, **280**, 18348-18354.
- Volk, K. A., Sigmund, R. D., Snyder, P. M., McDonald, F. J., Welsh, M. J. and Stokes, J. B. (1995) rENaC is the predominant Na⁺ channel in the apical membrane of the rat renal inner medullary collecting duct. *The Journal of clinical investigation*, **96**, 2748-2757.

- von Wöhrn, F., Berglund, G., Carlson, J., Mansson, H., Hedblad, B. and Melander, O. (2005) Genetic variance of SGK-1 is associated with blood pressure, blood pressure change over time and strength of the insulin-diastolic blood pressure relationship. *Kidney international*, **68**, 2164-2172.
- Vuagniaux, G., Vallet, V., Jaeger, N. F., Hummler, E. and Rossier, B. C. (2002) Synergistic activation of ENaC by three membrane-bound channel-activating serine proteases (mCAP1, mCAP2, and mCAP3) and serum- and glucocorticoid-regulated kinase (Sgk1) in *Xenopus* Oocytes. *The Journal of general physiology*, **120**, 191-201.
- Waerntges, S., Klingel, K., Weigert, C. et al. (2002) Excessive transcription of the human serum and glucocorticoid dependent kinase hSGK1 in lung fibrosis. *Cell Physiol Biochem*, **12**, 135-142.
- Wainford, R. D. and Kapusta, D. R. (2010) Hypothalamic Paraventricular Nucleus G α q Subunit Protein Pathways Mediate Vasopressin Dysregulation and Fluid Retention in Salt-Sensitive Rats. *Endocrinology*, **151**, 5403-5414.
- Waldegger, S., Barth, P., Forrest, J. N., Jr., Greger, R. and Lang, F. (1998) Cloning of sgk serine-threonine protein kinase from shark rectal gland - a gene induced by hypertonicity and secretagogues. *Pflugers Arch*, **436**, 575-580.
- Waldegger, S., Barth, P., Raber, G. and Lang, F. (1997) Cloning and characterization of a putative human serine/threonine protein kinase transcriptionally modified during anisotonic and isotonic alterations of cell volume. *Proceedings of the National Academy of Sciences of the United States of America*, **94**, 4440-4445.

- Waldegger, S., Gabrysch, S., Barth, P., Fillon, S. and Lang, F. (2000) h-sgk serine-threonine protein kinase as transcriptional target of p38/MAP kinase pathway in HepG2 human hepatoma cells. *Cell Physiol Biochem*, **10**, 203-208.
- Waldegger, S., Klingel, K., Barth, P., Sauter, M., Rfer, M. L., Kandolf, R. and Lang, F. (1999) h-sgk serine-threonine protein kinase gene as transcriptional target of transforming growth factor beta in human intestine. *Gastroenterology*, **116**, 1081-1088.
- Wan, S. L., Liao, M. Y. and Sun, K. (2002) Postnatal development of 11beta-hydroxysteroid dehydrogenase type 1 in the rat hippocampus. *Journal of neuroscience research*, **69**, 681-686.
- Wang, H., Huang, B. S. and Leenen, F. H. (2003a) Brain sodium channels and ouabainlike compounds mediate central aldosterone-induced hypertension. *American journal of physiology*, **285**, H2516-2523.
- Wang, H. and Leenen, F. H. (2002) Brain sodium channels mediate increases in brain "ouabain" and blood pressure in Dahl S rats. *Hypertension*, **40**, 96-100.
- Wang, H. and Leenen, F. H. (2003) Brain sodium channels and central sodium-induced increases in brain ouabain-like compound and blood pressure. *Journal of hypertension*, **21**, 1519-1524.
- Wang, H., White, R. and Leenen, F. H. (2003b) Stimulation of brain Na⁺ channels by FMRFamide in Dahl SS and SR rats. *American journal of physiology*, **285**, H2013-2018.

- Wang, H. W., Amin, M. S., El-Shahat, E., Huang, B. S., Tuana, B. S. and Leenen, F. H. (2010a) Effects of Central Sodium on Epithelial Sodium Channels in Rat Brain. *American journal of physiology*.
- Wang, H. W., Amin, M. S., El-Shahat, E., Huang, B. S., Tuana, B. S. and Leenen, F. H. (2010b) Effects of central sodium on epithelial sodium channels in rat brain. *American journal of physiology*, **299**, R222-233.
- Wang, J., Barbry, P., Maiyar, A. C., Rozansky, D. J., Bhargava, A., Leong, M., Firestone, G. L. and Pearce, D. (2001) SGK integrates insulin and mineralocorticoid regulation of epithelial sodium transport. *American journal of physiology*, **280**, F303-313.
- Wang, Q., Horisberger, J. D., Maillard, M., Brunner, H. R., Rossier, B. C. and Burnier, M. (2000) Salt- and angiotensin II-dependent variations in amiloride-sensitive rectal potential difference in mice. *Clinical and experimental pharmacology & physiology*, **27**, 60-66.
- Wang, Z., Takemori, H., Halder, S. K., Nonaka, Y. and Okamoto, M. (1999) Cloning of a novel kinase (SIK) of the SNF1/AMPK family from high salt diet-treated rat adrenal. *FEBS letters*, **453**, 135-139.
- Warnock, D. G. (1996) Polymorphism in the beta subunit and Na⁺ transport. *J Am Soc Nephrol*, **7**, 2490-2494.
- Warnock, D. G. (2001) Liddle syndrome: genetics and mechanisms of Na⁺ channel defects. *The American journal of the medical sciences*, **322**, 302-307.

- Warntges, S., Friedrich, B., Henke, G. et al. (2002) Cerebral localization and regulation of the cell volume-sensitive serum- and glucocorticoid-dependent kinase SGK1. *Pflugers Arch*, **443**, 617-624.
- Watanabe, E., Hiyama, T. Y., Kodama, R. and Noda, M. (2002) NaX sodium channel is expressed in non-myelinating Schwann cells and alveolar type II cells in mice. *Neuroscience letters*, **330**, 109-113.
- Watanabe, U., Shimura, T., Sako, N., Kitagawa, J., Shingai, T., Watanabe, E., Noda, M. and Yamamoto, T. (2003) A comparison of voluntary salt-intake behavior in Nax-gene deficient and wild-type mice with reference to peripheral taste inputs. *Brain research*, **967**, 247-256.
- Wedler, B., Brier, M. E., Wiersbitzky, M., Gruska, S., Wolf, E., Kallwellis, R., Aronoff, G. R. and Luft, F. C. (1992) Sodium kinetics in salt-sensitive and salt-resistant normotensive and hypertensive subjects. *Journal of hypertension*, **10**, 663-669.
- Wei, E. T. and Wu, Y. (1979) Pressor effects of intracisternal Na⁺ in normotensive and spontaneously hypertensive rats. *Brain research*, **169**, 605-609.
- Wei, S. G., Yu, Y., Zhang, Z. H., Weiss, R. M. and Felder, R. B. (2008) Angiotensin II-triggered p44/42 mitogen-activated protein kinase mediates sympathetic excitation in heart failure rats. *Hypertension*, **52**, 342-350.
- Weinberger, M. H. (1991) Salt sensitivity as a predictor of hypertension. *American journal of hypertension*, **4**, 615S-616S.
- Weinberger, M. H. (1993a) Racial differences in renal sodium excretion: relationship to hypertension. *Am J Kidney Dis*, **21**, 41-45.

- Weinberger, M. H. (1993b) Sodium sensitivity of blood pressure. *Current opinion in nephrology and hypertension*, **2**, 935-939.
- Weinberger, M. H. (1996a) Hypertension in African Americans: the role of sodium chloride and extracellular fluid volume. *Seminars in nephrology*, **16**, 110-116.
- Weinberger, M. H. (1996b) Salt sensitivity of blood pressure in humans. *Hypertension*, **27**, 481-490.
- Weinberger, M. H. (2000) Salt and blood pressure. *Current opinion in cardiology*, **15**, 254-257.
- Weinberger, M. H. (2004) Sodium and blood pressure 2003. *Current opinion in cardiology*, **19**, 353-356.
- Weinberger, M. H. (2006) Pathogenesis of salt sensitivity of blood pressure. *Current hypertension reports*, **8**, 166-170.
- Weinberger, M. H. and Fineberg, N. S. (1991) Sodium and volume sensitivity of blood pressure. Age and pressure change over time. *Hypertension*, **18**, 67-71.
- Weinberger, M. H., Fineberg, N. S., Fineberg, S. E. and Weinberger, M. (2001) Salt sensitivity, pulse pressure, and death in normal and hypertensive humans. *Hypertension*, **37**, 429-432.
- Weisz, O. A. and Johnson, J. P. (2003) Noncoordinate regulation of ENaC: paradigm lost? *American journal of physiology*, **285**, F833-842.
- Weisz, O. A., Wang, J. M., Edinger, R. S. and Johnson, J. P. (2000) Non-coordinate regulation of endogenous epithelial sodium channel (ENaC) subunit expression at the apical membrane of A6 cells in response to various transporting conditions. *The Journal of biological chemistry*, **275**, 39886-39893.

- Wen, H. T. N. C. S. (1973) The Yellow Emperors classic of internal medicine, translated by Veith, T. *University of California Press*.
- Whitescarver, S. A., Ott, C. E., Jackson, B. A., Guthrie, G. P., Jr. and Kotchen, T. A. (1984) Salt-sensitive hypertension: contribution of chloride. *Science (New York, N.Y)*, **223**, 1430-1432.
- Whitescarver, S. A., Ott, C. E., Tachman, M. and Kotchen, T. A. (1986) Sodium and chloride in salt-sensitive hypertension. *Hypertension*, **8**, 552.
- Widmer, H., Ludwig, M., Bancel, F., Leng, G. and Dayanithi, G. (2003) Neurosteroid regulation of oxytocin and vasopressin release from the rat supraoptic nucleus. *The Journal of physiology*, **548**, 233-244.
- Wiemuth, D., Lott, J. S., Ly, K., Ke, Y., Teesdale-Spittle, P., Snyder, P. M. and McDonald, F. J. (2010) Interaction of serum- and glucocorticoid regulated kinase 1 (SGK1) with the WW-domains of Nedd4-2 is required for epithelial sodium channel regulation. *PloS one*, **5**, e12163.
- Wilkie, G. S., Dickson, K. S. and Gray, N. K. (2003) Regulation of mRNA translation by 5'- and 3'-UTR-binding factors. *Trends in biochemical sciences*, **28**, 182-188.
- Wittkowski, W. (1998) Tanycytes and pituicytes: morphological and functional aspects of neuroglial interaction. *Microsc Res Tech*, **41**, 29-42.
- Wolf, K., Castrop, H., Riegger, G. A., Kurtz, A. and Kramer, B. K. (2001) Differential gene regulation of renal salt entry pathways by salt load in the distal nephron of the rat. *Pflugers Arch*, **442**, 498-504.
- Wotjak, C. T., Ludwig, M., Ebner, K., Russell, J. A., Singewald, N., Landgraf, R. and Engelmann, M. (2002) Vasopressin from hypothalamic magnocellular neurons

- has opposite actions at the adenohypophysis and in the supraoptic nucleus on ACTH secretion. *The European journal of neuroscience*, **16**, 477-485.
- Wotjak, C. T., Ludwig, M. and Landgraf, R. (1994) Vasopressin facilitates its own release within the rat supraoptic nucleus in vivo. *Neuroreport*, **5**, 1181-1184.
- Wright, E. M. (1970) Ion transport across the frog posterior choroid plexus. *Brain research*, **23**, 302-304.
- Wright, E. M. (1972a) Accumulation and transport of amino acids by the frog choroid plexus. *Brain research*, **44**, 207-219.
- Wright, E. M. (1972b) Mechanisms of ion transport across the choroid plexus. *The Journal of physiology*, **226**, 545-571.
- Wright, E. M. (1974) Active transport of iodide and other anions across the choroid plexus. *The Journal of physiology*, **240**, 535-566.
- Wright, E. M. (1977) Effect of bicarbonate and other buffers on choroid plexus Na⁺/K⁺pump. *Biochimica et biophysica acta*, **468**, 486-489.
- Wright, E. M. (1978) Transport processes in the formation of the cerebrospinal fluid. *Reviews of physiology, biochemistry and pharmacology*, **83**, 3-34.
- Wright, E. M. and Saito, Y. (1986) The choroid plexus as a route from blood to brain. *Annals of the New York Academy of Sciences*, **481**, 214-220.
- Wright, E. M., Wiedner, G. and Rumrich, G. (1977) Fluid secretion by the frog choroid plexus. *Experimental eye research*, **25 Suppl**, 149-155.
- Wulff, P., Vallon, V., Huang, D. Y. et al. (2002) Impaired renal Na⁽⁺⁾ retention in the sgk1-knockout mouse. *The Journal of clinical investigation*, **110**, 1263-1268.

- Yamada, H., Naruse, M., Naruse, K., Demura, H., Takahashi, H., Yoshimura, M. and Ochi, J. (1992) Histological study on ouabain immunoreactivities in the mammalian hypothalamus. *Neuroscience letters*, **141**, 143-146.
- Yamashita, Y., Takata, Y., Takishita, S., Tomita, Y., Tsuchihashi, T. and Fujishima, M. (1992) Cerebrospinal fluid sodium and enhanced hypertension in salt-loaded spontaneously hypertensive rats. *Journal of hypertension*, **10**, 741-747.
- Yang, H., Francis, S. C., Sellers, K. et al. (2002) Hypertension-linked decrease in the expression of brain gamma-adducin. *Circulation research*, **91**, 633-639.
- Yang, H., Reeves, P. Y., Katovich, M. J. and Raizada, M. K. (2004) Decrease in hypothalamic gamma adducin in rat models of hypertension. *Hypertension*, **43**, 324-328.
- Yang, L. E., Sandberg, M. B., Can, A. D., Pihakaski-Maunsbach, K. and McDonough, A. A. (2008) Effects of dietary salt on renal Na⁺ transporters' subcellular distribution, abundance, and phosphorylation status. *American journal of physiology*.
- Yang, L. M., Rinke, R. and Korbmacher, C. (2006) Stimulation of the epithelial sodium channel (ENaC) by cAMP involves putative ERK phosphorylation sites in the C termini of the channel's beta- and gamma-subunit. *The Journal of biological chemistry*, **281**, 9859-9868.
- Yau, J. L., Noble, J. and Seckl, J. R. (1999) Continuous blockade of brain mineralocorticoid receptors impairs spatial learning in rats. *Neuroscience letters*, **277**, 45-48.

- Ye, P., Kenyon, C. J., MacKenzie, S. M., Seckl, J. R., Fraser, R., Connell, J. M. and Davies, E. (2003) Regulation of aldosterone synthase gene expression in the rat adrenal gland and central nervous system by sodium and angiotensin II. *Endocrinology*, **144**, 3321-3328.
- Yoshika, M., Komiyama, Y. and Takahashi, H. (2011) An ouabain-like factor is secreted from immortalized hypothalamic cells in an aldosterone-dependent manner. *Neurochemistry international*.
- Yu, L., Eaton, D. C. and Helms, M. N. (2007) Effect of divalent heavy metals on epithelial Na⁺ channels in A6 cells. *American journal of physiology*, **293**, F236-244.
- Yu, L., Helms, M. N., Yue, Q. and Eaton, D. C. (2008) Single-channel analysis of functional epithelial sodium channel (ENaC) stability at the apical membrane of A6 distal kidney cells. *American journal of physiology*, **295**, F1519-1527.
- Zambotti-Villela, L., Marinho, C. E., Alponi, R. F. and Silveira, P. F. (2008) Hypothalamic activity during altered salt and water balance in the snake *Bothrops jararaca*. *J Comp Physiol B*, **178**, 57-66.
- Zecevic, M., Heitzmann, D., Camargo, S. M. and Verrey, F. (2004) SGK1 increases Na,K-ATP cell-surface expression and function in *Xenopus laevis* oocytes. *Pflugers Arch*, **448**, 29-35.
- Zemo, D. A. and McCabe, J. T. (2001) Salt-loading increases vasopressin and vasopressin 1b receptor mRNA in the hypothalamus and choroid plexus. *Neuropeptides*, **35**, 181-188.

- Zeuthen, T. and Wright, E. M. (1978) An electrogenic Na^+/K^+ pump in the choroid plexus. *Biochimica et biophysica acta*, **511**, 517-522.
- Zhang, D., Yu, Z. Y., Cruz, P., Kong, Q., Li, S. and Kone, B. C. (2009) Epigenetics and the control of epithelial sodium channel expression in collecting duct. *Kidney international*, **75**, 260-267.
- Zhang, W., Xia, X., Reisenauer, M. R., Hemenway, C. S. and Kone, B. C. (2006) Dot1a-AF9 complex mediates histone H3 Lys-79 hypermethylation and repression of ENaC α in an aldosterone-sensitive manner. *The Journal of biological chemistry*, **281**, 18059-18068.
- Zhang, W., Xia, X., Reisenauer, M. R., Rieg, T., Lang, F., Kuhl, D., Vallon, V. and Kone, B. C. (2007) Aldosterone-induced Sgk1 relieves Dot1a-Af9-mediated transcriptional repression of epithelial Na^+ channel α . *The Journal of clinical investigation*, **117**, 773-783.
- Zhang, Y. H., Alvarez de la Rosa, D., Canessa, C. M. and Hayslett, J. P. (2005) Insulin-induced phosphorylation of ENaC correlates with increased sodium channel function in A6 cells. *Am J Physiol Cell Physiol*, **288**, C141-147.
- Zhong, S. X. and Liu, Z. H. (2004) Immunohistochemical localization of the epithelial sodium channel in the rat inner ear. *Hear Res*, **193**, 1-8.
- Zhou, M. Y., Gomez-Sanchez, E. P., Cox, D. L., Cosby, D. and Gomez-Sanchez, C. E. (1995) Cloning, expression, and tissue distribution of the rat nicotinamide adenine dinucleotide-dependent 11 β -hydroxysteroid dehydrogenase. *Endocrinology*, **136**, 3729-3734.

- Zhou, R., Kabra, R., Olson, D. R., Piper, R. C. and Snyder, P. M. (2010) Hrs controls sorting of the epithelial Na⁺ channel between endosomal degradation and recycling pathways. *The Journal of biological chemistry*, **285**, 30523-30530.
- Zhou, R. and Snyder, P. M. (2005) Nedd4-2 phosphorylation induces serum and glucocorticoid-regulated kinase (SGK) ubiquitination and degradation. *The Journal of biological chemistry*, **280**, 4518-4523.
- Zhou, Z. H. and Bubien, J. K. (2001) Nongenomic regulation of ENaC by aldosterone. *Am J Physiol Cell Physiol*, **281**, C1118-1130.
- Zhu, A., Yoneda, T., Demura, M., Karashima, S., Usukura, M., Yamagishi, M. and Takeda, Y. (2009) Effect of mineralocorticoid receptor blockade on the renal renin-angiotensin system in Dahl salt-sensitive hypertensive rats. *Journal of hypertension*, **27**, 800-805.
- Zicha, J., Negrin, C. D., Dobesova, Z., Carr, F., Vokurkova, M., McBride, M. W., Kunes, J. and Dominiczak, A. F. (2001) Altered Na⁺-K⁺ pump activity and plasma lipids in salt-hypertensive Dahl rats: relationship to *Atp1a1* gene. *Physiological genomics*, **6**, 99-104.
- Zlokovic, B. V., Mackic, J. B., Wang, L., McComb, J. G. and McDonough, A. (1993a) Differential expression of Na,K-ATPase alpha and beta subunit isoforms at the blood-brain barrier and the choroid plexus. *The Journal of biological chemistry*, **268**, 8019-8025.
- Zlokovic, B. V., Wang, L., Mackic, J. B., Saraj, A. J., McComb, J. G. and McDonough, A. (1993b) Expression of Na,K-ATPase at the blood-brain interface. *Advances in experimental medicine and biology*, **331**, 55-60.